LATE QUATERNARY CHANGES IN THE
EASTERN MEDITERRANEAN CLIMATE AND HYDROGRAPHY
AND IMPLICATIONS FOR THE FORMATION OF SAPROPELS

Eelco J. Rohling

1991

LATE QUATERNARY CHANGES IN THE EASTERN MEDITERRANEAN CLIMATE AND HYDROGRAPHY AND IMPLICATIONS FOR THE FORMATION OF SAPROPELS

LAAT KWARTAIRE VERANDERINGEN IN HET KLIMAAT EN DE HYDROGRAFIE VAN DE OOSTELIJKE MIDDELLANDSE ZEE EN IMPLICATIES VOOR DE VORMING VAN SAPROPELEN

(met een samenvatting in het Nederlands)

proefschrift

ter verkrijging van de graad van doctor
aan de Rijksuniversiteit te Utrecht
op gezag van de Rector Magnificus, Prof. dr. J.A. van Ginkel
ingevolge het besluit van het College van Dekanen
in het openbaar te verdedigen
op woensdag 23 oktober 1991 te 14:30 uur

door

Eelco Johan Rohling

geboren op 19 september 1963 te Heiloo, Nederland

Promotor   Prof. dr. J.E. Meulenkamp

Co-promotor   dr. W.J. Zachariasse

To Jolanda
and my parents

CONTENTS

SUMMARY

The Mediterranean Sea is a marginal basin that is separated from the adjacent North Atlantic Ocean by a shallow sill in the Strait of Gibraltar. A more complex, but equally shallow sill-structure in the Strait of Sicily separates the western and eastern subbasins. The exchange of watermasses through both straits is typically two-layered, with an eastward surface flow and a westward subsurface flow. This pattern of exchange results from net buoyancy loss in the basins on the easterly side of the sills. Surface water flowing in through the Strait of Gibraltar is traceable through the Strait of Sicily into the eastern Mediterranean, although its salinity increases steadily towards the east.

Near Cyprus, surface water sinks to form Mediterranean Intermediate Water (MIW). This MIW spreads throughout the Mediterranean Sea, constituting a large part of the subsurface outflow across both the Sicilian sill and the sill at Gibraltar. There is no equivalent formation of intermediate water in the western Mediterranean. Both the eastern and the western Mediterranean have their own sources of deep water. This deep water settles below the MIW. Eastern Mediterranean Deep Water (EMDW) is formed mainly in the Adriatic Sea. Western Mediterranean Deep Water (WMDW) originates in the northern sector of the western Mediterranean, viz. the Gulf of Lyon and the Ligurian Sea. EMDW and WMDW are effectively separated by the Sicilian sill. EMDW contributes to the subsurface outflow, from the eastern into the western basin, through ernoulli flo - dragging water from below sill depth up and over the sill - and by basin-wide upward mixing into the lower portions of the MIW and subsequent entrainment in the subsurface flow across the sill. Similar processes account for the contribution of WMDW to subsurface outflow across the sill at Gibraltar, from the western Mediterranean into the Atlantic Ocean. The flushing-times of the eastern and western Mediterranean were recently estimated as 50 and 20 years, respectively.

A marked salinity gradient (halocline) exists between the surface waters and the MIW, whereas the thermal gradient between these layers is weak. Therefore, the density gradient (pycnocline) between surface water and MIW essentially parallels the halocline. At present, the eastern Mediterranean pycnocline resides well below the base of the euphotic layer and, as a result, the euphotic layer is extremely oligotrophic. In this thesis, I argue that the eastern Mediterranean pycnocline resided within the euphotic layer at times of sapropel[*] formation and at glacial times, ensuring high nutrient availability in the basal part of the euphotic layer with subsequent development of a Deep Chlorophyll Maximum, coinciding with increased rates of export production. A simple two-layered model is developed for the eastern Mediterranean to study which processes were responsible for the shoaling of the pycnocline.

At glacial times, pycnocline shoaling was largely due to sea level lowering, which invoked a decrease in the surface water inflow across the sills. The model suggests that a sea level lowering of 43 m, relative to the present, would cause shoaling of the eastern Mediterranean pycnocline to the base of the euphotic layer. At times of sapropel formation, pycnocline shoaling was essentially a response to reduction of the basin's freshwater bud et (F = evaporation E - total freshwater input P), which invoked a d crease in the surface water inflow. The

---

[*]	In this thesis, the term sapropel is applied to sediments deposited in dysoxic to anoxic bottom waters. Generally, these sediments are brown to black colored, and contain more than average amounts of pyrite and benthic foraminifera indicative of low bottom water oxygen concentrations. Also, benthic foraminifera may be completely absent from sapropelic sediments (so-called "benthic desert" conditions). Sometimes, sapropels are laminated. I do not follow strict definitions of sapropel, proto-sapropel, sapropelic, or non-sapropelic sediments based on subjective subdivision of organic carbon contents.

model suggests that, if sea level remained equal to the present, a reduction of the freshwater budget to 0.53 times its present-day value would result in shoaling of the pycnocline to the base of the euphotic layer. At times of sapropel formation, the eastern Mediterranean freshwater budget was reduced partly due to increased freshwater discharge from the river Nile, related to orbitally forced peak intensities of the Indian Ocean's summer (SW) monsoon, and partly due to increased activity of the westerly system of Mediterranean depressions, which invoked coeval decreases in evaporation and increases in precipitation and runoff.

The glacial hydrographic configuration, with a shallow pycnocline at or above the base of the euphotic layer, seems to have been quite similar to that at times of sapropel formation. An important difference, however, existed in deeper waters, since glacial sedimentation generally occurred in oxygenated bottom waters, whereas sapropels were formed in severely dysoxic to anoxic bottom waters. This difference is attributed to the fact that, at glacial times, the MIW to surface water salinity contrast was substantially increased, relative to the present, which would facilitate the formation of EMDW, whereas this contrast was decreased at times of sapropel formation, which would hamper the formation of EMDW. From this point of view, however, it was not possible to obtain a quantitative estimate of the rate of EMDW formation at times of sapropel formation, relative to the present.

The rate of EMDW formation could, however, be estimated by considering differences in the eastern Mediterranean phosphate budget between the present and times of sapropel formation. Thus, I obtained a rough estimate indicating that this rate should have been nearly 40 times lower at times of sapropel formation than it is today. This suggests that the flushing-time of the deep eastern Mediterranean had increased by a similar factor, to a value in the order of magnitude of a (few) thousand years.

Summarizing, lowering of the freshwater budget - consisting in part of an increase in runoff - resulted in: 1) shoaling of the pycnocline to a depth within the euphotic layer, ensuring increased nutrient availability for production; 2) enhanced input of nutrients via the Nile and Eurasian rivers; 3) a decrease in the MIW to surface water salinity gradient, which hampered the formation of EMDW. The former two effects would induce an increased transfer of organic matter from the euphotic layer to the deeper parts of the basin, and the latter effect would result in a decreased oxygen advection to deep (and bottom) waters. The combination of these effects would have been conducive to the formation of sapropels at depths below the "base" of the MIW, which probably coincided with the depth of the Sicilian sill.

SAMENVATTING

De Middellandse Zee is een marginaal bekken dat van de Noord Atlantische Oceaan gescheiden wordt door een ondiepe drempel in de Straat van Gibraltar. Een meer complexe, maar eveneens ondiepe drempel-structuur in de Straat van Sicilië scheidt de westelijke en oostelijke sub-bekkens. De uitwisseling van watermassa's door beide passages vindt plaats in twee lagen, met een oostwaarts transport in de oppervlakte-laag en een westwaarts transport in de diepere laag. Oppervlakte-water dat via de Straat van Gibraltar de Middellandse Zee binnenstroomt kan vervolgd worden via de Straat van Sicilië tot in het oostelijke bekken, hoewel de saliniteit geleidelijk toeneemt in oostelijke richting.

Nabij Cyprus zinkt oppervlakte-water, om zo het intermediaire water van de Middellandse Zee (MIW) te vormen. Dit MIW spreidt zich uit door de gehele Middellandse Zee en het vormt een hoofdbestanddeel van de diepere, westwaartse stroming door de Straten van Sicilië en Gibraltar. Er is geen vergelijkbare vorming van intermediair water in de westelijke Middellandse Zee. De oostelijke en westelijke Middellandse Zee bekkens kennen ieder hun eigen vorming van diep-water. Dit diep-water vult de bekkens op grote diepte, beneden het MIW. Diep-water van de oostelijke Middellandse Zee (EMDW) wordt met name gevormd in de Adriatische Zee. Diep-water van de westelijke Middellandse Zee (WMDW) ontstaat in de noordelijke sector van de de westelijke Middellandse Zee, nl. in de Golf van Lyon en de Ligurische Zee. EMDW en WMDW worden effectief van elkaar gescheiden door de Siciliaanse drempel. EMDW draagt bij aan de diepe uitstroming over de Siciliaanse drempel, vanuit het oostelijke naar het westelijke bekken, via Bernoulli-stroming - aanzuiging van water van diepten beneden de drempel-diepte tot over de drempel - en via opwaartse mixing, in het gehele oostelijke bekken, met de diepere delen van het MIW dat vervolgens uitstroomt over de drempel. Vergelijkbare processen bepalen de contributie van WMDW aan de diepe uitstroming over de drempel bij Gibraltar, van de westelijke Middellandse Zee naar de Atlantische Oceaan. De verversings-perioden van water in de oostelijke en westelijke Middellandse Zee werden recentelijk geschat op respectievelijk 50 en 20 jaar.

Er bestaat een opvallende saliniteits-gradiënt (halocline) tussen het oppervlakte-water en het MIW, terwijl de thermische gradiënt tussen deze lagen zwak is. Daardoor komt de dichtheids-gradiënt (pycnocline) in de oostelijke Middellandse Zee in essentie overeen met de halocline. Tegenwoordig ligt de pycnocline in de oostelijke Middellandse Zee ruim beneden de basis van de fotische zone en, dientengevolge, is de fotische zone bijzonder voedsel-arm (oligotroof). In dit proefschrift beredeneer ik dat de pycnocline zich binnen de fotische zone heeft bevonden ten tijde van sapropel[*] vorming en gedurende glacialen. Een dergelijke configuratie leidde tot hoge nutriënten-beschikbaarheid in het basale deel van de fotische zone en, daardoor, tot de ontwikkeling van een Diep Chlorophyll Maximum (DCM) en toename van de export produktie. Een simpel twee-lagen model is ontwikkeld voor de oostelijke Middellandse Zee, om te bestuderen welke processen verantwoordelijk waren voor dit verondiepen van de pycnocline.

---

[*]   In dit proefschrift wordt de term sapropel gebruikt voor sedimenten afgezet in zuurstof-arm (-loos) bodem-water. Over het algemeen zijn sapropelen bruin to zwart van kleur en bevatten ze meer dan gemiddelde hoeveelheden pyriet en benthische foraminiferen die aangeven dat het bodem-water zuurstof-arm was. Benthisch foraminiferen kunnen ook geheel ontbreken ("benthic desert"). Soms zijn sapropelen gelamineerd. Ik volg niet de strikte definities voor sapropel, proto-sapropel, sapropelic, of non-sapropelic, die gebaseerd zijn op subjectieve onderverdeling van organisch koolstof gehaltes.

Tijdens glacialen was het verondiepen van de pycnocline voornamelijk het gevolg van de verlaging van het zee-niveau, hetgeen een afname veroorzaakte van de instroming van oppervlakte-water over de drempels. Het model geeft aan dat een verlaging van het zee-niveau van 43 m, ten opzicht van het huidige niveau, een verondieping van de pycnocline tot aan de basis van de fotische zone zou veroorzaken, in de oostelijke Middellandse Zee. Ten tijde van sapropel vorming was het verondiepen van de pycnocline voornamelijk een reaktie op reduktie van het zoetwater budget in de oostelijke Middellandse Zee (zoetwater budget = verdamping - totale zoetwater toevoer). Het model geeft aan dat een reduktie van het zoetwater budget tot 0,53 maal de huidige waarde zou resulteren in een verondieping van de pycnocline tot aan de basis van de fotische zone, indien het zee-niveau gelijk bleef aan het huidige. Ten tijde van sapropel vorming was het zoetwater budget ten dele gereduceerd door een toename van het debiet van de Nijl, ten gevolge van astronomisch bepaalde piek intensiteiten van de zomer (ZW) moesson van de Indische Oceaan, en ten dele door toegenomen aktiviteit van het westelijke systeem van Mediterrane depressies. Dit laatste veroorzaakte een combinatie van afgenomen verdamping en toegenomen zoetwater toevoer (neerslag en rivier-water).

De glaciale hydrografische configuratie, met een ondiepe pycnocline aan of boven de basis van de fotische zone, vertoonde sterke overeeenkomst met de configuratie ten tijde van de vorming van sapropelen. Een belangrijk verschil bestond echter in de diepere delen van het bekken, aangezien glaciale sedimentatie over het algemeen plaats vond in goed belucht bodem-water, terwijl sapropelen gevormd werden in zeer slecht tot niet belucht bodem-water. Dit verschil wordt toegeschreven aan verschillen in de efficiëntie van diep-water (EMDW) vorming en, daardoor, het zuurstof transport naar de diepzee. Gedurende glacialen was het saliniteits-contrast tussen MIW en oppervlakte-water belangrijk toegenomen, hetgeen de vorming van EMDW zou vergemakkelijken. Ten tijde van sapropel vorming was dit saliniteits-contrast verzwakt, hetgeen de vorming van EMDW negatief zou beïnvloeden. Met een dergelijke benadering is het echter niet mogelijk een kwantitatieve schatting te maken van de hoeveelheid EMDW vorming ten tijde van sapropel vorming, ten opzichte van recent.

De hoeveelheid EMDW vorming kon echter wel worden geschat middels een beschouwing van verschillen in het fosfaat budget van de oostelijke Middellandse Zee tussen de recente situatie en die tijdens sapropel vorming. Op die manier bereikte ik een ruwe schatting die aangeeft dat de hoeveelheid EMDW vorming ten tijde van sapropel vorming ongeveer 40 maal lager was dan tegenwoordig. Dit suggereert dat de verversings-periode van de diepe oostelijke Middellandse Zee toegenomen was volgens eenzelfde factor, tot in de orde van grootte van een (paar) duizend jaar.

Samenvattend, reduktie van het zoetwater budget - ten dele veroorzaakt door toegenomen rivier-uitstroming - leidde tot: 1) verondieping van de pycnocline tot een diepte binnen de fotische zone, resulterend in een toename van de beschikbaarheid van nutriënten voor produktie; 2) verhoogde toevoeging van nutriënten via de Nijl en Eurasiatische rivieren; 3) een afname van de saliniteits-gradiënt tussen MIW en oppervlakte-water, hetgeen de vorming van EMDW negatief beïnvloedde. De eerste twee effecten leidden tot een verhoogde transfer van organisch materiaal vanuit de fotische laag naar de diepere delen van het bekken, en het laatstgenoemde effect leidde tot reduktie van het zuurstof transport naar diep- en bodem-water. De combinatie van deze effecten zou de ontwikkeling van sapropelen mogelijk hebben gemaakt op diepten beneden de "basis" van het MIW, welke waarschijnlijk ongeveer samenviel met de diepte van de Siciliaanse sill.

GENERAL INTRODUCTION

Some 40 years have elapsed since the discovery of sapropels in the eastern Mediterranean sediment cores collected during the 1947-1948 Swedish Deep Sea Expedition. During this time, much research has focused on the chronology and genesis of these late Quaternary sapropels. Sapropels were found to have developed during warm (interglacial) and - less frequently - during cool (glacial, interstadial) stages. Sapropel formation could, therefore, not be explained with mechanisms related to deglaciation. On the contrary, it has become well-established that sapropel formation coincided in time with minima in the cycle of precession, which occur every 21 000 years. A minimum in the cycle of precession implies that, in its ellipsoidal orbit, the earth is closest to the sun in Northern Hemisphere summer, which causes higher insolation during summer and lower insolation during winter, relative to the present (at present, the earth is closest to the sun in Northern Hemisphere winter). As a result, periods of minima in the cycle of precession are characterized by intensified (summer) monsoonal circulation, which invoked increased freshwater discharge into the eastern Mediterranean via the river Nile. This relation between the sapropel formation and minima in the cycle of precession seems to have existed already in the Pliocene. Evidence of increased humidity at times of sapropel formation has been found also in the northern borderlands of the eastern Mediterranean.

Generally, the work that has been devoted to the mechanism(s) of sapropel formation resulted in qualitative descriptions of the climatic and hydrograpic variations at times of sapropel formation. The small number of published quantitative modeling studies focused on the sensitivity of deep water ventilation to increased freshwater discharge, and on nutrient-budget calculations employed to determine the hydrographic configuration at times of sapropel formation.

In this thesis, I present interrelated estimates of the climatic and hydrographic variations which induced the formation of late Quaternary sapropels. The chapters 1 and 2 include qualitative descriptions of the climatic and hydrographic conditions during glacial periods and during sapropel formation, in comparison with the present-day conditions. The chapters 3 to 6 include quantitative elaborations of these descriptions, in which the results of previous quantitative modeling efforts, presented in the literature, have been incorporated.

Chapter 7, the synthesis, discusses the contribution of the results presented in the chapters 1 to 6 to previous research on the problem of sapropel formation. Also, some crucial parameters are mentioned, which need to be constrained in the future to enable a more accurate estimation of the magnitude of climatic and hydrographic variations inducing sapropel formation. Finally, I discuss the applicability of the presented results to the study of eastern Mediterranean faunal changes and sapropel formation during the Pliocene.

Three papers providing valuable background information, used in constructing and testing the presented hydrographic and climatic reconstructions and regularly referred to in the text, are added to the thesis in the form of appendices.

chapter 1

LATE QUATERNARY CHANGES IN MEDITERRANEAN INTERMEDIATE WATER DENSITY AND FORMATION RATE

LATE QUATERNARY CHANGES IN MEDITERRANEAN INTERMEDIATE WATER DENSITY AND FORMATION RATE

Eelco J. Rohling

Institute of Earth Sciences,
University of Utrecht,
The Netherlands

Winfried W. C. Gieskes

Department of Marine Biology
University of Groningen
The Netherlands

Abstract. Three recently acquired eastern Mediterranean cores containing Late Quaternary sediments display a marked faunal contrast between the Holocene and older sapropels. It is suggested that the absence of neogloboquadrinids in the Holocene sapropel and their abundance in older sapropels reflect differences in food availability related to the extent of development of a deep chlorophyll maximum layer (DCM) and the intensity of "new" primary production associated with this layer. The depth of such a layer, which consists of phytoplankton with a characteristic taxonomic composition, is determined by the vertical hydrodynamical structure. During deposition of the older sapropels, the pycnocline was apparently positioned well above the base of the euphotic layer, a situation that favors a pronounced DCM and an associated relatively high rate of new production. Shallowing of the pycnocline implies a relatively low density of the Mediterranean Intermediate Water (MIW). On the other hand, during deposition of the Holocene sapropel the pycnocline had apparently vanished due to termination of MIW formation.

1. INTRODUCTION

In the eastern Mediterranean, sapropels were first found in cores collected during the 1947-1948 Swedish Deep Sea Expedition [Kullenberg, 1952].

Their chronostratigraphic position was established with the aid of oxygen isotope stratigraphy. In spite of the fact that Mediterranean sediments display a larger variability in oxygen isotopic values than open ocean sediments, it appeared possible to correlate Quaternary oxygen isotopic records of the Mediterranean with those of the open ocean [amongst others Emiliani, 1955; Thunell and Williams, 1983; Vergnaud-Grazzini et al., 1977]. In general, sapropels were found to have developed during Quaternary warming phases, but also (less frequently) during cool isotopic stages [e.g., Cita et al., 1977; Muerdter and Kennett, 1984; Thunell et al., 1983a; Thunell et al., 1984; Vergnaud-Grazzini, 1985].

Olausson [1961] was the first to link sapropel formation to episodes of lowered surface water salinities and subsequent stagnation of the deeper waters. This hypothesis is supported by the excess lowering of the oxygen isotopic signal at times of sapropel development [Cita et al., 1977; Cita and Grignani, 1982; Calvert, 1983; Mangini and Schlosser, 1986; Thunell et al., 1984; Vergnaud-Grazzini et al., 1977; Williams et al., 1978].

Major potential source areas for a low-salinity surface layer are the Black Sea [amongst others Buckley et al., 1982; Cita et al., 1977; Ryan, 1972; Stanley and Blanpied, 1980; Williams et al., 1978] and the Nile river [amongst others Adamson et al., 1980; Rossignol-Strick, 1985; Rossignol-Strick et al., 1982; Street and Grove, 1979]. However, the Holocene sapropel appears to be younger than the main phase of postglacial melting [Rossignol-Strick et al., 1982; Rossignol-Strick, 1985; Shaw and Evans, 1984; Williams et al., 1978] but coincides with extensive flooding of the Nile [Adamson et al., 1980; Rossignol-Strick et al., 1982; Rossignol-

Strick, 1985] and a warm humid "pluvial" in tropical Africa [Street and Grove, 1979; Rognon, 1987].

A low-salinity surface layer in the eastern Mediterranean may have caused a reversal of the vertical circulation pattern from antiestuarine to estuarine [Buckley and Johnson, 1988; Calvert, 1983; Muerdter and Kennett, 1984; Stanley et al., 1975; Ten Haven, 1986; Thunell and Williams, 1989; Thunell et al., 1983a, 1984]. An estuarine circulation acts as a nutrienttrap, ensuring high nutrient levels that may be conducive to increased organic production. Enhanced organic production subsequently increases oxygen consumption in deeper waters.

This model of circulation reversal implies that stagnation is not a prerequisite for the formation of anoxic sediments [cf. Thunell and Williams, 1989]. In fact, De Lange and Ten Haven [1983] suggested that enhanced productivity exerted a major influence on the formation of eastern Mediterranean sapropels. They based their conclusions on variations of the organic carbon content in anoxic sediments underlying the brine-filled "Tyro Basin" south of Crete. Higher carbon concentrations, indicating an increased flux of organic matter, appeared to coincide with periods of sapropel formation in other parts of the eastern Mediterranean.

According to Ross and Kennett [1984], a circulation reversal cannot explain the changes in benthic foraminiferal associations in cores from the Strait of Sicily. They concluded that the present antiestuarine regime was not reversed, but merely weakened. Vergnaud-Grazzini et al. [1988] suggested that major influxes of low-salinity Atlantic water into the eastern Mediterranean surface layer occurred during both terminations Ia and Ib, causing a decrease in the aeration of the water column. They stated that this aeration further deteriorated during termination Ib, due to an additional amount of low-salinity riverine or Black Sea overflow waters that invaded the eastern Mediterranean, leading to stagnation of the deep eastern Mediterranean waters.

Furthermore, the circulation reversal hypothesis is not in accordance with the conclusions of Zahn and Sarnthein [1987]. These authors stated that, at Gibraltar, deep Mediterranean outflow occurred continuously during the last 140,000 years, although it was severely reduced at times of sapropel formation in the eastern basin. Zahn and Sarnthein's [1987] conclusions agree with the findings of Abrantes [1988], who recorded a decreasing upwelling intensity in the Alboran Sea between 14,000 and 10,000 years B.P., which she explained by the decrease in outflow of deeper Mediterranean waters over the Gibraltar sill at that time.

The circulation reversal hypothesis would imply increasing nutrient concentrations and primary production. An alternative mechanism is proposed by enhanced runoff which, itself, may provide sufficiently large nutrient influxes [Calvert, 1983; De Lange and Ten Haven, 1983; Rossignol-Strick et al., 1982; Ten Haven, 1986]. At the same time, increased runoff would dilute surface waters, leading to a more sluggish (but not necessarily ceased) circulation of the intermediate (Mediterranean Intermediate Water (MIW); see the next sections) and deeper waters. In this scenario, enhanced productivity, in combination with lowered oxygen supply to the deeper parts of the basin, enables the formation of sapropels. It is this combination that we regard as most likely to have caused the shifts in productivity and in oxygenation of deeper waters as discussed in this paper.

In this paper, a new contribution to the discussion on the causes of sapropel formation is presented. We introduce an aspect that has not been investigated before: fluctuations of the rate of "new" primary production in a deep chlorophyll maximum (DCM) as related to variations in the depth of the boundary between surface water and Mediterranean Intermediate Water (MIW). These fluctuations are inferred from striking and consistent frequency variations in the planktonic foraminiferal group of neogloboquadrinids found in the sediment.

2. MATERIALS AND METHODS

Three gravity cores were taken south of Crete in May 1987 with the Dutch research vessel *Tyro*. These cores (T87/2/13G, 306 m water depth; T87/2/20G, 707 m; and T87/2/27G, 607 m) were sampled at close intervals (Figure 2). The geographic positions of the cores are shown in Figure 1, and the lithology and sample positions are shown in Figure 2. The samples have been investigated for their planktonic foraminiferal contents, which resulted in respectively 71, 71, and 59 elaborated samples per core, respectively.

The samples were sieved with mesh widths of 595, 150, and 63 microns. The fractions between 150 and 595 microns were split into aliquots containing about 200 planktonic foraminifera. These foraminifera have been sorted and quantified as a percentage of the total in the aliquot.

3. TIME-STRATIGRAPHIC FRAMEWORK

The rough time-stratigraphic framework is provided by plotting cumulative frequencies of the species *Globigerinoides ruber, Globigerinella siphonifera, Globigerinoides tenellus, Globoturborotalita rubescens, Orbulina universa, Globigerina digitata, Globigerinoides trilobus* and *Hastigerina pelagica* (Figure 3.). This plot is considered to approximate the surface water temperature pattern
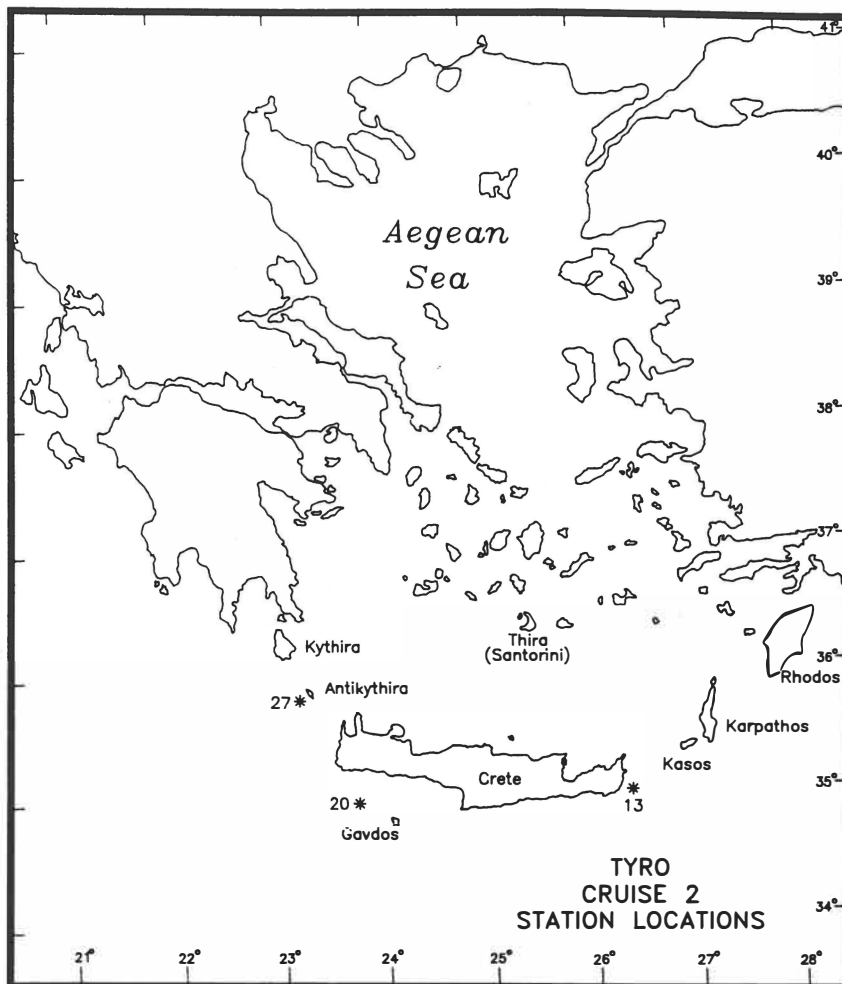
Fig. 1. Location map of cores T87/2/13G, T87/2/20G, and T87/2/27G.

through time. It has been correlated to a Mediterranean oxygen isotopic profile [Vergnaud-Grazzini et al., 1977; Vergnaud-Grazzini, 1985] for assessing the chronology of the sapropel sequence (Figure 3.).

The non-Holocene sapropels from the three cores presented in this study are correlated with the S_3, S_4, and S_5 succession (Figure 3), which is generally accepted to have developed in the interglacial oxygen isotopic stage 5 [Cita et al., 1977; Muerdter and Kennett, 1984; Rossignol-Strick, 1985; Thunell et al., 1984; Vergnaud-Grazzini et al., 1977; Vergnaud-Grazzini, 1985]. Therefore, these sapropels will in the following discussion be referred to as the isotope-5 (I-5) sapropels. The cold interval between the Holocene (I-1) and I-5 parts of the cores will be referred to as I-2, I-3, and I-4 glacial. The cold interval below the I-5 parts is called the I-6 glacial (Figure 3).

4. RESULTS AND DISCUSSION

4.1. *Downcore Distribution of Neogloboquadrinids*

Neogloboquadrinids have been counted as one category including two morphotypes: *Neogloboquadrina dutertrei* and dextrally coiled *Neogloboquadrina pachyderma*. Both types are considered to represent ecophenotypes within a cline, with *N. dutertrei* being the warm-water end-member and sinistrally coiled *N. pachyderma* the cold-water end-member [amongst others Srinivasan and Kennett, 1976; Van Leeuwen, 1989]. Dextrally coiled *N. pachyderma* (cf. P-D-intergrade morphotypes) [Kipp, 1976] is considered to occupy an intermediate position. Although *N. dutertrei* and *N. pachyderma* are not considered different species, we refrain from a strict approach and label them in italics as if they were.
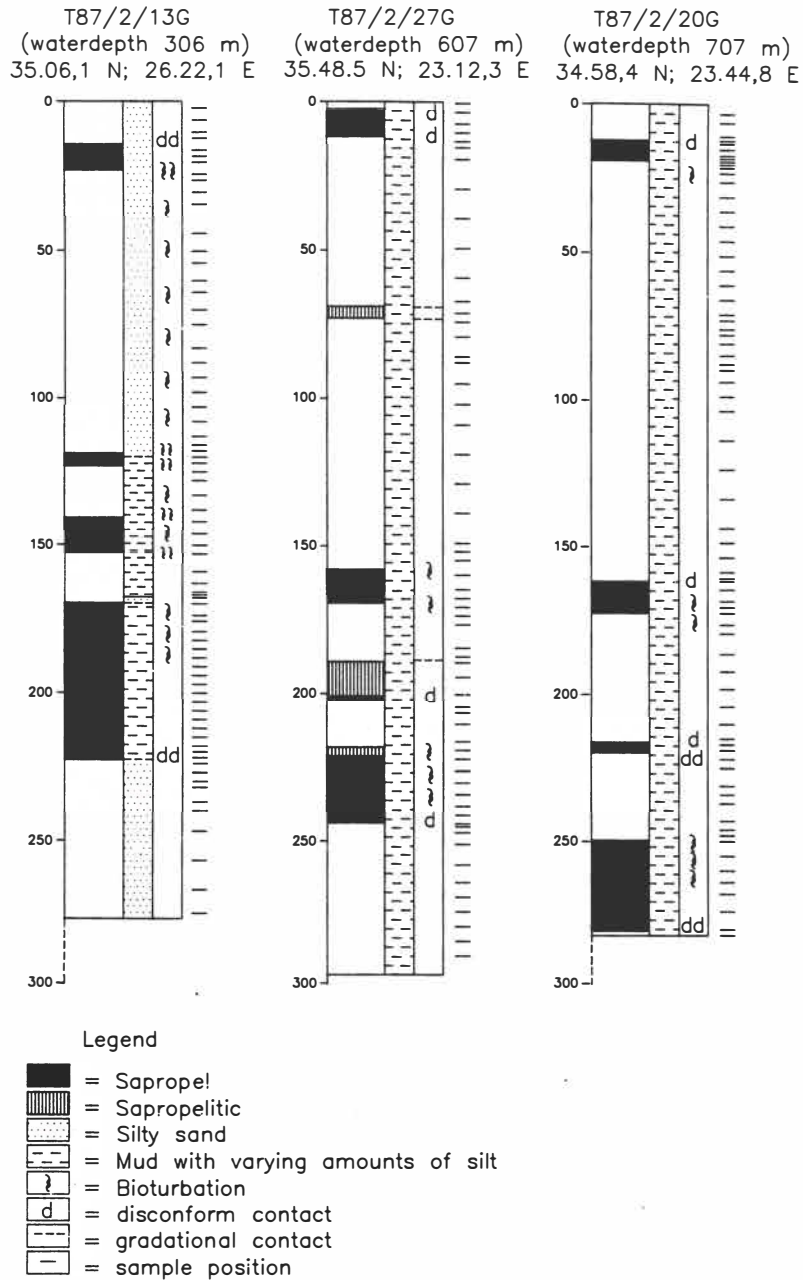
10

Fig. 2. Lithology and sample positions of cores T87/2/13G, T87/2/27G, and T87/2/20G.
The distinction between sapropel and sapropelitic is made purely visually.

The frequency distributions of neogloboquadrinids show a marked difference between the S_1 and the other sapropels in the three investigated cores. The S_1 is nearly devoid of neogloboquadrinids, whereas the other sapropels contain peak abundances of this group (Figure 4). A similar difference has been reported by Thunell et al. [1977].

Sinistrally coiled *N. pachyderma* appeared to be nearly absent in all three cores. The neogloboquadrinids in the I-5 parts of the cores were predominantly *N. dutertrei* types (especially in S_5), whereas dextrally coiled *N. pachyderma*-types dominate the glacial associations.

The abundance of *N. dutertrei* types in most

11
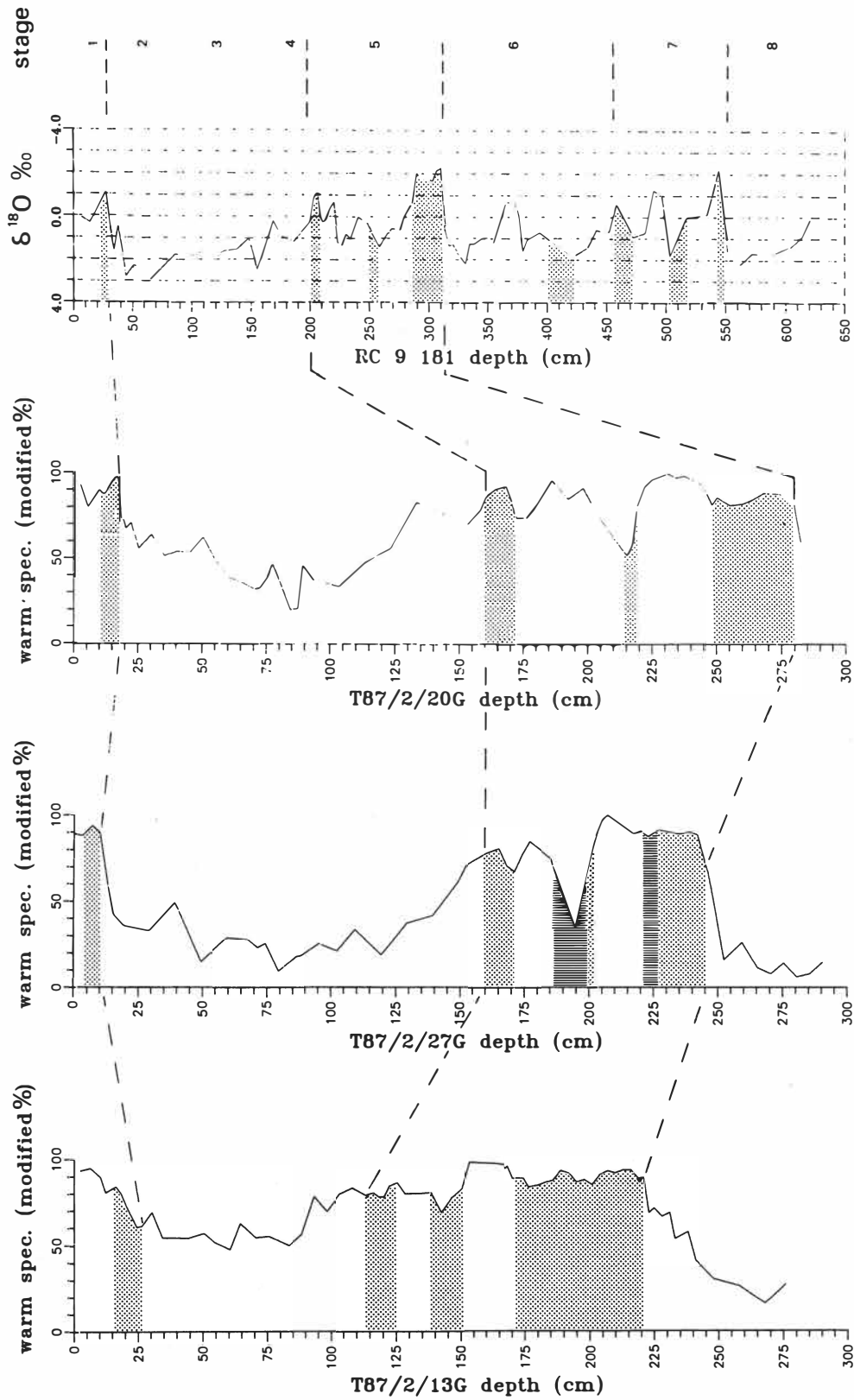
Fig. 3. (Opposite) Plots of the cumulative frequencies of *G. ruber*, *G. siphonifera*, *G. tenellus*, *G. rubescens*, *O. universa*, *G. digitata*, *G. trilobus*, and *H. pelagica* versus *G. quinqueloba*, *G. scitula*, *G. inflata*, *G. truncatulinoides*, *G. glutinata*, and *G. anfracta* for cores T87/2/13G, T87/2/27G, and T87/2/20G. These plots are considered to approximate the surface water temperature through time. They are compared with the oxygen isotope profile of *G. ruber* in core RC 9-181 (modified after Vergnaud-Grazzini [1985]) for assessing the chronology of the sapropel sequence. Sapropel (stippled) and sapropelitic (hatched) results are shown.

12

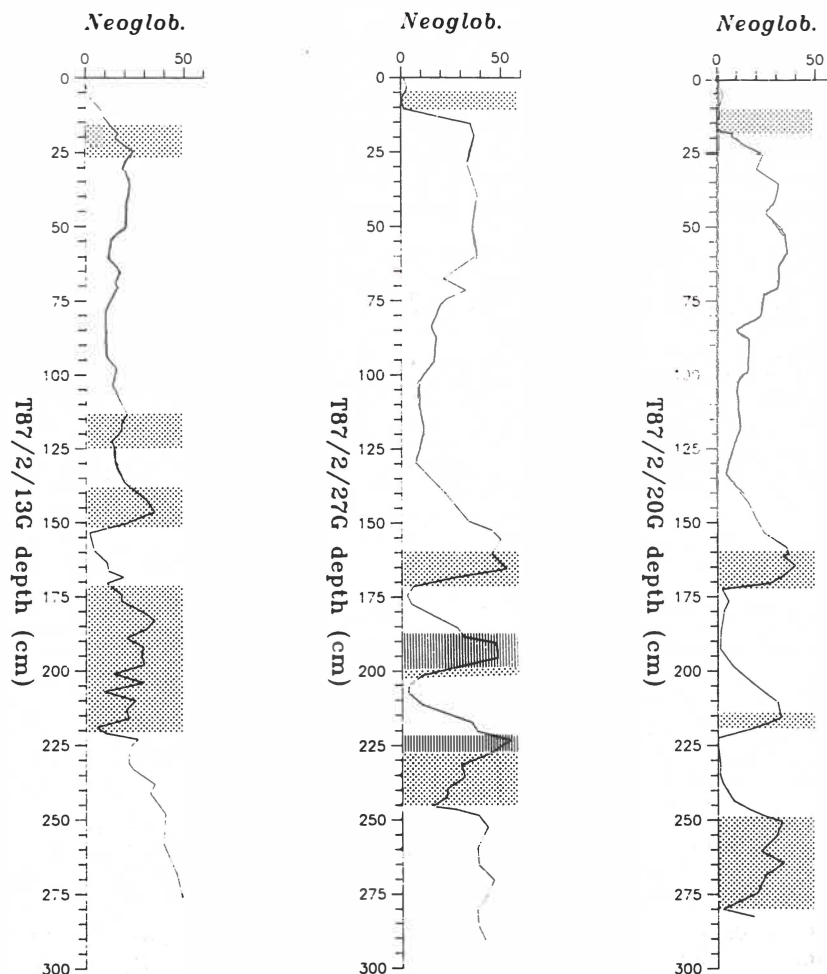Fig. 4. Downcore frequency distribution of neogloboquadrinids in cores T87/2/13G, T87/2/27G and T87/2/20G. Sapropel (stippled) and sapropelitic (hatched) distributions are shown.

late Quaternary sapropels was first noted by Kullenberg [1952] and later confirmed by others (Figure 5).

4.2. Recent Distribution of Neogloboquadrinids and Possible Relation to the Deep Chlorophyll Maximum

Neogloboquadrinids are rare to absent in oligotrophic waters such as the open ocean's central water masses [amongst others Bé and Hamlin, 1967; Kipp, 1976; Tolderlund and Bé, 1971; Schott, 1966], the eastern Mediterranean [Cifelli, 1974; Thunell, 1978], and the Gulf of Aqaba [Almogi-Labin, 1984]. On the other hand, they are well represented in eutrophic waters [amongst others Bé et al., 1985; Kipp, 1976; Tolderlund and Bé, 1971; Schott, 1966].

N. dutertrei appears most prolific in low-latitudinal oceanic divergences, particularly in the equatorial divergence [Cullen and Prell, 1984; Jones, 1967; Kipp, 1976; Parker and Berger, 1971]. Therefore, a high abundance of *N. dutertrei* has often been attributed to upwelling [Coulbourn et al., 1980; Duplessy et al., 1981; Kipp, 1976; Thunell et al., 1983b; Thunell and Reynolds, 1984; Thiede, 1975; Zhang, 1985]. Coastal upwelling zones, however, are usually dominated by *G. bulloides* rather than by neogloboquadrinids [cf. Coulbourn et al., 1980; Cullen and Prell, 1984; Duplessy et al., 1981; Schott 1966; Van Leeuwen, 1989; Zhang, 1985].

This faunal contrast between oceanic divergences and coastal upwelling zones is thought to be caused by differences in hydrodynamical conditions. In zones of large-scale divergence, the pycnocline (usually the thermocline) lies shallower than in nondivergent and convergent regions due to Ekman pumping [Bryan and Sarmiento, 1985; Pond and Pickard, 1983; Tolmazin, 1985; Wells,

Core	KS 09	Alb 189	Cobblestone 45	Cobblestone 6	Cobblestone 29	TR 171-24	TR 171-27	TR 172-22	Bannock 16-GC	CHN 61-25	LY II-3	BM 1966.0.435	BM 1960.199	BM 1960.203
Latitude (N)	35°09'	33°54'	36°16'	36°15'	35°50'	34°03'	33°50'	35°19'	35°52'	35°12.3'	35°02'	34°25'	35°18.5'	33°23'
Longitude (E)	20°09'	28°29'	17°43'	17°42'	20°50'	22°43'	25°59'	29°01'	20°46'	16°31.1'	16°42'	24°07'	20°08'	24°54'
Waterdepth (m)	2800	2664	3466	3466	2866	2380	2680	3150	2834	1460	2400	2044	2988	2341
S1			−	−		−	−	−			−		−	−
S2		−									+	+		
S3	+	+ +	+	+		+	+ +	+ +			+ +			
S4	+	+ +	+	+	●		+	+ +			+ +			
S5	+	+	●	●	+	+ +	+ +				+ +			
S6	+ +	+ +	+ +	+ +	+ +	+ +	+ +	+ +	+ +	+ +	+ +			
S7	−	−			+		+	+						
S8	+ +	+ +			+		+	+ +						
S9		−						+						
Authors	Vergnaud-Grazzini et al., 1977; Cita et al., 1977; Cita & Grignani, 1982	Vergnaud-Grazzini et al., 1977	Cita & Grignani, 1982	Cita & Grignani, 1982	Cita & Grignani, 1982	Thunell et al., 1977; Thunell & Williams, 1983	Thunell et al., 1977; Thunell & Williams, 1983	Thunell et al., 1977; Thunell & Williams, 1983	Thunell et al., 1983a	Muerdter, 1984; Muerdter & Kennett, 1984	Muerdter, 1984; Muerdter & Kennett, 1984	Buckley & Johnson, 1988	Buckley & Johnson, 1988	Buckley & Johnson, 1988

Legend

− = low frequencies or absence of neogloboquadrinids
● = intermediate frequencies of neogloboquadrinids
+ = high frequencies of neogloboquadrinids
+ + = very high frequencies of neogloboquadrinids

Fig. 5. Semiquantitative representation of neogloboquadrinid abundances for nine different sapropels in 14 cores (based on literature data).

1986]. Coastal upwelling tends to create a water mass that has rather uniform conditions which may extend throughout the upper 200 m [amongst others Dietrich et al., 1980; King, 1975; Tchernia, 1980].

In stratified regions a deep chlorophyll maximum (DCM) develops when the pycnocline lies close to the base of the euphotic zone (the layer where enough light for primary production penetrates). The maximum depth to which the DCM follows the pycnocline is regulated by the minimum light intensity necessary for the growth of phytoplankton at depth [Fairbanks and Wiebe, 1980]. Therefore, a distinct DCM is found only in areas where the pycnocline is situated at depths above or near the light compensation depth.

In areas where the pycnocline lies deeper than the euphotic zone, the nutricline is usually positioned in close vicinity to the pycnocline [Dortch et al., 1985; Goering et al., 1970; Hayward, 1987; Herbland et al., 1985; Hobson and Lorenzen, 1972; Spencer, 1975; M. Gilmartin, personal communication, 1988]. In areas where the pycnocline lies well within the euphotic zone, DCM development occurs at pycnocline depth and down to the base of the euphotic zone. Due to consumption of nutrients by autotrophs, the nutricline is

found to lie directly below the DCM in such a setting [Hayward, 1987; Herbland et al., 1985; Kiefer et al., 1976; Lohrenz et al., 1988]. In this case, the nutricline is no longer closely associated with the pycnocline. Where the pycnocline is shallow with respect to light and phytoplankton biomass, "eutrophication" by upward mixing of new nutrients into the euphotic zone fuels the development and maintenance of a DCM layer [Hayward, 1987; Klein and Steele, 1985], in which new production may equal total primary production [Gieskes and Kraay, 1986; Jenkins and Goldman, 1985].

Upward mixing of nutrients into the euphotic zone can be established by cross-isopycnal and along-isopycnal mixing. Along-isopycnal mixing is of a larger scale than that across isopycnals [Hayward, 1987; Pond and Pickard, 1983]. Therefore, it has to be considered as a major contributor to the supply of nutrients into waters above the nutricline if there are lateral nutrient gradients along isopycnals [Hayward, 1987; Lohrenz et al., 1988].

Gieskes and Kraay [1986] described the steep transition in the euphotic zone of the tropical Atlantic Ocean from a shallow (mixed-layer) phytoplankton assemblage to a deep assemblage

characteristic of the DCM layer. The mixed-layer phytoplankton assemblage of the open Atlantic is dominated by prokaryota (mainly cyanobacteria) and coccolithophorids. Primary production is coupled to rapid nutrient recycling within this layer [Gieskes and Kraay, 1986; Goering et al., 1970; Jenkins and Goldman, 1985]. On the other hand, the deep assemblage, near the base of the euphotic zone, consists mainly of eukaryota (green algae, coccolithophorids and chrysophyceae); it thrives at depth due to the influx of new nutrients into the lower euphotic zone (decribed above). Entrapment of new nutrients by the cells in the DCM was suggested by Anderson [1969] and Goering et al. [1970]. New (or net) primary production, derived from pulses of new nutrients from deeper water, is mainly restricted to the lower part of the euphotic zone [Jenkins and Goldman, 1985]. Up to 20% of the total primary production in the open tropical Atlantic was found to be new production [Gieskes and Kraay, 1986].

Such a vertical structure of two distinct phytoplankton assemblages in the euphotic layer does not only occur in the Atlantic Ocean but has also been reported from eastern Indonesian waters [Gieskes et al., 1988] and other parts of both the open Pacific and Atlantic oceans [Furuya and Marumo, 1983; Glover et al., 1985; Murphy and Haugen, 1985; Venrick, 1982]. In addition, differences in size class structure between the deep (mainly nannoplankton and picoplankton) and the shallow (mainly picoplankton) assemblages have been noted [Gieskes and Kraay, 1986; Herbland et al., 1985]. Similar differences have been found in the Adriatic Sea (M. Gilmartin, personal communication, 1988).

Shoaling of the pycnocline within the euphotic zone enables extension of the DCM into shallower waters with higher light intensities. This should enhance primary production in the DCM, and thus the chlorophyll concentrations, since most production at depth is new production (see the previous section). This relation between shoaling of the pycnocline and increasing chlorophyll concentrations in the DCM is illustrated by Gieskes and Kraay [1986, Figure 1]: a shallower DCM contains higher chlorophyll concentrations. In the "typical tropical system" [Herbland et al., 1983; Herbland and Voituriez, 1979], the subsurface primary production and chlorophyll maxima coincide in depth with the top of the nutricline, and integrated primary production correlates with nutricline depth [Hayward, 1987]. The DCM in the Gulf of Mexico varies significantly with changes in pycnocline depth [Hobson and Lorenzen, 1972]. Herbland et al. [1985] stated that the chlorophyll a maximum followed doming of the nutriclines in the Guinea Dome with higher values.

In the Panama Basin, Fairbanks and Wiebe [1980] and Fairbanks et al. [1982] demonstrated that

peak abundances of several nonspinose planktonic foraminiferal species, especially N. dutertrei, are associated with the DCM. A similar relationship between peak abundances of dextrally coiled N. pachyderma and the DCM has been observed in the Gulf of Alaska, where cyclonal circulation induces a shallow pycnocline position in winter [Reynolds and Thunell, 1986].

The occurrence of high abundances of N. dutertrei in areas with a distinct DCM supposedly is similar for the low-temperature variant N. pachyderma. This is actually confirmed by the fact that N. pachyderma blooms at North Atlantic high latitudes in summer [e.g. Tolderlund and Bé, 1971]. In summer only, a shallow pycnocline (within the euphotic layer) develops in these waters due to heating and decreased storm activity, and this creates favorable conditions for the development of a distinct DCM.

The relation between high abundances of neogloboquadrinids and a shallow pycnocline/nutricline (and therewith a high rate of new production in a DCM) may be indicative of their preferential grazing upon the deep phytoplankton assemblage, either because of a preference for the species typically found at depth, or due to a size preference (larger cells at depth; see above). Although their preferred food may also be present in the shallow phytoplankton assemblage, its higher density in the DCM will enable the existence of significant amounts of neogloboquadrinids. In fact, neogloboquadrinids are virtually absent in areas where the pycnocline/nutricline lies well below the euphotic zone. In such areas, for example the ocean's central water masses, there hardly is a distinct DCM; in other words there is no deep phytoplankton assemblage to support neogloboquadrinids.

Considering its present distribution pattern, we find no reasons to believe in any direct relation between a high abundance of N. dutertrei and lowered surface water salinities, as has been suggested by Ryan [1972], Thunell [1978], Thunell and Williams [1982, 1983], Vergnaud-Grazzini et al. [1977], and Williams et al. [1978].

4.3. The DCM in the Eastern Mediterranean

Since a DCM was also reported in the Levantine Basin of the eastern Mediterranean [Berman et al., 1984a, b], we assume that in that oligotrophic region, as well, two superimposed assemblages are present (conform section 4.2).

The pycnocline in the eastern Mediterranean is maintained by the salinity contrast between the nutrient-depleted surface waters and the somewhat more nutrient-rich Mediterranean Intermediate Water (MIW), as illustrated by property distribution profiles of McGill [1961] and Miller et al. [1970]. Therefore, the pycnocline and nutri-

cline depths are closely related and are affected in roughly the same way by changes in the MIW depth. The pycnocline lies at about 150 m depth in the area south of Crete and even deeper in non-divergent regions further west from the area where MIW formation takes place [Wüst, 1961; Miller et al., 1970]. Due to this deep pycnocline position, compared to the depth of the euphotic zone (about 120 m) in the eastern Mediterranean, there is no distinct DCM. This situation is similar to that in oceanic central gyres where the nutricline also lies deep with respect to light penetration.

The water below the pycnocline in the eastern Mediterranean Levantine Basin (the MIW) is much more depleted in nutrients than subpycnocline waters in the Atlantic Ocean. Although both regions do have a DCM, this nutrient limitation causes primary production in the DCM to be much lower in the Levantine Basin than in the Atlantic Ocean. Average chlorophyll concentrations in the Levantine Basin as reported by Berman et al. [1984b] are 1 order of magnitude lower than those in the tropical Atlantic [Gieskes and Kraay; 1986].

4.4. Interpretation of the Downcore Distribution of Neogloboquadrinids

A marked difference exists between the sapropel S_1, which is nearly devoid of neogloboquadrinids, and the older sapropels, which generally contain high abundances of this group (Figures 4 and 5). At times of deposition of the S_3, S_4, and S_5 sapropels, neogloboquadrinids were highly abundant, indicating favorable growth conditions, presumably (see section 4.2) due to high rates of primary production in a distinct DCM.

As we have argued above, enhanced production in a DCM can be realized by shallowing of the pycnocline to a depth that falls well within the euphotic layer. Therefore, the MIW to surface water density contrast should be decreased. This density contrast depends on climatic parameters such as evaporation rate and winter cooling. Since MIW spreads laterally from its source area, the MIW to surface water density contrast would decrease if prevailing dilution effects were relatively higher near the area of MIW formation than further away from it. Also, a relative decrease of surface temperature with increasing distance from the MIW source area (i.e., an increased east to west temperature gradient over the Mediterranean) would result in a decrease of the aforementioned density contrast. As argued in the introduction, we think that enhanced runoff triggered sapropel formation by both diluting surface waters and increasing nutrient concentrations. Since (1) the effects of dilution decrease with increasing distance from the diluting freshwater source(s) and

(2) modern MIW originates in the eastern Levantine Basin, one could reason that the major diluting source should have been the Nile river. It remains, however, to be proven that MIW always originated at its present location, since it may as well have been formed in other areas (e.g., parts of the Aegean). We will further restrict ourselves to interpreting the evolution of the vertical hydrodynamical structure through time, since the causative mechanisms still require much study.

A decreased MIW density would undoubtedly affect the rate of formation of eastern Mediterranean Deep Water (EMDW) [cf. Mangini and Schlosser, 1986]. EMDW is formed in the Adriatic Sea and possibly also in the Aegean Sea [Dietrich et al., 1980; King, 1975; Wüst, 1961]. Its formation occurs due to winter cooling and large-scale convection in areas where the MIW is brought close to the surface by persistent divergence in cyclonal circulations. High salinity (characteristic of the MIW), in combination with lowered surface water temperatures, generates water with densities higher than those of the MIW. This water then sinks to the deeper parts of the eastern Mediterranean Basin [Dietrich et al., 1980; King, 1975; Wüst, 1961].

We may therefore safely assume that a decrease in the MIW density caused a decline in the rate of EMDW production, thereby contributing to the preservation of organic material and thus to the formation of sapropels. Although Mangini and Schlosser [1986] showed that EMDW production in the Adriatic Sea would cease following even very small density decreases, we stress that even a diminution of EMDW production, combined with enhanced production during deposition of the 1-5 sapropels, could be conducive to the development of anoxic conditions (Figure 6).

The newly collected cores south of Crete indicate that the upper depth limit of S_3, S_4, and S_5 is at least as shallow as 300 m (core T87/2/13G). Even in this shallow core, the sapropelic sediments and near absence of benthic foraminifera (especially in S_5) seem to indicate that anoxic conditions prevailed at depths as shallow as 300 m and that the anoxic and dysoxic influence probably reached still shallower waters.

According to our reconstruction, the upper "limit" of the MIW was probably situated within the euphotic layer (<120 m) during the formation of S_3, S_4, and S_5. In that case, the upper limit of the anoxic conditions (<300 m) may have coincided with the top of the transitional water layer between EMDW and MIW (Figure 6), which at present lies at about 600 m depth (Figure 6) [King, 1975; Wüst, 1961]. If this is true, the MIW resided in a layer that was much thinner than at present; it probably was produced in smaller volumes, which may have caused reduction of the EMDW production as well as the lowered MIW densities did.
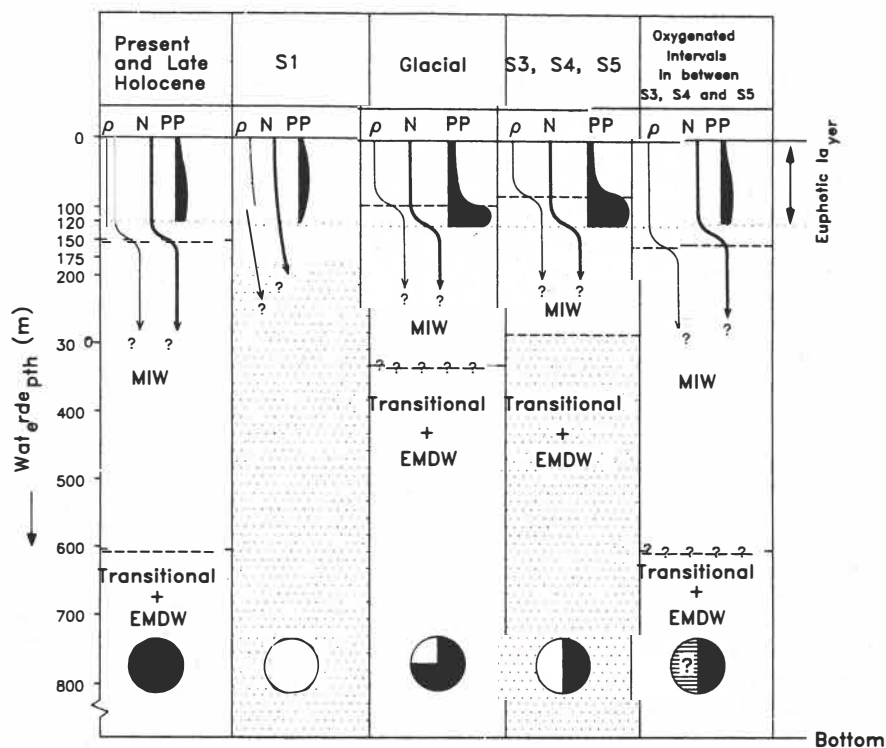
16

Fig. 6. Schematic presentation of depth changes of the pycnocline between MIW and surface waters and its influences on net primary production. Relative MIW densities and formation rates are reflected in the depth of the pycnocline and "thickness" of the MIW layer, which influence the EMDW formation rates.

During the deposition of S_1, conditions seem to have been very unfavorable for the neogloboquadrinids, indicating absence of a deep chlorophyll maximum layer. This may, as we explained above, have been caused by a deepening of the pycnocline far below the euphotic zone, or even by complete degradation of the pycnocline (Figure 6). The upper depth limit of S_1 lies at about 180 m, according to organic carbon measurements in several Aegean cores [Anastasakis, 1986]. Anoxic conditions thus prevailed below 180 m. This probably implies a (nearly) complete shutdown of MIW formation, causing a diminished oxygen supply at intermediate depths up to about 180 m, and at the same time a disintegration of the pycnocline

and associated DCM. The shutdown of the MIW production during deposition of S_1 curtailed EMDW production, thus allowing anoxic conditions to expand to even the deepest parts of the basin.

Recently, and in the late Holocene, neogloboquadrinids are rare in the region of the Cretan cores (Figure 4), as they generally are in the eastern Mediterranean [Cifelli, 1974; Thunell, 1978]. Since neogloboquadrinids are also rare in the I-5 non sapropelic intervals (Figure 4), we assume that the hydrodynamic structure during deposition of these intervals was much like that of the present day (Figure 6).

The glacial parts of the cores generally contain intermediate to very high frequencies of neoglobo-

quadrinids. Because of this abundance, glacial conditions can best be compared to conditions during formation of the I-5 sapropels. An important difference is the fact that glacial sedimentation appears to have occurred in oxygenated waters. The similarity between the glacial conditions and those during I-5 sapropel formation can be related to the fact that the MIW to surface water density contrast was of the same order of magnitude during these periods. The absolute densities may have differed considerably between the glacials and the I-5 sapropelic periods. According to Thunell et al. [1987], using a model developed by Bryden and Stommel [1984], salinities of glacial Mediterranean water masses far exceeded those in interglacials (see also Thunell and Williams [1989]).

Glacial primary production rates appear to have ranged from moderate to as high as during the I-5 sapropel formation. This, and the fact that anoxia did not develop during the entire glacial time span, leads to the hypothesis that EMDW production could take place more effectively during glacials than in I-5, causing a higher oxygen supply to deeper parts of the basin (Figure 6). Possibly, the lower glacial temperatures and higher salinity of the surface waters [Thunell et al., 1987] were the cause of this more effective glacial EMDW formation.

Sapropels have been found in some glacial intervals in the eastern Mediterranean (S_2, S_6, S_8; amongst others Cita et al. [1977], Muerdter and Kennett [1984], Thunell et al. [1983a, 1984] and Vergnaud-Grazzini et al. [1977]). According to our model, the occurrence of these sapropels can be attributed to (glacial) periods of less efficient EMDW production. The possibility of excess primary production, however, cannot be ruled out, especially for the S_6 sapropel which is known to contain excessive amounts of neogloboquadrinids (Figure 5).

5. CONCLUSIONS

A deep chlorophyll maximum layer is restricted to the base of the euphotic zone of oligotrophic water and develops when the vertical density structure is in support of the establishment of a deep phytoplankton population. We suggest that the faunal contrast between the S_1 and older sapropels reflects differences in primary production and food availability during their deposition. The new (i.e. net) primary production near the base of the euphotic zone in the deep chlorophyll maximum layer [Gieskes and Kraay, 1986; Jenkins and Goldman, 1985] supports neogloboquadrinids that feed on the DCM-related phytoplankton assemblage. Neogloboquadrinids should be (almost)

absent where a DCM is less pronounced or absent. Sapropel formation requires net production and, indeed, nearly all sapropels are associated with neogloboquadrinid blooms which are related to the high net primary production of the deep phytoplankton assemblage.

We have formulated the hypothesis that relates variations in the abundance of neogloboquadrinids to relative differences in the density and formation inten sity of the MIW. This mechanism has previously been mentioned as a possible nutrient regulator [Muerdter and Kennett, 1984]. The model we present accounts for the relative depth of the pycnocline between the MIW and the surface waters.

We propose that shoaling of the pycnocline is induced by relatively low surface water salinity in the MIW source area due to increased river runoff (during sapropel formation) and by possibly increased east to west surface temperature gradients (during glacials).

MIW production probably ceased when the S_1 developed. Relative MIW densities and formation rates were "intermediate" during the I-5 sapropel formation and during glacial periods. They were highest in I-5 nonsapropelic intervals, as they are in the present-day situation (Figure 6).

The Holocene sapropel S_1 developed under special conditions of absence of a deep chlorophyll maximum layer; there was no deep (DCM-related) phytoplankton assemblage. Since the remaining shallow phytoplankton assemblage, being recycled rapidly [cf. Gieskes and Kraay, 1986; Jenkins and Goldman, 1985], normally contributes only minutely to net production, oxygen advection due to MIW and EMDW flow must have been severely reduced in order to allow formation of the S_1 sapropel. This implies (nearly) total stagnation down from the upper depth limit of S_1 at 180 m.

REFERENCES

Abrantes, F., Diatom productivity peak and increased circulation during latest Quaternary: Alboran Basin (western Mediterranean), *Mar. Micropaleontol., 13*, 79-96, 1988.

Adamson, D. A., F. Gasse, F. A. Street, and M. A.

J. Williams, Late Quaternary history of the Nile, *Nature, 288,* 50-55, 1980.

Almogi-Labin, A., Population dynamics of planktic Foraminifera and Pteropoda -- Gulf of Aqaba, Red Sea, *Proc. K. Ned. Akad. Wet., Ser. B, Phys. Sci. 87*(4), 481-511, 1984.

Anastasakis, G. C., A new uppermost limit of sapropelic sequence deposition in the Aegean Sea, *Rapp. P. V. Reun. Comm. int. Explor. Sci. Mer Mediterr., Fasc. 2, 30,* 72, 1986.

Anderson, G. C., Subsurface chlorophyll maximum in the Northeast Pacific ocean, *Limnol. Oceanogr., 14,* 386-391, 1969.

Bé, A. W. H., and W. H. Hamlin, Ecology of Recent planktonic foraminifera, 3, Distribution in the North Atlantic during the summer of 1962, *Micropaleontology, 13,* 87-106, 1967.

Bé, A. W. H., J. K. B. Bishop, M. S. Sverdlove, and W. D. Gardner, Standing stock, vertical distribution and flux of planktonic foraminifera in the Panama Basin, *Mar. Micropaleontol., 9,* 307-333, 1985.

Berman, T., Y. Azov, and D. Townsend, Understanding oligotrophic oceans: Can the eastern Mediterranean be a useful model?, in *Marine Phytoplankton and Productivity,* edited by O. Holm-Hansen, L. Bolis, and R. Gills, pp. 101-111, Springer-Verlag, New York, 1984a.

Berman, T., D. W. Townsend, S. Z. El Sayed, C. C. Trees, and Y. Azov, Optical transparency, chlorophyll and primary productivity in the eastern Mediterranean near the Israeli coast, *Oceanol. Acta, 7,* 367-372, 1984b.

Bryan, K., and J. L. Sarmiento, Modeling ocean circulation, in *Advances in Geophysics, vol. 28, Issues in Atmospheric and Oceanic Modeling; Part A,* edited by S. Manabe, pp. 433-459, Academic, San Diego, Calif., 1985.

Bryden, H. L., and H. M. Stommel, Limiting processes that determine basic features of the circulation in the Mediterranean Sea, *Oceanol. Acta, 7,* 289-296, 1984.

Buckley, H. A., and L. R. Johnson, Late Pleistocene to Recent sediment deposition in the central and western Mediterranean, *Deep Sea Res., 35,* 749-766, 1988.

Buckley, H. A., L. R. Johnson, N. J. Shackleton, and R.A. Blow, Late glacial to recent cores from the eastern Mediterranean, *Deep Sea Res., 29,* 739-766, 1982

Calvert, S. E., Geochemistry of Pleistocene sapropels and associated sediments from the eastern Mediterranean, *Oceanol. Acta, 6,* 255-267, 1983.

Cifelli, R., Planktonic foraminifera from the Mediterranean and adjacent Atlantic waters (cruise 49 of the *Atlantis II,* 1969), *J. Foraminiferal Res., 4,* 171-183, 1974.

Cita, M. B., and D. Grignani, Nature and origin of late Neogene Mediterranean sapropels, in *Nature and Origin of Cretaceous Carbon-Rich Facies,* edited by S. O. Schlanger and M. B. Cita., pp. 165-196, Academic, San Diego, Calif., 1982.

Cita, M. B., C. Vergnaud-Grazzini, C. Robert, H. Chamley, N. Ciaranfi, and S. d'Onofrio, Paleoclimatic record of a long deep sea core from the eastern Mediterranean, *Quat. Res. 8,* 205-235, 1977.

Coulbourn, W. T., F. L. Parker, and W. H. Berger, Faunal and solution patterns of planktonic foraminifera in surface sediments of the North Pacific, *Mar. Micropaleontol., 5,* 329-399, 1980.

Cullen, J. L., and W. L. Prell, Planktonic foraminifera of the Northern Indian Ocean: Distribution and preservation in surface sediments, *Mar. Micropaleontol. 9,* 1-52, 1984.

De Lange, G. J., and H. L. Ten Haven, Recent sapropel formation in the eastern Mediterranean, *Nature, 305,* 797-798, 1983.

Dietrich, G., K. Kalle, W. Krauss, and G. Siedler, *General Oceanography,* 2nd ed., 626 pp., John Wiley, New York, 1980.

Dortch, Q., J. R. Clayton, S. S. Thoresen, J. S. Cleveland, S. L. Bresseler, and S. I. Ahmed, Nitrogen storage and use of biochemical indices to assess nitrogen deficiency and growth rate in natural plankton populations, *J. Mar. Res. 43,* 437-464, 1985.

Duplessy, J.-C., A. W. H. Bé, and P. L. Blanc, Oxygen and carbon isotope composition and biogeographic distribution of planktonic foraminifera in the Indian Ocean, *Palaeogeogr. Palaeoclimatol. Palaeoecol., 33,* 9-46, 1981.

Emiliani, C., Pleistocene temperature variations in the Mediterranean, *Quaternaria, 2,* 87-98, 1955.

Fairbanks, R. G., and P. H. Wiebe, Foraminifera and chlorophyll maximum: Vertical distribution, seasonal succession, and paleoceanographic significance, *Science, 209,* 1524-1525, 1980.

Fairbanks, R. G., M. Sverdlove, R. Free, P. H. Wiebe, and A. W. H. Bé, Vertical distribution of living planktonic foraminifera from the Panama Basin, *Nature, 298,* 841-844, 1982.

Furuya, K., and R. Marumo, The structure of the phytoplankton community in the subsurface chlorophyll maxima in the western North Pacific Ocean, *J. Plankton Res., 5,* 393-406, 1983.

Gieskes, W. W., and G. W. Kraay, Floristic and physiological differences between the shallow and the deep nannophytoplankton community in the euphotic zone of the open tropical Atlantic revealed by HPLC analysis of pigments, *Mar. Biol., 91,* 567-576, 1986.

Gieskes, W. W. C., G. W. Kraay, A. Nontji, D. Setiapermana, and Sutomo, Monsoonal alternation of a mixed and a layered structure in the phytoplankton of the euphotic zone of the Banda Sea (Indonesia): A mathematical analysis of algal pigment fingerprints, *Neth. J. Sea Res., 22*(2), 123-137, 1988.

Glover, H. E., A. E. Smith, and L. Shapiro, Diurnal

variations in photosynthetic rates: Comparisons of ultraphytoplankton with a larger phytoplankton size fraction, *J. Plankton Res.*, *7*, 519-535, 1985.

Goering, J. J., D. D. Wallen, and R. M. Naumann, Nitrogen uptake by phytoplankton in the discontinuity layer of the eastern subtropical Pacific Ocean, *Limnol. Oceanogr.*, *15*, 789-796, 1970.

Hayward, T. L., The nutrient distribution and primary production in the central North Pacific, *Deep Sea Res.*, *34*, 1593-1627, 1987.

Herbland, A., and B. Voituriez, Hydrological structure analysis for estimating the primary production in the tropical Atlantic Ocean, *J. Mar. Res.*, *37*, 87-101, 1979.

Herbland, A., R. Le Borgne, A. Le Bouteiller, and B. Voituriez, Structure hydrologique et production primaire dans l'Atlantique tropical oriental, *Oceanogr. Trop.*, *18*, 223-248, 1983.

Herbland, A., A. Le Bouteiller, and P. Raimbault, Size structure of phytoplankton biomass in the equatorial Atlantic Ocean, *Deep Sea Res.*, *32*, 819-836, 1985.

Hobson, L. A., and C. J. Lorenzen, Relationships of chlorophyll maxima to density structure in the Atlantic Ocean and Gulf of Mexico, *Deep Sea Res.*, *19*, 279-306, 1972.

Jenkins, W. J., and J. C. Goldman, Seasonal oxygen cycling and primary production in the Sargasso Sea, *J. Mar. Res.*, *43*, 465-491, 1985.

Jones, J. I., Significance of distribution of planktonic foraminifera in the Equatorial Atlantic Undercurrent, *Micropaleontology*, *13*, 489-501, 1967.

Kiefer, D. A., R. J. Olson, and O. Holm-Hansen, Another look at the nitrate and chlorophyll maxima in the central North Pacific, *Deep Sea Res.*, *23*, 1199-1208, 1976.

King, C. A. M., *Introduction to Physical and Biological Oceanography*, Edward Arnold, London, 1975.

Kipp, N. G., New transfer function for estimating past sea-surface conditions from sea-bed distribution of planktonic foraminiferal assemblages in the North Atlantic, Investigation of Late Quaternary Paleoceanography and Paleoclimatology, edited by R. M. Cline and J. D. Hays, *Mem. Geol. Soc. Am.*, *145*, 3-41, 1976.

Klein, P., and J. H. Steele, Some physical factors affecting ecosystems, *J. Mar. Res.*, *43*, 337-350, 1985.

Kullenberg, B., On the salinity of the water contained in marine sediments, *Medd. Oceanogr. Inst. Goteborg*, *21*, 1-38, 1952.

Lohrenz, S. E., D. A. Wiesenburg, I. P. DePalma, K. S. Johnson, and D. E. Gustafson Jr., Interrelationships among primary production, chlorophyll, and environmental conditions in frontal regions of the western Mediterranean Sea, *Deep Sea Res.*, *35*, 793-810, 1988.

Mangini, A., and P. Schlosser, The formation of Mediterranean sapropels, *Mar. Geol.*, *72*, 115-124, 1986.

McGill, D. A., A preliminary study of the oxygen and phosphate distribution in the Mediterranean Sea, *Deep Sea Res.*, *8*, 259-269, 1961.

Miller, A. R., P. Tchernia, H. Charnock, and D. A. McGill, *Mediterranean Sea Atlas of Temperature, Salinity, Oxygen: Profiles and Data From Cruises of R.V. Atlantis and R.V. Chain, With Distribution of Nutrient Chemical Properties*, edited by A. E. Maxwell et al., 190 pp., Alpine, Braintree, Mass., 1970.

Muerdter, D. R., Low salinity surface water incursions across the Strait of Sicily during late Quaternary sapropel intervals, *Mar. Geol.*, *58*, 401-414, 1984.

Muerdter, D. R., and J. P. Kennett, Late Quaternary planktonic foraminiferal biostratigraphy, Strait of Sicily, Mediterranean Sea, *Mar. Micropaleontol.*, *8*, 339-359, 1984.

Murphy, L. S., and E. Haugen, The distribution and abundance of phototrophic ultraplankton in the North Atlantic, *Limnol. Oceanogr.*, *30*, 47-58, 1985.

Olausson, E., Studies of deep-sea cores, *Rep. Swed. Deep Sea Exped. 1947-1948*, *8*, 353-391, 1961.

Parker, F. L., and W. H. Berger, Faunal and solution patterns of planktonic foraminifera in surface sediments of the South Pacific, *Deep Sea Res.*, *18*, 73-107, 1971.

Pond, S., and G. L. Pickard, *Introductory dynamical oceanography*, 329 pp., Bergamon, New York, 1983.

Reynolds, L. A., and R. C. Thunell, Seasonal production and morphologic variation of *Neogloboquadrina pachyderma* (Ehrenberg) in the northeast Pacific, *Micropaleontology*, *32*, 1-18, 1986.

Rognon, P., Aridification and abrupt climatic events on the Saharan northern and southern margins, 20,000 Y BP to present, *Abrupt Climatic Change: Evidence and Implications*, edited by W. H. Berger and L. D. Labeyrie, *NATO Adv. Study Inst., Ser. C, Math. Phys. Sc.*, *216*, 209-220, 1987.

Ross, C. R., and J. P. Kennett, Late Quaternary paleoceanography as recorded by benthonic foraminifera in Strait of Sicily sediment sequences, *Mar. Micropaleontol.*, *8*, 315-337, 1984.

Rossignol-Strick, M., Mediterranean Quaternary sapropels, and immediate response of the African monsoon to variations of insolation, *Palaeogeogr. Palaeoclimatol. Palaeoecol.*, *49*, 237-263, 1985.

Rossignol-Strick, M., V. Nesteroff, P. Olive, and C. Vergnaud-Grazzini, After the deluge; Mediterranean stagnation and sapropel formation, *Nature*, *295*, 105-110, 1982.

Ryan, W. B. F., Stratigraphy of late Quaternary sediments in the eastern Mediterranean, in *The*

Mediterranean Sea: A Natural Sedimentation Laboratory, edited by D. J. Stanley, pp. 149-169, Dowden, Hutchingson and Ross, Stroudsberg, Pa., 1972.

Schott, W., Foraminiferenfauna und stratigraphie der tiefsee sedimente im Nordatlantischen Ozean, *Rep. Swed. Deep Sea Exped. 1947-1948, Fasc. 8. Sediment Cores North Atlantic Ocean, 8,* 357-469, 1966.

Shaw, H. F., and G. Evans, The nature, distribution and origin of a sapropelic layer in sediments of the Cilicia Basin, northeastern Mediterranean, *Mar. Geol., 61,* 1-12, 1984.

Spencer, C. P., The micronutrient elements, in *Chemical Oceanography,* vol. 2, 2nd ed., edited by J. P. Riley and G. Skirrow, Academic, San Diego, Calif. pp. 245-300, 1975.

Srinivasan, M. S., and J. P. Kennett, Evolution and phenotypic variation in the late Cenozoic *Neogloboquadrina dutertrei* plexus, *Prog. Micropaleontol.,* 329-355, 1976.

Stanley, D. J., and C. Blanpied, Late Quaternary water exchange between the eastern Mediterranean and the Black Sea, *Nature, 266,* 537-541, 1980.

Stanley D. J., A. Maldonado, and R. Stuckenrath, Strait of Sicily depositional rates and patterns, and possible reversal of currents in the late Quaternary, *Palaeogeogr. Palaeoclimatol. Palaeoecol., 18,* 279-291, 1975.

Street, A. F., and A. T. Grove, Global maps of lake-level fluctuations since 30,000 Y BP, *Quat. Res., 12,* 83-118, 1979.

Tchernia, P., *Descriptive regional oceanography. Pergamon Mar. Ser.,* vol. 3, edited by J. C. Swallow, 253 pp., Pergamon, New York, 1980.

Ten Haven, H. L., Organic and inorganic geochemical aspects of Mediterranean late Quaternary sapropels and Messinian evaporitic deposits, *Geol. Ultraiectina, 46,* 1-206, 1986.

Thiede, J., Distribution of foraminifera in surface waters of a coastal upwelling area, *Nature, 253,* 712-714, 1975.

Thunell, R. C., Distribution of recent planktonic foraminifera in surface sediments of the Mediterranean Sea, *Mar. Micropaleontol., 3,* 147-173, 1978.

Thunell, R. C., and L. A. Reynolds, Sedimentation of planktonic foraminifera: Seasonal changes in species flux in the Panama Basin, *Micropaleontology, 30,* 243-262, 1984.

Thunell, R. C., and D. F. Williams, Paleoceanographic events associated with termination II in the eastern Mediterranean, *Oceanol. Acta, 5,* 229-233, 1982.

Thunell, R. C., and D. F. Williams, Paleotemperature and paleosalinity history of the eastern Mediterranean during the late Quaternary, *Palaeogeogr. Palaeoclimatol. Palaeoecol., 44,* 23-39, 1983.

Thunell, R. C., and D. F. Williams, Glacial-Holocene salinity changes in the Mediterranean Sea: Hydrographic and depositional effects, *Nature, 338,* 493-496, 1989.

Thunell, R. C., D. F. Williams, and J.P. Kennett, Late Quaternary paleoclimatology, stratigraphy and sapropel history in eastern Mediterranean deep-sea sediments, *Mar. Micropaleontol., 2,* 371-388, 1977.

Thunell, R. C., D. F. Williams, and M. B. Cita, Glacial anoxia in the eastern Mediterranean, *J. Foraminiferal Res., 13,* 283-290, 1983a.

Thunell, R. C., W. B. Curry, and S. Honjo, Seasonal variation in the flux of planktonic foraminifera: Time series sediment trap results from the Panama Basin, *Earth Planet. Sci. Lett., 64,* 44-45, 1983b.

Thunell, R. C., D. F. Williams, and P. R. Belyea, Anoxic events in the Mediterranean Sea in relation to the evolution of late Neogene climates, *Mar. Geol., 59,* 105-134, 1984.

Thunell, R. C., D. F. Williams, and M. Howell, Atlantic-Mediterranean Water exchange during the late Neogene, *Paleoceanography, 2(6),* 661-678, 1987.

Tolderlund, D. S., and A. W. H. Bé, Seasonal distribution of planktonic foraminifera in the western North Atlantic, *Micropaleontology, 17,* 297-329, 1971.

Tolmazin, D., *Elements of Dynamic Oceanography,* 181 pp., Allen and Unwin, Boston, 1985.

Van Leeuwen, R. J. W., Sea-floor distribution and late Quaternary faunal patterns of planktonic and benthic foraminifers in the Angola Basin, edited by C.W. Drooger, *Utrecht Micropaleontol. Bull., 38,* 288 pp., 1989.

Venrick, E. L., Phytoplankton in an oligotrophic ocean: Observations and questions, *Ecol. Monogr., 52,* 129-154, 1982.

Vergnaud-Grazzini, C., Mediterranean late Cenozoic stable isotope record: Stratigraphic and paleoclimatic implications, in *Geological Evolution of the Mediterranean Basin*, edited by D. J. Stanley and F. C. Wezel, pp. 413-451, Springer-Verlag, New York, 1985.

Vergnaud-Grazzini, C., W. B. F. Ryan, and M. B. Cita, Stable isotopic fractionation, climatic change and episodic stagnation in the eastern Mediterranean during the late Quaternary, *Mar. Micropaleontol., 2,* 353-370, 1977.

Vergnaud-Grazzini, C., A. M. Borsetti, F. Cati, P. Colantoni, S. D'Onofrio, J. F. Saliege, R. Sartori, and R.Tampieri, Palaeoceanographic record of the last deglaciation in the Strait of Sicily, *Mar. Micropaleontol., 13,* 1-21, 1988.

Wells, N., *The Atmosphere and Ocean; A Physical Introduction,* 337 pp., Taylor and Francis, London, 1986.

Williams, D. F., R. C. Thunell, and J. P. Kennett, Periodic fresh-water flooding and stagnation of

the eastern Mediterranean Sea during the late Quaternary, *Science, 201*, 252-254, 1978.

Wüst, G., On the vertical circulation of the Medi-. terranean Sea, *J. Geophys. Res., 66,* 3261-3271, 1961.

Zahn, R., and M. Sarnthein, Benthic isotope evidence for changes of the Mediterranean outflow during the late Quaternary, *Paleoceanography, 2*(6), 543-559, 1987.

Zhang, J., Living planktonic foraminifera from the Eastern Arabian Sea, *Deep Sea Res., 32,* 789-798, 1985.

W. W. C. Gieskes, Department of Marine Biology, University of Groningen, P. O. Box 14, 9750 AA Haren, The Netherlands.

E. J. Rohling, Department of Stratigraphy and Micropaleontology, Institute of Earth Sciences, University of Utrecht, P. O. Box 80.021, 3508 TA Utrecht, The Netherlands.

chapter 2

THE EASTERN MEDITERRANEAN CLIMATE AT TIMES OF SAPROPEL FORMATION; A REVIEW

THE EASTERN MEDITERRANEAN CLIMATE AT TIMES OF SAPROPEL FORMATION; A REVIEW

E.J. Rohling and F.J. Hilgen

Department of Stratigraphy and Micropaleontology, Institute of Earth Sciences, University of Utrecht, P.O.Box 80.021, 3508 TA Utrecht, The Netherlands

ABSTRACT

Sapropel formation in the eastern Mediterranean coincided closely with minima in the precession index. Such minima occur approximately every 21 000 years. At such times perihelion falls within Northern Hemisphere summer. Minima in the precession index are characterized by intensified Indian Ocean (summer) SW monsoonal circulation, which enhanced discharge of the river Nile into the eastern Mediterranean. However, by compiling paleoclimatological data from the literature, the influence of the monsoon is shown to have reached only as far as the southern Sinai Desert. Therefore, it does not account for contemporary humid phases in the northern borderlands of the eastern Mediterranean, which seem to have been characterized mainly by increased summer precipitation. We argue that increased (summer) precipitation along the northern borderlands of the eastern Mediterranean, at times of sapropel formation, was probably due to increased activity of Mediterranean (summer) depressions. Forming predominantly in the western Mediterranean and tracking eastwards, such depressions tend to lower the excess of evaporation from the eastern Mediterranean relative to that from the western basin. Picking up additional moisture along their eastward path, such depressions also redistribute freshwater within the complex eastern Mediterranean water balance. The increase in runoff and the related flux of nutrients and continental organic matter that resulted from the increased precipitation on the northern borderlands of the eastern Mediterranean, at times of sapropel formation, presumably provided a substantial addition to that which entered the eastern Mediterranean via the Nile.

INTRODUCTION

Present-day climatic conditions in the eastern Mediterranean

At present, the Mediterranean region forms a transition between the central and northern parts of Europe that remain under the influence of the westerlies for the entire year, and the deserts of North Africa which lie within the zone of the subtropical high pressure belt (Boucher 1975). In summer, the subtropical belt of high pressure is displaced to the north and most of the Mediterranean, especially the southeastern part, experiences drought. Polar front depressions may reach the western Mediterranean, but towards the east they become less frequent and they only exceptionally penetrate the eastern Mediterranean. Even when they do, there is little precipitation (Furlan 1977). During winter, the greatest activity of the polar front and the associated depressions occurs over the Mediterranean, especially over the southeastern part and the southern Balkan Peninsula. Accordingly, the frequency and amount of precipitation are highest there in winter (Mariolopoulos 1961, Furlan 1977).

Although cyclones may enter the Mediterranean from the Atlantic, the majority develops within the Mediterranean basin itself in preferred areas of cyclogenesis (Rumney 1968). They tend to be steered by the upper winds and move roughly eastwards (Trewartha 1966, Rumney 1968, Griffiths 1972, Boucher 1975, Furlan 1977). Cyclogenesis is much more frequent over the western Mediterranean than over the eastern basin, the activity being highest in the Gulf of Genoa (Trewartha 1966, Rumney 1968, Cantu 1977) and extending across the Plain of Lombardy to the northern Adriatic (Cantu 1977, Furlan 1977). Although a large number of depressions forms in the western Mediterranean, their central pressures are considerably higher than those of the

massive Atlantic storms. Mediterranean depressions should be regarded as secondary depressions, which are often related to much larger disturbances north of the Alps (Trewartha 1966, Boucher 1975). During winter, the Cyprus area becomes a significant centre of cyclogenesis as well (Trewartha 1966, Rumney 1968, Boucher 1975, Furlan 1977).

In present-day summers, a branch of the Asiatic depression (monsoon low) east of the northeastern Mediterranean invokes steady northwesterly winds over the southeastern Mediterranean (Goldsmith & Sofer 1983). This branch consists of an essentially thermal low, centred over the Iranian Plateau, and the resultant (dry) winds with a marked northerly component are known as the "Etesians" (Mariolopoulos 1961, Furlan 1977). The steady Etesians are characteristic of the summer circulation across southeastern Europe down to the Levantine area, and respond to the generally counterclockwise circulation around the dominant monsoon low. A secondary depression often develops over Cyprus in summer, augmenting the larger circulation (Rumney 1968).

The summer dryness, a present-day characteristic of the climate in most of the eastern Mediterranean, presumably developed in the Late Pliocene in response to the climatic modifications invoked by the uplift of the Tibetan Plateau. Uplift simulations by Ruddiman & Kutzbach (1989) show a change in the lower-level winds from westerly to northeasterly in the western limb of an intensified low-level cyclonic flow around the Tibetan Plateau, and in the eastern limb of the intensified North Atlantic subtropical high. Increased subsidence east of the elevated plateau also appeared to be of importance. Both a slight increase in winter wetness and a greater and significant increase in summer dryness developed due to the Tibetan Plateau uplift (Ruddiman & Kutzbach 1989).

Evidence of past climatic variations

Miocene to Recent sedimentary sequences show that the eastern Mediterranean's oceanographic (and climatic) conditions have been subject to considerable variations. Numerous brownish to black coloured beds are intercalated. These beds are relatively enriched in organic carbon and often well laminated, and are named sapropels.

Sapropels have been deposited in dysoxic to anoxic bottom waters, which allowed the preservation of organic matter in the sediments and caused the (near) absence of benthic fauna. Bottom water oxygen depletion may occur due to restricted deep water ventilation, due to a large flux of marine organic matter from the euphotic zone and/or continental organic matter via river run-off, or due to a combination of these processes.

Many workers argued that restricted deep water ventilation was the principal mechanism invoking sapropel formation. This restriction would be due to lowered salinities or higher temperatures at the sites of deep water formation, resulting in a more stable stratification which, in turn, inhibits large-scale convection. However, sapropels are known to have developed during pleniglacials as well as during interglacials, which suggests that warming was not the major agent invoking more stable stratification in the eastern Mediterranean. On the contrary, increased freshwater fluxes from various sources, at times of sapropel formation, have been positively identified (Rossignol-Strick et al. 1982, Shaw & Evans 1984, Rossignol-Strick 1985, Cramp et al. 1988, Appendix 3). Moreover, low $\delta^{18}O$ values within sapropels (see Fig. 1) strongly suggest generally lowered surface water salinities at that time (a.o. Cita et al. 1977, Vergnaud-Grazzini et al. 1977, Williams et al. 1978, Mangini & Schlosser 1986). Increased river run-off into the basin would not only lower the salinities, but it would also enhance the input of river-borne nutrients and continental organic matter.

A new model for sapropel formation, combining increased productivity with decreased deep water production and a more detailed assessment of the eastern Mediterranean's vertical

density-structure, has been proposed by Rohling and Gieskes (Chapter 1). In that model, increased freshwater fluxes into the basin resulted in a shoaling of the density gradient (pycnocline) between the Mediterranean Intermediate Water (MIW) and the surface water, to a depth within the euphotic layer. Thus, a Deep Clorophyll Maximum (DCM) could develop, between the top of the pycnocline and the base of the euphotic layer, as reflected by the planktonic foraminiferal record. At the same time, the nutrient concentration in the eastern Mediterranean would have increased as a result of increased riverine fluxes, favouring increased marine organic production.

Rossignol-Strick (1985) coupled the temporal occurrence of sapropels to an orbitally forced monsoonal index, and concluded that sapropel formation was invoked by Nile floods, which are related to monsoonal rains over eastern tropical Africa. In a later paper, Rossignol-Strick (1987) concluded that Eurasian river run-off, regulated by the "local" eastern Mediterranean climate, also contributed to the excess freshwater input which triggered sapropel formation. Furthermore, she concluded that increases in humidity in the Northern Borderlands of the Eastern Mediterranean (NBEM), at times of sapropel formation, were due in large part to precipitation in the summer season.

In this paper, we will discuss atmospheric circulation patterns that may have resulted in increased (summer) precipitation in the NBEM during sapropel formation. We end with a discussion of the major implications with respect to the Mediterranean freshwater budget and the formation of sapropels.

THE TEMPORAL OCCURRENCE OF SAPROPELS

It would seem most promising to try and unravel the climatic and oceanographic changes that initiated the formation of the youngest sapropel -the early Holocene S_1 sapropel - since its time of formation falls well within the age range covered by the AMS ^{14}C dating method. This dating method enables detailed correlation of changes in both the marine and the continental environment, within about the last 40 000 years.

The S_1 sapropel, with its age range between approximately 9 000 and 6 000 BP (see Fig. 1), however, has been deposited at about the Holocene warm Climatic Optimum, which followed the last major retreat of the Northern Hemisphere continental ice sheets. As stated before, such a coincidence with a warm Climatic Optimum is not typical for all sapropels, since they have been deposited also during glacials. Therefore, ice-cap geography cannot be considered as the dominant factor controlling the climatic initiation of sapropel formation.

Rossignol-Strick (1985) was the first to elaborate a relation between sapropel formation and orbital forcing. She calculated a monsoonal index from the caloric Northern Hemisphere insolation in tropical latitudes, and argued that sapropels were deposited at times of intense (northern) summer monsoons, since they coincided in time with maxima of the monsoonal index.

Hilgen (in press) demonstrated that sapropel formation coincided closely with minima in the precession index, which occur approximately every 21 000 years. A minimum in the precession index implies that perihelion falls within Northern Hemisphere summer, assuring greater Northern Hemisphere insolation in summer and less in winter. Consequently, the seasonal contrast on the Northern Hemisphere would be significantly increased. Since the heat capacity of water is much larger than that of land, the seasonal temperature contrast of the sea surface would be much less amplified than that of the land surface; according to Kutzbach & Guetter (1986) the range of the former would be about one-fifth of the latter. Consequently, land-sea temperature differences would be considerably larger at times of a precession-minimum than they are today. The relation between sapropel formation and precession minima is most obvious when considering Quaternary sapropels, which have been accurately placed in a time-stratigraphic framework (Rossignol-Strick

26

1985, Prell & Kutzbach 1987, Hilgen in press). Hilgen (in press) argued that this relation existed also throughout the Pliocene (Fig. 2). We emphasize that there seems to be a systematic phase-lag, the precession minima preceeding sapropel formation by approximately 2 000 to 3 000 years. As yet, there is no ready explanation for these lags.

Summarizing; ice-cap geography has differed considerably between individual phases of sapropel formation, and we should be careful not to overestimate its influence on the climatic constraints for sapropel formation. The correlation between minima in the precession index and the formation of sapropels suggests that orbital forcing is the major agent controlling the atmospheric circulation patterns which result in sapropel formation. On the Northern Hemisphere, the orbital configuration at times of sapropel development invoked increased seasonal and land-sea temperature contrasts and, consequently, enhanced (summer) monsoonal circulation.

DISCUSSION

In the literature, several models have been introduced that deal with geologically recorded wet phases in the Sahel, Magreb, central Sahara, Near East, eastern tropical Africa and the eastern Mediterranean countries in general. We will discuss the three major existing models with respect to literature-based information on the climate at times of sapropel formation. Furthermore, we will argue whether the prominent southeastern Black Sea precipitation system may have expanded towards the Aegean Sea at times of sapropel formation, a possibility which has not been discussed previously.

Monsoonal intensifications

Using the Community Climate Model (CCM) of the National Center for Atmospheric Research (NCAR), Kutzbach & Street-Perrott (1985) and Kutzbach & Guetter (1986) simulated an orbitally produced precipitation maximum from 12 000 to 6 000 BP, concentrated between 0° and 30° latitude in the Northern Hemisphere (see also COHMAP Members 1988). This precipitation maximum was due to increased vigour of the summer monsoon, in response to the increased heating of the Northern Hemisphere continental interiors when perihelion fell in northern summer (Kutzbach 1985). Also using the CCM, Prell & Kutzbach (1987) studied the monsoon variability over the past 150 000 years. They concluded that monsoonal strength and monsoonal precipitation were positively correlated to precession-caused peaks in the Northern Hemisphere summer radiation, over this interval of time.

Rossignol-Strick (1985) coupled the temporal occurrence of sapropels in the eastern Mediterranean to a monsoonal index, calculated from the caloric Northern Hemisphere insolation in tropical latitudes for the last 465 000 years. This insolation is controlled by variations of the orbital parameters, of which the precession cycle dominates at low latitudes. Peak values of the monsoonal index would relate to periods of intensified summer monsoons. Rossignol-Strick et al. (1982) and Rossignol-Strick (1985) reasoned that enhanced monsoonal precipitation, especially over the northern Ethiopian highlands, caused heavy Nile floods to reach the eastern Mediterranean some 35° of latitude north of the catchment area. Sapropel formation would then be triggered by the increased, high-nutrient, Nile discharge.

This hypothesis, considering Nile discharge as the exclusive cause of sapropel formation (Rossignol-Strick et al. 1982, Rossignol-Strick 1985) was rejected by Jenkins & Williams (1984) on the basis of a study of oxygen isotope records. Moreover, based on an oxygen isotopic study, Gudjonsson & Van der Zwaan (1985) concluded that European rivers, rather than the Nile, supplied the freshwater which caused anomalously low $\delta^{18}O$ values of foraminifera in Sicilian Pliocene sapropels.

Turkish and Greek rivers (Shaw & Evans 1984, Cramp et al. 1988, Zachariasse et al. Appendix 3) showed increased discharge rates at times of sapropel formation. Rossignol-Strick (1987) concluded that increases of humidity and winter mildness in the Northern Borderlands of the Eastern Mediterranean (NBEM) prevailed during sapropel formation, according to a revised interpretation of fossil pollen assemblages from northeastern Greece. Therefore, she adjusted her earlier theory by stating that, in addition to Nile flooding, precipitation in the NBEM played an important role in the initiation of sapropel formation. The oak pollen increases in northeastern Greece, which coincided with sapropel formation, would be primarily related to increased precipitation in the summer season (Rossignol-Strick, 1987). A similar increase in summer precipitation at times of sapropel formation was reconstructed from Macedonian pollen records by Wijmstra et al. (1990).

As argued above, there must be a mechanism controlling the humidity in the NBEM, which operates in phase with (or as part of) the Northern Hemisphere summer monsoon. Furthermore, the increased humidity in the NBEM during sapropel formation appeared to be largely due to increased precipitation in summer. Combined, this might suggest that the humidity in the NBEM should be interpreted as monsoonal precipitation, implying temporal expansion of the Indian Ocean's summer (SW) monsoon into the eastern Mediterranean.

The results from numerical climate simulations, summarized by the COHMAP Members (1988), show that the area receiving monsoonal precipitation had indeed expanded at 9 000 BP, compared to the present, reaching across tropical Africa - as far north as the Lybico-Egyptian desert - via the Arabian Peninsula, Pakistan and India into southeastern Asia and northwards into the Hoang Ho province of China. According to these simulations, however, the monsoonal precipitation did not reach into the eastern Mediterranean. According to Sarnthein (1978), the monsoonal summer rains of Africa reached their most northerly position at > 30° N in Lybia and the Atlas Mountains around 6 000 BP

Studying fluorescent bands in fossil corals, Klein et al. (1990) concluded that during the mid Holocene, as well as during other Quaternary periods of reef growth at high sea-level stands, a wet climate prevailed in the Sinai Desert, possibly with a summer rainfall regime. Klein et al. (1990) considered their observations as evidence for northward extension of the monsoon over the Sinai region. This seems to match with the numerically simulated northernmost extension of significant monsoonal precipitation in that region (COHMAP Members 1988). However, Prell & Kutzbach (1987) showed that the precession related intensifications of the summer monsoon were much less pronounced during glacials than during interglacials.

Goodfriend (1988) reconstructed a mid Holocene wet phase in the northern Negev desert (Israel), between 6 000 and 4 000 BP. He argued that the moisture increase in the Negev resulted from a southward shift of the rainfall isohyet pattern, rather than from an overall increase of rainfall troughout the southern Levant. Similarly, Goodfriend & Magaritz (1988) argued that strong north-south rainfall gradients, as today, existed during the wet phases in the northern Negev which occurred during globally warmer periods within the last glacial. These wet phases, at about 13 000 BP, 28 000 BP and 37 000 BP resulted in the formation of paleosols in the northern Negev. Goodfriend and Magaritz (1988) concluded that the source area of the precipitation was in the north or northwest, and that the periods were not the result of northward penetration of monsoonal rains from the Indian Ocean. Therefore, during wet phases in the northern Negev, both during interglacials (Goodfriend 1988) and during glacials (Goodfriend & Magaritz 1988), the moisture seems to have originated mainly in the north or northwest.

Summarizing, sapropel formation coincided with intensified (summer) monsoonal circulation, which invoked increased discharge of the river Nile. In addition, however, increased

(summer) precipitation rates have been recorded in the NBEM. Data from the Levant provide a means to study the northernmost extention of the monsoonal precipitation system. During interglacial wet phases, significant monsoonal precipitation reached the Sinai in summer. Meanwhile, the Negev desert benefited from a subtantial moisture supply from the north to northwest. At glacial times, the summer monsoon failed to reach as far as the Sinai. On the contrary, the northerly to northwesterly moisture flux towards the northern Negev did prevail during glacial (interstadial) wet phases. The principal moisture source for the Negev seems to have been the Mediterranean rather than the Indian Ocean, during interglacial as well as glacial (interstadial) wet phases. This implies that the temporal (summer) humidity in the NBEM may not be explained by intrusions of the (summer) monsoonal precipitation regime into the eastern Mediterranean.

Secondary depression tracks

Lamb (1966, 1969, 1977) reconstructed the climate of medieval times, also called the Little Climatic Optimum. According to Lamb (1977), the temperatures in this period regained values approaching those of the Holocene Cimatic Optimum. Also, he stated that the medieval circum-Mediterranean climate was more humid than at present, with greater rainfall in the Mediterranean and Near East and bigger, more frequent stream flow in the wadis of the African and Arabian deserts. At medieval times, the westerly track of cyclones (depression track) over the Atlantic had shifted considerably northwards, as far as 65-70° N (Lamb 1969, 1977) or 60-65° N (Flohn 1981c). As a consequence, a secondary depression-track could have developed across the Mediterranean, according to Lamb (1966, 1969, 1977).

In his reconstructions of medieval climate, Lamb indicated a secondary depression track in summer only east of Italy, in contrast to that in winter which he drew across the entire Mediterranean. Unfortunately, Lamb did not really explain what process would have invoked the summer depression track east of Italy. He suggested, however, that the medieval summers were characterized by a cold mid-tropospheric trough with its axis from the Barentz Sea down to the central Mediterranean. In such a configuration, the flow of cold air from the northwest favours cyclogenesis over the western Mediterranean, especially over the Gulf of Genoa (cf. Boucher 1975). The resultant Mediterranean depressions would have moved eastwards, which may explain the medieval summer depression track which Lamb suggested east of Italy.

Lamb's reconstruction of the medieval climate does suggest increased precipitation in the eastern Mediterranean, also along the northern limits of the basin. Therefore, accepting the medieval climate as an analogue to that around 9 000 BP would provide a means to explain the increased humidity in the NBEM during the formation of sapropel S_1. However, it remains doubtful whether we may really compare the two periods, since whatever external forcing may have acted upon the medieval climate, it certainly was not identical to that around 9 000 BP which was dominated by the summer perihelion. Consequently, the circulational response may also have differed significantly. Nevertheless, in the 9 000 BP simulations of Kutzbach & Guetter (1986), the subpolar jet in summer was found further north over the Atlantic Ocean (up to about 70° N) than at present. This suggests that the main depression track was displaced to the north as well, during the summers around 9 000 BP, much as it was during medieval times according to Lamb (1966, 1969, 1977).

Saharan depressions

Flohn (1981a) argued that a moist period affected northern Africa between 10 000 and 5 000 BP. He also stated that this moist phase was interrupted around 8 000 BP, for several cen-

turies, in the western and central Sahara, whereas it was not interrupted in East Africa and the Middle East. Flohn (1981a) suggested a relation between the first moist period and the occurrence of a warm Climatic Optimum in the Southern Hemisphere around 9 500 BP, while Scandinavia was still ice-covered. He argued that the second moist period - when Scandinavia was free of ice - was due to a quasi-permanent secondary mid-tropospheric trough, reaching across Central Europe into the western Sahara and caused by the extended remnants of the Laurentide Ice.

In another paper, Flohn (1981b) discussed teleconnections between the Sahelian and the western and eastern Mediterranean climates. He stated that a major connection could be attributed to the occurrence of Saharan depressions, which form within the tropical belt of easterly waves, cross the desert with heavy sandstorms, and develop convective rainstorms when approaching the moist air of the Mediterranean. Crane (1981) stated that a marked increase of such depressions would have occurred during the moist North African periods. Flohn (1981b) suggested that the Saharan depression mechanism would especially influence the Mediterranean rainfall in winter.

Flohn's mechanism of Saharan depressions cannot explain the increased humidity in the NBEM, since the influence of this mechanism is restricted to areas more to the south. Also, the humidity in the NBEM appeared to be substantially due to summer rains, whereas Flohn (1981b) suggested that the Saharan depression mechanism would especially influence the Mediterranean rainfall in winter. Moreover, we found no substantial evidence in favour of increased Saharan depression activity around 9 000 BP in the numerical simulations by Kutzbach & Guetter (1986) and Kutzbach & Gallimore (1988).

Expansion of the summer precipitation regime of the southeastern Black Sea towards the eastern Mediterranean ?

At present, a distinct summer precipitation system exists along the southeastern coast of the Black Sea, only 1 000 km east of the Aegean Sea. Although we have found no account in the literature as to whether this regime could have temporarily expanded westward to influence the NBEM, we think that this possibility should not be neglected without discussion.

Detailed descriptions of the climate around the eastern Mediterranean show that the Batumi region, southeast of the Black Sea, receives year-round precipitation and lacks a dry season (Trewartha 1966, Lydolph 1977). Annual precipitation in the Batumi region amounts to more than 2 500 mm yr^{-1} (Grasshoff 1975, Lydolph 1977). According to Trewartha (1966), the summer rainfall in this area is due to: 1) the fact that the Etesians are still more humid than further south and have not yet attained their genuinely stable characteristics, 2) cyclonic storms which, in these latitudes north of 40° N, are still active even in summer, especially along tracks entering the Black Sea, 3) humidification of the northwesterly air flow by the Black Sea itself, so that moderate precipitation develops when the air is forced upwards by highlands or convectional systems. Both types of upward forcing exist in the vicinity of the Caucasus mountains. The former due to topography, and the latter since (especially) the Armenian Plateau induces a local low pressure system in summer due to thermal effects (Lydolph 1977). Processes similar to those causing summer precipitation in the Batumi region invoke the summer precipitation along the southern coast of the Caspian Sea (Trewartha 1966).

Although the heaviest precipitation in the Batumi region originates from summertime thunderstorms, the winter maximum - associated with cyclonic storms moving in from the west - is generally considered to be the more characteristic feature of the Black Sea-Caucasus-Caspian Sea rainfall regime (Trewartha 1966, Lydolph 1977). Descriptively, the classical "Mediterranean climate", characterized by wet winters and dry summers, is modified by substantial summer rains in the Batumi region to a so called "humid subtropical climate" (Trewartha 1966). The summer

rains appear to be largely due to uplift of the moistened air in the vicinity of the Caucasus mountains (cf. Rumney 1968). Because of its dependance on topography, we envisage that the Batumi region's summer precipitation regime may not have expanded far enough to the west to cover the NBEM, as a response to insolation changes through times with about present-day topography.

Evaluation

The above considerations allow some restriction as to the origin of the increased humidity - largely summer precipitation - in the NBEM, at times of sapropel formation. In the present paper, we argue that neither Saharan depressions, nor westward expansions of the southeastern Black Sea's summer precipitation regime, would form a likely mechanism to invoke summer precipitation in the NBEM. Furthermore, we concluded that the temporal humidity in the NBEM may not be explained by intrusions of the monsoonal precipitation regime into the eastern Mediterranean.

It appears that the increases of summer precipitation in the NBEM simply reflect increased activity of summer depressions, which track eastwards across the Mediterranean. In addition, we emphasize that the (normal) winter precipitation in the NBEM was probably enhanced as well (Wijmstra et al., 1990). Therefore, we think that Lamb's reconstruction of the medieval climate may serve as a proxy for the climatic configuration during sapropel formation.

IMPLICATIONS FOR SAPROPEL FORMATION

As argued in the Introduction, Mediterranean depressions should be regarded as secondary depressions, which are often related to much larger disturbances north of the Alps. Cyclogenesis is most common in the western Mediterranean, especially in the Gulf of Genoa. A significant part of the moisture is collected in these formation areas, while more moisture may be picked up along the track eastwards. At present, summer depressions from the western Mediterranean are being notably reinforced when they cross the Aegean Sea (Trewartha 1966). The summer precipitation in the NBEM will, therefore, constitute 1) in part, a lowering of the excess evaporation from the eastern Mediterranean relative to that from the western basin, and 2) in part, a redistribution of freshwater within the complex eastern Mediterranean water balance.

The lowering of excess evaporation from the eastern Mediterranean relative to that from the western basin would decrease the contrast between the water budgets of these two basins. Consequently, the exchange of watermasses between the two basins across the Strait of Sicily may have been decreased, which would increase the residence time of water in the eastern Mediterranean.

We also concluded that sapropel formation occurred at times of minima in the precession index and, therefore, coincided in time with intensifications of the Indian Ocean's summer (SW) monsoon. Such intensifications enhanced freshwater fluxes into the eastern Mediterranean, via the Nile. Hence, the increased activity of Mediterranean depressions resulted in a greater flux of moisture of western origin, superimposed on an increased (monsoonal) moisture flux from the southeast.

The relative 'freshening' of the eastern basin due to increased summer and winter precipitation in the NBEM, in addition to that invoked by monsoonal intensification, may have invoked a decrease in the density difference between the surface and intermediate water masses, as compared to that at present. This would result in the processes described by Rohling and Gieskes (Chapter 1). Meanwhile, increased precipitation on the NBEM would, via the resulting increase of runoff, have enhanced the flux of river-borne nutrients, from the adjacent land into

31

the basin. Again, this process adds to the effect of monsoonal intensification, which augmented the flux of nutrients via the Nile.

CONCLUSIONS

Orbital forcing of the climate seems to control the formation of sapropels in the eastern Mediterranean. More specifically, the cycle of precession appears to be dominant. Furthermore, sapropels have been deposited during both interglacial and glacial intervals. Combined, this suggests that increased seasonal and land-sea temperature contrasts are more important for the climatic changes initiating sapropel formation than average warm (interglacial) or cool (glacial) conditions.

Rossignol-Strick's (1985) monsoonal theory fitted the requirement of being orbitally forced. Moreover, the coupling of monsoonal precipitation to orbital forcing has been confirmed by the numerical climate simulations of Kutzbach & Street-Perrott (1985), Kutzbach & Guetter (1986), Prell & Kutzbach (1987), Kutzbach & Gallimore (1988) and the COHMAP Members (1988). The Nile flood scenario as proposed by Rossignol-Strick (1985), however, did not account for humidity in the NBEM, as she concluded herself in a later paper (Rossignol-Strick 1987). Neither did the numerical simulations, but this was not noticed since - for some reason - the COHMAP Members (1988) interpreted the 9 000 BP paleoclimatic data from Greece and Turkey as indicative of conditions drier than present. Obviously, we disagree with this interpretation.

Rossignol-Strick (1987) and Wijmstra et al. (1990) stressed that the humid phases in the NBEM contain evidence of increased summer precipitation. Also, the (normal) winter precipitation seems to have been increased (Wijmstra et al. 1990). Since substantial summer precipitation would be the major deviation from the present-day climate, we focused on the mechanisms that may have invoked it. We conclude that the most likely mechanism consists of increased activity of Mediterranean summer depressions, the moisture sources being both the western Mediterranean Sea and the eastern Mediterranean Sea itself.

Sapropels were formed at times of distinct minima in the precession index. Such periods are characterized by intensified (summer) monsoons, which resulted in increased discharge of freshwater and nutrients via the Nile. The coeval increases of yearly precipitation in the NBEM also increased the fluxes of freshwater and river-borne nutrients, which added to the fluxes from the river Nile.

ACKNOWLEDGEMENTS

REFERENCES

Boucher, K. 1975 Global climate - The English Univ. Press Ltd. (London): 326 pp

Cantu, V. 1977 The climate of Italy. In: Wallén, C.C. (ed.): Climates of Central and Southern Europe -World Survey of Climatology, 6 - Elsevier (Amsterdam): 127-183

Cita, M.B. 1975 Planktonic foraminiferal biozonation of the Mediterranean Pliocene deep-sea record. A revision - Riv. Ital. Paleontol. Stratigr., 81: 527-544

Cita, M.B., C. Vergnaud-Grazzini, C. Robert, H. Chamley, N. Ciaranfi & S. d'Onofrio 1977 Paleoclimatic record of a long deep sea core from the eastern Mediterranean - Quat. Res., 8: 205-235

COHMAP Members 1988 Climatic changes of the last 18,000 years: observations and model simulations - Science, 241: 1043-1052

Cramp, A., M. Collins & R. West 1988 Late Pleistocene-Holocene sedimentation in the NW Aegean Sea: a palaeoclimatic plaeoceanographic reconstruction - Palaeogeogr., Palaeoclimatol., Palaeoecol, 68: 61-77

Crane, A.J. 1981 Techniques for reconstructing past climates. In: Berger, A. (ed.): Climatic variations and variability: facts and theories - NATO Adv. Study Inst., Ser. C, Math. Phys. Sc., 72: 739-750

Flohn, H. 1981a Tropical climate variations during late Pleistocene and early Holocene. In: Berger, A. (ed.): Climatic variations and variability: facts and theories - NATO Adv. Study Inst., Ser. C, Math. Phys. Sc., 72: 233-242

Flohn, H. 1981b Sahel droughts: recent climatic fluctuations in North Africa and the Mediterranean. In: Berger, A. (ed.): Climatic variations and variability: facts and theories - NATO Adv. Study Inst., Ser. C, Math. Phys. Sc., 72: 399-408

Flohn, H. 1981c Scenarios of cold and warm periods of the past. In: Berger, A. (ed.): Climatic variations and variability: facts and theories - NATO Adv. Study Inst., Ser. C, Math. Phys. Sc., 72: 689-698

Furlan, D. 1977 The climate of southeast Europe. In: Wallén, C.C. (ed.): Climates of Central and Southern Europe - World Survey of Climatology, 6 - Elsevier (Amsterdam): 185-235

Griffiths, J.F. 1972 The Mediterranean Zone. In: Griffiths, J.F. (ed.): Climates of Africa - World Survey of Climatology, 10 - Elsevier (Amsterdam): 37-74

Goldsmith, V. & S. Sofer 1983 Wave climatology of the southeastern Mediterranean: An integrated approach - Isr. J. Earth Sci., 32: 1-51

Goodfriend, G.A. 1988 Mid-Holocene rainfall in the Negev Desert from ^{13}C of land snail shell organic matter - Nature, 333: 757-760

Goodfriend, G.A. & M. Magaritz 1988 Palaeosols and late Pleistocene rainfall fluctuations in the Negev Desert - Nature, 332: 144-146

Grasshoff, K. 1975 The hydrochemistry of landlocked basins and fjords. In: Riley, J.P. & Skirrow, G. (eds.): Chemical Oceanography, 2 Academic (London): 455-597

Gudjonsson, L. & G.J. Van der Zwaan 1985 Anoxic events in the Pliocene Mediterranean: stable isotope evidence of run-off - Proc. K. Ned. Akad. Wet., Ser. B. Phys. Sci., 88: 69-82

Hilgen, F.J. (in press) Astronomical calibration of Gauss to Matuyama sapropels in the Mediterranean and implication for the Geomagnetic Polarity Time Scale - Earth Planet. Sci. Lett.

Jenkins, J.A. & D.F. Williams 1984 Nile water as cause of eastern Mediterranean sapropel formation: evidence for and against - Mar. Micropaleontol., 9: 521-534

Klein, R., Y. Loya, G. Gvirtzman, P.J. Isdale & M. Susic 1990 Seasonal rainfall in the Sinai Desert during the late Quaternary inferred from fluorescent bands in fossil corals - Nature, 345: 145-147

Kutzbach, J.E. 1985 Modeling of paleoclimates. In: Manabe, S. (ed.): Issues in atmospheric and oceanic modeling, A; climate dynamics - Adv. Geophys., 28: 161-196

Kutzbach, J.E. & R.G. Gallimore 1988 Sensitivity of a coupled Atmosphere/Mixed layer Ocean model to changes in orbital forcing at 9 000 years BP. - J. Geophys. Res., 93: 803-821

Kutzbach, J.E. & F.A. Street-Perrott 1985 Milankovitch forcing in the level of tropical lakes from 18 to 0 kyr BP - Nature, 317: 130-134

Kutzbach, J.E. & P.J. Guetter 1986 The influence of changing orbital parameters and surface boundary conditions on climate simulations for the past 18,000 years - J. Atmos. Sci., 43: 1726-1759

Lamb, H.H. 1966 The changing climate. Methuen & Co. (London): 236 pp

Lamb, H.H. 1969 Climatic fluctuations. In: Flohn, H. (ed.): General Climatology, 2 - World Survey of Climatology, 2 - Elsevier (Amsterdam): 173-249

Lamb, H.H. 1977 Climate: present, past and future. 2, Climatic history and the future. Methuen and Co. (London)

Lydolph, P.E. 1977 Climates of the Soviet Union - World Survey of Climatology, 7 - Elsevier (Amsterdam): 443 pp

Mariolopoulos, E.G. 1961 An outline of the climate of Greece - Publ. Metorol. Inst. Univ. Athens, 6: 51 pp

Mangini, A. & P. Schlosser 1986 The formation of Mediterranean sapropels - Mar. Geol., 72: 115-124

Prell, W.L. & J.E. Kutzbach 1987 Monsoon variability over the past 150 000 years - J. Geophys. Res., 92: 8411-8425

Raffi, I. & D. Rio 1979 Calcareous nannofossil biostratigraphy of DSDP Site 132 Leg 13 (western Mediterranean) - Riv. It. Paleontol. Stratigr., 85: 127-172

Rossignol-Strick, M. 1985 Mediterranean Quaternary sapropels, an immediate response of the African monsoon to variation of insolation - Palaeo geogr., Palaeoclimatol., Palaeoecol., 49: 237-263

Rossignol-Strick, M. 1987 Rainy periods and bottom water stagnation initiating brine accumulation and metal concentrations: 1. the Late Quaternary - Paleoceanography, 2: 333-360

Rossignol-Strick, M., W. Nesteroff, P. Olive & C. Vergnaud-Grazzini 1982 After the deluge: Mediterranean stagnation and sapropel formation - Nature, 295: 105-110

Ruddiman, W.F. & J.E. Kutzbach 1989 Forcing of Late Cenozoic Northern Hemisphere climate by Plateau uplift in southern Asia and the American West - J. Geophys. Res., 94: 18,409-18,427

Rumney, G.R. 1968 Climatology and the World's climates. Macmillan Cy. (New York): 656 pp

Sarnthein, M. 1978 Sand deserts during glacial maximum and climatic optimum - Nature, 272: 43-46

Shackleton, N.J., A. Berger & W.R. Peltier (in press) An alternative astronomical calibration of the Lower Pleistocene time scale based on ODP Site 677 - Trans. Royal Soc. Edinburgh

Shaw, H.F. & G. Evans 1984 The nature, distribution and origin of a sapropelic layer in sediments of the Cilicia Basin, northeastern Mediterranean - Mar. Geol., 61: 1-12

Spaak, P. 1983 Accuracy in correlation and ecological aspects of the planktonic foraminiferal zonation of the Mediterranean Pliocene - Utrecht Micropaleontol. Bull., 28: 160 pp

Trewartha, G.T. 1966 The earth's problem climates. Methuen & Co. (London): 334 pp

Vergnaud-Grazzini, C., W.B.F. Ryan & M.B. Cita 1977 Stable isotopic fractionation, climatic change and episodic stagnation in the eastern Mediterranean during the late Quaternary - Mar. Micropaleontol., 2: 353-370

Wijmstra, T.A., R. Young & H.J.L. Witte 1990 An evaluation of the climatic conditions during the Late Quaternary in northern Greece by means of multivariate analysis of palynological data and comparison with recent phytosociological and climatic data - Geol. Mijnbouw., 69: 243-251

Williams, D.F., R.C. Thunell & J.P. Kennett 1978 Periodic fresh-water flooding and stagnation of the eastern Mediterranean Sea during the late Quaternary - Science, 201: 252-254
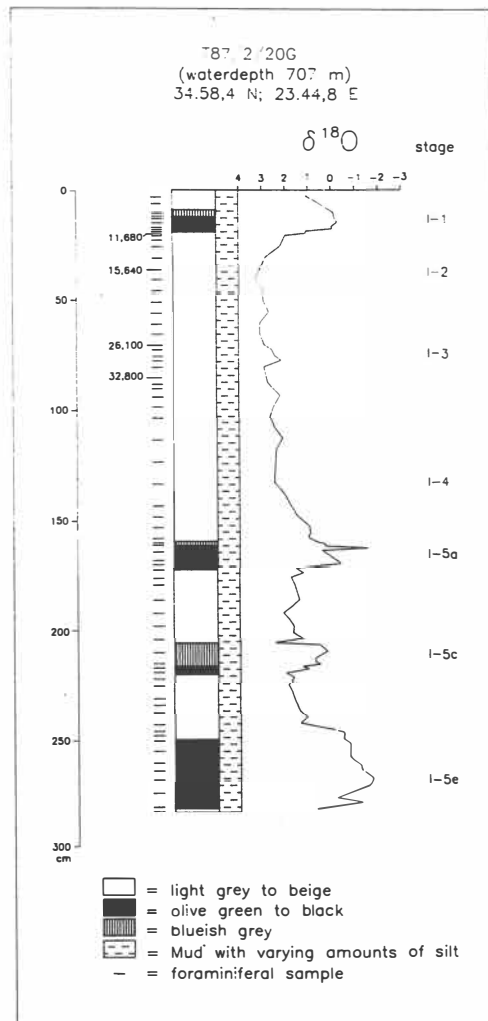
Figure 1. Highly detailed record of $\delta^{18}O$ values versus lithology in core T87/2/20G from the Crete perimeter (Chapter 1). Oxygen isotopic stages are indicated on the right side of the graph. Note the prominently low $\delta^{18}O$ values at the sapropelic levels (=black + hatched). The analyses were performed on the carbonaceous tests of the planktonic foraminiferal species *Globigerinoides ruber*. Small numbers at the left side of the core refer to AMS ^{14}C datings.

Figure 2. (Modified after Hilgen, in press) Calibration of Plio-Pleistocene sapropels in Mediterranean land-based sections and deep-sea cores to the astronomical record. This was established by correlating first the late Pliocene sapropels to the astronomical record, using oxygen isotope stage boundaries for calibration. The established phase-relations (individual sapropels correlate with 21 ka precession minima and sapropel-clusters with 100 and 400 ka eccentricity maxima) were subsequently employed to astronomically calibrate the late Pliocene-early Pleistocene sapropels. For further details, the reader is referred to Hilgen (in press). Note that eccentricity modulates the amplitude of precession variations in 100 and 400 ka cycles. Also shown is the correlation to the (resultant) astronomically calibrated Geomagnetic Polarity Time Scale of Shackleton et al. (in press) and Hilgen (in press), based on first order magnetostratigraphic records. Solid lines mark lithostratigraphic, magnetostratigraphic and astronomical correlations, dashed lines mark biostratigraphic correlations. Biozonations used are those of Cita (1975) and Spaak (1983) for the planktonic foraminifera, and Raffi & Rio (1979) for the calcareous nannofossils.
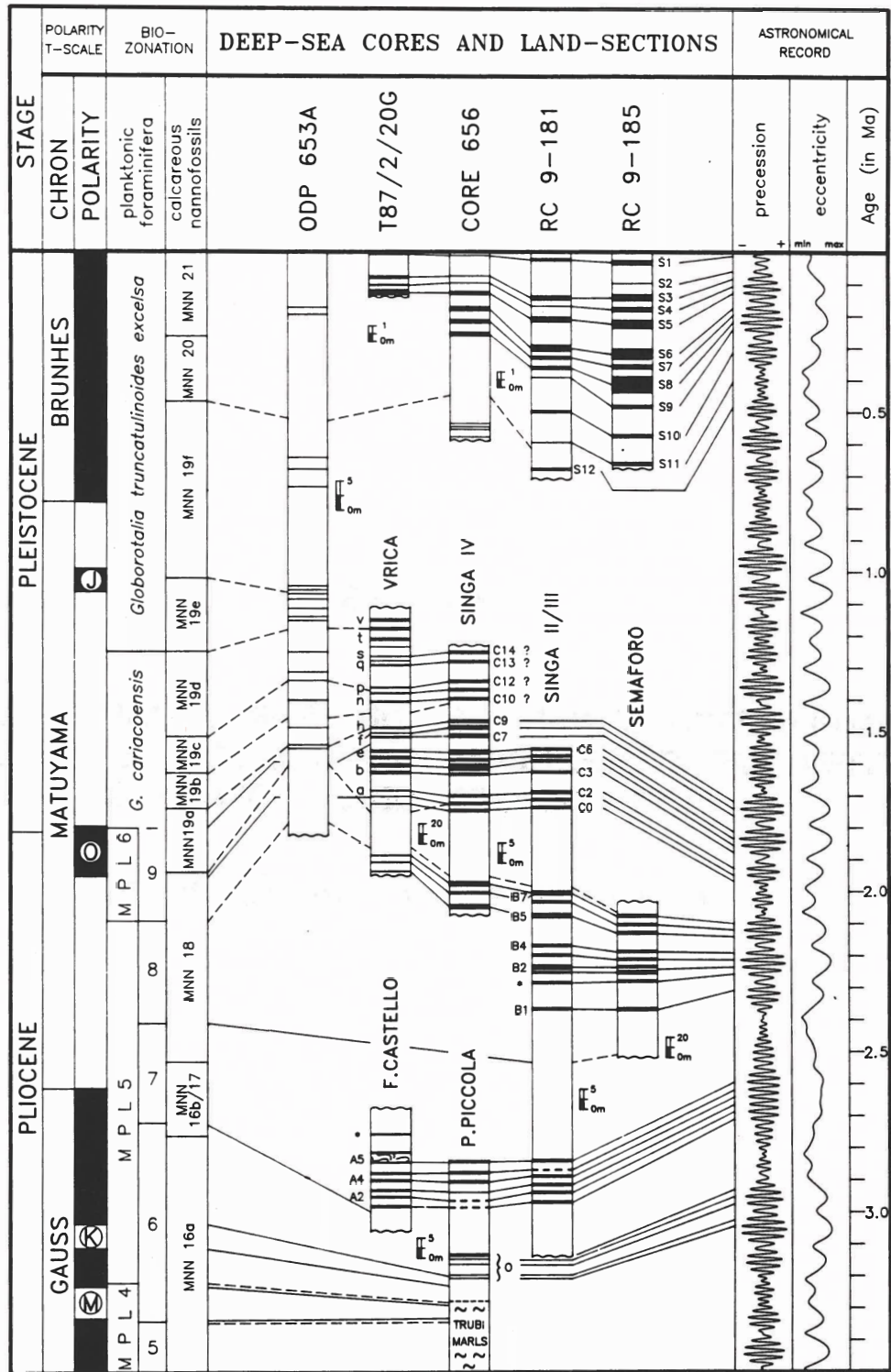
chapter 3

A SIMPLE TWO-LAYERED MODEL FOR SHOALING OF THE EASTERN MEDITERRANEAN PYCNOCLINE DUE TO GLACIO-EUSTATIC SEA LEVEL LOWERING

A SIMPLE TWO-LAYERED MODEL FOR SHOALING OF THE EASTERN MEDITERRANEAN PYCNOCLINE DUE TO GLACIO-EUSTATIC SEA LEVEL LOWERING

E.J. Rohling

Department of Stratigraphy and Micropaleontology, Institute of Earth Sciences, University of Utrecht, P.O.Box 80.021, 3508 TA Utrecht, The Netherlands

ABSTRACT

A simple two-layered model is developed to assess the depth of the permanent pycnocline in the eastern Mediterranean during glacial times. Shoaling of this pycnocline, from its present depth below the euphotic layer to a depth within that layer at glacial times, has been inferred from the planktonic foraminiferal record [Chapter 1]. In this paper, a two-layered model is applied to study the origin of the glacial shoaling of the permanent pycnocline. The model suggests that shoaling is due to glacial sea level lowering. Using literature-based glacial salinity and inflow reduction values, the model yields an estimated depth of about 80 m for the glacial pycnocline. This estimate represents an upper depth limit, since the model discards possible differences in the basin's heat loss between glacial and interglacial times.

INTRODUCTION

In the present-day eastern Mediterranean, the upper part of the permanent pycnocline resides at an average depth of about 150 m [Wüst, 1961; Miller et al., 1970]. This permanent pycnocline essentially is a halocline between the surface water and the Mediterranean Intermediate Water (MIW). Rohling and Gieskes [Chapter 1] discussed high abundances of the planktonic foraminiferal genus *Neogloboquadrina* in pleniglacial sediments of the eastern Mediterranean. They argued that these high abundances indicate that the permanent pycnocline had shoaled to a depth within the euphotic layer, which at present may extend as deep as 120 m. Rohling and Gieskes [Chapter 1], however, were not able to formulate a satisfactory explanation for the shoaling of the permanent pycnocline at glacial times.

In the present paper, a simple two-layered model is described for the eastern Mediterranean. This model is applied to estimate the pycnocline depth under glacial conditions. First, a scenario is evaluated in which the eastern Mediterranean freshwater budget is assumed to have remained equal to the present. Subsequently, an extremely arid glacial scenario is discussed in order to evaluate the effect of reduced glacial precipitation and run-off on pycnocline depth estimates. Finally, possible changes in the presented solutions, which may result from differences in the basin's thermal balance between glacial and interglacial times, are briefly evaluated.

BASIS OF THE MODEL

The eastern Mediterranean is considered very simplified as a two-layered system. The upper layer has temperature T_u, salinity S_u and density ρ_u. The deeper layer has temperature T_d, salinity S_d and density ρ_d. H represents the thickness of the upper layer, which is the approximate thickness of the surface layer above the top of the permanent pycnocline.

The buoyancy loss per unit area (B) necessary to transform a column of upper layer water of thickness H into deeper layer water can then be described [cf. Bryden and Stommel, 1984] as

$$B = (\rho_d - \rho_u) H g \qquad (1)$$

in which $g = 9.81$ m s^{-2} is the acceleration due to gravity.

In the simple two-layered model, the upper layer in the basin results from inflow across the Sicilian sill, and the deeper layer constitutes the outflow. The buoyancy loss (B), due to a net water deficit and heat loss, drives localized transformation of water with surface layer characteristics towards water with deep layer characteristics. As a result, a uniform density difference between the surface and deep layers prevails throughout the rest of the basin. Therefore, in the presented model, the density difference between the surface layer and the deep layer is the same as that between the inflowing and outflowing waters in the Strait of Sicily. As a consequence,

$$\rho_u V_u S_u = \rho_d V_d S_d$$

in which the ratio between the two densities is very close to 1 and the densities may, therefore, be omitted. V_u and V_d respectively indicate the volumes of inflow and outflow through the Strait of Sicily. These volumes are related to the basin's freshwater budget according to

$$V_d = V_u - F$$

in which F stands for the freshwater budget (E-P), i.e. evaporation minus total freshwater input (precipitation and runoff). Now, the difference between the deep layer salinity and the upper layer salinity is defined as dS (= S_d - S_u), so that

$$dS = \frac{S_u}{\dfrac{V_u}{F} - 1} \qquad (2)$$

EFFECTS OF SEA LEVEL LOWERING, USING THE PRESENT-DAY FRESHWATER BUDGET

At present, V_u is about 40 x 10^{12} m^3 yr^{-1} and F about 1.8 x 10^{12} m^3 yr^{-1} [Béthoux, 1979]. Hence, the present-day value of V_u/F is about 22. In this section, F is considered constant through time, but V_u is considered variable. Béthoux [1984] argued that a 100 m sea level lowering probably reduced the inflow across the Gibraltar sill to 60% of its present magnitude, and similar effects are to be expected at the Sicilian sill. If we apply an Inflow Reduction Factor (ϕ), which is the ratio between inflow at times of a sea level low-stand and inflow at present, equation 2 changes to

$$dS = \frac{S_u}{22\phi - 1} \qquad (3)$$

Equation 3 demonstrates that a reduction of inflow due to sea level lowering ($\phi < 1$) would invoke an increase in the salinity contrast between the upper and deeper layers.

The buoyancy loss (B) depends on the freshwater budget (F) of the basin, which is the difference between evaporation (E) and the total freshwater input (P). B also depends on the thermal balance of the basin. Béthoux [1979] emphasized that only about 10% of the heat loss is due to conduction, whereas about 90% results from a release of latent heat by evaporation. Therefore, variations of evaporation and the thermal balance are closely related. Since evaporation (E) was assumed constant through time, I will also assume that the thermal balance of the basin remained constant. In a later section, the possible modifications of the solution, related to variations in the thermal balance, will be evaluated.

Due to the assumption, in this section, that both the freshwater budget and the heat loss at glacial times were equal to those at present, the buoyancy loss (B) may be treated as a constant. Then, if the glacial depth of the interface equals α times its present value (H^P), the glacial value of ($\rho_d - \rho_u$) should equal $1/\alpha$ times the present day value (see equation 1).

As a result of the assumption that heat loss remained equal to the present, variations in $d\rho$ (= $\rho_d - \rho_u$) are linearly related to variations in dS (= $S_d - S_u$) [Béthoux, 1979; Bryden and Kinder, in press]. Furthermore, equation 1 indicates that the glacial $d\rho$ was $1/\alpha$ times the present-day $d\rho$, when the thickness of the surface layer at glacial times was α times that at present (H^P). As a consequence,

$$dS = \left(\frac{1}{\alpha}\right) dS^P \qquad (4)$$

in which the superscript p indicates the present-day value. Combining equations 3 and 4 gives

$$\alpha = \frac{22\phi - 1}{21} \frac{S_u^P}{S_u^g} \qquad (5)$$

in which the superscripts g and p indicate the glacial and present-day values, respectively.

Figure 1 shows the relations between α and S_u^P/S_u^g for several values of ϕ, as described by equation 5. Since αH^P yields the corresponding depth of the interface between the two layers, it is now possible to calculate the interface depth for any estimate of ϕ and S_u^P/S_u^g, using $H^P = 150$ m. The reconstructed interface depth may then be compared to the depth of the base of the euphotic layer (about 120 m), which corresponds to $\alpha = 0.8$.

APPLICATION OF LITERATURE-BASED GLACIAL CONDITIONS

Possible glacial values for ϕ, S_u^P and S_u^g, as suggested in the literature, can be inserted in equation 5. If Béthoux's [1984] proposed reduction of inflow through the Strait of Gibraltar to 60% of its present-day value at times of 100 m sea level lowering may be transposed to the Strait of Sicily, then $\phi = 0.6$, and

41

$$\alpha = 0.57 \frac{S_u^p}{S_u^g}$$

Using the salinity values which Thunell et al. [1987] calculated using the Bryden and Stommel [1984] overmixing model ($S_u^P = 38.2$ and $S_u^g = 40.5$ ppt) a glacial estimate of $\alpha = 0.54$ is found.

At present, the top of the eastern Mediterranean permanent pycnocline resides at an average depth of about 150 m. In terms of the two-layered model, the present-day thickness of the surface layer $H^P = 150$ m. The above calculated $\alpha = 0.54$ at glacial times would then imply that the pycnocline resided at $0.54*150 = 81$ m, which is well within the euphotic layer.

This result suggests that the shallow position of the permanent pycnocline at glacial times, which Rohling and Gieskes [Chapter 1] inferred from the planktonic foraminiferal record, was primarily due to the effects of sea level lowering.

TOTAL GLACIAL ARIDITY (P = 0) SCENARIO

In the two previous sections, the freshwater budget at glacial times was assumed to have been equal to that at present. However, glacial periods are characterized by increased aridity in most circum-Mediterranean countries. In this section, I will discuss to what extent the solution in equation 5 might change due to the incorporation of increased glacial aridity. Therefore, I will assume that total aridity prevailed, which implies that $P = 0$ and, consequently, that $F = E$. The magnitude of E has been derived from Béthoux [1979] as 2.7×10^{12} m^3 yr^{-1}.

In the total aridity scenario, the relation between the variations of dρ and the depth of the interface (equation 1) is somewhat different from that in the constant F scenario described above. This is due to the fact that the buoyancy loss (B) depends on the freshwater budget (F). I will proceed with B increasing proportionally to F. In the total aridity scenario, F is $2.7/1.8 = 1.5$ times larger than at present. Therefore, a similar change in B, to 1.5 times its present value, is used. Then, with the glacial depth of the interface being α times its present value (H^P), the value of d$\rho = (\rho_d - \rho_u)$ should be $1.5/\alpha$ times the present-day value (see equation 1).

Using $F = E = 2.7 \times 10^{12}$ m^3 yr^{-1} and the initial $V_u = 40 \times 10^{12}$ m^3 yr^{-1}, equation 2 gives

$$dS = \frac{S_u}{15\phi - 1} \tag{6}$$

From equation 1, using $H = \alpha H^P$, $B = 1.5 B^P$ and a linear relationship between dρ and dS, it follows that

$$dS = \left(\frac{1.5}{\alpha}\right) dS^P \tag{7}$$

The present-day difference between the salinity of the deeper layer and the salinity of the upper layer $dS^P = S_u^P/21$ (equation 3 with $\phi = 1$). In combination with equations 6 and 7, this gives

$$\alpha = \frac{15\phi - 1}{21} \frac{S_u^P}{S_u^g} \, 1.5 \tag{8}$$

This relation is very similar to the one decribed by equation 5, which indicates that the incorporation of increases in F does not substantially alter the solution obtained from the constant F scenario.

INFLUENCE OF CHANGES IN THE THERMAL BALANCE

In the previous calculations, possible differences in the basin's thermal balance between glacial and present-day times have been neglected. Changes in the thermal balance would induce changes in the buoyancy loss (B). If the net heat loss were greater, the buoyancy loss would be increased.

The minimal value of buoyancy loss increase necessary to 'deepen' the interface down to the base of the euphotic layer, can be calculated using the total glacial aridity scenario. Using the afore-mentioned values of $S_u^P/S_u^g = 0.94$ and $\phi = 0.6$ in that scenario, a 2.25 fold increase of the buoyancy loss (B) would be necessary to 'deepen' the interface position down to the base of the euphotic layer. This implies that the net heat loss from the basin should be increased, imposing a 1.5 fold increase on B superimposed on the 1.5 fold increase in B which resulted already from the change in the freshwater budget (F).

Note, however, that the extreme situation of total glacial aridity is purely hypothetical. If a more realistic increase in F would be applied, the possible change in the basin's thermal balance should impose an increase well over 1.5 times to 'push' the interface down to the base of the euphotic layer.

It is obvious that detailed reconstructions of glacial freshwater and thermal balances are required to determine the interface position more exactly. Nevertheless, our model strongly suggests that reduction of inflow through the Strait of Sicily invoked by glacio-eustatic sea level lowering would account for a shallow position of the interface, at a depth well within the euphotic layer.

CONCLUDING REMARKS

On the basis of their faunal analyses, it was argued by Rohling and Gieskes [Chapter 1] that the upper part of the eastern Mediterranean permanent pycnocline resided within the euphotic layer at glacial times. In order to determine which process(es) caused the glacial pycnocline to reside within the euphotic layer, a simple two-layered model was applied to estimate the surface layer thickness under glacial conditions.

The glacial pycnocline depth estimate from this simple model, discarding probable changes in the basin's thermal balance, ranges well within the euphotic layer. Using literature-based glacial salinity and inflow reduction values, a depth of approximately 80 m was determined for the permanent pycnocline in the pleniglacial eastern Mediterranean. This glacial estimate should be compared with the present-day average pycnocline depth of about 150 m and a euphotic layer thickness of about 120 m. Presumably, incorporation of a realistic increase in heat loss at glacial times, relative to the present, will not result in a deepening of the pycnocline to a depth below the base of the euphotic layer. Such an incorporation would, however, lead to a calculated pycnocline position at a somewhat greater depth than the 80 m mentioned above. Therefore, the latter figure should be considered as an 'upper depth limit'.

The presented model suggests that the shallow permanent pycnocline position in the glacial eastern Mediterranean, as envisaged in chapter 1, resulted from a reduction of surface water inflow through the Strait of Sicily. Béthoux [1984] demonstrated that the low pleniglacial sea level would have invoked an important reduction of water exchange through the Straits of Gibraltar and Sicily. The shallow permanent pycnocline position at pleniglacial times in the eastern Mediterranean seems, therefore, to have resulted essentially from glacio-eustatic sea level lowering.

ACKNOWLEDGEMENTS

REFERENCES

Béthoux, J.P., Budgets of the Mediterranean Sea. Their dependance on the local climate and on characteristics of the Atlantic waters. *Oceanol. Acta, 2*, 157-163, 1979.

Béthoux, J.P., Paléo-hydrologie de la Méditerranée au cours des derniers 20 000 ans. *Oceanol. Acta, 7*, 43-48, 1984.

Bryden, H.L., and T.H. Kinder, Steady two-layer exchange through the Strait of Gibraltar. *Deep-Sea Res.*, in press.

Bryden, H.L., and H.M. Stommel, Limiting processes that determine basic features of the circulation in the Mediterranean Sea. *Oceanol. Acta, 7*, 289-296, 1984.

Miller, A.R., P. Tchernia, H. Charnock, and D.A. McGill, *Mediterranean Sea Atlas of Temperature, Salinity, Oxygen: Profiles and Data from cruises of R.V. Atlantis and R.V. Chain. With distribution of Nutrient Chemical Properties*, edited by A.E. Maxwell et al., 190 pp., Alpine, Braintree, Mass., 1970.

Thunell, R.C., D.F. Williams, and M. Howell, Atlantic-Mediterranean water exchange during the Late Neogene. *Paleoceanography, 2*, 661-678, 1987.

Wüst, G., On the vertical circulation of the Mediterranean Sea. *J. Geophys. Res., 66*, 3261-3271, 1961.
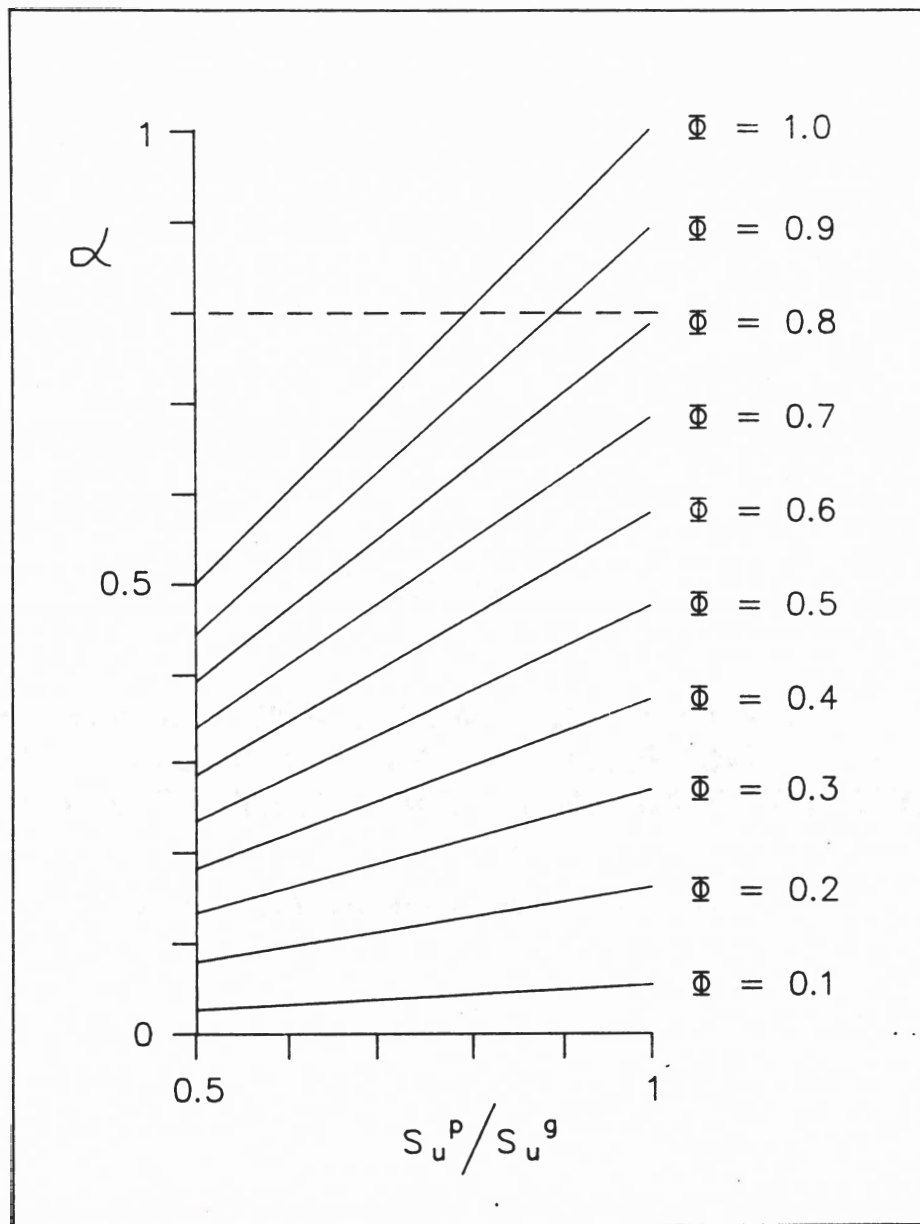
Figure 1. The relations between α and S_u^P/S_u^g for several values of the inflow reduction factor φ. The dashed line indicates the depth of the base of the euphotic layer (about 120 m), which corresponds to α = 0.8, using H = 150 m.

chapter 4

A SIMPLE TWO-LAYERED MODEL FOR VARIATIONS IN THE DEPTH OF THE EASTERN MEDITERRANEAN PYCNOCLINE DUE TO CHANGES IN THE FRESHWATER BUDGET

A SIMPLE TWO-LAYERED MODEL FOR VARIATIONS IN THE DEPTH OF THE EASTERN MEDITERRANEAN PYCNOCLINE DUE TO CHANGES IN THE FRESHWATER BUDGET

Eelco J. Rohling

Department of Stratigraphy and Micropaleontology, Institute of Earth Sciences, University of Utrecht, P.O.Box 80.021, 3508 TA Utrecht, The Netherlands

ABSTRACT

A simple two-layered model is applied to assess the relation between variations in the depth of the permanent pycnocline in the eastern Mediterranean and changes in the basin's freshwater budget. This study is performed to estimate the magnitude of changes in the freshwater budget at times of sapropel formation in the eastern Mediterranean. Pycnocline shoaling, from its present depth below the euphotic layer to a depth within that layer at times of sapropel formation, has been inferred from the planktonic foraminiferal record in chapter 1. The model suggests that a decrease of the eastern Mediterranean freshwater budget, which consists of evaporation minus total freshwater input, by ca. 8.5×10^{11} m^3 yr^{-1} would suffice to induce shoaling of the pycnocline to a depth within the euphotic layer. A consideration of the effects exerted by concomitant changes in the thermal balance suggests that the decrease of the freshwater budget may even have been smaller than the above estimate.

INTRODUCTION

Since the discovery of eastern Mediterranean sapropels in cores collected during the 1947-1948 Swedish Deep-Sea Expedition [Kullenberg, 1952], much effort has been devoted to unravel the oceanographic processes that led to the formation of these anoxic sediments. Olausson [1961] was the first to link sapropel formation to deep water stagnation induced by lowering of the surface water salinities. This hypothesis is supported by the excess lowering of the oxygen isotopic signal at times of sapropel formation [for example Cita et al., 1977; Vergnaud-Grazzini et al., 1977; Williams et al., 1978; Jenkins and Williams, 1984; Thunell and Williams, 1989]. Increased freshwater fluxes from various sources, coeval with sapropel formation, have been positively identified [Rossignol-Strick et al., 1982; Shaw and Evans, 1984; Rossignol-Strick, 1985; Cramp et al., 1988]. De Lange and Ten Haven [1983] suggested that enhanced primary production exerted a major influence on the formation of eastern Mediterranean sapropels.

A new model for sapropel formation, combining increased productivity with decreased deep water formation and a more detailed assessment of the eastern Mediterranean's vertical density structure, has been proposed by Rohling and Gieskes [Chapter 1]. Their model was primarily based on the high abundances of the planktonic foraminiferal genus *Neogloboquadrina* in sapropelic sediments. In the model of Rohling and Gieskes [Chapter 1], increased freshwater input into the basin resulted in shoaling of the density gradient (pycnocline) between the Mediterranean Intermediate Water (MIW) and the surface water, to a depth within the euphotic layer, which at present may extend as deep as 120 m. At present, the upper part of the permanent pycnocline (essentially a halocline) resides at an average depth of about 150 m. Shoaling of the pycnocline to a depth within the euphotic layer would have invoked increased nutrient availability to the euphotic layer, enabling the development of a Deep Chlorophyll Maximum (DCM) and a concomitant increase in the downward flux of organic matter from the euphotic layer (export production). In addition to an increase in

export production, Rohling and Gieskes [Chapter 1] argued that the formation rate of Eastern Mediterranean Deep Water (EMDW) would have decreased. This decrease would have resulted from reduction of the MIW to surface water salinity contrast which, in turn, resulted from increased freshwater input into the basin. Rohling and Gieskes [Chapter 1] envisaged that the combination of increased export production and decreased oxygen advection to deep waters resulted in the development of severely dysoxic to anoxic conditons in the bottom waters, enabling the formation of sapropels.

High abundances of *Neogloboquadrina* in pleniglacial intervals were also attributed to shoaling of the pycnocline to a depth within the euphotic layer [Chapter 1]. In chapter 3, a simple two-layered model was formulated for shoaling of the pycnocline at glacial times, which appeared to occur due to glacio-eustatic sea level lowering. Also, the model demonstrated that the MIW to surface water salinity contrast was increased at glacial times, compared to the present [Chapter 3].

In the present paper, the two-layered model is applied to calculate the magnitude of decreases in the freshwater budget related to pycnocline shoaling at times of sapropel formation in the eastern Mediterranean. Initially, the thermal balance is assumed to have remained equal to the present. Subsequently, I will discuss how incorporation of changes in the thermal balance would affect the presented estimates. In the discussion, the importance of the results for the formulation of an integrated model for sapropel formation is briefly evaluated.

BASIS OF THE MODEL [cf. Chapter 3]

The eastern Mediterranean is considered very simplified as a two-layered system. The upper layer has temperature T_u, salinity S_u and density ρ_u. The deeper layer has temperature T_d, salinity S_d and density ρ_d. H represents the thickness of the upper layer, which is the approximate thickness of the surface layer above the pycnocline.

The buoyancy loss per unit area (B) necessary to transform a column of upper layer water of thickness H to deeper layer water can then be described [cf. Bryden and Stommel, 1984] as

$$B = (\rho_d - \rho_u) H g \qquad (1)$$

in which $g = 9.81$ m s^{-2} is the acceleration due to gravity.

In the simple two-layered model, the upper layer in the basin results from inflow across the Sicilian sill, and the deeper layer consitutes the outflow. The buoyancy loss (B), due to a net water deficit and heat loss, drives localized transformation of water with surface layer characteristics towards water with deep layer characteristics. As a result, a uniform density difference between the surface and deep layers prevails throughout the rest of the basin. Therefore, in the presented model, the density difference between the surface layer and the deep layer is the same as that between the inflowing and outflowing waters in the Strait of Sicily. As a consequence,

$$\rho_u V_u S_u = \rho_d V_d S_d$$

in which the ratio between the two densities is very close to 1 and the densities may, therefore, be omitted. V_u and V_d respectively indicate the volumes of inflow and outflow across the Sicilian sill. These volumes are related to the basin's freshwater budget according to

$$V_d = V_u - F$$

in which F stands for the freshwater budget, which is defined as evaporation minus total freshwater input (F = E-P). Therefore, the difference between the deep layer salinity and the upper layer salinity is defined as dS (=S_d - S_u), so that

$$dS = \frac{S_u}{\dfrac{V_u}{F} - 1} \tag{2}$$

MODEL TO PORTRAY EFFECTS OF DECREASES IN THE FRESHWATER BUDGET

The model will now be applied to study changes in pycnocline depth due to decreases in the freshwater budget (F = E-P), a situation that prevailed at times of sapropel formation in the eastern Mediterranean (see introduction). In this section, I will assume that the thermal balance remained constant. Therefore, buoyancy loss (B) decreases proportionally to F.

The depth of the interface at times of sapropel formation is defined as α times its present value (H^p). The freshwater balance at times of sapropel formation is characterized as γ times its present value (F^p). Since we consider the variation in buoyancy loss (B) to be proportional to that in F, the buoyancy loss at times of sapropel formation is also defined as γ times its present value (B^p). Equation 1 then indicates that the density difference between the upper layer and the deeper layer, at times of sapropel formation, should equal γ/α times its present-day value $d\rho^p = (\rho_d - \rho_u)^p$. Summarized,

$$H = \alpha \, H^p$$
$$F = \gamma \, F^p$$
$$B = \gamma \, B^p$$
$$d\rho = \left(\frac{\gamma}{\alpha}\right) d\rho^p$$

in which the superscript p indicates present-day values. As argued before, sapropel formation coincided with decreased values of F and, therefore, $0 \le \gamma \le 1$. Furthermore, since the basin's freshwater budget influences the surface water inflow (V_u) through the Strait of Sicily, a decrease in F, relative to the present, will invoke a reduction of inflow. This reduction of inflow, imposed by variation of γ, is expressed by a coefficient Ω. As with γ, also $0 \le \Omega \le 1$. Hence,

$$F = \gamma \, F^p$$
$$V_u = \Omega \, V_u^p$$

At present, V_u is about 40×10^{12} m^3 yr^{-1} and F about 1.8×10^{12} m^3 yr^{-1} [Béthoux, 1979]. Therefore, the value of V_u^p/F^p is about 22, and

$$\frac{V_u}{F} = 22\left(\frac{\Omega}{\gamma}\right)$$

This relation may be used in combination with equation 2, so that the difference between salinities S_d and S_u can be expressed as

$$dS = \frac{S_u}{22\left(\dfrac{\Omega}{\gamma}\right) - 1} \qquad (3)$$

Since heat loss was assumed constant, variations in $d\rho$ are linearly related to variations in dS [Béthoux, 1979; Bryden and Kinder, in press]. Therefore,

$$dS = \left(\frac{\gamma}{\alpha}\right) dS^P \qquad (4)$$

Combining equations 3 and 4 gives

$$\alpha = \frac{22\Omega - \gamma}{21} \frac{S_u^P}{S_u^s} \qquad (5)$$

To solve equation 5, the relation between γ and Ω should be defined, expressing how changes in the eastern Mediterranean freshwater budget affect the volume of surface water flowing into the basin across the Sicilian sill. I will apply the result obtained by Bryden and Kinder [in press], which portrays the relation between the freshwater budget of the entire Mediterranean and inflow through the Straits of Gibraltar. This study suggested that, approximately, $\gamma = \Omega^2$.

Figure 1 shows the relations between α and S_u^P/S_u^s for several values of Ω. Since αH yields the corresponding depth of the interface between the two layers, it is now possible to calculate the interface depth for any estimate of Ω and S_u^P/S_u^s, using $H = 150$ m. The reconstructed interface depth may then be compared to the depth of the base of the euphotic layer (ca. 120 m), which corresponds to $\alpha = 0.8$.

APPLICATION OF LITERATURE-BASED CONDITIONS AT TIMES OF SAPROPEL FORMATION

In chapter 1, it was argued that the top of the eastern Mediterranean permanent pycnocline resided within the euphotic layer at times of sapropel formation and, therefore, that $\alpha < 0.8$. Also, the salinity of the eastern Mediterranean surface layer seems to have been considerably reduced at times of sapropel formation, compared to that at present. According to Thunell and Williams [1989], $S_u^s \approx 36$ ppt. These authors obtained this result from oxygen isotope values, calibrated to a present-day average surface layer salinity (S_u^P) of 38.8 ppt. Using these values and $\alpha < 0.8$, we find $\Omega < 0.73$ and, therefore, $\gamma < 0.53$.

In the eastern Mediterranean, the present-day value of F (= E-P) is about 1.8×10^{12} m^3 yr^{-1} [Béthoux, 1979]. At times of sapropel formation, the freshwater budget should have

been decreased, at least, to $\gamma = 0.53$ times its present value, which implies a reduction to 9.5 x 10^{11} m^3 yr^{-1}. That is 8.5 x 10^{11} m^3 yr^{-1} less than at present.

Béthoux [1984] calculated that an increase of the Nile discharge to 2.5 times its present (pre-Aswan) volume, which he derived from Rossignol-Strick et al. [1982], would invoke stagnant conditions below 1000 meters waterdepth in the eastern Mediterranean. Since the present-day (pre-Aswan) Nile discharge amounts to approximately 9 x 10^{10} m^3 yr^{-1} [Béthoux, 1984], however, a 2.5 fold increase would not suffice to account for the decrease of the freshwater budget by, at least, 8.5 x 10^{11} m^3 yr^{-1} as calculated above. In the hypothetical case that the Nile was the exclusive source for the total excess of freshwater and that the "local" eastern Mediterranean climate remained constant, the Nile's discharge should have been, at least, 10.4 times that at present (pre-Aswan).

If the estimate used by Béthoux [1984] is correct, which implies that the Nile's discharge was only 2.5 times greater than at present (pre-Aswan), then the Nile provided an excess freshwater input of 1.35 x 10^{11} m^3 yr^{-1}. Consequently, variations in the "local" eastern Mediterranean climate should have induced, at least, an additional 7.15 x 10^{11} m^3 yr^{-1} decrease in the freshwater budget (E-P) of the eastern Mediterranean.

Note, however, that variations in the freshwater budget depend on the amount of both evaporation (E) and freshwater input (P). Evaporation is entirely related to the "local" eastern Mediterranean climate. On the contrary, freshwater input is influenced both by the "local" eastern Mediterranean climate and, via the Nile river, by the "distant" monsoonal system of the Indian Ocean. It would be easiest to proceed calculating increases of freshwater input assuming a constant evaporation (E). However, such an assumption would be erroneous if part of the freshwater input resulted from "local" Mediterranean precipitation systems. Increased activity of such systems would not only increase the freshwater input, but also the amount of cloud-coverage and the moisture content of the air. These effects would invoke a significant reduction of the evaporation (E).

Following the above arguments, variations in the Nile river's discharge are not coupled to the evaporation rate in the eastern Mediterranean. Therefore, if the decrease of the freshwater budget at times of sapropel formation were entirely due to an increase in the Nile's discharge, the evaporation could be considered constant. On the contrary, as soon as variations in the "local" eastern Mediterranean climate are inferred, changes in the evaporation rate must be considered.

In the following, I will consider variations in evaporation (E) and variations in the "local" part of the freshwater input ($P_{loc.}$ = P - Nile discharge) as equally distributed according to their relative present-day proportions. At present, evaporation (E) amounts to 27 x 10^{11} m^3 yr^{-1} and total freshwater input (P) to 9 x 10^{11} m^3 yr^{-1} [Béthoux, 1979], while the (pre-Aswan) contribution of Nile discharge to the latter figure is 0.9 x 10^{11} m^3 yr^{-1} [Béthoux, 1984]. Hence, $P_{loc.}$ = 8.1 x 10^{11} m^3 yr^{-1}. The relative present-day proportions of E and $P_{loc.}$, therefore, are 3.3 : 1.

Previously, I concluded that, if the Nile's discharge at times of sapropel formation was indeed 2.5 times that at present, variations in the "local" eastern Mediterranean climate should, at least, have accounted for a decrease of 7.15 x 10^{11} m^3 yr^{-1} in the eastern Mediterranean freshwater budget (F = E-P). Using the ratio 3.3 : 1, this decrease in the freshwater budget can be subdivided into a decrease of E amounting 5.49 x 10^{11} m^3 yr^{-1}, and an increase of $P_{loc.}$ amounting 1.66 x 10^{11} m^3 yr^{-1}; variations of ca. 20%.

51

INFLUENCE OF CHANGES IN THE THERMAL BALANCE

In the previous sections, I have neglected changes in the thermal balance of the eastern Mediterranean, which would accompany changes in evaporation (E) since 90% of the heat loss results from release of latent heat by evaporation [Béthoux, 1979]. Hence, decreases in the buoyancy loss (B) were assumed to have been proportional to decreases in the freshwater budget (F = E-P). However, if E was not constant, but reduced, B would not have decreased proportionally to F, but faster. If β is applied as a coefficient describing the additional decrease in B resulting from variation in the thermal balance, with $0 \leq \beta \leq 1$, then

$$H = \alpha \; H^P$$
$$B = \beta\gamma \; B^P$$
$$d\rho = \left(\beta \frac{\gamma}{\alpha}\right) d\rho^P$$

As a result, equation 5 changes to

$$\alpha = \beta \; \frac{22\Omega - \gamma}{21} \; \frac{S_u^P}{S_u^s} \tag{6}$$

Equation 6 indicates that incorporation of the effects of decreased net heat loss allows a larger value for γ than the scenario in the previous sections, which assumed an invariable thermal balance. Therefore, using the invariable thermal balance scenario to calculate γ with $\alpha < 0.8$ results in a maximum estimate for the change of F necessary to raise the interface into the euphotic layer. Incorporation of possible changes in the thermal balance would result in a smaller estimate for the decrease of F.

These considerations obviate the need for detailed assessment of the eastern Mediterranean thermal balance, in both the present-day climatic configuration and that at times of sapropel formation.

DISCUSSION AND CONCLUSIONS

On the basis of their faunal analyses, Rohling and Gieskes [Chapter 1] argued that the permanent pycnocline in the eastern Mediterranean resided within the euphotic layer at times of sapropel formation. In chapter 3, I have formulated a simple two-layered model to assess pycnocline depth variations in the eastern Mediterranean resulting from sea-level lowering. In the present paper, this model was adapted to study the relation between pycnocline depth variations and decreases in the eastern Mediterranean freshwater budget (F = E-P), assuming that sea level remained equal to the present. At first, the thermal balance of the basin was also assumed constant. Afterwards, I briefly discussed how variations in the thermal balance would affect the solution.

Using the invariable thermal balance scenario, it was calculated that the eastern Mediterranean freshwater budget (F = E-P) should have decreased by, at least, 8.5×10^{11} m^3 yr^{-1} to induce shoaling of the pycnocline into the euphotic layer. If this were exclusively due to an increase in the Nile river's discharge, the calculated change in the freshwater budget would indicate that the Nile discharged, at least, 10.4 times the present (pre-Aswan) volume, at times of sapropel formation.

Rohling and Hilgen [Chapter 2] reviewed paleoclimatological reconstructions concerning times of sapropel formation. They concluded that, although the Nile river was important, it certainly was not the only enhanced freshwater source. The "local" eastern Mediterranean precipitation was substantially increased as well. Presumably, this increase of "local" precipitation resulted from increased activity of Mediterranean depressions, which invoke a net transport of moisture from the west towards the eastern Mediterranean [Chapter 2]. In the present paper, I emphasized that such an increased activity would, additionally, induce a decrease in the eastern Mediterranean evaporation (E), due to increases in cloud-coverage and moisture content of the air. Both the increase of net moisture transport from the west and the decrease of evaporation, as consequences of increased activity of Mediterranean depressions, tend to lower the eastern Mediterranean freshwater budget (F = E-P).

Considering a similar increase in the Nile river discharge at times of sapropel formation as did Béthoux [1984], which is 2.5 times the present (pre-Aswan) flux, the Nile accounted for an excess of only 1.35×10^{11} m^3 yr^{-1} freshwater. Since the freshwater budget (F) should have been decreased by, at least, 8.5×10^{11} m^3 yr^{-1} to invoke pycnocline shoaling into the euphotic layer, the "local" climate should account for a decrease in F amounting 7.15×10^{11} m^3 yr^{-1}. I argued that this may be accomplished by coeval variations of ca. 20% in evaporation (E; decreased) and "local" freshwater input (P_{loc}; increased). These variations suggest a (roughly) 20% increased intensity of the westerly system of Mediterranean depressions at times of sapropel formation.

A brief assessment of the effects exerted by changes in the thermal balance, which would accompany variations of evaporation, shows that the freshwater balance may have been decreased even less than calculated with the invariable thermal balance scenario. Unfortunately, however, it is not yet possible to make a detailed reconstruction of the thermal balance through geologic time.

Importance of the results for the formulation of an integrated model of sapropel formation

Since $\gamma \approx \Omega^2$, while $0 \leq \gamma \leq 1$, equation 3 shows that a reduction of the freshwater budget, to γ times the present-day value, would result in a lowering of dS, which is the salinity contrast across the pycnocline. As envisaged already in chapter 1, such a decrease in the MIW to surface water salinity contrast would affect the rate of formation of Eastern Mediterranean Deep Water (EMDW) in the Adriatic Sea [cf. Mangini and Schlosser, 1986]. On the large Adriatic shelf, surface waters of relatively low salinity are subject to cold and dry northeasterly winds ("Bora") in the winter season. As a result, a subsurface outflow develops, which consists of cold water with an increased salinity. The salinity of this subsurface outflow, however, remains lower than that of the MIW. Upon interaction with MIW, which has a higher temperature and salinity, densification generates water (EMDW) which, although lower in salinity, is cooler and of higher density than MIW. As a consequence, EMDW settles below MIW, filling the deeper parts of the eastern Mediterranean basin [Artegiani et al., 1989]. The process of densification, which generates EMDW from the two initial components, would be negatively influenced by a decrease in the MIW to surface water salinity (i.e. density) contrast, during periods with a decreased freshwater budget relative to the present. As a consequence, the EMDW formation rate would also be decreased during such periods, inducing a reduction of oxygen advection to deeper waters.

The reduction of the freshwater budget necessary to invoke pycnocline shoaling into the euphotic layer, as estimated with the two-layered model, can serve as a basis for the determination of differences in the eastern Mediterranean phosphate budget between times of

sapropel formation and the present. Such a study will give an order of magnitude estimation for the EMDW formation rate and, therefore, the flushing-time of the eastern Mediterranean at times of sapropel formation [see Chapter 5].

ACKNOWLEDGEMENTS

REFERENCES

Artegiani, A., R. Azzolini, and E. Salusti, On the dense water in the Adriatic Sea, *Oceanol. Acta, 12*, 151-160, 1989.

Béthoux, J.P., Budgets of the Mediterranean Sea. Their dependance on the local climate and on characteristics of the Atlantic waters. *Oceanol. Acta, 2*, 157-163, 1979.

Béthoux, J.P., Paléo-hydrologie de la Méditerranée au cours des derniers 20 000 ans. *Oceanol. Acta, 7*, 43-48, 1984.

Bryden, H.L., and T.H. Kinder, Steady two-layer exchange through the Strait of Gibraltar. *Deep-Sea Res., in press.*

Bryden, H.L., and H.M. Stommel, Limiting processes that determine basic features of the circulation in the Mediterranean Sea. *Oceanol. Acta, 7*, 289-296, 1984.

Cita, M.B., C. Vergnaud-Grazzini, C. Robert, H. Chamley, N. Chiaranfi, and S. d'Onofrio, Paleoclimatic record of a long deep sea core from the eastern Mediterranean, *Quat. Res., 8*, 205-235.

Cramp, A., M. Collins, and R. West, Late Pleistocene-Holocene sedimentation in the NW Aegean Sea: a palaeoclimatic palaeoceanographic reconstruction, *Palaeogeogr., Palaeoclimatol., Palaeoecol, 68*, 61-77, 1988.

De Lange, G.J., and H.L. Ten Haven, Recent sapropel formation in the eastern Mediterranean, *Nature, 305*, 797-798, 1983.

Jenkins, J.A., and D.F. Williams, Nile water as cause of eastern Mediterranean sapropel formation: evidence for and against. *Mar. Micropaleontol, 9*, 521-534, 1984.

Kullenberg, B., On the salinity of the water contained in marine sediments, *Medd. Oceanogr. Inst. Goteborg, 21*, 1-38, 1952.

Olausson, E., Studies of deep-sea cores, *Rep. Swed. Deep Sea Exped. 1947-1948, 8*, 353-391, 1961.

Rossignol-Strick, M., W. Nesteroff, P. Olive, and C. Vergnaud-Grazzini, After the deluge: Mediterranean stagnation and sapropel formation. *Nature, 295*, 105-110, 1982.

Rossignol-Strick, M., Mediterranean Quaternary sapropels, an immediate response of the African monsoon to variations of insolation, *Palaeogeogr., Palaeoclimatol., Palaeoecol., 49*, 237-263, 1985.

Shaw, H.F. and G. Evans, The nature, distribution and origin of a sapropelic layer in sediments of the Cilicia Basin, northeastern Mediterranean, *Mar. Geol., 61*, 1-12, 1984.

Thunell, R.C., and D.F. Williams, Glacial-Holocene salinity changes in the Mediterranean Sea: hydrographic and depositional effects. *Nature, 338*, 493-496, 1989.

Vergnaud-Grazzini, C., W.B.F. Ryan, and M.B. Cita, Stable isotope fractionation, climatic change and episodic stagnation in the eastern Mediterranean during the late Quaternary, *Mar. Micropaleontol.*, *2*, 353-370, 1977.

Williams, D.F., R.C. Thunell, and J.P. Kennett, Periodic fresh-water flooding and stagnation of the eastern Mediterranean Sea during the late Quaternary, *Science*, *201*, 252-254, 1978.
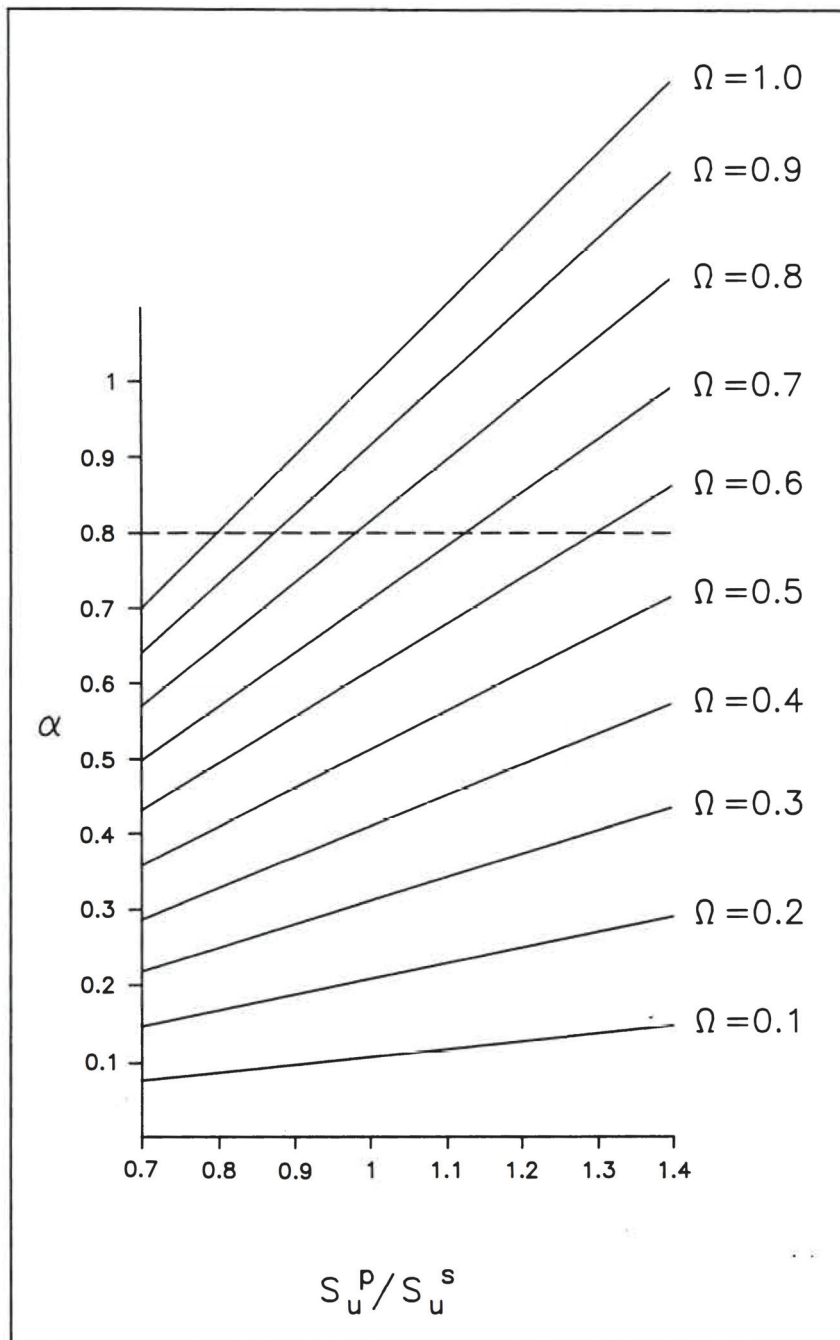
Figure 1. The relations between α and S_u^P/S_u^s for several values of the inflow reduction factor Ω. The dashed line indicates the depth of the base of the euphotic layer (about 120 m), which corresponds to $\alpha = 0.8$, using $H = 150$ m. The reduction of the freshwater budget, expressed by the coefficient γ, can be derived directly from Ω, using $\gamma = \Omega^2$.

chapter 5

ESTIMATING THE FLUSHING-TIME OF THE EASTERN MEDITERRANEAN AT TIMES OF SAPROPEL FORMATION

ESTIMATING THE FLUSHING-TIME OF THE EASTERN MEDITERRANEAN AT TIMES OF SAPROPEL FORMATION

Eelco J. Rohling

Department of Stratigraphy and Micropaleontology, Institute of Earth Sciences, University of Utrecht, P.O.Box 80.021, 3508 TA Utrecht, The Netherlands

ABSTRACT

A calculation is presented of the eastern Mediterranean phosphate budget at times of sapropel formation. This calculation is based on the freshwater budget reduction determined in chapter 4 with a model relating pycnocline depth variations to changes in the freshwater budget. The phosphate budget calculations give an estimate of the contribution of Eastern Mediterranean Deep water to the subsurface outflow across the Sicilian sill, at times of sapropel formation. This estimate is used to calculate the flushing-time of the deep eastern Mediterranean, relative to the present-day flushing-time of ca. 50 years. The flushing-time at times of sapropel formation is determined at approximately 1800 years. The average phosphate concentration of the subsurface flow across the Sicilian sill into the western Mediterranean would, according to the model, have been increased from its present-day value of 0.2 to a value of 0.25 μmol l^{-1} at times of sapropel formation, i.e. an increase of 30%.

INTRODUCTION

The qualitative model for sapropel formation in the eastern Mediterranean, which Rohling and Gieskes [Chapter 1] proposed, combined increases in export production with reductions of deep water formation. Increased export production, i.e. increased downward flux of organic matter from the euphotic layer, would have resulted from shoaling of the eastern Mediterranean pycnocline to a depth within the euphotic layer. Such a shoaling would be conducive to increased nutrient availability in the sub-pycnoclinal part of the euphotic layer and the consequent development of a Deep Chlorophyll Maximum (DCM), as reflected in the planktonic foraminiferal record [Chapter 1]. The inferred decrease in the formation rate of Eastern Mediterranean Deep water (EMDW) would have resulted from a decrease in the density gradient between the surface water and the Mediterranean Intermediate Water (MIW). Both the shoaling of the pycnocline, which essentially is a halocline between the surface water and the MIW, and the decrease in EMDW formation rate would have resulted from increased freshwater input into the basin [Chapter 1].

In chapter 4 a model was presented for pycnocline depth variations in the eastern Mediterranean, resulting from changes in the freshwater budget of that basin. In this model, sea level was assumed to have remained equal to the present. The model showed that a decrease in the eastern Mediterranean freshwater budget (= evaporation - total freshwater input) to 0.53 times its present value would suffice to raise the pycnocline to the base of the euphotic layer. I also calculated that such a 47% decrease in the freshwater budget could have resulted from coeval increases in the freshwater discharge from the Nile (by 150%) and the activity of Mediterranean depressions (by 20%). Furthermore, the model presented in chapter 4 indicated that a reduction of the eastern Mediterranean freshwater budget would indeed induce a decrease in the MIW to surface water salinity (i.e. density) gradient, as envisaged in chapter 1. Such a reduction in the MIW to surface water salinity would favor a decline in the EMDW formation rate.

The inferred decline of the EMDW formation rate would imply that oxygen advection to deeper (and bottom) waters would decrease. The combination of increased export production and decreased oxygen advection to deeper waters would result in the development of dysoxic conditions in deeper waters. The truly anoxic conditions that prevailed during the formation of most sapropels, as witnessed by the frequent presence of "benthic deserts", may have been restricted to thin layers at the sea-floor [Rohling et al., in prep.]. Such an oxygen minimum at the sea-floor might develop due to mineralization of organic particles that have rapidly sunk through the water-column, and it would imply that most of the water-column may still have contained some oxygen (dysoxic conditions), while truly anoxic conditions were present only in a "blanket" at the bottom.

The model presented in chapter 4 did provide an estimate for the reduction in the freshwater budget necessary to invoke pycnocline shoaling into the euphotic layer. The relation between reduction of the MIW to surface water salinity gradient and variations in the EMDW formation rate, however, could not be quantitatively expressed. Other methods should provide an estimate of the order of magnitude of EMDW formation and, therefore, of the flushing-time of the deep eastern Mediterranean at times of sapropel formation, relative to the present.

In their discussion on the cause of eastern Mediterranean anoxic events, Sarmiento et al. [1988] focused on the distribution of phosphate, a limiting nutrient, in the water column. Sarmiento et al. [1988] concluded that only an extremely weak anti-estuarine circulation or a reversed (estuarine) circulation in the eastern Mediterranean might explain the phosphate distributions they inferred from the literature. In this paper, I will discuss variations in the phosphate budget according to the model for the hydrographic configuration at times of sapropel formation as formulated in the chapters 1 and 4. This model places much less severe constraints to the circulation than the solutions presented by Sarmiento et al. [1988]. As a result, an order of magnitude estimate of the rate of EMDW formation - at times of sapropel formation - can be determined.

THE PHOSPHATE BUDGET
The solution is based on the following prerequisites [cf. Sarmiento et al., 1988]:

1) severely dysoxic to anoxic conditions prevailed in the bottom waters, which implies that (nearly) all oxygen had been consumed by mineralization, and nutrient concentrations had been increased accordingly. The Redfield ratio may, therefore, be used to link variations in the oxygen and nutrient concentrations.

2) the extra input of nutrients via rivers is delimited by the 47% decrease of the freshwater budget necessary to invoke shoaling of the pycnocline into the euphotic layer [Chapter 4], in combination with the average nutrient content of river water which is assumed to have remained constant through time.

3) export of nutrients via subsurface outflow towards the western Mediterranean should be low enough to prevent the western Mediterranean from becoming loaded with nutrients. This prerequisite is based on the fact that there has been no known sapropel formation in the western Mediterranean, coeval with the formation of sapropels in the eastern basin [Sarmiento et al., 1988].

Similar to Sarmiento et al. [1988], I will assume that the PO_4 concentration of inflow across the Sicilian sill was constant through time, at 0.126 μmol l^{-1}. The present-day phosphate concentration of outflow was set at an average 0.2 μmol l^{-1}. Sarmiento et al. [1988] used the Redfield ratio to calculate deep water PO_4 concentrations - $[PO_4]_d$ - at times of sapropel

formation, assuming that the deep water had gone completely anoxic - $[O_2]_d = 0$ µmol l^{-1}. This was performed using

$$[O_2]_d = [O_2]_u - R \, [PO_4]_d \qquad (4)$$

where R is the Redfield ratio, the subscript d indicates deep water value and the subscript u indicates surface water (upper layer) value. In the present paper, a value will be used of $R \approx$ 169, similar to that used by Sarmiento et al. [1988] (after Takahasi et al. [1985]). Sarmiento et al. [1988] reasoned that $[O_2]_u \approx 231$ µmol l^{-1}. Using $[O_2]_d = 0$ µmol l^{-1}, equation 4 gives $[PO_4]_d$ = 1.37 µmol l^{-1}. Note that this figure would be smaller if the deep water would not have gone completely anoxic, but only dysoxic with an anoxic "blanket" at the sea-floor. Sarmiento et al. [1988], on the contrary, argued that the estimated value of $[PO_4]_d = 1.37$ µmol l^{-1} may even be too low. In the following discussion of the phosphate budget at times of sapropel formation, the value of $[PO_4]_d = 1.37$ µmol l^{-1} will be applied.

Since the model presented in chapter 4 was based on the volumes of the exchange transport across the Sicilian sill and the freshwater budget determined by Béthoux [1979], I will continue to use these values, in spite of the fact that they are significantly larger than the values used by Sarmiento et al. [1988]. Thus, the volume of inflow across the Sicilian sill V_u = 1268 x 10^6 l s^{-1}, and the volume of outflow V_d = 1211 x 10^6 l s^{-1}. The present-day phosphate concentration of the inflowing water $[PO_4]_u = 0.126$ µmol l^{-1}, and that of outflowing water $[PO_4]_d = 0.2$ µmol l^{-1} [Sarmiento et al., 1988]. Therefore, inflow accounts for an influx of phosphate of 160 mol s^{-1}, while outflow accounts for an efflux of 240 mol s^{-1}. In order to maintain a steady state, the input rate of phosphate into the eastern Mediterranean from the atmosphere and via rivers should be 80 mol s^{-1} (see Table 1)

PRESENT			
	Volume (x 10^6 l s^{-1})	[PO$_4$] (µmol l^{-1})	PO$_4$ flux (mol s^{-1})
inflow	1268	0.126	160
freshwater budget	57		
outflow	1211	0.2	240
PO$_4$ input via rivers and atmosphere			80

Table 1. Volumes, phosphate concentrations and resultant phosphate fluxes in the present-day situation. Volumes as determined by Béthoux [1979]. Phosphate concentrations as determined by Sarmiento et al. [1988].

As stated before, the model presented in chapter 4 indicates that a reduction in the freshwater budget to 0.53 times the present-day value would invoke shoaling of the pycnocline to the base of the euphotic layer. Also in chapter 4, I argued that such a reduction may have resulted from an increase in the Nile river discharge (by 150%; see also Béthoux [1984]) and an intensification of the westerly system of Mediterranean depressions (by 20%). A 150% increase of Nile discharge corresponds to an excess freshwater flow of 4.3 x 10^6 l s^{-1}. A 20% intensification of the Mediterranean depression activity would not only result in a 20% decrease in

evaporation, but also in an excess freshwater input of 5.3×10^6 l s^{-1}, in the form of both precipitation and runoff [see Chapter 4]. For the phosphate budget, the excess amount of precipitation is not very interesting, but it is very important to estimate the excess amount of runoff. According to Tchernia [1980], the ratio between precipitation and runoff is about 2.5 in the Mediterranean. Therefore, a 20% intensification of the depression activity would invoke a runoff excess of ca. 1.5×10^6 l s^{-1}. Combining this figure with the excess flow from the Nile, it appears that the 47% reduction in the freshwater budget calculated in chapter 4 would have consisted, in part, of an excess freshwater input from the Nile and other rivers, amounting 5.8×10^6 l s^{-1}.

Sarmiento et al. [1988] summarized that the average phosphate concentration in the rivers discharging into the eastern Mediterranean is ca. 4.7 μmol l^{-1}. Assuming that the average phophate concentration in river water remained constant through time, the above calculated 5.8×10^6 l s^{-1} of excess runoff would produce an excess phosphate flux into the eastern Mediterranean of 27.3 mol s^{-1}, in addition to the background (= present-day) flux of 80 mol s^{-1} (cf. Table 1). Such an excess influx of PO$_4$ would be balanced by an outflow of 19.9×10^6 l s^{-1} deep water, since we determined earlier in this paper that $[PO_4]_d = 1.37$ μmol l^{-1} (equation 1, with $R = 169$, $[O_2]_u = 231$ μmol l^{-1} and $[O_2]_d = 0$ μmol l^{-1}). In other words, an outflow of 19.9×10^6 l s^{-1} of water from deep anoxic layers would balance the excess phosphate influx resulting from the increase in runoff (see Table 2).

SAPROPEL - TIME			
	Volume (x 10^6 l s^{-1})	[PO$_4$] (μmol l^{-1})	PO$_4$ flux (mol s^{-1})
inflow	0.73 x 1268 = 925.6	0.126	116.6
freshwater budget	0.53 x 57 = 30.2		
input via rivers and atmosphere: background (=present-day input)			80
excess input via Nile and Eurasian rivers	5.8	4.7	27.3
OUTFLOW total	925.6 - 30.2 = 895.4		
anoxic	19.9	1.37	27.3
other	895.4 - 19.9 = 875.5	0.22	196.6

Table 2. Volumes, phosphate concentrations and resultant phosphate fluxes at times of sapropel formation, calculated using the model for the hydrographic configuration presented in chapter 4. In that model, the freshwater budget was reduced to 0.53 times its present-day value, resulting in a reduction of inflow across the Sicilian sill to 0.73 times its present-day value. In the present paper, it was argued that the 47% reduction of the freshwater budget consisted, in part, of an excess river discharge of 5.8×10^6 l s^{-1}, which has an average phosphate concentration of 4.7 μmol l^{-1} [Sarmiento et al., 1988]. The total volume of outflow could be determined as: 0.73 times the present-day inflow minus 0.53 times the present-day freshwater budget. Outflow has been subdivided in an anoxic part, which should have had a

phosphate concentration of ca. 1.37 µmol l^{-1} (as calculated with equation 1) and which should have balanced the excess riverine phosphate input, and a part named "other outflow", which accounts for the difference between total outflow and anoxic outflow.

In chapter 4, I calculated that inflow across the Sicilian sill would be reduced to 0.73 times its present-day value, if the freshwater budget were reduced to 0.53 times the present-day value. This means that the inflow across the Sicilian sill was reduced to 925.6 x 10^6 l s^{-1}. The outflowing volume, equal to inflow minus the freshwater budget, would then amount to 895.4 x 10^6 l s^{-1} (Table 2). The amount of outflow from deep anoxic layers (with [PO$_4$] = 1.37 µmol l^{-1}) was determined at 19.9 x 10^6 l s^{-1} and, therefore, "other outflow" consists of a volume of (895.4 - 19.9) x 10^6 = 875.5 x 10^6 l s^{-1}. Consequently, the average phosphate concentration of this "other outflow" would be ca. 0.22 µmol l^{-1} (Table 2).

In the described scenario, the total of deep outflow across the Sicilian sill consists of 2 components, viz. 875.5 x 10^6 l s^{-1} with an average [PO$_4$] ≈ 0.22 µmol l^{-1} and 19.9 x 10^6 l s^{-1} of water from deep anoxic layers with [PO$_4$] = 1.37 µmol l^{-1}. The average phophate concentration of subsurface outflow across the Sicilian sill into the western Mediterranean would, therefore, be 0.25 µmol l^{-1}, which is very similar to the present-day value of 0.2 µmol l^{-1}. This demonstrates that the presented solution of the phosphate budget would not drive the western Mediterranean to an extreme nutrient trap, which is a major requirement defined by Sarmiento et al. [1988].

The very low contribution of anoxic water (19.9 x 10^6 l s^{-1} with [PO$_4$] = 1.37 µmol l^{-1}) to the total subsurface outflow across the Sicilian sill suggests that the deep anoxic layers were characterized by very poor ventilation. Thus, a pattern of the vertical circulation at times of sapropel formation emerges, which consists of three layers. The upper layer consists of the surface water flowing into the basin from the western Mediterranean, the intermediate layer accounts for most of the subsurface outflow towards the western Mediterranean, and the deepest layer has become dysoxic/anoxic as a result of increased oxygen consumption and poor ventilation.

THE FLUSHING-TIME OF THE DEEP EASTERN MEDITERRANEAN AT TIMES OF SAPROPEL FORMATION

At present, outflow through the Strait of Sicily drags water from depths well below sill-depth. This so-called Bernoulli flow depends on the density stratification below sill depth, and the velocity of outflow near the bottom of the strait [Stommel et al., 1973]. There is no consensus as to whether the present-day Bernoulli flow over the Sicilian sill is powerful enough to be the exclusive mechanism responsible for ventilation of even the deepest eastern Mediterranean basins. Béthoux [1984] determined that this is indeed the case, but Bryden and Stommel [1984] calculated, using their overmixing model, that deep water from only a few hundred meters below sill depth can be involved. Besides Bernoulli flow, upward flow over the whole interior of the basin, mixing with the lower portions of MIW and subsequent entrainment in the subsurface outflow through the Strait of Sicily, also enables deep water to escape from the basin [cf. Stommel et al., 1973]. As a result, MIW accounts for about 40% and EMDW for about 60% of the subsurface outflow across the Sicilian sill, according to a rough estimation by Béthoux [1980].

Béthoux [1984] argued that a 150% increase of the Nile discharge would already suffice to induce stagnant conditions below 1000 m in the eastern Mediterranean. As calcula-

ted in chapter 4, however, the freshwater budget should be reduced by 47% to induce shoaling of the pycnocline to the base of the euphotic layer at times with a sea level equal to the present. This implies that the freshwater budget should be reduced by 8.5×10^{11} m^3 yr^{-1}, which corresponds in magnitude to a ca. 950% increase of the Nile discharge. This suggests that the upper limit of poorly ventilated conditions may have resided much shallower than the 1000 m calculated by Béthoux [1984]. In fact, Rohling and Gieskes [Chapter 1] found sapropels in a core from only 300 m waterdepth, indicating that, at least locally, anoxic bottom water conditions may have extended up to that depth.

Rohling and Gieskes [Chapter 1] reasoned that the boundary between dysoxic/anoxic and well-oxygenated waters probably coincided with the "base" of actively flowing MIW, and that the poor ventilation below that level concerned the EMDW. In chapter 4, I argued that the decrease in the MIW to surface water salinity gradient, which is related to the decrease in the freshwater budget, would have caused a decline in the EMDW formation-rate. This, in turn, would cause a decrease in the oxygenation of the watercolumn below the "base" of the MIW, in agreement with the expectations of Rohling and Gieskes [Chapter 1].

A decrease of Bernoulli flow, in combination with a decline in the EMDW formation rate, would have curtailed the contribution of EMDW to the total subsurface outflow across the Sicilian sill. Consequently, poorly ventilated conditions prevailed in the watercolumn below the "base" of the MIW which, according to Rohling and Gieskes [Chapter 1], may have resided at an average waterdepth of ca. 300 m. Therefore, the calculated 19.9 10^6 l s^{-1} outflow of water from severely dysoxic to anoxic layers ($[PO_4]$ = 1.37 μmol l^{-1}) is thought to represent a remnant of the EMDW contribution to subsurface outflow across the Sicilian sill.

At present, EMDW accounts for roughly 60% of the total outflow. This implies that approximately 725 x 10^6 l s^{-1} of EMDW is entrained in the subsurface flow towards the western Mediterranean. That is ca. 36 times more than at times of sapropel formation (19.9 10^6 l s^{-1}, calculated above) and the flushing-time of the deep eastern Mediterranean would, consequently, have been approximately 36 times longer at times of sapropel formation than at present. According to Béthoux et al. [1990], the present-day flushing-time of the eastern Mediterranean is approximately 50 years. At times of sapropel formation, therefore, the flushing-time of the deep eastern Mediterranean may have been in the order of 1800 years.

SUMMARY

In the present paper, simple balancing calculations on the eastern Mediterranean phosphate budget have been presented. The freshwater budget reduction by 47% [Chapter 4] was subdivided in a decrease of evaporation, an increase in precipitation directly on sea, and an increase of runoff. Subsequently, the runoff increase was multiplied with the average phosphate concentration in river waters, as determined by Sarmiento et al. [1988], to calculate the excess riverine phosphate input. In order to preserve a steady state, this excess should leave the basin across the Strait of Sicily. Assuming that the deep waters had become anoxic due to mineralization of organic material, deep water phosphate concentrations may be calculated using the Redfield ratio [cf. Sarmiento et al., 1988]. The volume of outflow from these deep, anoxic layers is subsequently calculated, assuming that it constitutes the principal mechanism of balancing for the excess riverine phosphate input into the basin. Thus, a contribution of deep, anoxic waters of ca. 20 x 10^6 l s^{-1} to the total outflow could be determined. At present, EMDW accounts for a portion of ca. 725 x 10^6 l s^{-1} of the total outflow and, therefore, the EMDW contribution to outflow at times of sapropel formation seems to have been reduced by a factor of 36, relative to the present. Such a reduction should, to preserve a steady state, also

have occurred in the formation rate of EMDW. The flushing time of the deep eastern Mediterranean would, consequently, have been 36 times longer than at present. At present, the eastern Mediterranean flushing-time is ca. 50 years [Béthoux et al., 1990]. At times of sapropel formation, therefore, the flushing-time of the deep eastern Mediterranean would have been ca. 1800 years.

Considering the assumptions involved in the model presented in chapter 4 and in the phosphate budget calculations in the present paper, the solution can only be considered as an order of magnitude approximation. Hence, the flushing-time of the deep eastern Mediterranean, at times of sapropel formation, appears to have been in the order of magnitude of a (few) thousand years, compared to the present-day eastern Mediterranean flushing-time of ca. 50 years.

The transfer of the excess riverine phosphate input to deep waters occurred via increased export production, which developed in response to shoaling of the pycnocline into the euphotic layer due to reduction of the eastern Mediterranean freshwater budget. The decrease of EMDW formation probably resulted mainly from a reduction of the MIW to surface water salinity contrast, also due to a decrease in the eastern Mediterranean freshwater budget.

ACKNOWLEDGEMENTS

REFERENCES

Béthoux, J.P., Budgets of the Mediterranean Sea. Their dependance on the local climate and on chracteristics of the Atlantic waters, *Oceanol. Acta, 2*, 157-163, 1979.

Béthoux, J.P., Mean water fluxes across sections in the Mediterranean Sea, evaluated on the basis of water and salt budgets and of observed salinities, *Oceanol. Acta, 3*, 79-88, 1980.

Béthoux, J.P., Paléo-hydrologie de la Méditerranée au cours des derniers 20 000 ans, *Oceanol. Acta, 7*, 43-48, 1984.

Béthoux, J.P., B. Gentili, J. Raunet, and D. Tailliez, Warming trend in the western Mediterranean deep water, *Nature, 347*, 660-662, 1990.

Bryden, H.L. and H.M. Stommel, Limiting processes that determine basic features of the circulation in the Mediterranean Sea, *Oceanol. Acta, 7*, 289-296, 1984.

Sarmiento, J.L., T. Herbert, and J.R. Toggweiler, Mediterranean nutrient balance and episodes of anoxia. *Global Biogeoch. Cycles, 2*, 427-444, 1988.

Stommel, H., H. Bryden, and P. Mangelsdorf, Does some of the Mediterranean Outflow come from great depth, *Pure and Applied Geophysics, 105*, 879-889, 1973.

Takahashi, T., W.S. Broecker, and S. Langer, Redfield ratio based on chemical data from isopycnal surfaces, *J. Geophys. Res, 90*, 6907-6924, 1985.

Tchernia, P., *Descriptive regional oceanography, Pergamon Mar. Ser.*, vol. 3, edited by J.C. Swallow, 253 pp., Pergamon, New York, 1980.

chapter 6

AN INTEGRATED MODEL FOR PYCNOCLINE DEPTH VARIATIONS IN THE EASTERN MEDITERRANEAN

AN INTEGRATED MODEL FOR PYCNOCLINE DEPTH VARIATIONS IN THE EASTERN MEDITERRANEAN

E.J. Rohling

Department of Stratigraphy and Micropaleontology, Institute of Earth Sciences, University of Utrecht, P.O.Box 80.021, 3508 TA Utrecht, The Netherlands

ABSTRACT

A model is presented for depth variations of the eastern Mediterranean pycnocline due to sea level changes and/or variations in the basin's freshwater budget (F = E-P). The model is applied to demonstrate that the post-glacial sea level rise has probably been the principal mechanism invoking a shift of the eastern Mediterranean pycnocline from a depth within the euphotic layer at glacial times to its present-day depth well below the base of the euphotic layer. According to the model, the pycnocline passed the base of the euphotic layer as sea level passed the -43 m level, relative to the present. Furthermore, the model is applied to formulate a tentative explanation for the exceptional faunal characteristic of the Holocene sapropel S_1, compared to that of other Quaternary sapropels. The model suggests that the freshwater budget was reduced by less than 33%, relative to the present, at times of the formation of sapropel S_1. Finally, it is argued that an increase in the salinity contrast between Mediterranean Intermediate Water (MIW) and surface water, resulting from sea level lowering, would facilitate the formation of Eastern Mediterranean Deep Water (EMDW) in the Adriatic Sea, whereas a decrease in that salinity contrast, resulting from reduction of the freshwater budget, would hamper the formation of EMDW. This might explain the observed differences in bottom water oxygenation between glacial times (dominated by lowered sea level) and times of sapropel formation (when the freshwater budget was reduced).

INTRODUCTION

On the basis of eastern Mediterranean Quaternary records of the planktonic foraminiferal genus *Neogloboquadrina*, Rohling and Gieskes [Chapter 1] argued that the upper part of the eastern Mediterranean permanent pycnocline resided within the euphotic layer at pleniglacial time and at times of sapropel formation. At present, the upper part of this pycnocline, which is essentially maintained by the salinity contrast between the Mediterranean Intermediate Water (MIW) and the surface water, resides at an average depth of ca. 150 m, which is well below the base of the euphotic layer (ca. 120 m) [cf. Chapter 1].

In an effort to portray the mechanisms responsible for the pycnocline depth variations described by Rohling and Gieskes [Chapter 1], a simple two-layered model has been developed for the eastern Mediterranean [Chapter 3; Chapter 4].

In chapter 3, I demonstrated that pycnocline shoaling at pleniglacial times resulted essentially from restriction of the surface water inflow through the Strait of Sicily, in response to glacio-eustatic sea level lowering. The model also showed that the MIW to surface water salinity (i.e. density) contrast would be increased as a result of sea level lowering.

In chapter 4, I demonstrated that pycnocline shoaling during periods with a reduced freshwater budget, a characteristic of times of sapropel formation, would predominantly result from a reduction of surficial inflow across the Sicilian sill that is directly related to the decrease in the freshwater budget. According to Bryden and Kinder [in press], who studied a similar relationship at the Strait of Gibraltar, the reduction of inflow is approximately equal to the square root of the reduction of the freshwater budget. Although the model presented in chapter 4 showed that the primary cause for shoaling of the pycnocline was the decrease in

surficial inflow, instead of a decrease in the MIW to surface water density contrast envisaged by Rohling and Gieskes [Chapter 1], the model did confirm that the MIW to surface water salinity (i.e. density) contrast would indeed be reduced at times of a decreased freshwater budget (F = E-P).

In this paper, I will present an integration of the models for shoaling of the eastern Mediterranean pycnocline presented in chapters 3 and 4. Subsequently, I will use the integrated model to assess the probable causes of the disappearance of *Neogloboquadrina* from the foraminiferal record at the base of the Holocene and the exceptional faunal characteristic of the Holocene sapropel S_1. Also, I will briefly discuss the relationship between pycnocline shoaling and the formation rate of Eastern Mediterranean Deep Water (EMDW).

AN INTEGRATED MODEL FOR PYCNOCLINE DEPTH VARIATIONS IN THE EASTERN MEDITERRANEAN

In the simple two-layered approach of the eastern Mediterranean vertical circulation, as applied in chapter 3 to study the influence of sea level lowering, and in chapter 4 to study the influence of a reduced freshwater budget, the salinity difference dS (= deeper layer salinity S_d - upper layer salinity S_u) was described as, respectively,

$$dS = \frac{S_u}{22\phi - 1}$$

and

$$dS = \frac{S_u}{22\left(\frac{\Omega}{\gamma}\right) - 1}$$

Combined, these statements give

$$dS = \frac{S_u}{22\left(\frac{\phi\Omega}{\gamma}\right) - 1} \tag{1}$$

where ϕ is an inflow reduction factor related to sea level lowering, and Ω is an inflow reduction factor related to a freshwater budget reduction factor γ. According to Bryden and Kinder [in press], who studied a similar relation for the Strait of Gibraltar, $\gamma \approx \Omega^2$.

The relation between the present-day value of dS (= dS^P) and the value of dS at times with a freshwater budget reduced to γ times its present-day value was described in chapter 4 as

$$dS = \left(\frac{\gamma}{\alpha}\right) dS^p \qquad (2)$$

where α is a coefficient of pycnocline shoaling, so that αH^p gives the depth of the pycnocline (H^p is the present-day average pycnocline depth of ca. 150 m), and the superscript p indicates the present-day value.

Combining equations 1 and 2 with the relation between the present-day version of equation 1 (with the present-day values of $\phi = \gamma = \Omega^2 = 1$), which is

$$dS^p = \frac{S_u^p}{21}$$

gives

$$\alpha = \frac{22\phi\Omega - \gamma}{21} \frac{S_u^p}{S_u} \qquad (3)$$

With $\alpha = 0.8$, the depth of the pycnocline would correspond to 120 m, which approximately is the base of the euphotic layer. In figure 1, the relations between ϕ and S_u^p/S_u are plotted for several values of Ω, as described by equation 3 with $\alpha = 0.8$. Corresponding values of γ can be derived directly from figure 1, using $\gamma = \Omega^2$ (see examples[♦]).

DISCUSSION

The integrated model indicates which process(es) would invoke shoaling of the pycnocline to a depth within the euphotic layer, a situation conducive to the development of a DCM with a concomitant increase in the downward flux of organic matter from the euphotic layer (increase in export production) [Chapter 1]. Since variations in both the freshwater budget and sea level are measured relative to the present, the model essentially predicts which

[♦]   For example, using $S_u^p/S_u = 1.08$ [see Chapter 4], Ω should be 0.73 to satisfy the condition $\alpha = 0.8$ when $\phi = 1$. This means that, if there is no sea-level lowering ($\phi = 1$) relative to the present, the surficial inflow through the Strait of Sicily should be reduced to $\Omega = 0.73$ times its present value, in order to raise the pycnocline to the base of the euphotic layer ($\alpha = 0.8$). Since $\gamma = \Omega^2$, this implies that the freshwater budget ($F = E-P$) should be reduced to 0.53 times its present value. If the freshwater budget were reduced even further, the pycnocline would rise to an even shallower position within the euphotic layer.

If, however, there was sufficient sea-level lowering to invoke $\phi = 0.8$, using the same upper layer salinity ratio as above, $\Omega = 0.93$ would already satisfy the condition $\alpha = 0.8$. This implies that, under these circumstances, the freshwater budget ($F = E-P$) should be reduced to only 0.87 times its present value, in order to raise the pycnocline to the base of the euphotic layer.

Note that the above mentioned decreases in the freshwater budget are measured relative to the present-day freshwater budget. Compared to the present, however, glacial periods were characterized by increased aridity in most circum-Mediterranean countries. In other words, the initial value of the glacial freshwater budget ($F = E-P$) most probably was considerably larger than the present-day value. The above calculation of the freshwater budget reduction to 0.87 times the present-day value - necessary to satisfy $\alpha = 0.8$ when $\phi = 0.8$ - suggests a decrease by only 13%. However, if the initial value of the glacial freshwater budget was larger than that at present, the true decrease - relative to this initial glacial value - should have been larger than 13%.

changes in either the freshwater budget or sea level, or in a combination of those parameters, would have to occur at present to invoke pycnocline shoaling into the euphotic layer. These predicted requirements are, subsequently, used as proxies for the conditions prevailing during past events of pycnocline shoaling as reflected in the record of *Neogloboquadrina* [cf. Chapter 1]. Sea level variation probably is the best constrainable parameter used in the model, and highly detailed sea level records are available already for the interval from the last glacial maximum to the present [Bard et al., 1989; Fairbanks, 1989]. However, it may prove to be very hard, or even impossible, to determine the magnitude of the freshwater budget at any time-slice in the past. Hence, all variations in the freshwater budget have to be expressed relative to the present-day value, although the true variations - relative to an initial value in the past - may have been considerably larger, or smaller (see examples[*]).

In the following sections, I will use the integrated model to discuss the disappearance of *Neogloboquadrina* from the eastern Mediterranean foraminiferal record at the base of the Holocene, as described by Rohling et al. [Appendix 1] and Jorissen et al. [Appendix 2], and the exceptional faunal characteristic of the Holocene sapropel S_1. Furthermore, I will briefly discuss the relation between pycnocline shoaling and oxygen advection to deep (and bottom) waters.

Pycnocline depth variation across the Pleistocene-Holocene transition

In the model, the reduction of inflow across the sill was expressed with the coefficient ϕ, which decreases as a result of sea level lowering. At present, $\phi = 1$ and at times of ca. 100 m sea level lowering, $\phi \approx 0.6$ [cf. Béthoux, 1984]. Assuming a linear relationship between ϕ and the magnitude of sea level lowering, which implies that a rectangular cross-section is assumed for the strait which limits the exchange transports, a value of $\phi = 0.8$ would correspond to a sea level lowering of ca. 50 m.

This assumption allows for a speculation on the cause of the disappearance of *Neogloboquadrina* from the eastern Mediterranean foraminiferal record at the base of the Holocene [Appendix 1; Appendix 2]. Assuming that the freshwater budget was about equal to the present ($\gamma = \Omega^2 = 1$), and $S_u P / S_u \approx 0.97$ (mean of the pleniglacial value 0.94 [Chapter 3] and the present-day value 1.0), the pycnocline would have resided at the base of the euphotic layer ($\alpha = 0.8$) when $\phi \approx 0.83$. If the relation between ϕ and the magnitude of sea level lowering is assumed linear, as discussed above, then $\phi \approx 0.83$ would correspond to a sea level position at ca. 43 m below the present.

The disappearance of *Neogloboquadrina* was dated by Jorissen et al. [Appendix 2] at 9 600 YBP. According to the highly detailed sea level reconstruction by Fairbanks [1989], sea level passed -43 m around 9 400 YBP (around 9 600 YBP sea level stood at -46 m). Although the two-layered model is a highly simplified and idealized representation of the true circulation, the match between the calculated -43 m at 9 600 YBP and Fairbanks' [1989] sea level reconstruction is striking. It suggests that the post-glacial rise of sea level to less than ca. -43 m at the base of the Holocene may indeed have been the principal mechanism invoking the disappearance of *Neogloboquadrina* from the eastern Mediterranean foraminiferal record.

On the exceptional faunal characteristic of the Holocene sapropel S_1

As Rohling and Gieskes [Chapter 1] pointed out already, the Holocene sapropel S_1 is an exception, with respect to the other Quaternary sapropels, in that it is devoid of neogloboquadrinids. Rohling et al. [Appendix 1] and Jorissen et al. [Appendix 2], however, reported a short-term reappearance of neogloboquadrinids in the topmost part of S_1. This level represents

the only part of the Holocene sequence that contains neogloboquadrinids. As discussed above, the pycnocline may have moved below the base of the euphotic layer at the Pleistocene-Holocene transition due to the post-glacial rise of sea level to less than -43 m. Apparently, the pycnocline did not move up into the euphotic layer during the formation of S_1. Still, there is ample evidence that increased precipitation / runoff did occur during the formation of S_1, as it did during the formation of the other sapropels. As yet, I can only offer one possible explanation for the anomalous faunal record of S_1.

Possibly, the pycnocline did rise during the formation of S_1, but not sufficiently to reach the base of the euphotic layer. This scenario would imply that $\alpha > 0.8$. At times of the deposition of S_1, between 8 730 and 7 970 YBP [Troelstra et al., 1990], sea level stood approximately 25 m below the present-day level [Fairbanks, 1989]. Using a linear relationship between ϕ and the magnitude of sea level lowering (see above), this would imply that $\phi \approx 0.9$. Taking $S_u^P/S_u = 1.08$ [Chapter 4], equation 3 indicates that $\Omega > 0.82$, which implies that $\gamma > 0.67$. During the formation of sapropel S_1, the freshwater budget seems to have been reduced by less than 33%, relative to the present, since the pycnocline does not seem to have reached the base of the euphotic layer. The short Holocene reappearance of *Neogloboquadrina* in the topmost part of S_1 might represent a brief phase during which the pycnocline did reach the base of the euphotic layer, suggesting that the freshwater budget was temporarily reduced by 33% or slightly more, relative to the present.

This scenario implies that the freshwater budget at times of the formation of S_1 was not as radically altered as during the formation of other sapropels. Note that one should primarily consider such differences between S_1 and other sapropels formed during episodes with a sea level lowering of 25 m or less ($\phi \geq 0.9$), relative to the present, because a decrease in ϕ tends to induce an increased sensitivity to variations in the freshwater budget (see equation 3 and figure 1). This tentative explanation seems to be confirmed by the much greater $\delta^{18}O$ depletion (-2 ppt) in the sapropel S_5, deposited during the penultimate interglacial, as compared to the depletion (-0.5 ppt) in S_1 [cf. Chapter 2].

The relation between pycnocline shoaling and bottom water oxygenation

As discussed above, shoaling of the eastern Mediterranean pycnocline seems to result essentially from restriction of the surficial inflow through the Strait of Sicily. Two processes were found to have a profound influence on the volume of inflow, viz. glacio-eustatic sea level lowering [cf. Chapter 3] and decreases in the freshwater budget (F = E-P) of the basin [cf. Chapter 4]. The former process is largely responsible for the high pleniglacial abundances of *Neogloboquadrina*, while the latter would be the main cause of high *Neogloboquadrina* abundances in sapropels. Apparently, as argued also in chapter 1, the hydrographic configuration within the euphotic layer at glacial times was quite similar to that at times of sapropel formation. An important difference, however, existed in deeper waters, since glacial sedimentation generally occurred in oxygenated bottom waters, whereas sapropels were formed in severely dysoxic to anoxic bottom waters. Rohling and Gieskes [Chapter 1] suggested that this difference originated from variations in the intensity of Eastern Mediterranean Deep Water (EMDW) formation and, therefore, in the intensity of oxygen advection to deep waters.

In chapter 4, I argued that the process of densification - which generates EMDW when cold, relatively low-salinity Adriatic subsurface water mixes with high-salinity, relatively warm MIW - would be negatively influenced by a decrease in the MIW to surface water salinity contrast. The model presented in chapter 4 showed that this contrast would be substantially decreased during periods with a reduced freshwater budget (F = E-P). As a

consequence, the EMDW formation rate would also be decreased during such periods, which would explain the inferred decrease in oxygen advection to deeper waters, at times of sapropel formation. Unfortunately, such an approach is not very promising for estimating the magnitude of the deep water formation rate at times of sapropel formation, relative to the present. Such an estimate could, however, be made on the basis of a calculation of the phosphate budget at times of sapropel formation, using the scenario of sapropel formation with present-day sea level discussed in chapter 4. Thus, I tentatively determined a 36 fold decrease in the deep water formation rate, relative to the present [Chapter 5]. This figure depends on many assumptions, but it indicates - if nothing else - that the flushing-time of the deep eastern Mediterranean at times of sapropel formation was in the order of magnitude of a (few) thousand years, compared to the present-day eastern Mediterranean flushing-time of ca. 50 years [Béthoux et al., 1990].

At glacial times, with a substantial sea level lowering and a freshwater budget equal to, or even greater than the present, the MIW to surface water salinity (i.e. density) contrast was larger than at present [Chapter 3]. Consequently, an increase in the EMDW formation rate is envisaged at glacial times. This would explain the fact that glacial sedimentation occurred in oxygenated bottom waters, although export production was probably larger than at present. Note that Rohling and Gieskes [Chapter 1] could not satisfactorily explain the oxygenated nature of most glacial sediments, because they attributed pycnocline shoaling to a decrease in the MIW to surface water density contrast. The model presented in chapter 3 has solved this discrepancy, by showing that the density contrast had increased rather than decreased, and that pycnocline shoaling at glacial times was essentially a result of sea level lowering.

CONCLUSIONS

In this paper, an integration is presented of the model for shoaling of the eastern Mediterranean pycnocline due to sea level lowering [Chapter 3] and that for pycnocline shoaling due to reduction of the freshwater budget [Chapter 4]. The integrated model indicates that lowering of sea level increases the sensitivity to decreases in the freshwater budget (relative to the present). This implies that, as sea level is lowered, smaller variations in the freshwater budget are necessary to invoke pycnocline shoaling to the base of the euphotic layer.

However, since glacials are known as periods of increased aridity in most circum-Mediterranean countries, sea level lowering may have coincided with increased values of the freshwater budget (F = E-P). Therefore, model-based decreases of the freshwater budget, necessary to invoke shoaling of the pycnocline to the base of the euphotic layer, may underestimate the true decreases in the freshwater budget (relative to an intitial value in the past, which may have been larger than that at present).

According to the model, the pycnocline should have moved to a depth below the base of the euphotic layer as the post-glacial sea level rise passed -43 m, relative to the present. Jorissen et al. [Appendix 2] dated this event, reflected by the disappearance of *Neogloboqua-drina* from the eastern Mediterranean planktonic foraminiferal record, at 9 600 YBP. The detailed sea level reconstruction of Fairbanks [1989] showed that sea level passed the -43 m level around 9 400 YBP (around 9 600 YBP sea level stood at -46 m). The match between the sea level position predicted by the model and the detailed sea level reconstruction of Fairbanks [1989] is striking, which suggests that the post-glacial sea level rise was the principal cause of the disappearance of *Neogloboquadrina* at the base of the Holocene.

With respect to the exceptional faunal characteristic of the Holocene sapropel S_1, which is devoid of neogloboquadrinids except for a minor abundance-peak in the topmost part [Appendix 1; Appendix 2], the model predicts that the freshwater budget may have been decreased during the formation of S_1, but by no more than 33%, relative to the present.

The fact that pycnocline shoaling into the euphotic layer and resultant increases in export production occurred both at glacial times (dominated by lowered sea level) and during sapropel formation (when the freshwater budget was reduced), suggests that the hydrographic configuration within the euphotic layer during these periods was quite similar. In deeper waters, however, an important difference existed, since glacial sedimentation occurred in oxygenated bottom waters, whereas sapropels were formed in severely dysoxic to anoxic bottom waters. This difference probably resulted from differences in the MIW to surface water salinity contrast. At glacial times, this contrast was increased, relative to the present, which would favor efficient formation of deep water, ensuring well-ventilated conditions in the deep (and bottom) water layers. At times of sapropel formation, the MIW to surface water salinity contrast was decreased, relative to the present, which would hamper the formation of deep water, resulting in restricted oxygen advection to deep (and bottom) waters. In chapter 5, I argued that the decline of deep water formation at times of sapropel formation should have invoked an increase in the deep eastern Mediterranean's flushing-time from the present-day ca. 50 years [Béthoux et al., 1990] to a value in the order of magnitude of a (few) thousand years.

ACKNOWLEDGEMENTS

REFERENCES

Bard, E., R. Fairbanks, M. Arnold, P. Maurice, J. Duprat, J. Moyes, and J.-C. Duplessy, Sea-level estimates during the last deglaciation based on $\delta^{18}O$ and Accelerator Mass Spectrometry ^{14}C Ages measured in *Globigerina bulloides*, *Quat. Res.*, *31*, 381-391, 1989.

Béthoux, J.P., Paléo-hydrologie de la Méditerranée au cours des derniers 20 000 ans, *Oceanol. Acta*, *7*, 43-48, 1984.

Béthoux, J.P., B. Gentili, J. Raunet, and D. Tailliez, Warming trend in the western Mediterranean deep water, *Nature*, *347*, 660-662, 1990.

Bryden, H.L. and T.H. Kinder, Steady two-layer exchange through the Strait of Gibraltar, *Deep-Sea Res.*, in press.

Fairbanks, R.G., A 17,000-year glacio-eustatic sea level record: influence of glacial melting rates on the Younger Dryas event and deep-ocean circulation, *Nature*, *342*, 637-642, 1989.

Troelstra, S.R., G.M. Ganssen, and G.T. Klaver, High resolution analysis of eastern Mediterranean sapropel S_1; chronostratigraphy, oxygen isotopes and geochemistry, *Abstracts Volume IX R.C.M.N.S. Congress Barcelona 1990*, p. 349, 1990.
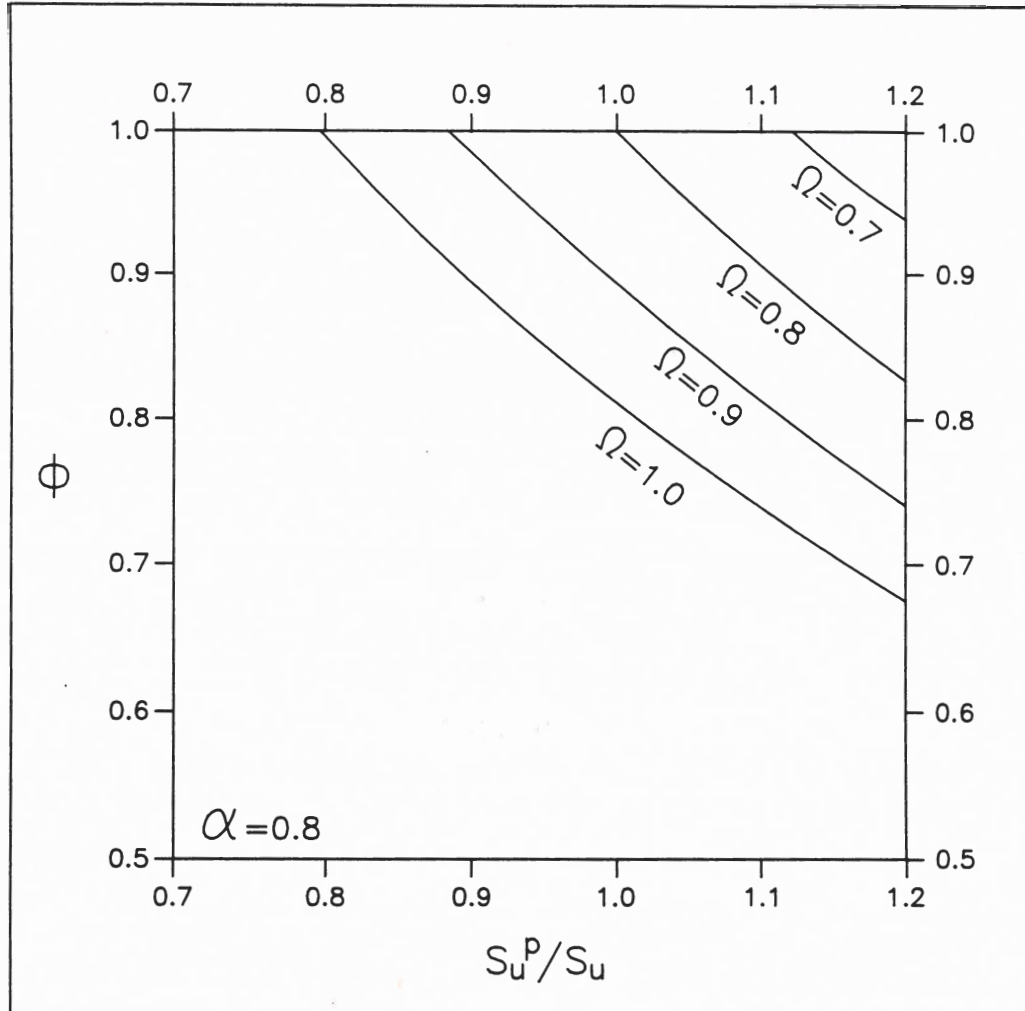
Figure 1. The relations between ϕ - the coefficient of inflow reduction due to sea level lowering - and S_u^P/S_u for several values of Ω - the coefficient of inflow reduction due to decrease in the freshwater budget - plotted in the scenario that $\alpha = 0.8$, which implies that the pycnocline had shoaled to the base of the euphotic layer. The reduction of the freshwater budget - expressed by the coefficient γ - can be derived directly from Ω, using $\gamma = \Omega^2$.

chapter 7

SYNTHESIS

SYNTHESIS

E.J. Rohling

Department of Stratigraphy and Micropaleontology, Institute of Earth Sciences, University of Utrecht, P.O.Box 80.021, 3508 TA Utrecht, The Netherlands

BACKGROUND AND NEW DEVELOPMENTS

Since the discovery of eastern Mediterranean sapropels in cores collected during the 1947-1948 Swedish Deep Sea Expedition [Kullenberg, 1952], a large number of scientists has attempted to portray the mechanism of their formation. Sapropels were found to have been deposited in dysoxic to anoxic bottom waters, which allowed the preservation of organic matter in the sediments and caused the (near) absence of benthic fauna. Bottom water oxygen depletion may develop due to restricted deep water ventilation, due to a large flux of marine organic matter from the euphotic layer and/or continental organic matter via river runoff, or due to a combination of these processes.

The chronology of the sapropel-sequence has been established with the aid of oxygen isotope stratigraphy. In spite of the fact that Mediterranean sediments display a larger variability in oxygen isotopic values than open ocean sediments, it appeared possible to correlate Quaternary oxygen isotopic records of the Mediterranean with those of the open ocean [a.o. Emiliani, 1955; Vergnaud-Grazzini et al., 1977; Thunell and Williams, 1983]. In general, sapropels were found to have developed during warm (interglacial) stages but also - less frequently - during cool (glacial, interstadial) stages [Cita et al., 1977; Thunell et al., 1983; 1984; Muerdter and Kennett, 1984; Vergnaud-Grazzini, 1985]. Moreover, $\delta^{18}O$ records based on planktonic foraminiferal carbonate show an excess depletion in most sapropels, which suggests that the surface water salinity was lowered and/or that the surface water temperature was increased, during their deposition [Cita et al., 1977; Vergnaud-Grazzini et al., 1977; Williams et al., 1978]. Both anomalies would tend to increase the stability of the watercolumn. The fact that sapropels have developed during cool as well as warm stages suggests that warming was not the principal mechanism invoking more stable stratification in the eastern Mediterranean. On the contrary, increased freshwater fluxes from various sources - coeval with sapropel formation - have been positively identified [Rossignol-Strick et al., 1982; Shaw and Evans, 1984; Rossignol-Strick, 1985; Cramp et al., 1988; Appendix 3].

More stable stratification would hamper large-scale convection and, therefore, invoke a restriction of the deep water ventilation. As a consequence, the oxygen advection to deeper parts of the basin would be substantially reduced, enabling the development of bottom water anoxia. This, in turn, would account for a better preservation of organic material and the (near) absence of benthic life ("benthic desert" conditions).

The lowered surface water salinities at times of sapropel formation, as inferred from excess $\delta^{18}O$ depletions, formed the basis of the so-called "circulation reversal theory" [a.o. Stanley et al., 1975; Calvert, 1983; Thunell et al., 1983; 1984; Muerdter and Kennett, 1984; Thunell and Williams, 1989]. This theory states that the vertical circulation in the eastern Mediterranean had changed from an anti-estuarine mode, as it is today, to an estuarine mode at times of sapropel formation. An estuarine circulation acts as a nutrient-trap, ensuring high nutrient levels in surface waters, which favor increased organic production. Enhanced export production rates would, in turn, lead to increased oxygen consumption in deeper waters. In

order to change the vertical circulation from anti-estuarine to estuarine, however, the eastern Mediterranean freshwater budget should have been converted from the present-day net evaporative mode to a mode of net freshwater input. In addition to previously published arguments against the "circulation reversal theory" [for overview see Chapter 1], a reversal does not seem to be a very realistic possibility because of the huge volume of freshwater necessary to change the mode of the freshwater budget. In the hypothetical scenario that all excess freshwater would be derived from the river Nile, the required volume would imply a 21 times increase in the volume of Nile discharge, relative to the present.

An alternative reconstruction of the eastern Mediterranean hydrography at times of sapropel formation has been proposed in chapter 1. It was argued that the upper part of the eastern Mediterranean pycnocline resided at a depth within the euphotic layer at times of sapropel formation. This pycnocline is essentially maintained by the salinity contrast between the Mediterranean Intermediate Water (MIW) and the surface water. At present, the upper part of the eastern Mediterranean pycnocline resides at an average depth of ca. 150 m, which is well below the base of the euphotic layer (ca. 120 m). The inference that the pycnocline resided within the euphotic layer at times of sapropel formation is based on high abundances of the planktonic foraminiferal genus *Neogloboquadrina* within Quaternary sapropels. In the present-day oceans, neogloboquadrinids are most prolific in areas where a distinct Deep Chlorophyll Maximum (DCM) is developed. In the eastern Mediterranean, the development of a distinct DCM can be realized by shoaling of the pycnocline to a depth that falls well within the euphotic layer. Shoaling of the pycnocline would induce high nutrient availability in the sub-pycnoclinal part of the euphotic layer. As a result, the development of a distinct DCM in the eastern Mediterranean would be accompanied by an increase in the downward flux of organic matter from the euphotic layer (increase in export production).

Furthermore, it was shown in chapter 1 that neogloboquadrinids are not only abundant in sapropels, but also in glacial sediments. Therefore, I concluded that the hydrographic configuration at glacial times was quite similar to that at times of sapropel formation, with a shallow pycnocline within the euphotic layer. In an effort to portray the mechanisms responsible for shoaling of the pycnocline at glacial times and at times of sapropel formation, a simple two-layered model was developed for the eastern Mediterranean [Chapter 3; Chapter 4]. The primary cause for pycnocline shoaling in the eastern Mediterranean was found to be reduction of the surface water inflow through the Strait of Sicily, resulting either from lowering of sea level which dominated during glacial times, or from reduction of the basin's freshwater budget (F = evaporation E - total freshwater input P) at times of sapropel formation. In chapter 6, the results were combined into an integrated model for pycnocline depth variations due to sea level changes and/or variations in the basin's freshwater budget. Additionally, I argued that the observed differences in bottom water oxygenation between glacial times and times of sapropel formation should be attributed to an increase in the MIW to surface water salinity contrast at glacial times and an opposite change at times of sapropel formation [Chapter 6]. This salinity contrast is important for the process of formation of Eastern Mediterranean Deep Water (EMDW) in the Adriatic Sea and, therefore, the oxygen advection to deep (and bottom) waters. An increase in the MIW to surface water salinity contrast, resulting from sea level lowering, would facilitate the formation of EMDW. A decrease in the salinity contrast due to a reduction of the freshwater budget would hamper the formation of EMDW.

In chapter 2, a review was presented of paleoclimatic reconstructions concerning times of sapropel formation. It was concluded that intensity maxima of the Northern Hemisphere summer monsoonal circulation, related to minima in the cycle of precession which occur every

76

21 000 years, resulted in intensified freshwater transport towards the eastern Mediterranean via the river Nile. Also, however, reports were found of increased humidity in the Northern Borderlands of the Eastern Mediterranean (NBEM), at times of sapropel formation, which could not be related to the intensified monsoonal circulation. Apparently, not only had the monsoon reached maximum intensity, but also the "local" eastern Mediterranean precipitation was increased substantially, at times of sapropel formation. The increased "local" precipitation seems to have resulted from increased activity of Mediterranean depressions, which invoke a net transport of moisture from the west towards the eastern Mediterranean. Additionally, such an increased activity would induce a reduction of the eastern Mediterranean evaporation, due to increased cloud-coverage and moisture content of the air. Both the increase in net moisture transport from the west and the reduction of evaporation, as consequences of increased activity of Mediterranean depressions, would tend to lower the eastern Mediterranean freshwater budget (F = E-P).

A major result of the model presented in chapter 4 is the estimation of the decrease in the freshwater budget necessary to invoke shoaling of the pycnocline to the base of the euphotic layer, at times with a sea level equal to the present. The model indicated that a decrease in the freshwater budget to 0.53 times its present-day value would suffice. Such a decrease could be accomplished by coeval increases in the Nile discharge - by a literature-based amount of 150% - and the activity of the westerly system of Mediterranean depressions - by ca. 20%. Incorporation of possible changes in the thermal balance of the basin would result in an estimate for the necessary freshwater budget reduction of less than the 47% mentioned above [Chapter 4]. Also, incorporation of the influences of possibly lowered sea level at times of sapropel formation, compared to the present, would result in a lower estimate than the 47% mentioned above [Chapter 6]. Note that the 47% reduction is measured relative to the present-day value of the freshwater budget and that, therefore, true reductions may have been larger or smaller, relative to an initial value in the past that may have been higher or lower than that at present.

In chapter 5, I calculated, on the basis of differences in the basin's phosphate budget between times of sapropel formation and the present, that a reduction of the freshwater budget by 47%, accomplished by a 150% increase in Nile discharge and a 20% increase in the activity of Mediterranean depressions, would imply that the outflow from deep, anoxic layers with an average phosphate concentration of 1.37 μmol l^{-1} had a volume of ca. 20 x 10^6 l s^{-1}. This rough estimate would imply that the contribution of Eastern Mediterranean Deep Water (EMDW) to total subsurface outflow across the Sicilian sill had decreased by a factor of 36, relative to the present, indicating that the waters below the "base" of the MIW were poorly ventilated. Moreover, the flushing-time of the deep eastern Mediterranean would have been increased by a similar factor, which would imply that this flushing-time was in the order of magnitude of a (few) thousand years, at times of sapropel formation.

PERSPECTIVES AND NEW PROBLEMS

The results described above have yielded estimates for several factors that governed the development of sapropels, such as reduction of the freshwater budget and the related shoaling of the pycnocline (influencing export production) and the EMDW formation rate (influencing oxygen advection to deep - and bottom - waters). Moreover, the influence of a possibly lower sea level at times of sapropel formation, relative to the present, on the calculated reduction of the freshwater budget could be quantitatively expressed.

However, the relation envisaged in chapter 4, between variations in the MIW to surface water salinity contrast and changes in the magnitude of the deep water formation rate, could not yet be defined quantitatively. At present, variations in these parameters can only be determined independently via separate budgeting calculations, from different points of view. Possibly, this relation may be approximated in the future with the aid of detailed numerical models of the eastern Mediterranean circulation. Furthermore, the importance of determining accurate values for the thermal balance at glacial times and at times of sapropel formation was stressed in chapters 3 and 4. This requires the development and application of new methods to measure paleotemperatures, which should be more accurate than the existing methods based on $\delta^{18}O$ values or foraminiferal transfer functions.

The modeling effort presented in chapters 1 to 6 focused on the formation of Quaternary sapropels, which was found to be related to minima in the cycle of precession. However, Pliocene sedimentary sequences in the eastern Mediterranean also contain sapropels, which have also been deposited at times of minima in the cycle of precession [Hilgen, in press; Chapter 2]. Therefore, it is tempting to assume that the calculated constraints concerning the formation of Quaternary sapropels would be valid for the Pliocene sapropels as well. There are some major objections to such a simplistic approach.

Firstly, the morphology of the Straits of Sicily and Gibraltar is very important, since it limits the exchange transport of watermasses between the basins on either side. The importance of strait morphology is evident from the profound effects of sea level lowering in the model for pycnocline shoaling [Chapter 3; Chapter 6]. Before the results of the study on Quaternary sapropel formation can be applied to the Pliocene, detailed paleogeographic and paleobathymetric reconstructions of the Mediterranean should become available, with special emphasis on the connecting straits.

Secondly, the Pliocene freshwater budget may have deviated substantially from the present, due to differences in the large-scale atmospheric circulation related to the uplift history of mountain ranges. For example, Ruddiman and Kutzbach [1989] argued that distinct summer dryness, a present-day characteristic of the climate in large parts of the eastern Mediterranean, developed in the Late Pliocene in response to climatic modifications invoked by the uplift of the Tibetan Plateau. Before the model results can be applied to the Pliocene, the Pliocene climatic conditions should be described. These Pliocene climatic conditions should be documented well enough to provide a "reference configuration" versus which climatic variations associated with the formation of Pliocene sapropels can be measured, analogous to the present-day climatic "reference configuration" in the presented study on Quaternary sapropel formation. It may prove to be necessary to define several of such "reference configurations" through the Pliocene, because of the gross tectonic reorganisations, on Mediterranean and global scale, within that period.

REFERENCES

Calvert, S.E., Geochemistry of Pleistocene sapropels and associated sediments from the eastern Mediterranean, *Oceanol. Acta*, 6, 255-267, 1983.

Cita, M.B., C. Vergnaud-Grazzini, C. Robert, H. Chamley, N. Chiaranfi, and S. d'Onofrio, Paleoclimatic record of a long deep sea core from the eastern Mediterranean, *Quat. Res.*, 8, 205-235, 1977.

Cramp, A., M. Collins, and R. West, Late Pleistocene-Holocene sedimentation in the NW Ae gean Sea: a palaeoclimatic palaeoceanographic reconstruction, *Palaeogeogr., Palaeoclimatol., Palaeoecol, 68*, 61-77, 1988.

Emiliani, C., Pleistocene temperature variations in the Mediterranean, *Quaternaria, 2*, 87-98, 1955.

Hilgen, F.J., Astronomical calibration of Gauss to Matuyama sapropels in the Mediterranean and implications for the Geomagnetic Polarity Time Scale, To appear in *Earth Planet. Sci. Lett.*

Kullenberg, B., On the salinity of the water contained in marine sediments, *Medd. Oceanogr. Inst. Goteborg, 21*, 1-38, 1952.

Muerdter, D.R. and J.P. Kennett, Late Quaternary planktonic foraminiferal biostratigraphy, Strait of Sicily, Mediterranean Sea, *Mar. Micropaleontol., 8*, 339-359, 1984.

Rossignol-Strick, M., Mediterranean Quaternary sapropels, an immediate response of the A frican monsoon to variations of insolation, *Palaeogeogr., Palaeoclimatol., Palaeoecol., 49*, 237-263, 1985.

Rossignol-Strick, M., V. Nesteroff, P. Olive, and C. Vergnaud-Grazzini, After the deluge; Mediterranean stagnation and sapropel formation, *Nature, 295*, 105-110, 1982.

Ruddiman, W.F. and J.E. Kutzbach, Forcing of Late Cenozoic Northern Hemisphere climate by Plateau uplift in southern Asia and the American West, *J. Geophys. Res., 94*, 18409-18427, 1989.

Shaw, H.F. and G. Evans, The nature, distribution and origin of a sapropelic layer in sediments of the Cilicia Basin, northeastern Mediterranean, *Mar. Geol., 61*, 1-12, 1984.

Stanley, D.J., A. Maldonado, and R. Stuckenrath, Strait of Sicily depositional rates and pat terns, and possible reversal of currents in the late Quaternary, *Palaeogeogr., Palaeoclimatol., Palaeoecol., 18*, 279-291, 1975.

Thunell, R.C. and D.F. Williams, Paleotemperature and paleosalinity history of the eastern Mediterranean during the late Quaternary, *Palaeogeogr., Palaeoclimatol., Palaeoecol., 44*, 23-39, 1983.

Thunell, R.C. and D.F. Williams, Glacial-Holocene salinity changes in the Mediterranean Sea: Hydrographic and depositional effects, *Nature, 338*, 493-496, 1989.

Thunell, R.C., D.F. Williams, and M.B. Cita, Glacial anoxia in the eastern Mediterranean, *J. Foraminiferal Res., 13*, 283-290, 1983.

Thunell, R.C., D.F. Williams, and P.R. Belyea, Anoxic events in the Mediterranean Sea in relation to the evolution of late Neogene climates, *Mar. Geol., 59*, 104-134, 1984.

Vergnaud-Grazzini, C., Mediterranean late Cenozoic stable isotope record: Stratigraphic and paleoclimatic implications, in *Geological Evolution of the Mediterranean Basin*, edited by D.J. Stanley and F.C. Wezel, pp. 413-451, Springer-Verlag, New York, 1985.

Vergnaud-Grazzini, C., W.B.F. Ryan, and M.B. Cita, Stable isotope fractionation, climatic change and episodic stagnation in the eastern Mediterranean during the late Quaternary, *Mar. Micropaleontol., 2*, 353-370, 1977.

Williams, D.F., R.C. Thunell, and J.P. Kennett, Periodic fresh-water flooding and stagnation of the eastern Mediterranean Sea during the late Quaternary, *Science, 201*, 252-254, 1978.

appendix 1

NORTHERN LEVANTINE AND ADRIATIC QUATERNARY PLANKTONIC FORAMINIFERA; AN ENVIRONMENTAL COMPARISON

NORTHERN LEVANTINE AND ADRIATIC QUATERNARY PLANK-TONIC FORAMINIFERA; AN ENVIRONMENTAL COMPARISON

E.J. Rohling[1], F.J. Jorissen[1], C. Vergnaud-Grazzini[2], and W.J. Zachariasse[1]

1. *Department of Stratigraphy and Micropaleontology, Institute of Earth Sciences, University of Utrecht, P.O.Box 80.021, 3508 TA Utrecht, The Netherlands*

2. *Laboratoire d'Océanographie Dynamique et de Climatologie, Université Pierre et Marie Curie, Tour 12, 2ᵉ étage; 4, Place Jussieu – 75252 Paris Cedex 05, France*

ABSTRACT

A detailed study of the planktonic foraminiferal records of three cores, recovered near Crete, shows very consistent changes. The record of one core (T87/2/13G), however, has been severely smoothed by bioturbation in the top 150 cm. The mutual record of the other two (T87/2/20G and T87/2/27G) extends down to about 125 000 YBP. Principal Components Analyses performed on the combined records of T87/2/20G and T87/2/27G yield two axes that can be interpreted paleoecologically, viz. a temperature-axis and an 'annual stability' axis. The latter is a measure of 'stratification' within the euphotic layer.

We consider T87/2/20G and T87/2/27G to be reference-cores for the eastern Mediterranean. Subsequently, we interpret the faunal variation in two cores from the Adriatic Sea (IN68-5 and IN68-9), containing records extending down to 15 000 and 18 000 YBP, in the context of these reference-cores. This is done by calculating scores of the Adriatic records along the two relevant PCA axes derived from the northern Levantine records. Also, cluster analyses of the Adriatic and northern Levantine records are compared.

On the average, the Adriatic Sea appears to have been considerably colder than the region around Crete, during the past 18 000 years. This temperature difference was largest during the pleniglacial and only small during the Holocene. Remarkably, there is no distinct expression of a Younger Dryas cooling event in the Adriatic records. This contradicts with previous paleoclimatic reconstructions, based mainly on paleobotanical evidence, which suggest that the Younger Dryas event greatly influenced circum-Mediterranean countries. As yet, we have no ready explanation for this discrepancy.

Low annual stability values dominate both the pleniglacial and the Holocene intervals of the Adriatic records. This suggests that homothermal conditions were as prevalent in the Adriatic euphotic layer at pleniglacial times as they are at present. In the present-day Adriatic, homothermal conditions are associated with deep convection and subsequent Eastern Mediterranean Deep Water (EMDW) formation. The similarity between annual stability values in the pleniglacial and Holocene intervals suggests that EMDW formation was as effective at pleniglacial times as it is at present. High annual stability values in the transitional interval, from 12 700 to 9 600 YBP, in the Adriatic records are suggestive of low EMDW formation-rates at that time. In combination with high productivity throughout the eastern Mediterranean, which has previously been inferred from the planktonic foraminiferal record, these low EMDW formation-rates may have precon-ditioned the eastern Mediterranean for sapropel formation, by invoking a gradual decrease in the bottom water oxygen concentrations.

1. INTRODUCTION

In the marine pelagic ecosystem, planktonic foraminifera are essentially distributed, geographically as well as vertically, according to their preferences for specific temperature-ranges and food requirements. Nearly all species thrive within the euphotic layer. Within that layer, significant vertical differentiation of food quality and concentration may occur, so-called shallow and deep phytoplankton assemblages can be distinguished (for overview see Chapter 1). This

vertical differentiation is reflected in the assemblages of planktonic foraminifera, which directly graze upon the phytoplankton or predate/scavenge on other organisms that do so.

Extensive studies on Northern Atlantic sediment cores have shown that the geographical distribution of planktonic foraminifera has shifted through time, as a result of changes in hydrography and climate (e.g. Ruddiman and McIntyre, 1976; Crowley, 1981). Due to shifts in the bio-geographical distribution, different North Atlantic assemblages successively occupied the waters in front of the Mediterranean gateway at Gibraltar. This invoked compositional changes in the planktonic assemblages transported into the Mediterranean by the surface flow. An example of this process are the repeated invasions of *Neogloboquadrina atlantica* in the Mediterranean late Pliocene. This species was continuously present in the middle to high latitude North Atlantic (Poore and Berggren, 1975). Zachariasse et al. (1990) demonstrated that, at times of Northern Hemisphere glaciations, the geographical distribution of *N. atlantica* periodically reached south of the Gibraltar passage, which enabled *N. atlantica* to migrate into the Mediterranean.

Within the Mediterranean, as anywhere, the abundance of planktonic foraminiferal species will be controlled by local environmental conditions. An outstanding example of abundance control by local environmental conditions is the distinct faunal contrast between the eastern and western Mediterranean subbasins (Thunell, 1978; Vergnaud-Grazzini et al., 1986). Such differences in planktonic foraminiferal abundances arise mainly from differences in average food concentration, seasonal food availability and density structure of the watercolumn, and also from temperature differences.

In this paper, we will analyze the Late Quaternary changes in the planktonic foraminiferal records of three cores from the northern Levantine Basin. According to our $\delta^{18}O$ record, these cores extend back in time into the penultimate glacial (oxygen isotopic stage 6). Adding to the interpretation of Rohling and Gieskes (Chapter 1), who focused on the record of the genus *Neogloboquadrina* in these cores, we will try to understand which processes dominated the variations in the total planktonic foraminiferal record.

We will then compare the records of two cores from the deep part of the Adriatic Sea to those of the northern Levantine cores. According to the $\delta^{18}O$ record, the Adriatic cores reach into the last glacial maximum, which is confirmed by a large number of AMS ^{14}C datings discussed by Jorissen et al. (Appendix 2). By comparing the northern Levantine records to the two selected Adriatic records, we aim to show the history of environmental differences between the rather oceanic northern Levantine Basin and the Adriatic Sea, which has a much more continental setting and into which the Po river discharges huge amounts of freshwater loaded with nutrients.

2. MATERIAL AND METHODS

Three gravity cores were taken in the northern Levantine Basin near Crete with the Dutch research vessel *Tyro, in May 1987*. These cores (T87/2/13G, 306 m waterdepth; T87/2/20G, 707 m; and T87/2/27G, 607 m) were sampled at close intervals; the average sample distance is 3 cm. Geographic positions of the cores are shown in figure 1, the core lithologies in figure 2. All samples were sieved with mesh widths of 63, 150 and 595 microns. We studied planktonic foraminifera in the fraction between 150 and 595 microns, from 71, 71 and 59 samples per core, respectively. The position of these samples has been indicated in figure 2a. Seven AMS ^{14}C datings were performed on samples from the upper parts of the cores T87/2/20G and T87/2/27G (figure 2).

Core T87/2/20G, our most complete core, has been used for constructing a highly detailed oxygen isotope record, based on the carbonaceous tests of the planktonic foraminiferal species *Globigerinoides ruber*. T87/2/13G appeared to be quite heavily bioturbated upwards from 150 cm

coredepth, while the top of T87/2/27G is truncated just above the youngest sapropel (figure 2). Oxygen isotopes have therefore been analyzed from 90 samples of core T87/2/20G. The isotopic record, and the isotopic stages are shown in figure 2.

Two cores from the Adriatic Sea (figure 1) have been selected from a study by Jorissen et al. (Appendix 2). The lithology of the two Adriatic cores, IN68-5 and IN68-9, is shown in figure 3. The planktonic foraminiferal records of IN68-5 and IN68-9 consist of 32 and 22 samples, respectively. Based on *G. ruber*, an oxygen isotope record has been constructed for core IN68-5 (figure 3). The Adriatic cores have been accurately dated with the AMS ^{14}C technique (Appendix 2), who used these datings to date three planktonic foraminiferal biozones, which they described in the interval from 18 000 YBP to Recent. The positions of the boundaries between these foraminiferal zones are indicated in figure 3.

3. THE NORTHERN LEVANTINE CORES

In order to place the three northern Levantine cores in a time-stratigraphic framework, Rohling and Gieskes (Chapter 1) constructed a plot of warm-water versus cool-water species. They coupled these plots to an oxygen isotope record of the Mediterranean standard core RC9-181 (Vergnaud-Grazzini et al., 1977). In this paper (figure 2), we present a highly detailed oxygen isotope record of core T87/2/20G and seven AMS ^{14}C dates in T87/2/20G and T87/2/27G. The results show that the correlation proposed in chapter 1 was correct. The four sapropels present in each core were successively identified as S_1, S_3, S_4 and S_5. As mentioned before, core T87/2/13G was found to be heavily bioturbated from 150 cm upwards. Below that level, the faunal pattern is quite similar to that of the other two cores.

In figure 2, hatched intervals have been indicated above several sapropels. There, a sharp and distinct colour change, marking the presently visible top of a sapropel, is followed by a relatively minor colour-change a few centimeters upcore. The depths of these minor colour changes in the cores T87/2/20G and T87/2/27G are listed in table I, and they are indicated with dashed lines in the planktonic foraminiferal records displayed in the figures 4, 5, and 6. The hatched intervals represent blueish grey clays which are lighter in colour than the sapropel below, but still somewhat darker than the clay above.

This might indicate that the sapropels initially were thicker, extending up to the (at present) minor colour change, and that they have been partly oxydized downwards when the bottom waters were oxygenated again. Such a process has been described by De Lange et al. (1989) as 'burning down'. Another interpretation (Hilgen, 1987) regards the blueish grey layer as genuine and characteristic of a wet climatic phase, in which the incorporated sapropel would represent the extreme.

We favor the first interpretation, the blueish grey (hatched) intervals being reoxidized continuations of the sapropels. We do so because this interpretation seems to be endorsed by the fact that intervals poor in benthic fauna extend above the presently visible tops of the sapropels (reflected by high values of the plankton percentage ($100*P/\{P+B\}$) in figures 4, 5 and 6). This suggests that dysoxic to anoxic bottom water concentrations prevailed, which seems characteristic of a sapropel. Additionally, the more important faunal changes do not seem to correspond with the tops of the presently visible sapropels. Table II lists the differences in core depth between the presently visible sapropel extents and such faunal changes. A fair correspondence is suggested at the sapropel bases, but offsets occur at the tops.

Therefore, we will in the following consider the sapropels not to be delimited to the presently olive green to black coloured intervals. We include the blueish grey (presumably reoxidized) intervals.

3.1. Faunal records

The planktonic foraminiferal records of the three northern Levantine cores are shown in figures 4, 5 and 6. The present-day habitat of the taxa is discussed in the added Ecological Notes. Figure 7 presents a dendrogram of the different taxa in the cores T87/2/20G and T87/2/27G. It illustrates the clustering of various -individually low frequent- species into the so-called SPRUDTS-group, which will in the following be treated as one entity (see discussion in Ecological Notes).

There is a marked consistency in the three faunal records, especially between those of T87/2/20G and T87/2/27G. The consistent pattern of neogloboquadrinids has been discussed already by Rohling and Gieskes (Chapter 1). The frequency distribution of pink coloured *G. ruber*, counted only in T87/2/20G and T87/2/27G, is very consistent as well. If this variety should indeed be considered as indicative of optimum warm conditions (Ecological Notes), temperature optima are suggested during the formation of S_1 and (the lower part of) S_5.

The conspicuous peak of indeterminable specimens which occurs above the S_5 sapropel in all three cores (figures 4, 5 and 6) is caused by the abundance of heavily encrusted foraminifera. Nearly all foraminifera that could still be determined showed some coating as well. Moreover, encrustation has been observed on all species present in the interval, and we suspect that it is an early diagenetic feature. Although we cannot rule out completely that some species are affected more than others, we think that our countings are still representative for the associations.

On the average, a rough gradient appears in the percentages of *T. quinqueloba* and *G. scitula* versus *G. ruber* and the SPRUDTS-group, going from T87/2/13G via T87/2/20G to T87/2/27G (approximately from east to west). *T. quinqueloba* and *G. scitula* are indicative of low temperatures and most frequent in T87/2/27G (west). *G. ruber* and the SPRUDTS-group reflect higher temperatures and are most frequent in T87/2/13G (east). This suggests a general pattern of eastwards increasing temperatures throughout the last 125 000 years, the time-span covered by all three cores. This temperature increase also exists at present (Vergnaud-Grazzini, 1985; Stanev et al., 1989).

Within the consistent faunal changes of the three northern Levantine records, one important peculiarity should be noticed, viz. the marked increase of *G. bulloides*, passing upwards from the last glacial into S_1 in core T87/2/27G, whereas no such trend exists in the other two cores. T87/2/27G has been recovered from the Antikythira Straits, a passage between the western part of the Aegean Sea and the Levantine Basin. Therefore, we envisage that this increase of *G. bulloides* may be related to a similar increase in core SK1, which was recovered from the Sporades Basin, south of Skopelos Island (western Aegean). It was probably invoked by increased nutrient concentrations during the S_1 formation, which resulted from enhanced river run-off in northern Greece and extended southward by the western branch of the generally cyclonic Aegean circulation (Appendix 3).

3.2. Principal Components Analysis

Because of intensive bioturbation upwards from 150 cm in core T87/2/13G, we excluded this core from the statistical processing. The SPRUDTS-group was treated as one category (see Ecological Notes), and the sapropels are considered to incorporate the blueish grey, presumably reoxidized, intervals.

A Principal Components Analysis (PCA; Davis, 1973) has been performed on the combined records of T87/2/20G and T87/2/27G (in total 130 samples). Both the standardized and the non-

standardized mode of PCA have been applied; the first relying on the correlation-coefficients, and the latter on covariances between the different taxa.

From the standardized PCA, the first two components are considered; PC1 which describes 32.27 %, and PC2 which describes 22.31 % of the variation (Table IIIa). Table IVa lists the loadings of the taxa on these two axes. From the non-standardized PCA, as well, the first two components are considered; PC1 which describes 56.33 %, and PC2 which describes 20.42 % of the variation (Table IIIb). Table IVb lists the loadings of the taxa on these two axes.

The standardized PC1 (table IVa) shows highly positive loadings of *G. ruber* and the SPRUDTS-group, versus very negative loadings of *T. quinqueloba*, *G. scitula*, neogloboquadrinids, *G. glutinata* and *G. inflata*. As summarized in the Ecological Notes, the positively loading taxa thrive in warm, subtropical waters, while the negatively loading taxa prefer cool/cold conditions or seem to be quite indifferent to temperature (*G. glutinata*, and neogloboquadrinids as a group). The standardized PC1 may, therefore, be interpreted as a temperature axis, with higher temperatures towards its positive side. However, the influence of food concentrations inevitably interferes with the temperature axis. This problem arises from the fact that the warm side is dominated by typical subtropical mixed layer dwellers. The mixed layer is usually deprived of nutrients due to the (seasonal) density discontinuity which marks its base, since this discontinuity hampers turbulent advection of nutrients from below. Usually, the density discontinuity is a (summer) seasonal thermocline, developing due to insolational heating of the surface waters in the absence of frequent storms which would cause its desintegration. Thus, apart from being warmer, the mixed layer waters are oligotrophic with respect to the water below the density discontinuity. In winter, there is no density discontinuity hampering nutrient advection from below. On the cool side of the temperature axis, species are gathered which do not prefer the warm, oligotrophic mixed layer conditions. Some thrive below the mixed layer, down to the base of the euphotic layer, when a (seasonal) pycnocline resides within the euphotic layer. Others prefer the winter situation of cool/cold temperatures and fairly eutrophic conditions throughout the euphotic layer. The quality of our standardized PC1 is, therefore, reduced to a rough approximation of temperature. The downcore scores are plotted in figures 8 and 9.

The non-standardized PC1 (table IVb) predominantly opposes *G. ruber* and the neogloboquadrinids. The downcore scores are plotted in figures 8 and 9. Evidently, the interference of different environmental parameters is much more extreme than on the standardized PC1. On the non-standardized PC1, temperature-induced modulations in the *G. ruber* record interfere with information on Deep Chlorophyll Maximum (DCM) development stored in the neogloboquadrinid record. Such an interference is not very informative, and we will not use this axis for paleoenvironmental interpretation. Temperature fluctuations can better be approximated with the standardized PC1. With respect to the history of DCM development, better information can be obtained directly from the neogloboquadrinid frequency variations, and this has been done already for the three northern Levantine cores by Rohling and Gieskes (Chapter 1).

The standardized PC2 and the non-standardized PC2 yield quite similar results (figures 8, 9). Our interpretation, however, is confined to the non-standardized PC2 (table IVb) since the standardized PC2 (table IVa) shows highest positive loadings of *G. glutinata*, which is a cosmopolitan species from which no conclusive paleoenvironmental information can be derived yet.

The non-standardized PC2 has high positive loadings of neogloboquadrinids, the SPRUDTS group and *G. ruber*. The first prevail in areas with a well-developed 'deep' (DCM) habitat and the latter two occur predominantly in the 'shallow' (mixed layer) system (see Ecological Notes). Some members of the SPRUDTS group are known to thrive in the DCM during part of their life-cycle. Summarized, the association of these species is suggestive of a well-

stratified euphotic zone, with a relatively oligotrophic mixed layer above the (seasonal) pycnocline and a DCM below it down to the base of the euphotic layer. On the negative side of the non-standardized PC2, a grouping occurs of *T. quinqueloba G. bulloides* and *G. inflata*. The first two species were grouped also by Van Leeuwen (1989), who interpreted them as upwelling-indicators. Upwelling areas generally are characterized by a homothermal water column and high food levels. *G. inflata* is a species which requires a (season with a) homothermal water column and intermediate food levels (see Ecological Notes). Moreover, these three species are found to flourish in winter in the western Mediterranean (Vergnaud-Grazzini et al., 1986), when the seasonal thermocline is disrupted and a homogeneous watercolumn exists throughout the euphotic zone.

The non-standardized PC2 may, therefore, be interpreted as a measure of 'annual stability'. A shift towards more positive scores indicates that the watercolumn has been longer stratified within the euphotic zone, as averaged over a year. A shift towards more negative values reflects prevalent homothermal conditions. It has to be noted that, in the vicinity of river mouths, blooms of *G. bulloides* may be invoked due to the riverine discharge of particulate organic matter. In such settings, the flux of particulate organic matter may, therefore, substantially influence the scores on the non-standardized PC2, pushing them to negative values. The complex play of environmental variations influencing the scores on the non-standardized PC2 is schematically represented in figure 10.

Summarizing, there are two axes which seem to yield relevant paleoenvironmental information. The standardized PC1 approximates temperature variations, and the non-standardized PC2 probably approximates 'annual stability'.

3.2.1. Downcore scores on the two relevant PCA axes

The downcore fluctuations along the standardized PC1 (figures 8 and 9) are very similar to the temperature records of the cores T87/2/20G and T87/2/27G presented in chapter 1, which were based on an *a priori* grouping of warm and cool water indicators. This similarity illustrates that our standardized PC1 provides an applicable temperature approximation, in spite of the loadings of some temperature indifferent taxa, such as *G. glutinata* and the neogloboquadrinids (as a group).

Glacial and interglacial intervals are clearly distinguishable, although neither the distinct peak glacials, nor the warmer interstadials show up. The same restriction applies for the temperature curves as constructed by Rohling and Gieskes (Chapter 1). Also in the oxygen isotope record of core T87/2/20G (figure 2), the interstadial stage 3 cannot be distinguished from the glacial stages 2 and 4 without ambiguity. As yet, we cannot provide a satisfactory explanation.

Apparently, the entire curve along the standardized PC1 for core T87/2/27G (figure 9) is displaced towards more negative (colder) values compared to that for T87/2/20G (figure 8), which suggests that the temperature near Antikythira island has consistently been somewhat lower than that near Gavdos island during the last 125 000 years.

Sapropels S_1 and S_5 appear to be deposited at highest temperatures, S_3 during a slightly cooler phase and S_4 during a short, remarkably cold period. A Holocene temperature optimum within S_1 is strongly suggested in both T87/2/20G and T87/2/27G. No conspicuous temperature optimum is reflected within S_5 (figures 8 and 9), in contrast to what we expected -an optimum in the lower half of this sapropel- on the basis of high frequencies of pink *G. ruber*.

As argued in the previous section, the non-standardized PC2 may be an indication of 'annual stability'. In the eastern Mediterranean, the annual stability within the euphotic layer may be increased in two ways (see figure 10). Firstly, by means of shortening of the stormy season with deep vertical mixing, which implies a lengthening of the part of the year during which a seasonal

thermocline is present. Secondly, by rising of the permanent pycnocline, up to a depth within the euphotic layer (cf. Chapter 1). The permanent pycnocline essentially is a halocline between the Mediterranean Intermediate Water (MIW) and the surface water.

In interglacial non-sapropelic intervals, the values for annual stability are fairly high (figures 8 and 9). According to Rohling and Gieskes (Chapter 1), these periods were probably characterized by a permanent pycnocline at a position comparable to that at present, viz. below the base of the euphotic zone. Temperature was high during these periods, and we envisage that the fairly high annual stability values reflect a significant persistence of the seasonal thermocline during a large part of the year.

Surprisingly, the upper half of the last glacial interval, which should contain the Last Glacial Maximum, displays a high annual stability which is consistent in both cores. This may, however, be explained by persistence of the permanent pycnocline within the euphotic zone during this interval of time. Rohling and Gieskes (Chapter 1) argued that the conditions within the euphotic zone at glacial times were probably quite similar to those during the deposition of S_3, S_4 and S_5. The shallow position of the permanent pycnocline probably resulted from the sea-level lowering of 100 meters or more, at glacial times, which limited inflow and outflow across the Sicilian sill (Chapter 3).

However, in the lower half of the last glacial interval, the annual stability appears to be consistently low in both cores. Apparently, the hydrographic conditions in the euphotic zone were not uniform throughout the last glacial, and homothermality of the watercolumn was much more dominant in the earlier part than in the later part. This may be interpreted as an indication of either a deeper position of the permanent pycnocline and/or a longer season of storm-activity in the earlier part of the last glacial. As yet we cannot offer a sound explanation as to which of these two possibilities dominated.

The sapropels S_3 and S_5 are characterized by high annual stability values. The same applies to S_4 in core T87/2/27G, although less distinctly, to T87/2/20G. Annual stability during the S_1 formation appears to have been about equal to that during the S_4 formation in core T87/2/20G, but less as compared to that during the S_4 formation in core T87/2/27G. Rohling and Gieskes (Chapter 1) reasoned that the pycnocline probably resided within the euphotic layer during the formation of S_3, S_4 and S_5, and this would indeed explain high annual stability for S_3 and S_5. The lower values for S_4, however, may indicate a longer season of homothermality during the formation of this sapropel as compared to that during the formation of S_3 and S_5. On the standardized PC1, our inferred temperature axis (figures 8 and 9), S_4 also occupied an exceptional position - relative to S_3 and S_5 - in being significantly colder. We envisage that there is a link between the lower temperatures during the formation of S_4 and its somewhat lower annual stability as compared to S_3 and S_5.

The sapropel S_1 bears no indication of a (shallow) position of the permanent pycnocline within the euphotic zone (Chapter 1), but still annual stability appears to have been fairly high (figures 8 and 9). Until further details become available, we assume that this is due to strong prevalence of the seasonal thermocline, which may be related to the high temperatures during the S_1 formation suggested by the standardized PC1.

Summarizing our suggestions with respect to S_1 and S_4, we assume (cf. Chapter 1) that the permanent pycnocline was not positioned within the euphotic layer during the S_1 formation and that it, on the contrary, did reside within that layer during the S_4 formation. This should invoke low annual stability values for S_1 and high values for S_4. In fact, however, the values for these sapropels do not deviate much from one another. Therefore, we envisage that the warm optimum conditions during the S_1 formation invoked the homothermal season to be short, which raised the

nual stability values in S_1 to intermediate levels. Similarly, we think that the cold conditions prevailing during the S_4 formation induced a longer than normal homothermal season, which consequently lowered the annual stability values in S_4 to intermediate levels.

4. THE ADRIATIC CORES COMPARED TO THE NORTHERN LEVANTINE CORES

The figures 11 and 12 show the planktonic foraminiferal records of the cores IN68-5 and IN68-9 from the Adriatic Sea. The core locations are shown in figure 1, the descriptions in figure 3. The time-stratigraphic framework for the Adriatic cores is provided by the oxygen isotope record for core IN68-5 (figure 3), and by several AMS ^{14}C datings presented in appendix 2. The sapropel found in both cores IN68-5 and IN68-9 was identified as the Holocene sapropel S_1.

In figures 3, 11 and 12 we indicated the zonal boundaries as defined in appendix 2. Zone III is full glacial, the II/III boundary (12 700 YBP) approximately matches the end of Termination 1a. Zone II spans the interval from 12 700 to 9 600 YBP, and the Zone I/II boundary matches with Termination 1b. Zone I is the Holocene interglacial, containing the S_1 sapropel. According to Jorissen et al. (Appendix 2), the S_1 sapropel formed between about 8 200 and 5 600 YBP. These ages, however, were acquired by interpolation and may include large errors if the sedimentation-rate did not remain constant across the interval containing S_1. Troelstra et al. (1990; 1991) dated bottom and top of sapropel S_1 at 8 730 and 7 970 YBP, respectively.

As expected, the faunal records of the two Adriatic cores are very similar, since these cores were recovered from sites only about 100 km apart. They are remarkably different, however, from the records of the three northern Levantine cores. Due to the very low sedimentation rates in the northern Levantine cores, the three zones defined by Jorissen et al. (Appendix 2) cannot be recognized without ambiguity. Especially Zone II is difficult to discern in the northern Levantine cores. In the Adriatic cores, Zone II represents the interval between the top of Zone III (temporal exit *G. scitula*) and the base of Zone I (temporal exit neogloboquadrinids + marked increase *G. ruber*). These boundary criteria, however, suffered from bioturbation in the low sedimentation rate cores from the northern Levantine Basin. Especially in core T87/2/13G, the zonal discrimination appears impossible due to the intense bioturbation upwards from 150 cm coredepth. For T87/2/20G and T87/2/27G (figures 5 and 6), however, we tentatively indicated the zones I and III and also the interval which roughly corresponds in age to Zone II of the Adriatic cores. From the Adriatic cores, no distinct criterion could be obtained to describe the base of Zone III. Based on core T87/2/20G and T87/2/27G, we propose to place the base of Zone III at the temporal exit of *G. inflata*, which roughly coincides with a marked increase of *G. scitula*. This proposed base of Zone III is also indicated in figures 5 and 6.

The species *G. ruber* is nearly absent in the Adriatic Zone III (figures 11 and 12), whereas it is continuously present in the northern Levantine records (figures 5 and 6). *G. scitula* reaches higher percentages in the Adriatic Zone III than anywhere in the northern Levantine records. These differences suggest that the Adriatic Sea was characterized by substantially lower temperatures than the northern Levantine Basin, during the last glacial.

G. bulloides reaches high percentages in the Adriatic Zone I (figures 11 and 12), whereas it remains fairly constant in the northern Levantine cores (figures 5 and 6), from the last glacial to the Holocene (except in T87/2/27G, as discussed in section 3.1). The frequency distribution of *G. bulloides* in the Adriatic is likely to be influenced by variations in food concentrations induced by the nearby Po river's discharge.

Both in the Adriatic records (figures 11 and 12) and in the northern Levantine records (figures 5 and 6), neogloboquadrinids abound in the last pleniglacial up to a marked frequency-drop to zero at the glacial-Holocene transition. The extreme peak in the neogloboquadrinid

frequencies of the Adriatic Zone II, however, has no equivalent in the northern Levantine records. This discrepancy is genuine, since the almost continuous sampling below S_1 in T87/2/20G should have revealed at least traces of a distinct frequency peak just prior to the Holocene (i.e. in Zone II), if such a peak were present. This discrepancy in (Zone II) neogloboquadrinid frequencies between the Adriatic and the northern Levantine records is discussed in section 4.2.2.

4.1. A brief comparison of cluster analyses

Cluster analyses (program DENDRO; Drooger, 1982) were performed on 1. the combined records of T87/2/20G and T87/2/27G, which will serve as a northern Levantine standard, and 2. the combined records of IN68-5 and IN68-9, two standard cores for the Adriatic Sea (Appendix 2). Unfortunately, it was not possible to run DENDRO only on the youngest part (last 18 000 years) of the northern Levantine records, because that part contains too little samples in these low sedimentation rate cores. Although we realize that there is a problem when we compare records spanning very different intervals of time, we apply DENDRO to show major differences and similarities between the general faunal groupings of the two areas.

The Adriatic dendrogram (figure 13) differs substantially from the northern Levantine dendrogram (figure 14). The main difference lies in the position of *G. bulloides*, an indicator of eutrophication due to upwelling or riverine influxes (Ecological Notes). In the Adriatic, this species appears strongly coupled to the warm-water group (i.e. *G. ruber* + SPRUDTS group). This would suggest that the Po river discharge had the greatest influence during the warm (Holocene) interval in the Adriatic records.

Additionally, the Adriatic dendrogram deviates from the northern Levantine dendrogram in as much that *G. inflata*, *G. glutinata* and *G. truncatulinoides* correlate negatively with the cool/cold-water group in the Adriatic records, whereas *G. inflata* and *G. glutinata* correlate negatively with the warm-water group in the northern Levantine records. Since these species are known neither as typical warm-water dwellers, nor as typical cold-water dwellers (Ecological Notes), their affinity to the warm-water group in the Adriatic, and to the cool/cold-water group in the Cretan records might be interpreted in terms of a lower average temperature in the Adriatic records than in the northern Levantine records.

4.2. Comparison of the northern Levantine and Adriatic records using PCA

We will not present separate Principal Components Analyses of the Adriatic cores IN68-5 and IN68-9, since it would be difficult to compare with T87/2/20G and T87/2/27G owing to the relatively short time-span covered by the Adriatic records. Instead, we considered cores T87/2/20G and T87/2/27G as reference-cores for the central and eastern Mediterranean. We then interpreted the faunal variation in the Adriatic cores in the context of the much longer northern Levantine records, by using the two paleoecologically relevant PCA axes of the latter.

In the non-standardized mode, we calculated the downcore scores of IN68-5 and IN68-9 by multiplying the relative frequencies of all taxa with their loadings on the PCA axes of the northern Levantine cores.

In the standardized mode, we standardized census data of IN68-5 and IN68-9 using the means and standard deviations from the matrix of the northern Levantine cores. Thereafter, the procedure was identical to the one in the non-standardized mode.

We realize that the described procedures, henceforth called FPCA (Fixed Principal Components Analysis), is only allowed in a region where specific paleoenvironmental fluctuations are expressed by similar faunal responses. We envisage that this is (approximately) the case for the central and eastern Mediterranean.

Figures 15 and 16 show the downcore FPCA scores of IN68-5 and IN68-9 (based on the fixed PCA axes of T87/2/20G + T87/2/27G). The only 'fixed axes' presented are the standardized PC1 and non-standardized PC2 of T87/2/20G, since these are the only two yielding relevant paleoenvironmental information.

4.2.1. Fluctuations along the standardized FPC1; the temperature axis

The temperature differences between the Adriatic Sea and the northern Levantine Basin, which we inferred before (the former being cooler than the latter), are confirmed by the FPCA procedure. Especially the very negative values along the temperature axis (standardized FPC1) in the Adriatic full glacial interval (Zone III; figures 15 and 16) differ from those in the corresponding interval of the northern Levantine records (figures 8 and 9). Glacial temperatures appear to have been considerably lower in the Adriatic Sea than in the northern Levantine Basin. The temperature difference between the two areas appears to have been distinctly smaller during the Holocene than at glacial times. Nevertheless, the Adriatic Sea seems to have remained somewhat cooler than the northern Levantine Basin during the Holocene, as it is at present (Stanev et al., 1989). The glacial to interglacial temperature gradient appears to be much larger in the Adriatic Sea than in the northern Levantine Basin.

Although, in the Adriatic cores, the basal part of the interval between 12 700 to 9 600 YBP (Zone II) seems to be characterized by somewhat higher temperatures than the upper part of that zone (figures 15 and 16), no distinct Younger Dryas cooling event can be indentified with our temperature proxy axis. This would suggest that the Younger Dryas, which so dramatically affected the Northern Atlantic realm (e.g. Berger et al., 1987; Mangerud, 1987), hardly had a noticable effect on temperature in the Adriatic Sea. We find this difficult to believe, since previous paleoclimatic reconstructions suggested a great influence of the Younger Dryas event on the circum-Mediterranean climate (a.o. Guiot, 1987; Magaritz and Goodfriend, 1987; Pons et al., 1987; Rognon, 1987). As yet, we have no ready explanation for this discrepancy.

The temperature optimum during the formation of the S_1 sapropel, which is most prominent in the record of T87/2/20G, is much less conspicuous in the Adriatic records. However, a distinct early Holocene temperature increase seems to prelude the S_1 formation in the Adriatic. Just above S_1, a short recursion to lower values and a subsequent recuperation is suggested both in the Adriatic records and in that of T87/2/20G.

4.2.2. Fluctuations along the non-standardized FPC2; 'annual stability'

Along this axis, the Adriatic records (figures 15 and 16) display a very conspicuous tripartition. Zone III (glacial) and Zone I (Holocene interglacial) contain scores of comparable magnitude, whereas the transitional Zone II is characterized by much higher scores. This pattern differs completely from that in the northern Levantine records (figures 8 and 9), where the last glacial to Holocene values remain more or less in the same range. The northern Levantine values range intermediate to the high values of the Adriatic Zone II and the low values of the Adriatic Zones I and III.

The presence of neogloboquadrinids in the Adriatic glacial interval (Zone III; figures 11 and 12) suggests that stratified conditions prevailed in the Adriatic euphotic layer during a substantial part of the year. The high neogloboquadrinid abundances in the last pleniglacial interval of the northern Levantine cores (Zone III; figures 5 and 6) have been attributed to a shallow position of the permanent pycnocline, within the euphotic layer (Chapter 1). This shoaling, which seems to have occurred basin-wide in the eastern Mediterranean was probably invoked by glacio-eustatic sea-level lowering (Chapter 3). Since the fauna in the glacial part (Zone

III) of the Adriatic cores indicates, at least seasonal, predominance of stratified conditions in the euphotic layer, this suggests a density structure which was quite similar to that in the rest of the eastern Mediterranean. Therefore, one would expect the annual stability scores to be as high in the Adriatic glacial interval as they are in the northern Levantine glacial interval. This expectation is, however, not supported by the actual values. Much lower scores occur along the non-standardized FPC2 in the Adriatic full glacial interval (Zone III; figures 15 and 16), as compared to those in the corresponding interval of the northern Levantine records (figures 8 and 9). We will now consider two processes which may account for the surprisingly low annual stability values in the full glacial intervals of the Adriatic cores, as compared to those in the corresponding interval of the northern Levantine cores.

Firstly, the Adriatic may have been characterized by a substantially longer season of homothermal conditions, resulting from thorough mixing of the surface waters, which may be due to its more continental setting as compared to the region around Crete. This seems to match with our previous observation that the Adriatic Sea probably was significantly colder than the northern Levantine Basin at glacial times. Secondly, the Po river's influence may have disturbed the signal along FPC2 by causing abundance increases of *G. bulloides*. Increased influence of the river's nutrient release, in the glacial interval, is not necessarily due to to enhanced discharge. It may also reflect a smaller distance between the rivermouth and the sites of IN68-5 and IN68-9, invoked by sea-level lowering.

Considering the faunal similarity between the pleniglacial intervals and the sapropels S_3, S_4 and S_5, Rohling and Gieskes (Chapter 1) stated that the higher than average primary production rates in the pleniglacial eastern Mediterranean should have invoked a significant lowering of bottom water oxygen concentrations, unless substantial Eastern Mediterranean Deep Water (EMDW) formation occurred. Assuming that the Adriatic was the primary site of EMDW formation during the pleniglacial, as it is at present, their argument favors the hypothesis of a much longer homothermal season in the Adriatic Sea than in the northern Levantine Basin. A season of thoroughly mixed, homothermal, conditions would accompany EMDW formation through the process of deep convection.

The very high scores on the non-standardized FPC2 in Zone II of the Adriatic records (figures 15 and 16) are almost entirely due to the extremely high frequencies of the neogloboquadrinids (> 60 %) in that interval (figures 11 and 12). As argued before, no such extreme peak is found just prior to the Holocene in the northern Levantine records. There, the neogloboquadrinid frequencies -just before the abrupt abundance drop at the base of the Holocene- are similar to those of the last pleniglacial. We envisage that a DCM, related to a shallow pycnocline position within the euphotic layer, occurred throughout the eastern Mediterranean (including the Adriatic) during the pleniglacial and until about 9 600 YBP (i.e. top of Zone II). However, some additional factor caused a more vigorous bloom of neogloboquadrinids in the Adriatic between 12 700 and 9 600 YBP (Zone II). An argument inverse to the one applied to the pleniglacial section would imply that the season of homothermality was much shorter in the Adriatic than in the northern Levantine Basin between 12 700 and 9 600 YBP. In turn, this might imply that EMDW formation in the Adriatic was not very effective at that time. In combination with fairly high production rates throughout the eastern Mediterranean, this may have preconditioned the eastern Mediterranean for sapropel formation, by inducing a gradual decrease in the deep water oxygen concentrations. This would match with the findings of Troelstra et al. (1990; 1991), who reported that processes resulting in complete bottom water anoxia (from 8 730 to 7 970 YBP) started as early as 13 800 YBP, in the Ionian Basin.

91

The scores on the non-standardized FPC2 in Zone I, the Holocene, of the Adriatic records (figures 15 and 16) are markedly lower than those in the northern Levantine records (figures 8 and 9). This would suggest that, during the Holocene, homothermality was more pronounced in the Adriatic than in the northern Levantine Basin. Such an interpretation would agree with the fact that the Adriatic is the major site of EMDW formation.

However, we have to be careful in interpreting the Holocene scores. Rossignol-Strick (1987) stated that from about 11 000 YBP onwards and culminating during the formation of the S_1 sapropel, an increase of deciduous oak pollen occurred in the northern borderlands of the eastern Mediterranean. She also stated that this increase reflects an increase in (summer) precipitation. Therefore, the frequencies of *G. bulloides* may have been enhanced by an increase of the Po river's budget and subsequent nutrient flux. Our cluster analysis of the Adriatic records showed a coupling of *G. bulloides* with *G. ruber* and the SPRUDTS-group, a major difference compared to its position together with *G. inflata* in the more oceanic northern Levantine records. We interpreted this anomaly by assuming that the Po river's influence had increased in close parallel to temperature. The low Holocene scores on the Adriatic non-standardized FPC2, therefore, may also be explained by an increased abundance of *G. bulloides* related to nutrient discharge of the Po river.

5. CONCLUSIONS

Throughout the last 125 000 years, an eastward increase of temperature seems to have existed from the site of T87/2/27G, near Antikythira island, via that of T87/2/20G, near Gavdos island, to that of T87/2/13G, just east of Crete.

Generally, the sapropels S_1 and S_5 have been deposited at highest temperatures, S_3 during a slightly cooler phase and S_4 during a remarkably cold period.

On the average, the Adriatic Sea has been significantly colder than the region around Crete during the last 18 000 years. This difference was largest during the pleniglacial and only small during the Holocene.

Apart from an approximate temperature axis, our PCA analysis also yield an axis which seems to reflect 'annual stability', which indicates the relative dominance of stratified or homothermal conditions in the euphotic layer.

In cores T87/2/20G and T87/2/27G, annual stability values are high in the upper part of the last glacial intervals and in the sapropels S_3 and S_5. This probably results from a shallow position of the permanent pycnocline, within the euphotic layer. As well as temperature, annual stability seems to have been low during the S_4 formation, which may indicate that, at that time, the season with a well-mixed watercolumn was longer than during the formation of S_3 and S_5. Annual stability during the formation of S_1 appears to have been moderate, although there are no indications of a shallow permanent pycnocline position (within the euphotic layer). We think that the moderate annual stability during the formation of S_1 is due to long persistence of the seasonal thermocline, since temperature at that time was high.

In the Adriatic cores IN68-5 and IN68-9, no distinct Younger Dryas cooling event could be identified with our temperature proxy axis. This is not in accordance with previous paleoclimatic reconstructions of the circum-Mediterranean climate, which suggested a great impact of the Younger Dryas event. Also, it is hard to discern interstadials within the last glacial in the northern Levantine records, even in the highly detailed oxygen isotope record of T87/2/20G. As yet, we cannot offer a satisfactory explanation.

Low annual stability values in the last pleniglacial of the Adriatic cores contrast with high values in the corresponding interval of the northern Levantine cores. This may indicate that

homothermality of the watercolumn was more common in the Adriatic than in the northern Levantine realm. This suggests that, during the pleniglacial, significant formation of Eastern Mediterranean Deep Water (EMDW) may have occurred in the Adriatic. High annual stability values in the interval between 12 700 and 9 600 YBP in the Adriatic records suggest low EMDW formation-rates at that time. In combination with fairly high productivity throughout the eastern Mediterranean, this may have caused a gradual decrease in bottom water oxygen concentrations, thus preconditioning the eastern Mediterranean for sapropel formation.

6. ACKNOWLEDGEMENTS

7. REFERENCES

Almogi-Labin, A., 1984. Population dynamics of planktonic foraminifera and pteropoda -- Gulf of Aqaba, Red Sea. Proc. K. Ned. Akad. Wet. Ser. B. Phys. Sci., 87(4): 481-511.

Barmawidjaja, D.J., Van der Borg, K., De Jong, A.F.M., Van der Kaars, W.A., and Zachariasse, W.J., 1989. Kau Basin, Halmahera, a Late Quaternary paleoenvironmental record in a poorly ventilated basin. Proc. Snellius II Symp. Jakarta, Neth. J. Sea Research., 24: 591-605.

Bé, A.W.H., 1969. Distribution of selected groups of Marine Invertebrates in waters south of 35° S Latitude. In: Antarctic Map Folio Series, 11: 9-12.

Bé, A.W.H., Bishop, J.K.B., Sverdlove, M.S., and Gardner, W.D., 1985. Standing stock, vertical distribution and flux of planktonic foraminifera in the Panama Basin. Mar. Micropaleontol., 9: 307-333.

Berger, W.H., Burke, S., and Vincent, E., 1987. Glacial Holocene transition: climate pulsations and sporadic shutdown of NADW production. In: W.H. Berger and L.D. Labeyrie (eds.), Abrupt climatic change, NATO Adv. Study Inst., Ser. C, Math. Phys. Sc.: 279-297.

Brummer, G.J.A. and Kroon, D., 1988. Genetically controlled planktonic foraminiferal coiling ratios as tracers of past ocean dynamics. In: Brummer, G.J. and Kroon, D., Planktonic foraminifers as tracers of ocean-climate history. Free University Press, Amsterdam, The Netherlands: 293-298.

Coulbourn, W.T., Parker, F.L., and Berger, W.H., 1980. Faunal and solution patterns of plaktonic foraminifera in surface sediments of the North Pacific. Mar. Micropaleontol., 9: 329-399.

Crowley, T.J., 1981. Temperature and Circulation changes in the eastern North Atlantic during the last 150 000 years: evidence from the planktonic foraminiferal record. Mar. Micropaleontol., 6: 97-129.

Davis, J.C., 1973. Statistics and data analysis in geology: 550 pp. Wiley and Sons, New York.

De Lange, G.J., Middelburg, J.J., and Pruysers, P.A., 1989. Discussion: Middle and Late Quaternary depositional sequaences and cycles in the eastern Mediterranean. Sedimentology, 36: 151-156.

Drooger, M.M., 1982. Quantitative range chart analysis. Utrecht Micropaleontol. Bull., 26: 227 pp.

Duplessy, J.-C, Bé, A.W.H. and Blanc, P.L., 1981. Oxygen and Carbon isotope composition and biogeographic distribution of planktonic foraminifera in the Indian Ocean. Palaeogeogr. Palaeoclimatol. Palaeoecol., 33: 9-46.

Fairbanks, R.G., Sverdlove, M., Free, R., Wiebe, P.H., and Bé, A.W.H., 1982. Vertical distribution of living planktonic foraminifera from the Panama Basin. *Nature, 298*: 841-844.

Fairbanks, R.G., Wiebe, P.H., and Bé, A.W.H., 1980. Vertical distribution and isotopic composition of living planktonic foraminifera in the western North Atlantic. *Science, 207*: 61-63.

Ganssen, 1983. Dokumentation von küstennahen Auftrieb anhand stabiler Isotope in rezenten Foraminiferen vor Nordwest-Afrika: *"Meteor" Forsch.-Ergeb., Reihe C, 37*: 1-46.

Guiot, J., 1987. Late Quaternary climatic change in France estimated from multivariate pollen time series. *Quat. Res., 28*: 100-118.

Hemleben, Ch. and Spindler, M., 1983. Recent advances in research on living planktonic foraminifera. In: J.E. Meulenkamp (ed.), Reconstruction of marine paleoenvironments. *Utrecht Micropaleontol. Bull. 30*: 141-170.

Hemleben, Ch., Spindler, M., and Anderson, O.R., 1989. *Modern planktonic foraminifera*: 363 pp., Springer-Verlag New York.

Hilgen, F.J., 1987. Sedimentary rhythms and high-resolution chronostratigraphic correlations in the Mediterranean Pliocene. *Newsl. Stratigr., 17*: 109-127.

Hutson, W.H., 1977. Variations in planktonic foraminiferal assemblages along North-South transects in the Indian Ocean. *Mar. Micropaleontol. 2*: 47-66.

Kipp, N.G., 1976. New transfer function for estimating past sea-surface conditions from sea-bed distribution of planktonic foraminiferal assemblages in the North Atlantic. In: R.M. Cline and J.D. Hays (eds.), Investigation of Late Quaternary Paleoceanography and Paleoclimatology, *Mem. Geol. Soc. Am., 145*: 3-41.

Kroon, D., Wouters, P.F., Moodley, L., Ganssen, G., and Troelstra, S.R., 1988. Phenotypic variation of *Turborotalita quinqueloba* (Natland) tests in living populations and in the Pleistocene of an eastern Mediterranean piston core. In: Brummer, G.J. and Kroon, D. *Planktonic foraminifers as tracers of ocean-climate history*. Free University Press, Amsterdam, The Netherlands: 131-147.

Lohmann, G.P. and Schweitzer, P.N., 1990. *Globorotalia truncatulinoides'* growth and chemistry as probes of the past thermocline: 1. shell size. *Paleoceanography, 5*: 55-75.

Magaritz, M. and Goodfriend, G.A., 1987. Movement of the desert boundary in the Levant from latest Pleistocene to early Holocene. In: W.H. Berger and L.D. Labeyrie (eds.), Abrupt climatic change, *NATO Adv. Study Inst., Ser. C, Math. Phys. Sc.*: 173-183.

Mangerud, J., 1987. The Alleröd / Younger Dryas boundary. In: W.H. Berger and L.D. Labeyrie (eds.), Abrupt climatic change, *NATO Adv. Study Inst., Ser. C, Math. Phys. Sc.*: 163-171.

Overpeck, J.T, Peterson, L.C., Kipp, N., Imbrie, J., and Rind, D., 1989. Climate change in the circum-North Atlantic region during the last deglaciation. *Nature, 338*: 353-357.

Pons, A., De Beaulieu, J.-L., Guiot, J., and Reille, M., 1987. The Younger Dryas in southwestern Europe: an abrupt climatic change as evidenced from pollen records. In: W.H. Berger and L.D. Labeyrie (eds.), Abrupt climatic change, *NATO Adv. Study Inst., Ser. C, Math. Phys. Sc.*: 195-208.

Poore, R.Z. and Berggren, W.A., 1975. The morphology and classification of *Neogloboquadrina atlantica* (Berggren). *J. Foraminiferal Res., 5*: 692-694.

Pujol, C. and Vergnaud-Grazzini, C., 1989. Palaeoceanography of the Last Deglaciation in the Alboran Sea (Western Mediterranean). Stable Isotopes and Planktonic Foraminiferal Records. *Mar. Micropaleontol., 15*: 153-179.

94

Reynolds, L.A. and Thunell, R.C., 1989. Seasonal succession of planktonic foraminifera: results from a four-year time-series sediment trap experiment in the northeast Pacific. *J. Foraminiferal Res.*, *19*: 253-267.

Rognon, P., 1987. Aridification and abrupt climatic events on the Saharan northern and southern margins, 20 000 Y BP to present. In: W.H. Berger and L.D. Labeyrie (eds.), Abrupt climatic change, *NATO Adv. Study Inst., Ser. C, Math. Phys. Sc.*: 209-220.

Rossignol-Strick, M., 1987. Rainy periods and bottom water stagnation initiating brine accumulation and metal concentrations: 1. the Late Quaternary. *Paleoceanography*, *2*: 333-360.

Ruddiman, W.F. and McIntyre, A., 1976. Northeast Atlantic paleoclimatic changes over the past 600 000 years. *Mem. Geol. Soc. Am.*, *145*: 111-146.

Stanev, E.V., Friedrich, H.J., and Botev, S.V., 1989. On the seasonal response of intermediate and deep water to surface forcing in the Mediterranean Sea. *Oceanol. Acta, 12*: 141-149.

Thiede, J., 1983. Skeletal plankton and nekton in upwelling water masses off northwestern South America and northwest Africa. In: E. Suess and J. Thiede, *Coastal upwelling, pt. A.*, Plenum Publishing Corp.: 183-207.

Thunell, R.C., 1978. Distribution of recent planktonic foraminifera in surface sediments of the Mediterranean Sea. *Mar. Micropaleontol., 3*: 147-173.

Thunell, R.C. and Reynolds, L.A., 1984. Sedimentation of planktonic foraminifera: Seasonal changes in species flux in the Panama Basin. *Micropaleontology, 30*: 243-262.

Tolderlund, D.S. and Bé, A.W.H., 1971. Seasonal distribution of planktonic foraminifera in the western North Atlantic. *Micropaleontology, 17*: 297-329.

Troelstra, S.R., Ganssen, G.M. and Klaver, G.T., 1990. High resolution analysis of eastern Mediterranean sapropel S_1; chronostratigraphy, oxygen isotopes and geochemistry. *IX R.C.M.N.S. Congress, Barcelona 1990*: p. 349.

Troelstra, S.R., Ganssen, G.M., Van der Borg, K. and De Jong, A.F.M., 1991. A Late Quaternary stratigraphic framework for eastern Mediterranean sapropel S_1 based on AMS ^{14}C dates and stable oxygen isotopes. *Radiocarbon, 33*: 15-21.

Van Leeuwen, R.J.W., 1989. Sea-floor distribution and late Quaternary faunal patterns of planktonic and benthic foraminifera in the Angola Basin. C.W. Drooger (ed.), *Utrecht Micropaleontol. Bull., 38*: 288 pp.

Vergnaud-Grazzini, C., 1985. Mediterranean late Cenozoic stable isotope record: Stratigraphic and paleoclimatic implications. In: D.J. Stanley and F.C. Wezel (eds.), *Geological evolution of the Mediterranean Basin*. Springer-Verlag, New York: 413-451.

Vergnaud-Grazzini, C., Ryan, W.B.F. and Cita, M.B., 1977. Stable isotopic fractionation, climatic change and episodic stagnation in the eastern Mediterranean during the late Quaternary. *Mar. Micropaleontol., 2*: 353-370.

Vergnaud-Grazzini, C., Glaçon, G., Pierre, C., Pujol, C. and Urrutiaguer, M.J., 1986. Foraminiferes planctoniques de Méditerranée en fin d'été. Relations avec les structures hydrologiques. *Mem. Soc. Geol. It., 36*: 175-188.

Zachariasse, W.J., Gudjonsson, L., Hilgen, F.J., Langereis, C.G., Lourens, L.J., Verhallen, P.J.J.M., and Zijderveld, J.D.A., 1990. Late Gauss to early Matuyama invasions of *Neogloboquadrina atlantica* in the Mediterranean and associated record of climatic change. *Paleoceanography, 5*: 239-252.

Zhang, J., 1985. Living planktonic foraminifera from the Eastern Arabian Sea. *Deep Sea Res., 32*: 789-798.

ECOLOGICAL NOTES

<u>Globigerinoides ruber</u>

- mixed layer species (Fairbanks et al., 1982; Hemleben and Spindler, 1983; Almogi-Labin, 1984; Thunell and Reynolds, 1984; Bé et al., 1985; Vergnaud-Grazzini et al., 1986; Hemleben et al., 1989; Pujol and Vergnaud-Grazzini, 1989; Van Leeuwen, 1989).
- $\delta^{18}O$ reflects summer sea surface temperatures (Ganssen, 1983).
- $\delta^{13}C$ reflects that of surface ΣCO_2 (Pujol and Vergnaud-Grazzini, 1989).
- Temperature range 13.3 to 29.5^{o}C, optimum above 21.3^{o}C; pink variety most abundant at T > 24.4^{o}C (Tolderlund and Bé ,1971).
** conclusions: reliable warm-water indicator; pink variety possibly reflects highest temperatures.

Although the following seven species do not live in completely identical habitats, their individually low frequencies and their tendency to group in cluster analyses (see figure 3), led us to lump them into one category, the SPRUDTS-group. Members of the SPRUDTS-group have been grouped in several other studies as well (e.g. Tolderlund and Bé, 1971; Thunell, 1978; Hemleben and Spindler, 1983; Almogi-Labin, 1984; Van Leeuwen, 1989).

<u>Globoturborotalita rubescens</u>, <u>Globigerinoides sacculifer</u> and <u>Hastigerina pelagica</u>

- often reported as mixed layer species (Hutson, 1977; Hemleben and Spindler, 1983; Almogi-Labin, 1984; Thunell and Reynolds, 1984; Bé et al., 1985; Vergnaud-Grazzini et al., 1986; Pujol and Vergnaud-Grazzini, 1989).
- also deeper occurrences, however, for <u>G. sacculifer</u> (Fairbanks et al., 1982; Hemleben and Spindler, 1983; Bé et al., 1985) and <u>H. pelagica</u> (Hemleben and Spindler, 1983; Almogi-Labin, 1985; Bé et al., 1985). These probably represent specimens in reproducing stage, sunk due to spine shedding and/or breakdown of cytoplasm (Hemleben and Spindler, 1983).

<u>Orbulina universa</u>

- both in mixed layer (Bé et al., 1985; Vergnaud-Grazzini et al., 1986; Reynolds and Thunell, 1989) and deeper waters (Fairbanks et al., 1982; Almogi-Labin, 1984; Bé et al., 1985). Lives surficially during spiral stage and deeper during spherical stage (Bé et al., 1985).

<u>Globigerinella siphonifera</u> and <u>Globoturborotalita tenella</u>

- in deeper waters (Almogi-Labin, 1984; Bé et al., 1985).

<u>Globigerinella digitata</u>

- poorly known, but may be restricted to deeper waters (Hemleben et al., 1989).

Several members of SPRUDTS-group have optimum temperatures of about 20 ^{o}C or higher (Tolderlund and Bé, 1971).
** conclusions: SPRUDTS group applicable as warm (subtropical) water indicator, especially when considered in combination with <u>G. ruber.</u>

<u>Globorotalia inflata</u>

- probably lives in deeper waters (Hutson, 1977; Pujol and Vergnaud-Grazzini, 1989). However, seems to calcify in mixed layer (Fairbanks et al., 1980).
- isotopic composition reflects winter sea surface temperatures (Ganssen, 1983).
- peak abundances related to seasons of strong vertical mixing and a consequently homothermal watercolumn (Tolderlund and Bé, 1971; Hutson, 1977; Pujol and Vergnaud-Grazzini, 1989; Van Leeuwen, 1989).
- one of the authors (C. V.-G.) recently observed high <u>G. inflata</u> abundances in a frontal system in the Alboran Sea.
- distribution also reflects intermediate food levels (Van Leeuwen, 1989).
- Temperature-range 2.2 to 22.6 ^{o}C, optimum between 10.6 and 17.3 ^{o}C (Tolderlund and Bé, 1971).
** conclusions: indicative of well-mixed, cool environment with intermediate food-levels.

<u>Globigerinita glutinata</u>

- most abundant in surficial (mixed layer) waters (Fairbanks et al., 1982; Bé et al., 1985; Thunell and Reynolds, 1984; Hemleben et al., 1989; Reynolds and Thunell, 1989), but may live in deeper waters as well (Almogi-Labin, 1984).
- encompasses the entire temperature and salinity ranges studied by Tolderlund and Bé (1971). Greatest abundances occurred at very different, not overlapping, temperature ranges.
** conclusions: cosmopolitan species.

96

Turborotalita quinqueloba

- shallow (mixed layer) dweller (Hutson, 1977; Vergnaud-Grazzini et al., 1986; Hemleben et al., 1989; Pujol and Vergnaud-Grazzini, 1989; Reynolds and Thunell, 1989; Van Leeuwen, 1989).
- considered as upwelling indicator in the Angola Basin, together with Globigerina bulloides (Van Leeuwen, 1989).
- temperature range 2.2 to 16 ^{o}C, although lower limit may even be about 1 ^{o}C and upper limit about 21.5 ^{o}C according to sparse findings; optimum between 4.6 and 10.8 ^{o}C (Tolderlund and Bé, 1971).
- test size seems inversely correlated to temperature (Kroon et al., 1988).
** conclusions: tolerant to fairly low salinities and indicative of low temperatures and/or enhanced fertility in surficial waters (Hemleben, pers. comm. Cambridge 1989).

Neogloboquadrina spp.

- category of neogloboquadrinids in this study comprises predominantly dextrally coiled pachyderma types and quite tightly coiled dutertrei types. Both the reason to group them, and the records from three northern Levantine cores, are treated by Rohling and Gieskes (Chapter 1).
- abundance closely linked to development of a Deep Chlorophyll Maximum (DCM) (Chapter 1; and references therein).
- often described as pycnocline-dwellers (also: Fairbanks et al., 1982; Hemleben and Spindler, 1983; Thunell and Reynolds, 1984; Bé et al., 1985; Hemleben et al., 1989; Pujol and Vergnaud-Grazzini, 1989; Reynolds and Thunell, 1989; Van Leeuwen, 1989).
- as a group, they have a very wide temperature range.
** conclusions: thrive in deeper, eutrophic, waters, below mixed layer and, therefore, indicative of stratified conditions within euphotic layer.

Globorotalia scitula

- probably thrives in very deep waters (Bé, 1969).
- although little is known, it seems to behave more or less like Globorotalia truncatulinoides (see below), calcifying at very great depths. In spring, offshore Bermuda, G. scitula appears near surface as very thin shelled specimen and subsequently sinks to deep water (Hemleben et al., 1989).
- characteristic for subpolar waters, together with T. quinqueloba and N. pachyderma (Bé, 1969; Thunell and Reynolds, 1984).
- occurs in temperate regions (Hemleben et al., 1989).
** conclusions: occurs down to great depths, in cool to cold waters.

Globigerina bulloides

- inhabits both mixed-layer (Bé, 1969; Bé et al., 1985; Hemleben et al., 1989; Reynolds and Thunell, 1989; Van Leeuwen, 1989) and deeper waters (Almogi-Labin, 1984; Hemleben et al., 1989; Pujol and Vergnaud-Grazzini, 1989).
- characterizes upwelling conditions (Kipp, 1976; Coulborn et al., 1980; Duplessy et al., 1981; Thiede, 1983; Zhang, 1985; Hemleben et al., 1989; Overpeck et al., 1989; Van Leeuwen, 1989). - also high standing stocks near river mouths (Barmawidjaja et al. 1989; Van Leeuwen, 1989).
- occurs in very warm tropical waters (Barmawidjaja et al., 1989) as well as in water with temperatures as low as 0 ^{o}C (Tolderlund and Bé, 1971).
- may occur in warmer waters only when the food level is high, and in cooler waters also at more variable food levels (Van Leeuwen, 1989).
** conclusions: no depth preference, but highly dependent on food levels enhanced by upwelling or river-input.

Globorotalia truncatulinoides

- very deep dwelling species (Tolderlund and Bé, 1971; Hutson, 1977; Hemleben and Spindler, 1983; Vergnaud-Grazzini et al., 1986; Hemleben et al., 1989).
- near Bermuda, G. truncatulinoides seems to reproduce in winter near the surface and continues to grow as it sinks to great depths (> 1000 m) (Hemleben et al., 1989). Lohmann and Schweitzer (1990), on the contrary, think that G.truncatulinoides reproduces at about 600 m waterdepth, and that vertical mixing down to that depth is required to return juveniles to surface.
- size distribution may be indication of thermocline depth (Lohmann and Schweitzer, 1990)

- temperature range between 10.5 and 28.1 $^{\circ}$C, optimum between 15.4 and 22 $^{\circ}$C (Tolderlund and Bé, 1971).
- marked preference for coiling either sinistral or dextral (Tolderlund and Bé, 1971; Brummer and Kroon, 1988; Hemleben et al., 1989).
- left-coiling shells spend only winter months in shallow water, while right-coiling shells persist there throughout the year (Lohmann and Schweitzer, 1990)
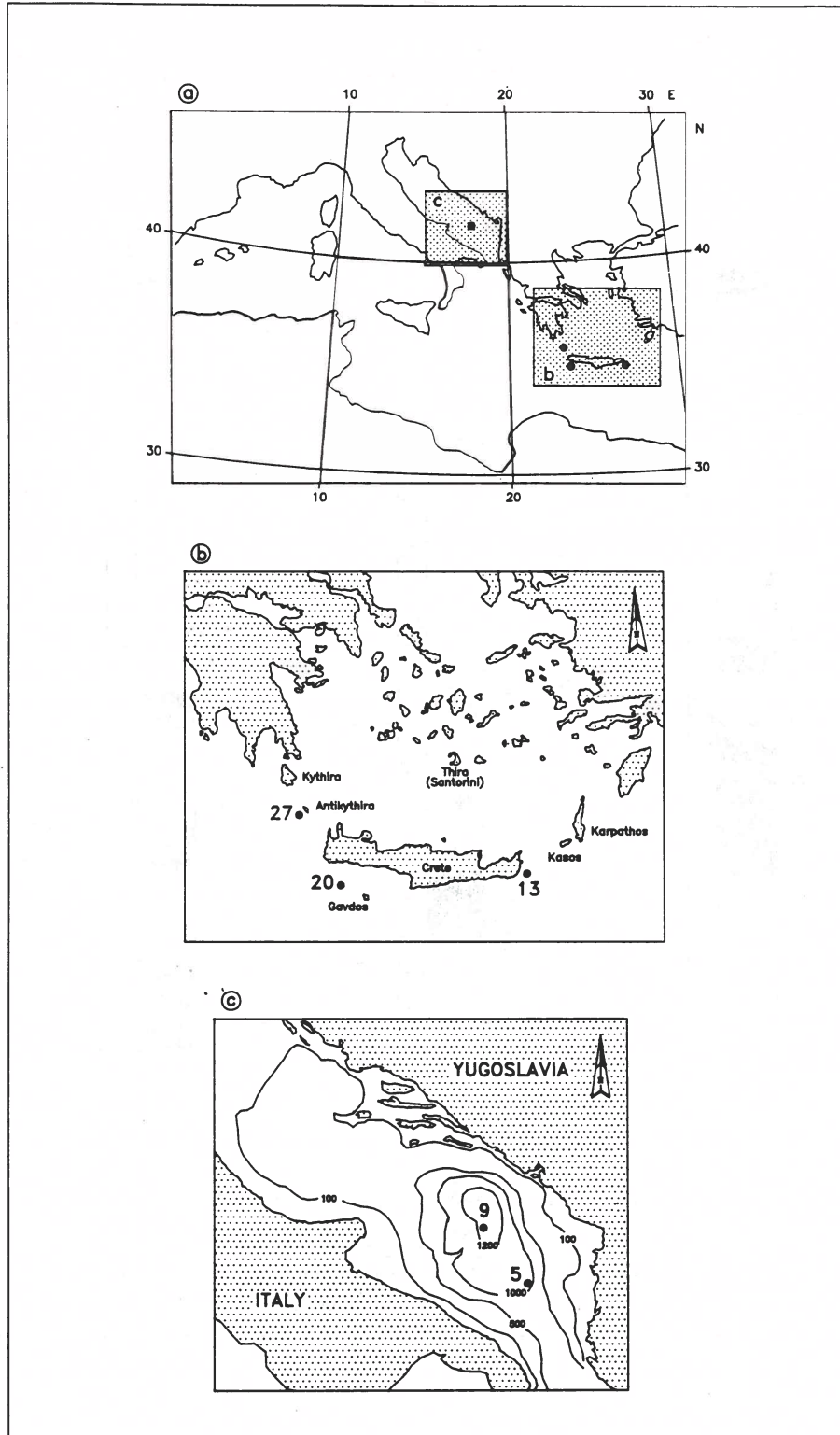** conclusions: occurs down to great depths, in fairly cool waters.

Figure 1. Locations of the cores T87/2/13G, T87/2/20G, T87/2/27G, IN68-5 and IN68-9.
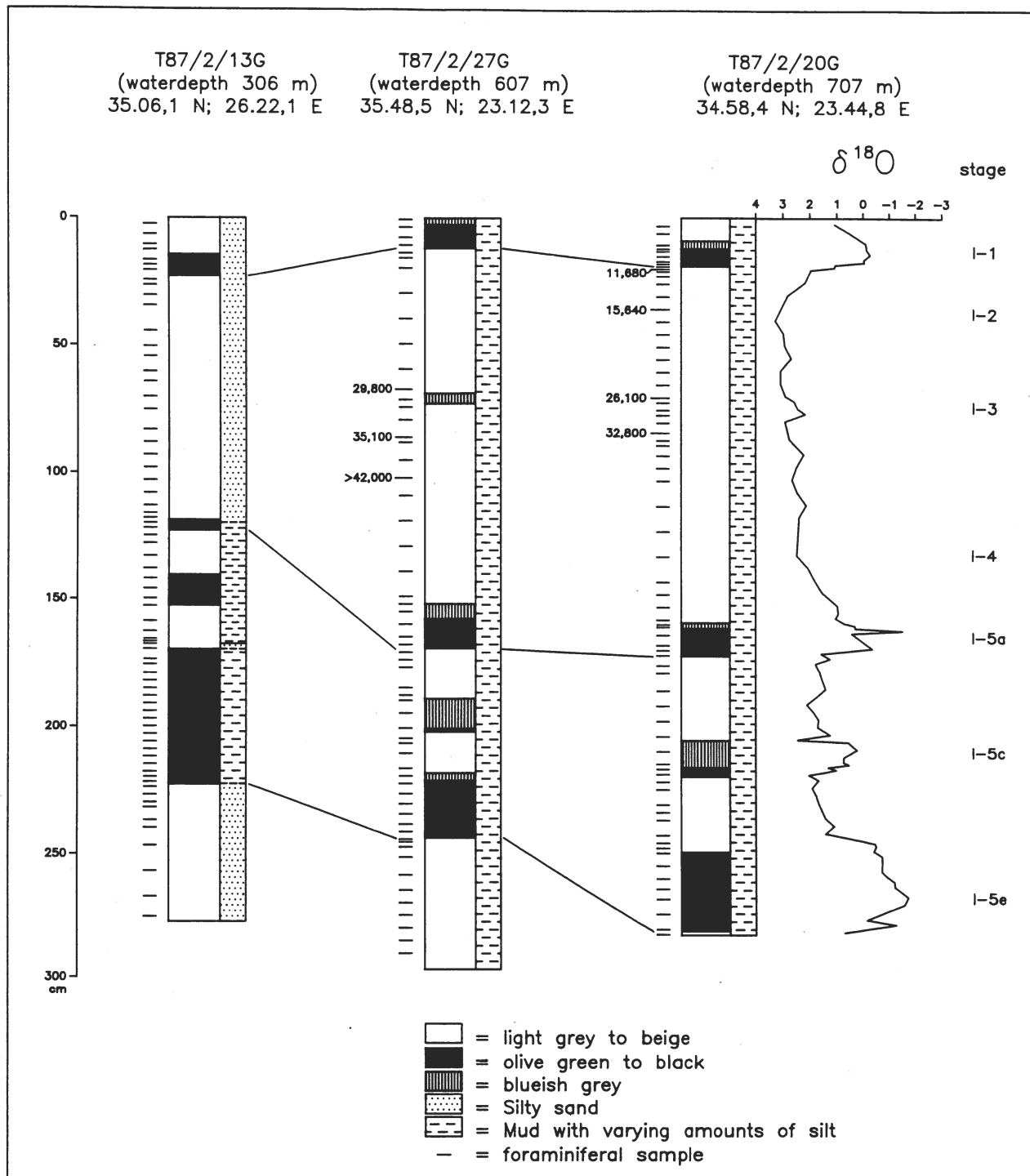
Figure 2. Lithology and sample positions of cores T87/2/13G, T87/2/20G and T87/2/27G (modified after Rohling and Gieskes, 1989). Small numerals along T87/2/20G and T87/2/27G represent AMS ^{14}C dates. The curve represents the oxygen isotopic record of T87/2/20G and a rough subdivision in isotopic stages is indicated.
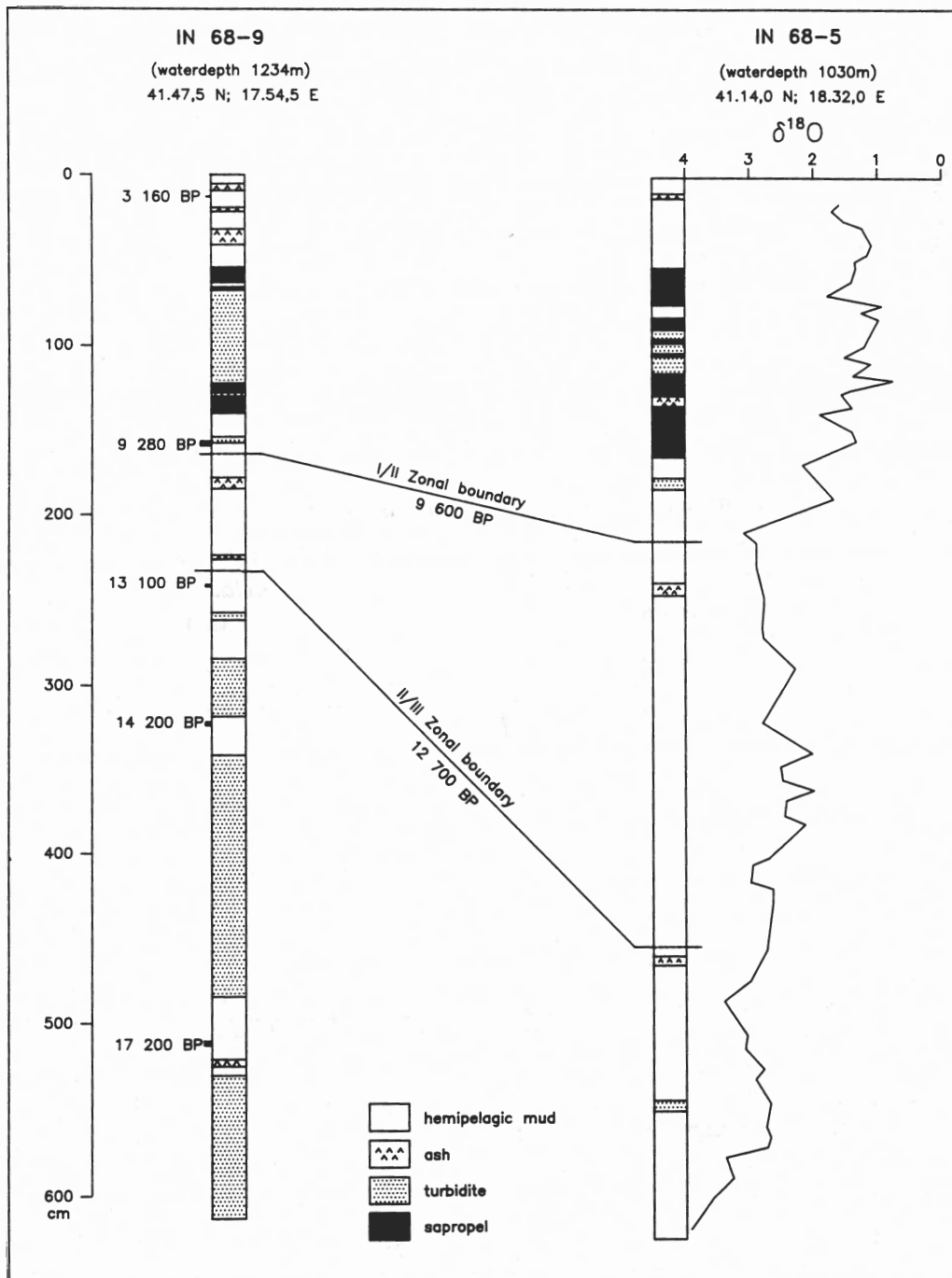
Figure 3. Lithology of cores IN68-5 and IN68-9, with planktonic foraminiferal zonal boundaries I/II and II/III, dated at 9 600 YBP and 12 700 YBP, respectively. Curve on right hand side represents oxygen isotope record of core IN68-5, based on carbonaceous tests of *G. bulloides.*
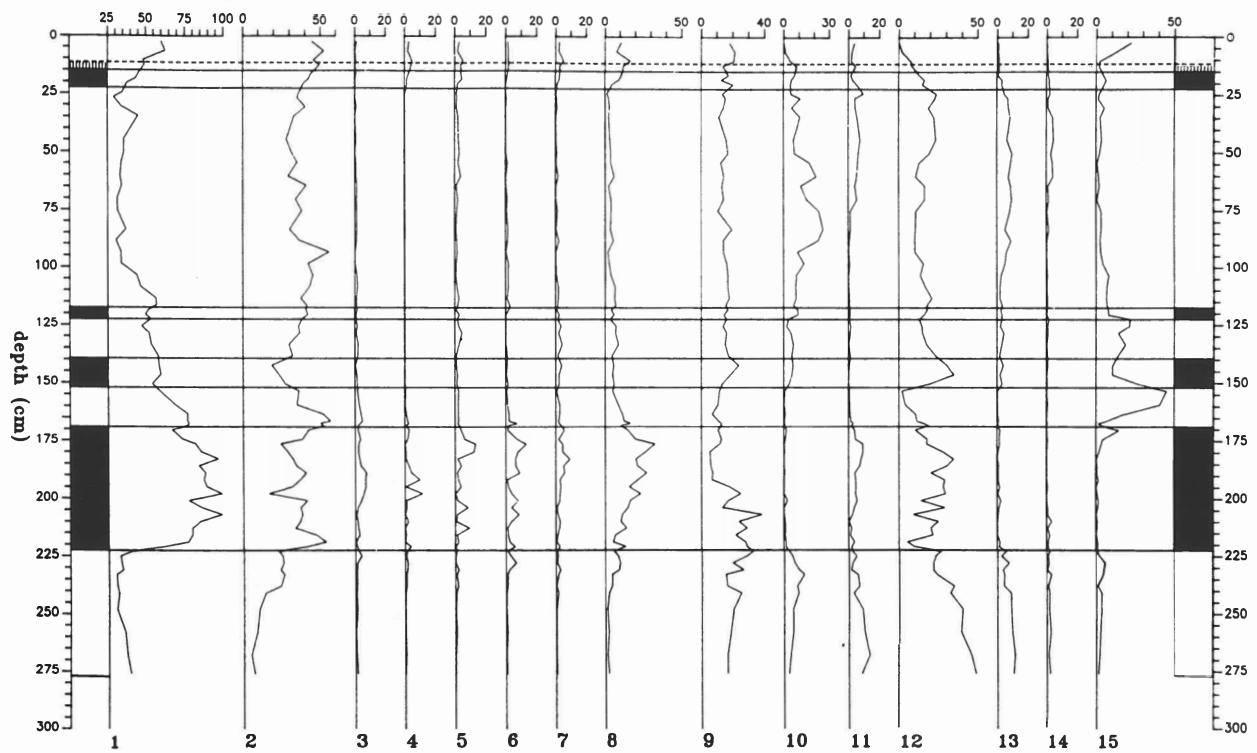
Figure 4. Planktonic foraminiferal frequency distribution in T87/2/13G.
1= 100*P/(P+B); 2= *G. ruber*; 3= *O. universa*; 4= *G. sacculifer*; 5= *G. rubescens*; 6= *G. tenella*; 7= *G. siphonifera*; 8= SPRUDTS-group; 9= *G. bulloides*; 10= *G. inflata*; 11= *G. glutinata*; 12= neogloboquadrinids; 13= *T. quinqueloba*; 14= *G. scitula*; 15= indeterminable.
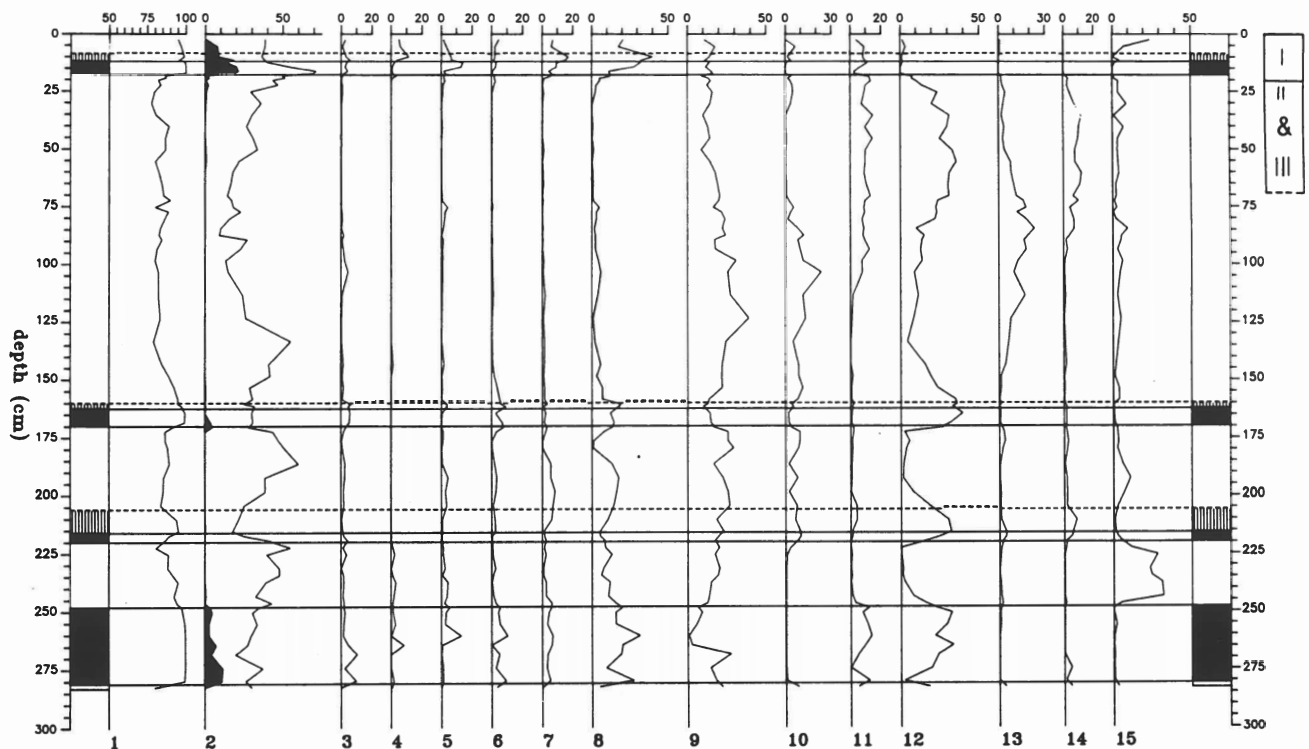
Figure 5. Planktonic foraminiferal frequency distribution in T87/2/20G. Numbers correspond to those in the caption of figure 4. Within the distribution of *G. ruber*, the black coloured portion indicates the frequency of the pink variety. Roman numerals indicate the faunal zones as defined by Jorissen et al. (Appendix 2).
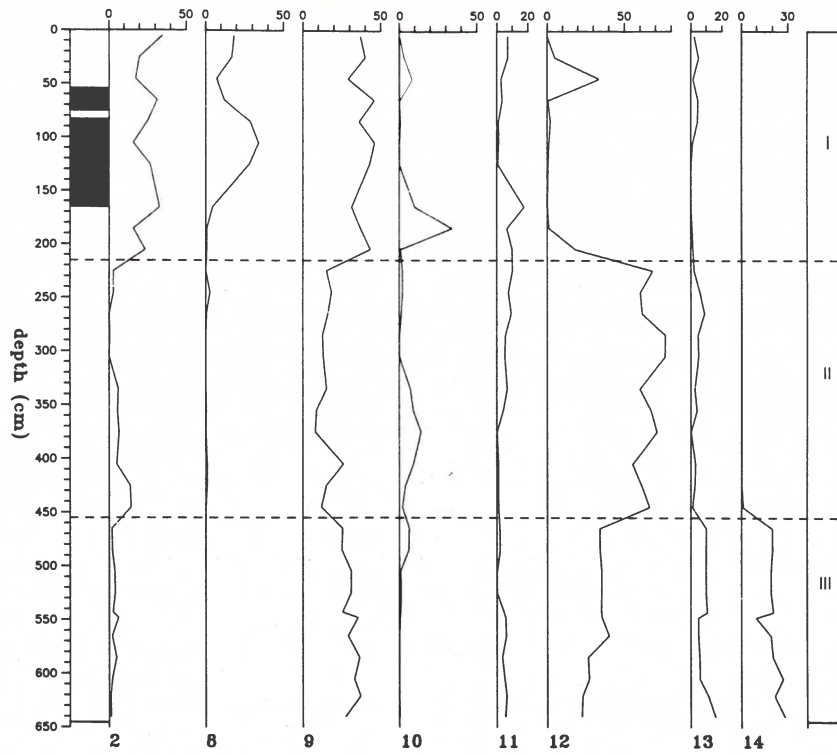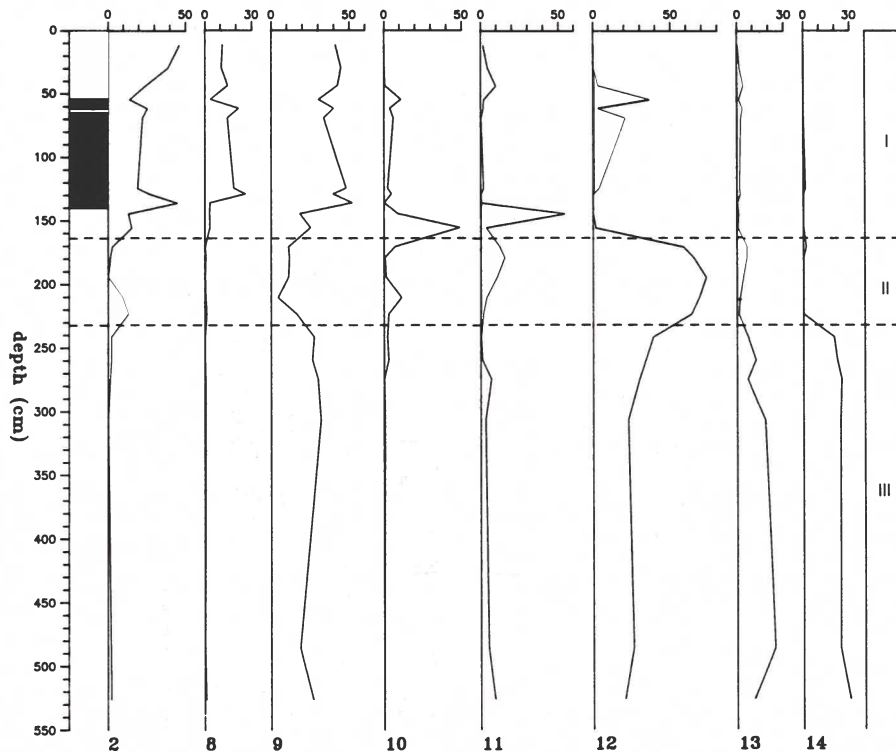
102
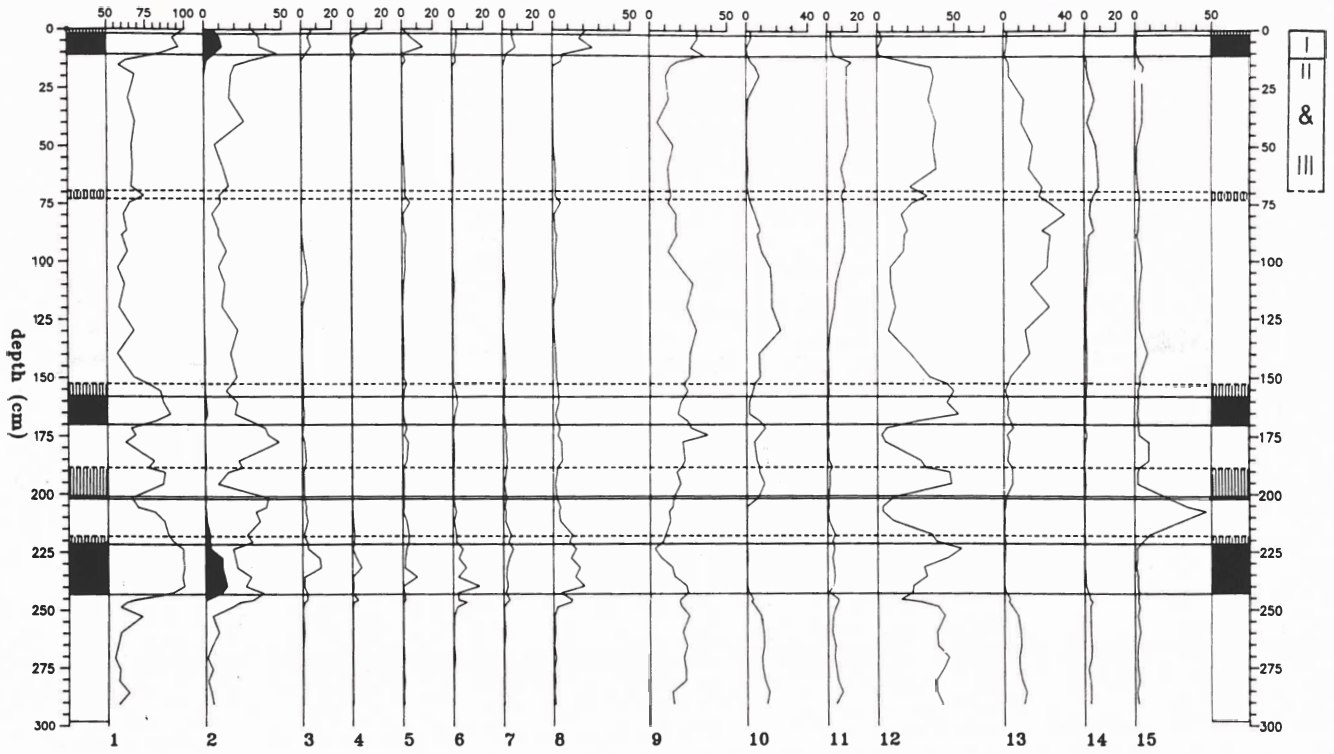
Figure 6. Planktonic foraminiferal frequency distribution in T87/2/27G. Numbers correspond to those in the caption of figure 4. Within the distribution of *G. ruber*, the black coloured portion indicates the frequency of the pink variety. Roman numerals indicate the faunal zones as defined by Jorissen et al. (Appendix 2).
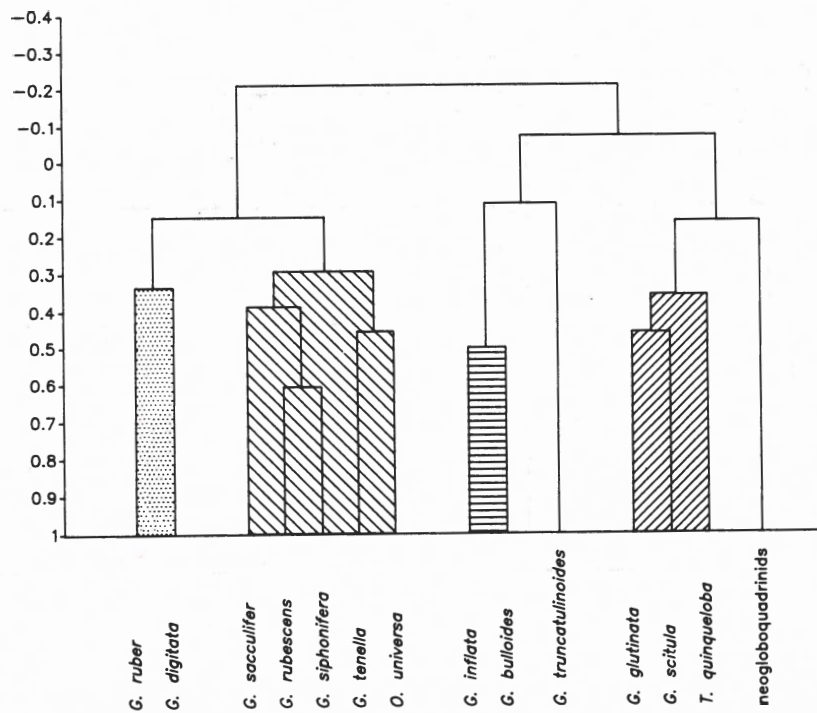
Figure 7. Dendrogram of combined record of T87/2/20G and T87/2/27G. This illustrates the gathering of several -individually low frequent- species into the so-called SPRUDTS-group (see Ecological Notes). Y-axis shows correlation coefficients.
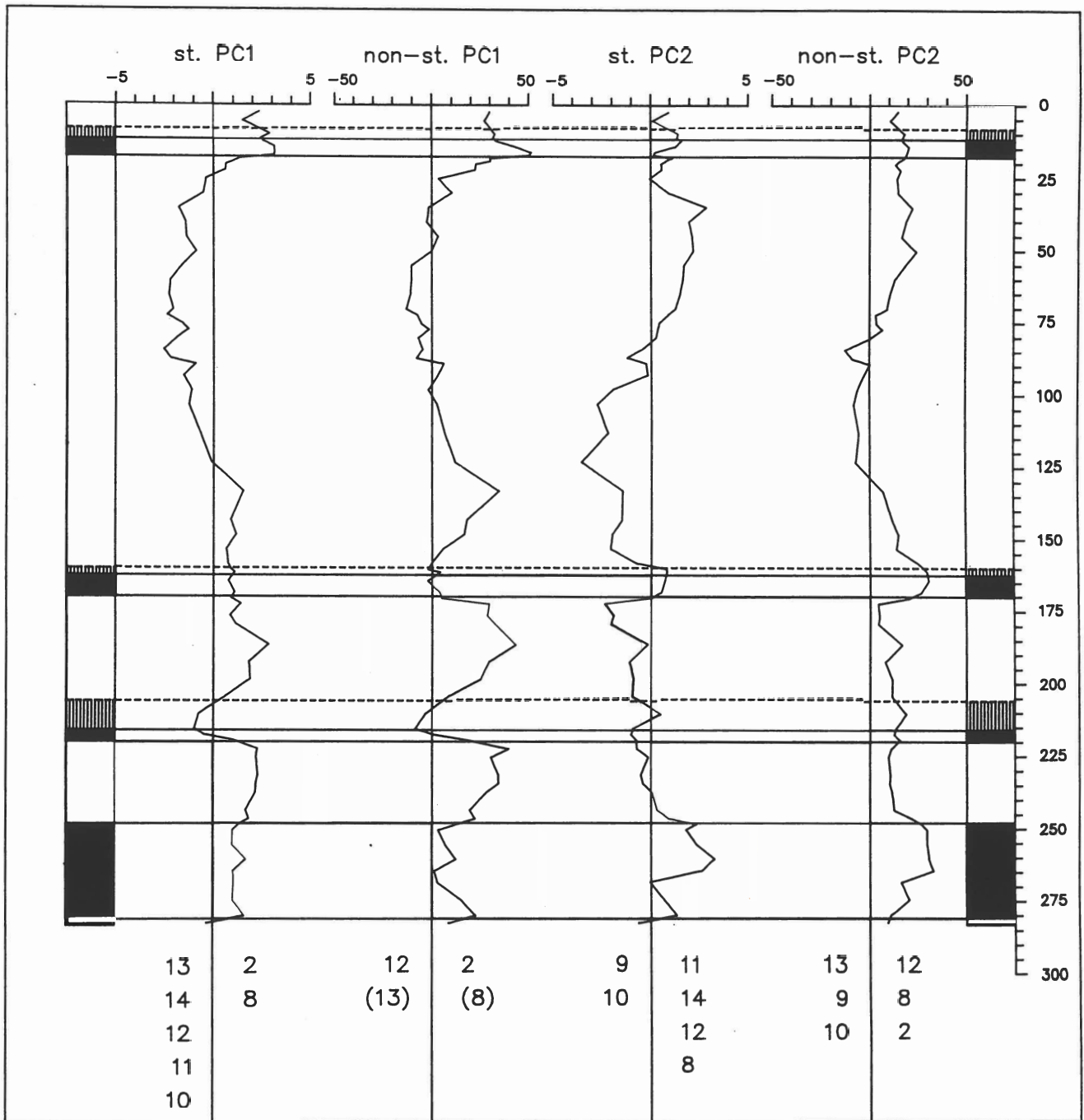
Figure 8. Downcore scores on the four PCA axes for core T87/2/20G. Numbers below the axes correspond to those in the caption of figure 4, and indicate the species dominating the positive or negative sides of the axes (cf. Table IV).
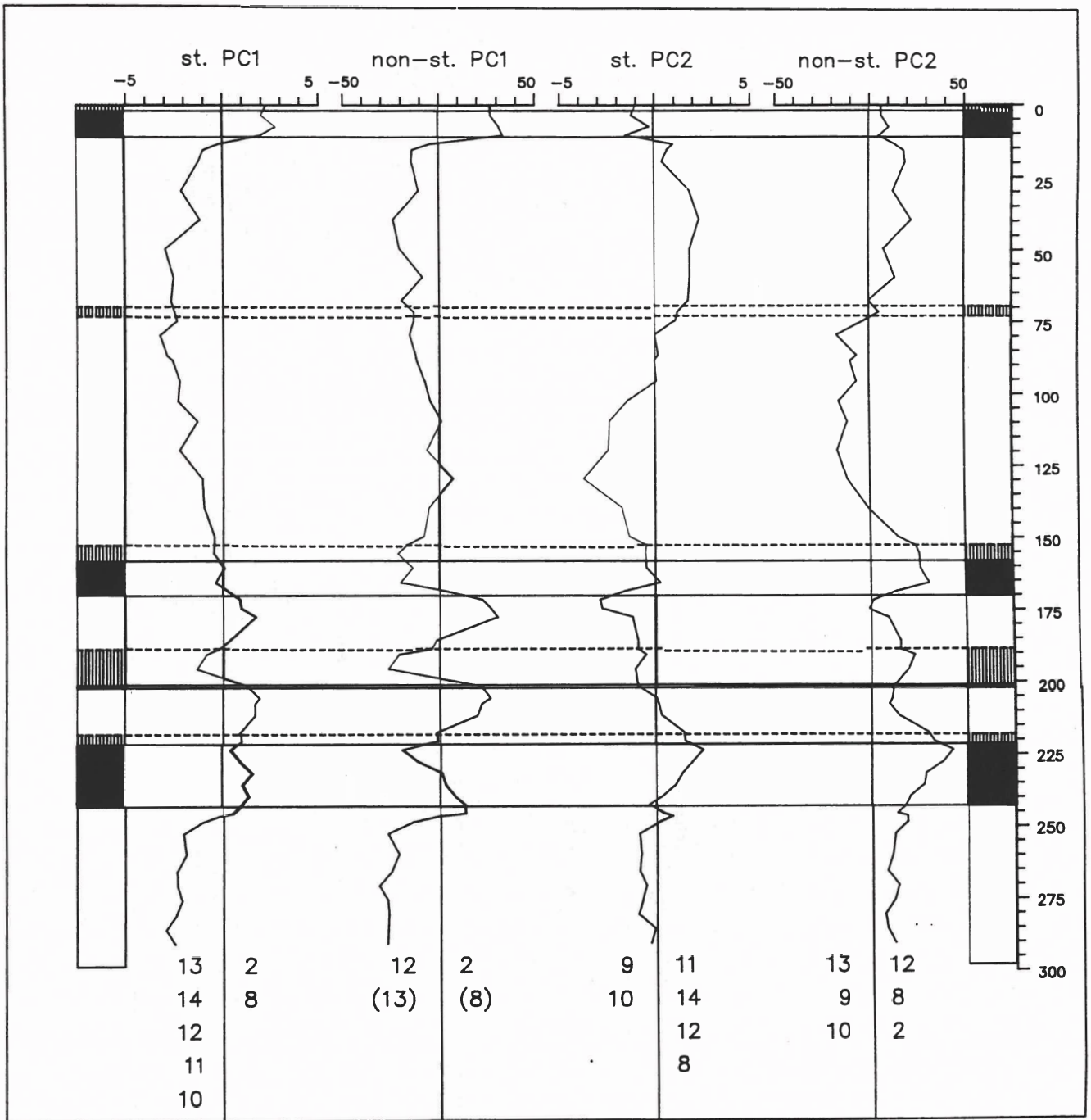
Figure 9. Downcore scores on the four PCA axes for core T87/2/27G. Numbers below the axes correspond to those in the caption of figure 4, and indicate the species dominating the positive or negative sides of the axes (cf. Table IV).
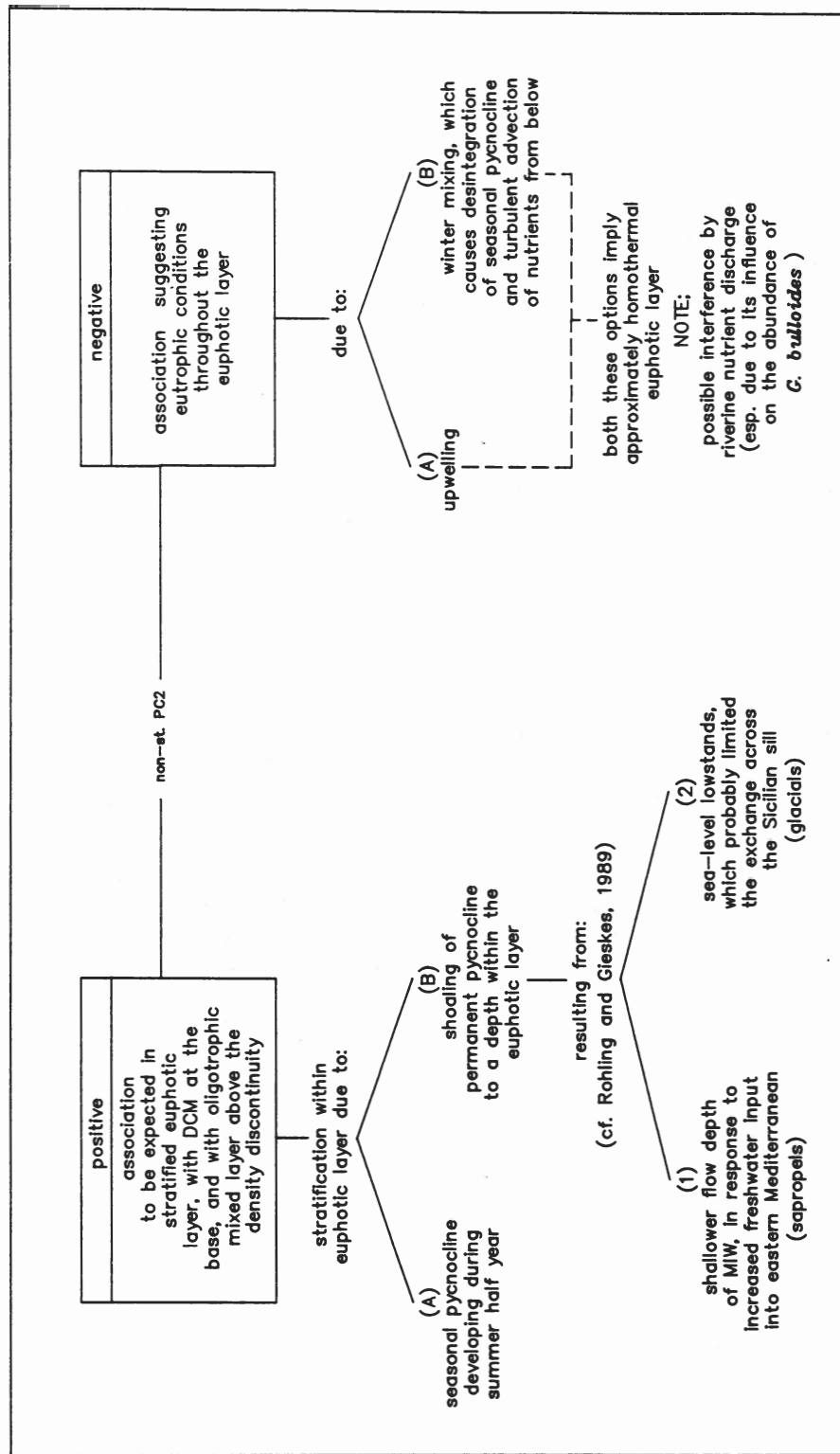
Figure 10. Schematic representation of the complex play of environmental parameters influencing the scores along the non-standardized PC2.

Figure 11. Planktonic foraminiferal frequency distribution in IN68-5. Numbers correspond to those in the caption of figure 4. Roman numerals indicate the faunal zones as defined by Jorissen et al. (Appendix 2).

Figure 12. Planktonic foraminiferal frequency distribution in IN68-9. Numbers correspond to those in the caption of figure 4. Roman numerals indicate the faunal zones as defined by Jorissen et al. (Appendix 2).

107
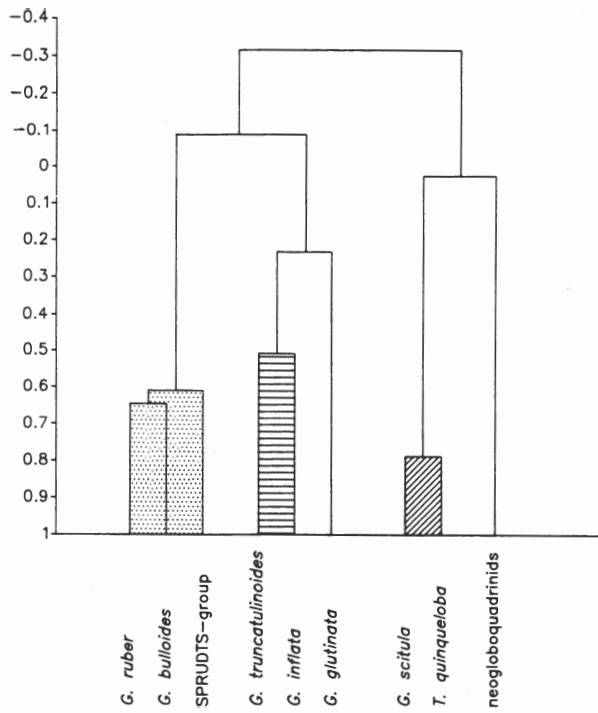
Figure 13. Dendrogram of the combined record of the Adriatic cores IN68-5 and IN68-9. Y-axis shows correlation coefficients.
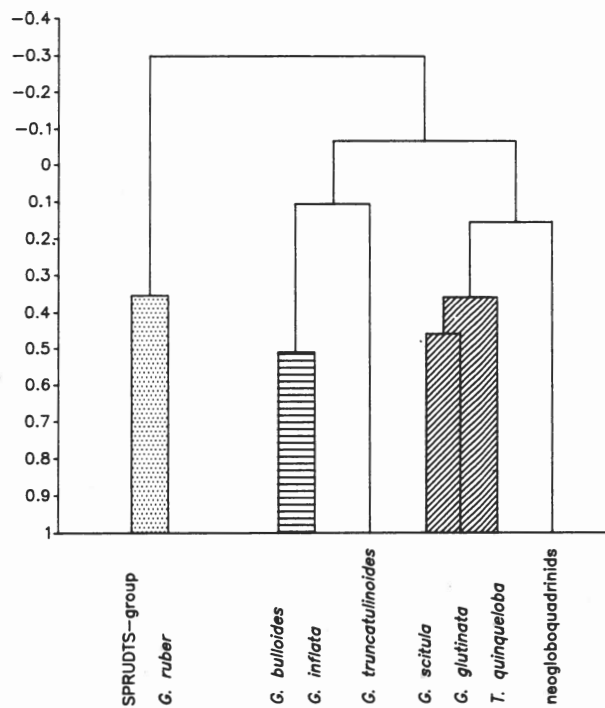
Figure 14. Dendrogram of the combined record of the northern Levantine cores T87/2/20G and T87/2/27G. Y-axis shows correlation coefficients.
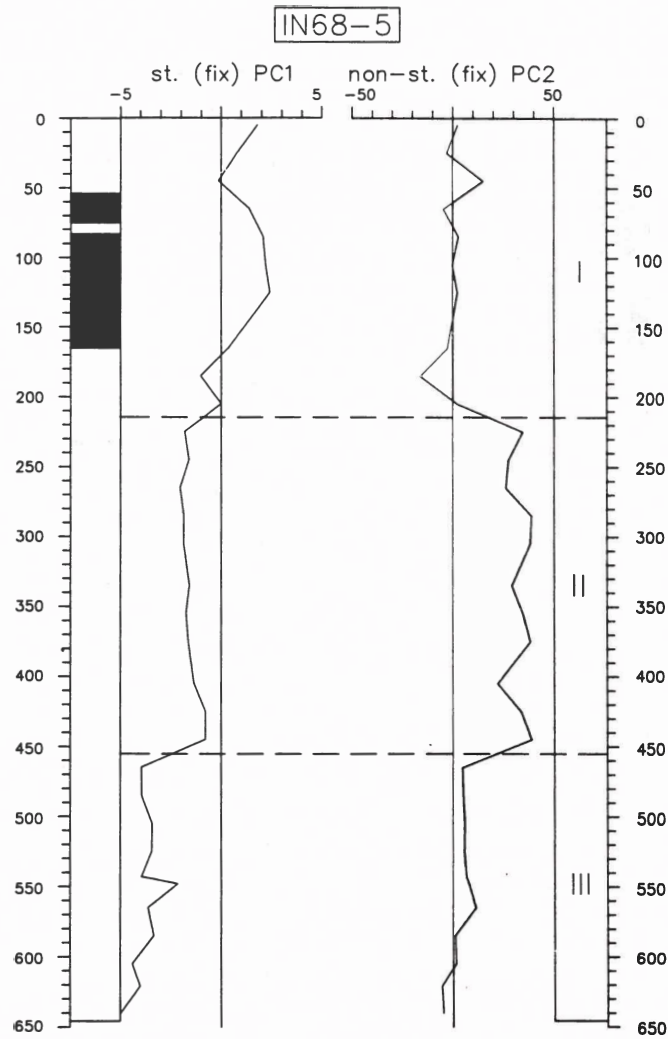
108

Figure 15. Downcore scores on the two FPCA axes for core IN68-5. Loadings of species along these axes are displayed in Table IV. Roman numerals indicate the faunal zones as defined by Jorissen et al. (Appendix 2).
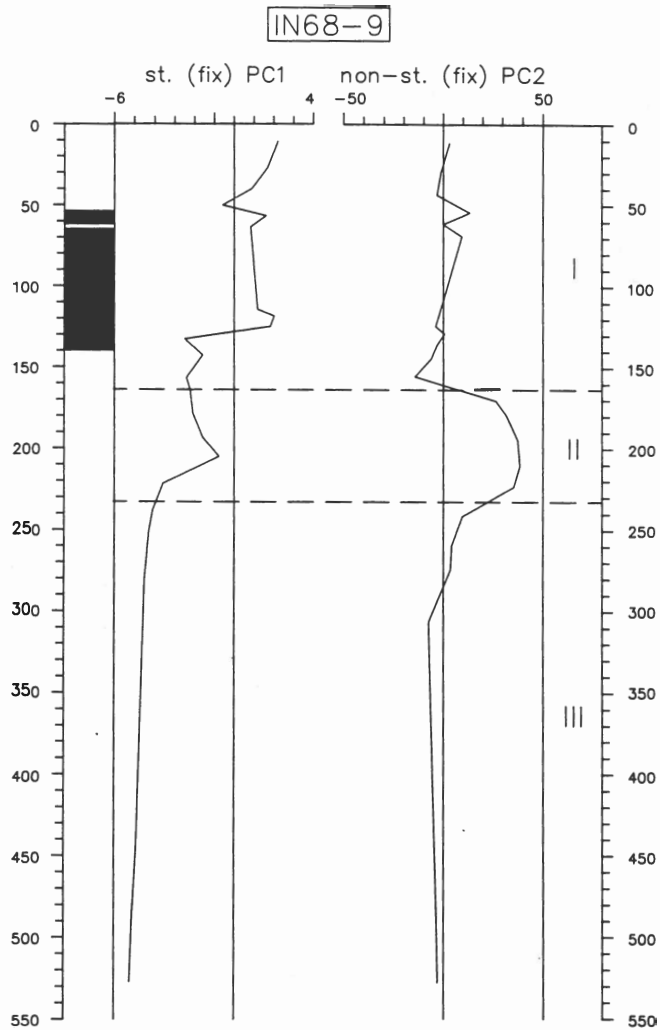
Figure 16. Downcore scores on the two FPCA axes for core IN68-9. Loadings of species along these axes are displayed in Table IV. Roman numerals indicate the faunal zones as defined by Jorissen et al. (Appendix 2).

TABLE I	
Core T87/2/20G	
Above S_1	colour change between 8 and 9 cm
Above S_3	colour change at about 160 cm
Above S_4	colour change at 206 cm
Core T87/2/27G	
Above S_1	no change visible in the 2 cm recovered above S_1
Above S_3	colour change between 152 and 153 cm
Above S_4	colour change between 188 and 189 cm
Above S_5	not obvious, sample at 217.5 cm may as well seem to be part of S_5 due to bioturbational mixing

Table I. The upper limits of the blueish grey layer which occurs above most sapropels in the northern Levantine cores T87/2/20G and T87/2/27G.

TABLE II			
Core T87/2/20G			
sapropel		presently visible	major faunal changes
S_1	top	12	between 5.5 & 10.0
	base	18	between 17.5 & 18.5
S_3	top	162.5	between 158.5 & 160.5
	base	172	between 170.5 & 172.5
S_4	top	216	between 204.5 & 210.5
	base	220	between 219.5 & 222.5
S_5	top	248	between 246.5 & 248.5
	base	281	between 280.0 & 282.5
Core T87/2/27G			
sapropel		presently visible	major faunal changes
S_1	top	2	above 0.5 (?)
	base	11	between 10.5 & 13.5
S_3	top	158	between 149.5 & 152.5
	base	170	between 168.5 & 171.5
S_4	top	201	between 185.5 & 188.5
	base	202	between 201.5 & 205.5
S_5	top	218	between 211.5 & 217.5
	base	243	between 242.5 & 245.5

Table II. The offsets between the limits of the presently visible sapropels and the major faunal changes in the northern Levantine cores T87/2/20G and T87/2/27G.

TABLE III					
A			**B**		
standardized PCA on T87/2/20G + T87/2/27G			non-standardized PCA on T87/2/20G + T87/2/27G		
axis	% trace	% cumulative	axis	% trace	% cumulative
1	32.27	32.27	1	56.33	56.33
2	22.31	54.58	2	20.42	76.75
3	12.66	67.24	3	9.89	86.64
4	12.04	79.28	4	7.70	94.35
5	9.13	88.41	5	2.20	96.54
6	5.11	93.77	6	1.80	98.34
7	3.26	96.77	7	1.11	99.45
8	2.48	99.25	8	0.50	99.95
9	0.75	100.00	9	0.05	100.00

Table III. **A)** The percentages of the variation explained by each PCA axis separately and the cumulative percentage. The result for the standardized run on the combined record of T87/2/20G and T87/2/27G.

B) The percentages of the variation explained by each PCA axis separately and the cumulative percentage. The result for the non-standardized run on the combined record of T87/2/20G and T87/2/27G.

TABLE IV	
A	**B**
Cores T87/2/20G + T87/2/27G	Cores T87/2/20G + T87/2/27G
ranking on *standardized* PC1	ranking on *non-standardized* PC1
G. ruber +0.49 SPRUDTS−group +0.41 G. truncatulinoides +0.05 G. bulloides −0.03 G. inflata −0.24 G. glutinata −0.26 neogloboquadrinids −0.32 G. scitula −0.38 T. quinqueloba −0.46	G. ruber +0.68 SPRUDTS−group +0.21 G. bulloides +0.03 G. truncatulinoides 0.00 G. glutinata −0.06 G. scitula −0.06 G. inflata −0.07 T. quinqueloba −0.22 neogloboquadrinids −.065
ranking on *standardized* PC2	ranking on *non-standardized* PC2
G. glutinata +0.42 G. scitula · +0.23 neogloboquadrinids +0.22 SPRUDTS−group +0.22 G. ruber −0.01 T. quinqueloba −0.10 G. truncatulinoides −0.16 G. inflata −0.54 G. bulloides −0.59	neogloboquadrinids +0.60 SPRUDTS−group +0.31 G. ruber +0.30 G. truncatulinoides 0.00 G. scitula −0.03 G. glutinata −0.04 G. inflata −0.25 G. bulloides −0.34 T. quinqueloba −0.52

Table IV. **A)** Ranking of the species along the first and second PCA axis, together with their loadings. The result for the standardized run on the combined record of T87/2/20G and T87/2/27G.

B) Ranking of the species along the first and second PCA axis, together with their loadings. The result for the non-standardized run on the combined record of T87/2/20G and T87/2/27G.

appendix 2

LATE QUATERNARY CENTRAL MEDITERRANEAN BIOCHRONOLOGY

LATE QUATERNARY CENTRAL MEDITERRANEAN BIOCHRONO-LOGY

F.J. Jorissen[1], A. Asioli[2], A.M. Borsetti[3], L. Capotondi[2], A.F.M. De Jong[4], J.P. De Visser[1], L. Gudjonsson[1], F.J. Hilgen[1], E.J. Rohling[1], K. Van der Borg[4], C. Vergnaud-Grazzini[5] and W.J. Zachariasse[1]

1. *Department of Stratigraphy and Micropaleontology, Institute of Earth Sciences, University of Utrecht, P.O.Box 80.021, 3508 TA Utrecht, The Netherlands*

2. *Universita degli Studi di Parma, Istituto di Geologia, Via Kennedy 4, 43100 Parma, Italy*

3. *Istituto di Geologia Marina del CNR, Via Zamboni, 65, I 40127 Bologna, Italy*

4. *Robert J. van de Graaff Laboratorium, University of Utrecht, P.O.Box 80.000, 3508 TA Utrecht, The Netherlands*

5. *Laboratoire d'Océanographie Dynamique et de Climatologie, Université Pierre et Marie Curie, Tour 12, 2ᵉ étage; 4, Place Jussieu - 75252 Paris Cedex 05, France*

ABSTRACT

A high-resolution biochronology is presented for the Late Quaternary of the central Mediterranean. In the Late Pleistocene-Holocene successions three assemblage zones are distinguished on the basis of frequency patterns of planktonic foraminifera. These zones are calibrated with the absolute time scale by Accelerator Mass Spectrometry (AMS) ^{14}C dates. The zonal boundaries are dated 12,700 YBP (the end of termination Ia) and 9600 YBP (the end of termination Ib), respectively. The AMS dates conclusively show that major changes in the planktonic and benthic realms occurred synchronously over wide areas, although especially in the benthic records, different taxa may be involved in the various subareas. In the areas studied, resedimentation processes, revealed by anomalies in the successions of ^{14}C dates, play a far more important role than was expected on the basis of the sedimentological and micropaleontological data. Especially the very high accumulation rates in the glacial zone III can be attributed to these processes. Although the AMS technique has increased the accuracy of ^{14}C-ages, admixture of older carbonate may still lead to substantial age differences between areas with different sedimentary regimes.

INTRODUCTION

The last glacial cycle is one of the best documented examples of abrupt climatic change. Research has concentrated on high-sedimentation open-ocean records. In the Mediterranean, accumulation rates are generally low, and thus, few detailed studies on the last 15,000 years have been conducted (e.g. Buckley et al., 1982; Buckley and Johnson, 1988; Caralp, 1988; Vergnaud-Grazzini et al., 1988). In the Adriatic Sea, which is characterized by high sedimentation rates, a large number of high quality piston-cores have been recovered in recent decades (e.g. Colantoni and Galignani, 1977). The papers dealing with these cores lack a reliable time-stratigraphic frame (e.g. D'Onofrio, 1959, 1973; Cita and Chierici, 1962; Bottema and Van Straaten, 1966; Van Straaten, 1966, 1967, 1972, 1985; Cita and D'Onofrio, 1967; Breman, 1975; Van der Zwaan, 1980). Only with the advent of Accelerator Mass Spectrometry (AMS) it has become possible to obtain accurate ^{14}C-ages with small quantities of calcium carbonate. It is the

primary scope of the present paper to provide a central Mediterranean high-resolution biochronology which allows comparison with the open ocean deglaciation records.

Stanley (1985) opens a paper discussing the influence of redepositonal processes on mud sedimentation in the Mediterranean by stating that "fine-grained sediments, forming the bulk of unconsolidated Plio-Quaternary series on Mediterranean margins and basins, are largely of redepositional origin." Obviously, much caution is needed when interpreting faunal assemblages from these sediments.

If redepositional processes are wide-spread in the low-accumulation extra-Adriatic regions, then such processes will certainly be important in the Adriatic Sea. It is of primary importance to establish whether the Adriatic Sea sediments are affected by redepositional processes, and if so, to what extent these processes have distorted the original faunal signal. Unfortunately, most of the sediment cores studied in this paper were sampled in 1968, when the influence of redepositional processes was still not fully appreciated, and it was not yet common practice to take X-ray radiographs.

In this paper we will focuss on a number of aspects related to the core stratigraphy. Since the benthic system is much more affected by local environmental parameters than the pelagic system, we based our biozonation on the succession of planktonic foraminifera (in the southern Adriatic Sea). The successions of benthic foraminifera are used for local refinements of the biozonation. The applicability of our zonation outside the Adriatic Sea is tested in two sediment cores from the Strait of Sicily and the Tyrrhenian Sea. The paleoecology of the Late Quaternary planktonic foraminiferal assemblages is treated by Rohling et al. (Appendix 1).

MATERIAL AND METHODS

We selected 11 sediment cores from the Adriatic Sea (fig. 1, Table I), where according to core descriptions (Colantoni and Galignani, 1977; UU.OO. Gruppo Bacini Sedimentari, 1979) a minimum of down-slope transport and a maximum of hemipelagic muds could be expected. For comparison two cores from the Strait of Sicily and the Tyrrhenian Sea were selected.

In total some 400 samples were studied; the samples were washed over sieves with meshwidths of 63, 150 and 595 microns. The 150-595 micron fraction was split in suitable aliquots of at least 200 planktonic foraminifera and of 250 benthic foraminifera respectively. The identified taxa were quantified as a percentage of the total number of planktonic or benthic foraminifera.

For the planktonic foraminifera we largely followed the taxonomic concept of Hemleben et al. (1989). The benthic foraminiferal taxonomy is basically similar to that of Jorissen (1987,1988). A faunal reference list is given in the added taxonomical notes.

$\delta^{18}O$ values of the planktonic foraminifer Globigerina bulloides were measured for cores IN 68-9 and IN 68-21. Standard laboratorium procedures, as described by Shackleton and Opdyke (1973), were followed. Sira 24 mass-spectrometer measurements are reported as %-deviations from the PDB-1 standard (Epstein et al., 1953).

Accelerator Mass Spectrometry ^{14}C datings were performed on 45 samples. For shallow sites we used carbonate of mixed benthic organisms (foraminifera, molluscs, bryozoans), whereas carbonate of mixed pelagic organisms (foraminifera, pteropods) was used at deeper sites. In three cases ^{14}C-datings have been performed on both pelagic and benthic material.

The biogenic material used for the ^{14}C dates was hand-picked and pretreated with 4 % HCL. The evolved CO_2 gas was reduced to graphite using finely divided iron powder in the presence of excess hydrogen at $920°K$ (Hut et al., 1986). Subsequently, the mixture was pressed into a hole of an aluminium holder and the $^{14}C/^{12}C$ ratio was analysed, using the Utrecht tandem

accelerator (Van der Borg et al., 1987). The ^{14}C results are expressed in radiocarbon years, corrected for fractionation according to the $\delta^{13}C$-values (Stuiver, 1983), and reported with $1-\sigma$ error including the reproducibility and background. The $\delta^{13}C_{PDB}$ values were routinely measured at the Utrecht Institute of Earth Sciences. No corrections have been made for the mean apparent ^{14}C-age of surface sea water (reservoir age), which at low and middle latitudes is estimated to be about 400 years (Bard, 1988; Broecker et al., 1988; Bard et al., 1990).

PLANKTONIC FORAMINIFERAL ZONATION

The zonation proposed here is based on major compositional changes in the succession of planktonic foraminifera in the southern part of the Adriatic Sea. It consists of three zones, which roughly correspond with the succession of pleniglacial, transitional and postglacial phases. A fourth (older) zone is not yet well-defined, because this zone has only been penetrated at two sites, at both of which the successions of ^{14}C-dates indicate major disturbances in the basal part of the record. The three zones defined in the southern Adriatic basin are equally recognizable in the central Adriatic basin (IN 68-21), the Strait of Sicily (CS 73-34) and the Tyrrhenian Sea (BS 78-12). Although the zones are numbered from top to bottom, faunal changes will be discussed in actual (stratigraphic) order, viz. from bottom to top.

The abundance patterns of the dominating species in the various cores are shown in figs. 2 and 3. For reasons explained by Rohling and Gieskes (Chapter 1), all morphotypes of Neogloboquadrina are lumped together. The species Globigerinella siphonifera, Hastigerina pelagica, Globoturborotalita rubescens, Orbulina universa, Globigerina digitata, Globoturborotalita tenella and Globigerinoides sacculifer, which show significant positive correlations in a large number of statistical analyses performed on the present data set, will hereafter be treated as one category ("SPRUDTS"-group) (see also Appendix 1).

Zone I is characterized by the continous presence (> 1%) of the SPRUDTS-group (except for the very basal part of the zone), the (near-)absence of Globorotalia scitula (< 1%), high relative frequencies of (both white and pink) Globigerinoides ruber (> 7.5 %), and low numbers of Turborotalita quingueloba (< 7.5 %). Globorotalia truncatulinoides, which is always scarce, displays a predominantly sinistral coiling. Except for some specific levels, Neogloboquadrina spp. and Globorotalia inflata are absent in zone I. In the most complete (and densely sampled) records (IN 68-5 and IN 68-9) there is a clear succession of peak-frequencies of various species (figs. 2,3). A spike of G. inflata at the base of the zone is followed directly by a peak frequency of Globigerinita glutinata. Higher up in zone I, a level with abundant Neogloboquadrina and G. inflata appears to be followed by sediments with raised frequencies of G. glutinata. These short-term peak occurrences are positioned around sapropel S_1, which is well-developed in the southern Adriatic Sea, and consists of two laminated parts, separated by a thin interval of homogeneous mud. The peak amplitudes, which are very variable, seem to be strongly influenced by the sample width, which unfortunately varies from 1 to 10 cm. Apart from these S_1-related peaks, the main characteristics of zone I are very similar throughout the central Mediterranean (Figs. 2-3).

Zone II is characterized by the (near-)absence (< 1%) of G. scitula and the SPRUDTS-group and by high frequencies of Neogloboquadrina spp. (> 17.5 %). Pink-coloured specimens of G. ruber are scarce. In the basal part of the zone the coiling direction in the low frequent G. truncatulinoides changes from predominantly dextral to predominantly sinistral. The lower part of zone II shows raised percentages of G. inflata and G. ruber in combination with suppressed numbers of T. quinqueloba and G. glutinata; the reversed pattern is present in the upper part of the zone. Although the near-absence of G. scitula and the SPRUDTS-group are

116

consistent throughout the Mediterranean, the high frequencies of Neogloboquadrina are prone to considerable geographic variation. The maximal frequencies in zone II are typical for the southern Adriatic Sea; in the Strait of Sicily and Tyrrhenian Sea Neogloboquadrina are equally abundant in zones II and III, in the central Adriatic Sea they are relatively low-frequent throughout.

Zone III is characterized by the presence of G. scitula (> 1%), the (near-)absence of the SPRUDTS-group (< 1%), and relatively high abundances of T. quinqueloba (> 3.5 %). G. inflata is absent, except for the very top of zone III (there always < 7.5%). G. ruber, which is relatively low-frequent (< 22.5 %), is always white-coloured. G. truncatulinoides is virtually absent in zone III. These zonal criteria are also applicable in the Strait of Sicily and the Tyrrhenian Sea. However, time-equivalent levels in the central Adriatic basin contain a totally different fauna, which is strongly dominated by T. quinqueloba (figs. 2-3).

Since presence/absence levels are strongly influenced by various processes of sediment mixing, we avoided their use as much as possible for the positioning of zonal boundaries, but tried to use quantitative and sequence criteria instead. The I/II zonal boundary is placed at the very abrupt upward frequency drop of Neogloboquadrina. Generally this event is coincident with a sudden increase in G. ruber, and slightly precedes an increase in the SPRUDTS-group (figs. 2-3). The II/III zonal boundary is placed at the strong diminution of G. scitula. Generally, frequencies of this species rapidly fall to zero, but at sites with lower accumulation rates (e.g. IN 68-7) bioturbation has resulted in the presence of G. scitula in significantly younger levels (fig. 3). Usually this drop in G. scitula is slightly preceded by the re-appearance level of G. inflata. G. scitula is absent in core IN 68-21 from the central Adriatic basin, where the II/III zonal boundary is placed at the dramatic frequency drop in T. quinqueloba. The base of zone III is tentatively placed at the temporal disappearance level of G. inflata, which is only present in cores IN 68-7 (southern Adriatic Sea) and CS 73-34 (Strait of Sicily). Unfortunately, in both cores the ^{14}C-ages suggest major disturbances in the part of the sedimentary record where this event is positioned.

Although the zonal bodies and boundaries can be identified all over the central Mediterranean, there are substantial geographic variations in the faunal composition. In core IN 68-21 from the central Adriatic basin, the fauna in zone III differs completely from that of all other areas. Subsurface dwelling planktonic foraminifera such as globorotaliids and neogloboquadrinids are (almost) absent, whereas the surface-dwelling cool-water species T. quinqueloba strongly dominates the fauna (up to 90%). Also in zones I and II of core IN 68-21, the relative frequencies of most taxa differ considerably from those in the southern Adriatic basin (e.g. lower percentages of G. inflata and Neogloboquadrina). Nevertheless, trends of individual species are comparable. A first attempt to apply our zonation in the eastern Mediterranean proved to be successful. The faunal succession in a core from the Aegean Sea (Sporades Basin) is remarkably similar to that in the southern Adriatic Sea; even the short-term peaks of G. inflata and Neogloboquadrina around sapropel S_1 are present there (Zachariasse et al., Appendix 3).

^{14}C STRATIGRAPHY AND PLANKTONIC FORAMINIFERAL BIOCHRONOLOGY

In order to determine the age and synchroneity of our biozones, 45 samples were dated (table II). For three samples two ^{14}C-dates were obtained, one on benthic foraminifera, and one on pteropods. Age differences between these pairs are minimal, and apparently random, indicating that planktonic and benthic organisms can be used indifferently for a ^{14}C-date in this region. In these three cases of "duplicate" dates, we used the younger ages.

The succession of ^{14}C-ages is very consistent down to 15,000 YBP in all cores (fig. 4). Below that level the chronology shows major anomalies in three cores (IN 68-29, IN 68-7 and CS 73-34). In our opinion these anomalous successions of ^{14}C ages can only be explained by slumping

of larger sedimentary units. Core 68-7 shows a turbiditic level between 2.58 and 2.73 m (Colantoni and Galignani, 1977). The sample dated 23,200 YBP (2.5 m) is positioned slightly above this interval, and could therefore belong to the fine-grained top of this turbidite. The very quick passage from 18,500 YBP at 3.35 m to > 42,000 YBP at 4.03 m in the same core strongly suggests the presence of a second major discontinuity. Although there are no clear indications for massive slumping in the two other cores showing an anomalous ^{14}C-stratigraphy (IN 68-29, CS 73-34), we see no other explanation for the apparent mixing of sedimentary units.

Wherever possible, ages of the I/II and II/III zonal boundaries were determined by linear interpolation between ^{14}C-dates (tables III and IV). Before interpolating all ash-layers and turbidites were omitted from the sedimentary record. The maximal age difference is 1270 years for the I/II zonal boundary and 950 years for the II/III zonal boundary. In the cores with the best time-control (IN 68-5 and IN 68-9) interpolation of ^{14}C-ages provided age constraints for a number of lithological horizons which were used by Van Straaten (1967, 1972, 1985) for intercore correlations within the Adriatic Sea (fig. 5). The ages of these apparently correlative ash-layers and turbidites, and also of our zonal boundaries, are systematically older in core IN 68-5 than in core IN 68-9. The age difference varies from 300 to 1400 years. Since both cores are located in the southern Adriatic Sea (only about 100 km apart), it seems highly improbable that the lithological horizons, or the faunal changes which define the zonal boundaries, are diachronous. The position of core IN 68-5 at the base of a relatively steep slope (fig. 1b), and the much higher accumulation rate than at site IN 68-9 (fig. 4) suggest that the older ages in core IN 68-5 result from down-slope transport of older foraminiferal tests.

Since there are a number of processes that can lead to an increase of apparent ^{14}C ages (e.g. input of older foraminiferal tests by downslope transport, bioturbation), we decided to use the youngest ages for constraining the ages of our bioevents. These youngest ages are found in core IN 68-9, which also is the core with the most detailed ^{14}C-record. The apparent ages of the most notable events in the planktonic foraminiferal record of core In 68-9 are given in table V.

Subsequently, we recalibrated all cores using the ages of a number of selected events dated in core IN 68-9 (fig. 6). These selected events are the I/II and II/III zonal boundaries (9600 YBP and 12,700 YBP respectively) and ash-levels 2 (2900 YBP) and 4 (4500 YBP) of van Straaten (1985). In the older parts of the cores (below the II/III zonal boundary), where the number of reliable correlative levels is limited, we preferred to calibrate the records on the basis of the actual ^{14}C-ages (fig. 6). Only for cores IN 68-28 and In 68-38, which lack ^{14}C-ages, we used ash 8 of Van Straaten (1985; age in IN 68-9: 17,900 YBP). In case of anomalous sequences of ^{14}C-ages, we only used the younger ages.

Based on these age recalibrations, sediment accumulation curves were constructed for all cores (fig. 6). These curves reveal that accumulation rates are generally lower in zone I than in zones II and III. Apparently the maximal accumulation rates in zone III result mainly from resedimentation processes, and not so much from an increase in the rate of hemi-pelagic sedimentation.

Subsequently, time-abundance plots of the most important taxa were constructed for all cores (figs. 7-8). In the southern Adriatic Sea cores, the position of (the double) sapropel S_1 has been indicated on the basis of its age in standard core IN 68-9. The basal part of five of the cores has been hatched horizontally as an indication of poor time control. In the case of cores IN 68-29, IN 68-7 and CS 73-34, poor time control was inferred from anomalous successions of ^{14}C ages (fig. 4). Moreover, the lowest 66 cm of core IN 68-7 have been omitted, because interpolation in that part of the core would certainly be erroneous. In the case of cores IN 68-28 and IN 68-38 the

basal part has been hatched because of the lack of ^{14}C-dates and the anomalous record of G. inflata.

Figures 7 and 8 show that, as could be expected, the planktonic foraminiferal records in zones I and II are indeed very similar. In most cases, time differences between bio-events in individual cores are less than 500 years. Unfortunately, the temporal disappearance of G. inflata, on which we tentatively defined the base of zone III, could not be dated with certainty. Both in cores IN 68-7 and CS 73-34, this bioevent is positioned in a section with anomalous ^{14}C-ages. Nevertheless, the fact that the temporal disappearance of G. inflata is not found in core IN 68-29, which yields a maximum ^{14}C-age of 27,100 YBP, suggests that the species disappeared from the central Mediterranean before that time. This is in agreement with the age of 36,000 YBP which Muerdter and Kennett (1984) assign to this event.

Biochronologies for the last glacial cycle with similar resolution as the one presented here have been published by Buckley and Johnson (1988) and Vergnaud-Grazzini et al. (1988). Unfortunately, the study of Buckley and Johnson (1988) is based on an assessment of the 250 micron size fraction, which seriously hampers a detailed comparison with our results. However, their timing of faunal events is consistent with our results, with a few notable exceptions. G. ruber shows much higher frequencies in the data set of Buckley and Johnson (1988) than in our cores. In our opinion these higher frequencies can only be explained by the use of a larger size fraction. We disagree with the interpretation of their core 3, which shows frequency patterns very similar to our core BS 78-12. The presence of G. inflata and the absence of G. scitula indicates that the basal part of this core (30-70 cm) does not contain full glacial sediments, but belongs to our zone II, and should be younger than 14,000 YBP. This is confirmed by the fact that a considerable part of G. ruber still consists of pink morphotypes here (fig. 3b in Buckley and Johnson, 1988).

The succession of faunal acmes and paracmes in core CS 70-5 from the Strait of Sicily (Vergnaud-Grazzini et al., 1988) is nearly identical to our records. However, the amplitudes of most taxa show considerable differences, what is probably again caused by the employment of a different size fraction (125 versus 150 microns).

BENTHIC FORAMINIFERAL BIOCHRONOLOGY

Essentially, the main changes in the benthic foraminiferal record are coincident with those in the planktonic foraminiferal record. In nearly all cases zonal boundaries could be positioned correctly on the basis of benthic foraminifera alone. In the southern and central Adriatic Sea the three zones cannot only be recognized on the basis of changes in the frequency distributions, but also by entries and exits of a number of highly indicative benthic foraminiferal taxa (Table VI). The frequencies of the most indicative taxa are plotted versus the apparent ^{14}C-ages in figures 9 to 12. Again, parts of the cores with poor time control are hatched horizontally, and sapropel S_1 is indicated according to the age constraints determined in standard core IN 68-9.

Since regional variations in species composition are substantial, we will first discuss the southern Adriatic cores, and will subsequently describe the regional deviations from this pattern. The succession in core IN 68-29, which, as far as the benthic foraminiferal record is concerned, seems to occupy an intermediate position between southern and central Adriatic Sea has been neglected in the following discussion on the southern Adriatic basin.

In the southern Adriatic Sea Zone I is characterized by the virtual absence of a number of taxa; Bolivina albatrossi, Cibicides wuellerstorfi, Siphotextularia affinis and Trifarina angulosa show an exit at or just above the zone I/II-boundary (Table VI, figs. 10-11). All these species are generally present in fair numbers below the I/II zonal boundary. Zone I is further characterized by high percentages of Uvigerina mediterranea, Gyroidina altiformis, Gyroidina orbicularis and

Hoeglundina elegans (figs. 9-10). However, typical low-oxygen tolerant taxa such as Globobulimina pyrula, Chilostomella czizeki, Cassidulinoides bradyi, Bulimina costata and Uvigerina peregrina dominate the assemblages in and around S_1 (figs. 9-11), where the afore-mentioned taxa may even be absent.

In the southern Adriatic Sea zone I can roughly be subdivided in 5 successive intervals on the basis of the succession of acmes and paracmes:

-- 9600 - 8500 YBP: a diversified fauna, in which Bolivina albatrossi, Bolivina spathulata and Siphotextularia affinis are still present.

-- 8500 - 6000 YBP: acmes of Chilostomella czizeki, Globobulimina pyrula, Cassidulinoides bradyi, Bulimina costata and Uvigerina peregrina indicate that the faunas are affected by low oxygen conditions. In the inner part of S_1 benthic faunas may even be absent.

-- 6000 - 4500 YBP: faunas without B. albatrossi, B. spathulata and S. affinis, and with fairly high percentages of Gyroidina altiformis, Gyroidina orbicularis and Nonion barleeanum. Uvigerina mediterranea does not exceed 15%.

-- 4500 - 3000 YBP: faunas with abundant Uvigerina mediterranea (> 20%) and Hoeglundina elegans. Nonion barleeanum is virtually absent.

-- 3000 YBP - Recent (missing interval in most cores): faunas differ from those of the previous interval by raised percentages of Cassidulina crassa and by the presence of Cassidulina subglobosa. Cassidulina subglobosa is only found in the topmost sample of five cores (fig. 9), in relative frequencies varying from 1 - 10%. Although extrapolated ages of these youngest samples vary considerably, we suppose that the entry of this taxon in the Mediterranean region is a synchronous, and very recent, phenomenon. The same holds for the frequency increase of Cassidulina crassa in the topmost samples of seven cores. If the presence of C. subglobosa and the peak value of C. crassa in the topmost sample indeed indicate that the actual sediment top has been sampled, then the large differences between the apparent ages of these samples would point to a Holocene phase of low accumulation rates, or even non-deposition, of variable duration.

The I/II zonal boundary (9600 YBP) coincides with a strong upward frequency decrease of Cibicides pachydermus (fig. 11). At the same level Trifarina angulosa shows a temporary exit.

In zone II (unlike zone I), Bolivina albatrossi, Cibicides wuellerstorfi, Siphotextularia affinis and Trifarina angulosa are present throughout. Just as in zone I, Karreriella bradyi is absent (fig. 12). Bulimina costata, Bulimina marginata, Hyalinea balthica and Nonion barleeanum are present in fair numbers (figs. 10,12). Two distinct intervals can be recognized within zone II:

-- 12,700 YBP - 11,000 YBP; Gyroidina altiformis and Uvigerina peregrina show relative maxima, whereas Cibicides pachydermus is low frequent or even absent.

-- 11,000 YBP - 9600 YBP: Cibicides pachydermus shows peak frequencies (up to 70 %), and in turn G. altiformis and U. peregrina are low frequent or even absent.

The II/III zonal boundary (12,700 YBP) coincides with the exit of Sigmoilina sellii and Karreriella bradyi (fig. 12). Gyroidina altiformis and Hoeglundina elegans enter at this level.

In zone III Bolivina albatrossi, Cibicides wuellerstorfi, Siphotextularia affinis as well as Karreriella bradyi are present. The assemblages are dominated by Bolivina spathulata, Cibicides pachydermus, Uvigerina peregrina and Pyrgo depressa. Two intervals can be distinguished on the basis of the relatively brief presence interval of Sigmoilina sellii:

-- older than 15,000 YBP: Sigmoilina sellii is absent.

-- 15,000 YBP - 12,700 YBP: Sigmoilina sellii is present.

In core IN 68-7 the exit level of Epistominella rugosa is positioned one sample below the temporary disappearance of the planktonic foraminifer Globorotalia inflata, on which we tentatively placed the basis of zone III. In core CS 73-34 (Strait of Sicily) the exit of E. rugosa is positioned 80 cm lower. Possibly also the exit of E. rugosa is a synchronous event, slightly preceding the temporal exit of G. inflata.

The afore-mentioned zonal characteristics can easily be recognized in all cores from the central Adriatic Sea. The faunas in the much shallower central Adriatic basin differ substantially from those found in the southern Adriatic basin. There, zone I is dominated by Uvigerina mediterranea, which shows a very rapid increase in frequency at the I/II zonal boundary. In the central Adriatic Sea, zone I contains fair numbers of Bolivina spathulata, Bulimina marginata, Cibicides pachydermus and Trifarina angulosa, which contrasts with their absence from zone I in the southern Adriatic Sea.

In the central Adriatic zone II Bolivina spathulata, Hoeglundina elegans and Nonion barleeanum are absent, whereas Cibicides pachydermus and Uvigerina mediterranea are low frequent. Bulimina marginata, Hyalinea balthica, Trifarina angulosa and Uvigerina peregrina dominate the assemblages. The II/III zonal boundary precisely coincides with the exit of Sigmoilina sellii. Just as in the southern Adriatic basin, the presence of Sigmoilina sellii is typical for the upper part of zone III. In the central Adriatic Sea zone III this species occurs in very high numbers, together with abundant Scutuloris sp. A and fair numbers of Glandulina laevigata. However, in the central Adriatic Sea S. sellii is, although less abundant, also present in the lower part of zone III, where the faunas are strongly dominated by Cassidulina laevigata. The central Adriatic zone III faunas are incomparable to any other Holocene or Pleistocene Mediterranen faunas. A paleoenvironmental study of the Pleistocene deposits of the central Adriatic basin is in progress.

Core CS 73-34 from the Strait of Sicily contains only a very basal part of zone I. The entry of C. subglobosa in the highest sample, with an extrapolated age of 8300 YBP, is remarkable. If the entry of this taxon is indeed a recent phenomenon, then this would imply that non-deposition prevailed during most of the Holocene. No S_1-related interval has been found, neither lithologically nor faunistically, which may be explained by discontinuity of the sedimentary record. The frequency plots of Bolivina albatrossi, Siphotextularia affinis and Cibicides wuellerstorfi (all with an exit around the I/II zonal boundary) are remarkably similar to those of the southern Adriatic basin. However, no Cibicides pachydermus acme has been found in zone II, and the marker species Sigmoilina sellii and Pyrgo depressa are absent from zone III. Karreriella bradyi was only found in one sample. The presence of Epistominella rugosa in the basal part of core CS 73-34 has been discussed before.

Rather surprisingly, the benthic foraminiferal record in core BS 78-12 from the western Tyrrhenian Sea is more similar to that of the southern Adriatic Sea, than the record of the Strait of Sicily. Although no S_1 has developed here, a number of taxa (e.g. Bolivina spathulata, Hyalinea balthica) disappear at about 8000 YBP, just as they do in the southern Adriatic Sea. Between 8000 YBP and 6000 YBP (the top of the core) the Tyrrhenian Sea faunas are dominated by Nonion barleeanum. Cassidulina subglobosa is absent, which could indicate that the actual sediment top has not been sampled. The records of Bolivina albatrossi and Siphotextularia affinis (both with an exit at the I/II zonal boundary) are similar to those from the southern Adriatic Sea, but now the exit of Cibicides wuellerstorfi is positioned somewhat earlier, at about 11,500 YBP. Just as in the Strait of Sicily core, no C. pachydermus acme has been found in zone II. The marker species Sigmoilina sellii and Karreriella bradyi are present in small amounts in zone III, but Pyrgo depressa is absent.

STABLE ISOTOPE STRATIGRAPHY

In fig. 13 $\delta^{18}O$-values of G. bulloides from cores IN 68-21 (central Adriatic Sea) and IN 68-5 (southern Adriatic Sea) are plotted versus time, together with two previously published surface water oxygen isotope records from the central Mediterranean. The oxygen isotope chronology for core KET 8216 from the southern Adriatic Sea (G. ruber; Fontugne et al., 1989) is based on AMS ^{14}C-dates, but that for core CS 70-5 from the Strait of Sicily (G. bulloides; Vergnaud-Grazzini et al., 1988) is based on conventional radiocarbon dates, performed on bulk carbonate of the larger than 50 micron fraction. Since AMS-dating of small (hand-picked) quantities generally produce ages younger than those determined by conventional radiocarbon dates, in core CS 70-5 we recalibrated the part of the $\delta^{18}O$ record relevant to this study. Instead of using the ages of 9460 YBP and 13,500 YBP of Vergnaud-Grazzini et al. (1988), we recalculated the chronology of the record on the basis of the ages of our zone I/II- and zone II/III-boundaries, which we placed in the faunal curves of Vergnaud-Grazzini et al. (1988) at 1.8 and 3.4 m respectively. This procedure resulted in a shift to younger ages for the entire curve. No faunal data are available for core KET 8216 (Fontugne et al., 1989), which is rather unfortunate because these could provide additional control on the oxygen istope chronology and on the position of the basis of S_1, which is somewhat too old in comparison with our southern Adriatic data (fig. 13).

Figure 13 shows that the four records are highly comparable, although in detail some differences due to correlation problems can be observed. Termination Ib can easily be distinguished in all cores; the end of termination Ib coincides with our zone I/II-boundary. The age range from 10,500 YBP to 9000 YBP (not reservoir-corrected) for termination Ib accords with similar ages reported in the literature (e.g. Duplessy et al., 1981; Mix and Ruddiman, 1985; Broecker et al., 1988). A (Younger Dryas) cooling event between 11,000 and 10,000 YBP can only be recognized with certainty in the core from the Strait of Sicily. It is not clearly noticeable in the oxygen isotope record from the Adriatic Sea, where a phase with rather constant isotope values is present between 12,700 and 10,000 YBP.

Termination Ia is well perceptable in the oxygen isotope records from the central Adriatic and the Strait of Sicily, but not in the central Adriatic Sea (fig. 13). Termination Ia matches the uppermost part of zone III; the zone II/III-boundary probably reflects the end of termination Ia. The age range of termination Ia, 14,800 YBP to 12,700 YBP, accords with the youngest ages derived from the literature (e.g. Mix and Ruddiman, 1985; Bard et al., 1987). In core CS 70-5, termination Ia may be slightly too old, because the chronology is based on linear extrapolation of the accumulation rate in zone II, which usually is lower than that of zone III (fig. 6). It should be

122

noted that our interpretation of the oxygen isotope record of core CS 70-5 differs from the one given by Vergnaud-Grazzini et al. (1988), who place termination Ia at a level (between 3.0 and 3.7 m), which according to the faunal data falls in our zone II. This level ranges from 12,700 - 12,000 YBP, and could coincide with the start of a warming phase at the end of an Older Dryas event. The same warming phase can possibly also be recognized in the curve of core IN 68-5.

In core IN 68-21 from the shallow central Adriatic basin, termination Ia cannot be recognized. In contrast to the other cores, oxygen isotope values in the upper part of zone III do not differ from those in zone II (fig. 13). The most plausible explanation for this anomaly is that during glacial times, when sea-level stood some 120 m below the present level (Fairbanks, 1989), core IN 68-21 was positioned directly in front of the Po outlet. At the beginning of the last deglaciation, meltwater discharge into the central Adriatic basin may have resulted in lower surface water salinities and, consequently, in lighter isotope values. If so, the effect of meltwater on the isotope composition in the central Adriatic Sea diminished during the deglaciation, when the Po outlet shifted to its present-day position due to the rising sea-level.

CONCLUSIONS

AMS ^{14}C dates obtained from hand-picked foraminifera from the larger than 150 micron fraction reveal that in the central Mediterranean resedimentation processes play a far more important role than could be expected on the basis of sedimentological descriptions and faunal signals alone. In all central Mediterranean cores an undisturbed record seems to be present down to about 15,000 YBP. Older parts of the records frequently show anomalous ^{14}C sequences, indicating that resedimentation processes were very active during glacial times, causing the substantially higher accumulation rates observed there. However, also in the last 15,000 years, where no indications for large-scale redepositional phenomena are found, admixture of older foraminiferal tests seems to have resulted in too old ^{14}C ages.

In addition to resedimentation processes which distorted most of the original glacial faunal signal, a second complication is the absence of the youngest part of the Holocene in most cores; at two sites even the last 8000 years are missing. These missing late Holocene sections may result from coring inadequacies, but if Cassidulina subglobosa indeed entered the central Mediterranean very recently, then there are a number of sites were non-depositional conditions prevailed during the Holocene.

There are no significant differences in three duplo-sets of ^{14}C dates, based on planktonic and benthic organisms from the same samples, respectively. This suggests that, at the considered locations, the bottom waters had not aged significantly relative to the surface waters, during the time-slices involved in these duplo-exercises.

The Late Quaternary planktonic foraminiferal records are very comparable throughout the central Mediterranean. The main changes take place synchronously. However, in our re-calibrated planktonic foraminiferal curves (figs. 7-8) a clear difference can be noticed between groups of taxa. A number of taxa (G. ruber, G. scitula, T. quinqueloba and the SPRUDTS-group) show very comparable successions of presence, absence and acme intervals in all cores, whereas a second group (Neogloboquadrina spp., G. inflata, G. glutinata and G. bulloides) appears to be much more prone to regional variation. In our opinion the first group contains taxa largely influenced by temperature, whereas the second group consists of more nutrient-dependent taxa. Temperature-influenced species are more suitable for biozonation purposes than nutrient-dependent taxa.

Major changes in the planktonic foraminiferal record at 12,700 YBP and 9600 YBP are used to subdivide the Late Quaternary sequences from the central Mediterranean into three zones,

coinciding with the pleniglacial, a transitional phase, and the Holocene interglacial. The oxygen isotope record reveals that these major breaks in the Late Quaternary faunal record correspond with the final stages of terminations Ia and Ib, respectively.

Globorotalia inflata and (the benthic foraminifer) Epistominella rugosa are only found in cores IN 68-7 and CS 73-34, the only cores yielding radiocarbon ages older than 30,000 YBP. The fact that both species are completely absent in core IN 68-29, which shows a maximal radiocarbon age of 27,100 YBP suggests that the exit of these taxa should be placed before this date. This would be in agreement with the age of 36,000 YBP which Muerdter and Kennett (1984) assign to the exit of G. inflata.

Although different taxa may be involved in different areas, the main events in the benthic foraminiferal record are unexpectedly synchronous, and coincide with the breaks in the pelagic record. Local variations in the benthic records allow a further refinement of our biozonation.

The sapropelitic layer S_1 was only found in the southern Adriatic Sea, where it consists of two (laminated) intervals. The intrapolated age (8200 - 5600 YBP) determined in the present paper agrees well with those given in the literature (review in Vergnaud-Grazzini et al., 1986). However, since the sedimentation rate during deposition of the S_1 may have been increased, and extrapolations have been made on the basis of average sedimentation rates in zone I, the estimated age of the top of the S_1 may be too young.

The biozonation presented in this paper is very comparable to the zonation based on pelagic molluscs used by Van Straaten (1967, 1969, 1972, 1985). The zonal boundaries are in perfect agreement, and also the ages estimated by Van Straaten (on the basis of conventional radiocarbon dates) do not differ significantly from ours. In the present paper, the age of a number of in the southern Adriatic Sea very consistent ash layers and turbidites (Van Straaten, 1967, 1985) could be estimated very precisely (fig. 5). However, Van Straaten overestimated the correlatability of turbiditic layers in the oldest parts of some of the cores.

REFERENCES

Bard, E., 1988. Correction of accelerator mass spectrometry ^{14}C ages measured in planktonic foraminifera: paleoceanographic implications. Paleoceanography, 3: 635-645.

Bard, E., Arnold, M., Maurice, P., Duprat, J., Moyes, J. and Duplessy, J.C., 1987. Retreat velocity of the North Atlantic polar front during the last deglaciation determined by 14C accelerator mass spectometry. Nature, 328: 791-794.

Bard, E., Hamelin, B., Fairbanks, R.G. and Zindler, A., 1990. Calibration of the ^{14}C timescale over the past 30,000 years using mass spectrometric U-Th ages from Barbados corals. Nature, 345: 405-409.

Borsetti, A.M., Iaccarino, S., Jorissen, F.J., Poignant, A., Sztrakos, K., Van der Zwaan, G.J. and Verhallen, P.J.J.M., 1986. The Neogene development of Uvigerina in the Mediterranean. In: G.J. Van der Zwaan, Jorissen, F.J., Verhallen, P.J.J.M. and Von Daniels, C.H. (eds), Atlantic- European Oligocene to Recent Uvigerina. Utrecht Micropal. Bull., 35: 183-234.

Bottema, S. and Van Straaten, L.M.J.U., 1966. Malacology and palynology of two cores from the Adriatic sea floor. Marine Geol., 4: 553-564.

Brady, H.B., 1884. Report on the foraminifera dredged by H.M.S. Challenger during the years 1873-1876. Rep. Sci. Res. Explor. Voyages H.M.S. Challenger, Zool., 9, 814 pp.

Breman, E., 1975. Ostracodes from a bottom core from the deep southeastern basin of the Adriatic Sea. I. Proc. Kon. Ned. Akad. Wetensch., B, 78: 197-218.

Broecker, W.S., Andree, M., Wolfli, W., Oeschger, H., Bonani, G., Kennett, J. and Peteet, D., 1988. The chronology of the last deglaciation: implications to the cause of the Younger Dryas event. Paleoceanography, 3: 1-19.

Broecker, W.S., Andree, M., Bonani, G., Wolfli, W., Klas, M., Mix, A. and Oeschger, H., 1988. Comparison between radiocarbon ages obtained on coexisting planktonic foraminifera. Paleoceanography, 3: 647-657.

Buckley, H.A. and Johnson, L.R., 1988. Late Pleistocene to recent sediment deposition in the central and western Mediterranean. Deep-Sea Research, 35: 749-766.

Buckley, H.A., Johnson, L.R., Shackleton, N.J. and Blow, R.A., 1982. Late glacial to recent cores from the eastern Mediterranean. Deep-Sea Research, 29: 739-766.

Caralp, M.H., 1988. Late Glacial to Recent deep-sea benthic foraminifera from the northeastern Atlantic (Cadiz Gulf) and western Mediterranean (Alboran Sea): paleooceanographic results. Marine Micropal., 13: 265-289.

Cita, M.B. and Chierici, M.A., 1962. Crociera talassographica Adriatica 1955. V. Ricerche sui foraminiferi contenuti in 18 carote prelevate sul fondo del mare Adriatico. Arch. Oceanogr. Limnol., Venezia, 12: 297-359.

Cita, M.B. and D'Onofrio, S., 1967. Climatic fluctuations in submarine cores from the Adriatic Sea (Mediterranean). Progress in Oceanography, 4: 161-178.

Colantoni, P. and Galignani, P., 1977. Le carote raccolte dal laboratorio per la geologia marina del C.N.R. nel canale di Sicilia, Mare Ionio e Mare Adriatico meridionale dal 1967 al 1976. C.N.R., Lab. Geol. Marina, Bologna, Rapp. Tecn., 5, 175 pp.

D'Onofrio, S., 1959. Foraminiferi di una carota sottomarina del medio Adriatico. Giorn. di Geol., ser. 2a, 27: 147-194.

D'Onofrio, S., 1973. Globigerina pachyderma and Globigerinoides ruber: paleoclimatic indicators in submarine cores in the Adriatic Sea. Rapp. Comm. int. Mer Médit., 21, 11: 905-908.

Duplessy, J.C., Delibrias., G., Turon., J.L., Pujol, C. and Duprat, J., 1981. Deglacial warming of the northeastern Atlantic Ocean: correlation with the paleoclimatic evolution of the European continent. Paleogeogr. Palaeoclimat. Palaeoecol., 35: 121-144.

Epstein, S., Buchsbaum, R., Lowenstam, H. and Urey, H.C., 1953. Revised carbonate-water isotopic temperature scale. Geol. Soc. Am. Bull., 64: 1315-1326.

Fairbanks, R.G., 1989. A 17,000-year glacio-eustatic sea level record: influence of glacial melting rates on the Younger Dryas event and deep-ocean circulation. Nature, 342: 637-642.

Fontugne, M.R., Paterne, M., Calvert, S.E., Murat, A., Guichard., F. nd Arnold, M., 1989. Adriatic Deep water formation during the Holocene: implication for the reoxygenation of the deep eastern Mediterranean Sea. Paleoceanography, 4: 199-206.

Hemleben, C. and Spindler, M., 1983. Recent advances in research on living planktonic foraminifera. Utrecht Micropal. Bull., 30: 141-170.

Hemleben, C., Spindler, M. and Anderson, O.R., 1989. Modern Planktonic Foraminifera. Springer-Verlag New York.

Hut, G., Ostlund, H.G. and Van der Borg, K., 1986. Fast and complete CO_2-to-graphite conversion for 14C Accelerator Mass Spectometry. In Stuiver, M. and Kra, R.S. (eds.): Proc. 12th International 14C Conference; Radiocarbon, 28, 186-190.

Jorissen, F.J., 1987. The distribution of benthic foraminifera in the Adriatic Sea. Marine Micropal., 12: 21-48.

Jorissen, F.J., 1988. Benthic foraminifera from the Adriatic Sea; principles of phenotypic variation. Utrecht Micropal. Bull., 37, 176 pp.

Kohl, B., 1985. Early Pliocene benthic foraminifers from the Salina Basin, southeastern Mexico. Bull. American Paleont., 88, n. 322, 173 pp.

Loeblich, A.R. and Tappan, H., 1964. Saccodina chiefly Thecamoebians and Foraminiferida. In: R.C. Moore (ed.), Treatise on Invertebrate Paleontology., part C, Protista 2, vols. 1-2. Geol. Soc. Am., Univ. Kansas Press, 900 pp.

Mix, A.C. and Ruddiman, W.F., 1985. Structure and Timing of the last deglaciation: oxygen-isotope evidence. Quaternary Science Rev., 4: 59-108.

Muerdter, D.R. and Kennett, J.P., 1984. Late Quaternary planktonic foraminiferal biostratigraphy, Strait of Sicily, Mediterranean Sea. Mar. Micropal., 8: 339-359.

Parker, F.L., 1958. Eastern Mediterranean foraminifers. Rep. Swed. Deep-Sea Exped., 1947-1948, 8: 217-283.

Shackleton, N.J. and Opdyke, N., 1973. Oxygen isotope and paleomagnetic stratigraphy of equatorial Pacific core V28-238: Oxygen isotope temperatures and ice volume on a 10^5 and 10^6 year scale. Quat. Res., 3: 39-55.

Stanley, D.J., 1985. Mud redepositional processes as a major influence on Mediterranean margin-basin sedimentation. In: Stanley, D.J. and Wezel, F.C. (eds.): Geological evolution of the Mediterranean Basin. Springer, New York., 377-410.

Stuiver, M., 1983. International agreements and the use of the new oxalic acid standard. In Stuiver, M. and Kra, R.S. (eds.): Proc. 11th international 14C Conference., Radiocarbon, 25, 793-795.

UU.OO. Gruppo Bacini Sedimentari, 1979. Primi dati geologici sul Bacino della Corsica (Mar Tirreno). Conv. Scient. Naz., P.F. Oceanogr. e Fondi Marini., 713-727.

Van der Borg, K., Alderliesten, C., Houston, C.M., de Jong, A.F.M. and Van Zwol, N.A., 1987. Accelerator Mass Spectometry with 14C and ^{10}Be in Utrecht. Nucl. Instr. and meth. B29: 143-145.

Van der Zwaan, G.J., 1980. The impact of climatic changes on deep sea benthos. A micropaleontological investigation of a deep sea core from the S.E. Adriatic. Proc. Kon. Ned. Akad. Wetensch., B, 83: 379-397.

Van Straaten, L.M.J.U., 1966. Micro-malacological investigation of cores from the southeastern Adriatic Sea. Proc. Kon. Ned. Akad. Wetensch., B, 69: 429-445.

Van Straaten, L.M.J.U., 1967. Turbidites, ash layers and shell beds in the bathyal zone of the southeastern Adriatic Sea. Rev. Géogr. Phys. et Géol. Dyn., 9: 219-240.

Van Straaten, L.M.J.U., 1972. Holocene stages of oxygen depletion in deep waters of the Adriatic Sea. In: D.J. Stanley (ed.), The Mediterranean Sea., pp. 631-643.

Van Straaten, L.M.J.U., 1985. Molluscs and sedimentation in the Adriatic Sea during late-Pleistocene and Holocene times. Giorn. di Geol., ser. 3a, 47: 181-202.

Vergnaud-Grazzini, C., Devaux, M. and Znaidi, J., 1986. Stable isotope "anomalies" in Mediterranean Pleistocene records. Marine Micropal., 10: 35-69.

Vergnaud-Grazzini, C., Borsetti, A.M., Cati, F., Colantoni, P., D'Onofrio, S., Saliège, J.F., Sartori, R. and Tampieri, R., 1988. Palaeoceanographic record of the last deglaciation in the Strait of Sicily. Marine Micropal., 13, 1-21.

Von Daniels, C.H., 1970. Quantitative oecologische Analyse der zeitlichen und raumlichen Verteilung rezenter Foraminiferen im Limski-kanal bei Rovinj (nordliche Adria). Göttinger Arb. Geol. Palaeont., 8, 180 pp.

TAXONOMICAL NOTES

<u>Benthic foraminifera - faunal reference list</u>

The benthic foraminiferal taxa referred to in this article are listed in the order of Loeblich and Tappan (1964). To illustrate the taxonomic concept used, for each taxon an adequate reference is given. The species in open nomenclature will be treated in more detail in forthcoming papers dealing with the paleoecology of the benthic foraminiferal faunas.

<u>Siphotextularia affinis</u> (Fornasini 1883) - Kohl (1985).

<u>Karreriella bradyi</u> (Cushman 1911) - Parker (1958): <u>Eggerella bradyi</u> + <u>K. bradyi.</u>

<u>Pyrgo depressa</u> (D'Orbigny 1826) - Brady (1884): <u>Biloculina depressa.</u>

<u>Sigmoilina sellii</u> D'Onofrio 1959. - Van der Zwaan (1980): pl. 2, fig. 5; determined as <u>Quinqueloculina seminula.</u>

<u>Scutuloris</u> sp. A. - a keeled morphotype with a weakly developed apertural flap.

<u>Glandulina laevigata</u> (D'Orbigny 1826) - Loeblich and Tappan (1964). Microspheric and megalopspheric stages (uniserial troughout) are present in equal quantities.

<u>Bolivina albatrossi</u> Cushman 1922 - Parker (1958).

<u>Bolivina spathulata</u> (Williamson 1858) - Von Daniels (1970). Also very broad types (Parker 1958: <u>B. dilatata dilatatissima</u>) have been included here.

<u>Cassidulinoides bradyi</u> (Norman 1881) - Brady (1884): <u>Cassidulina bradyi.</u>

<u>Bulimina costata</u> D'Orbigny 1852 - Parker (1958).

<u>Bulimina marginata</u> D'Orbigny 1826 - Jorissen (1987,1988). In all areas except the shallow central Adriatic Sea the assemblages are strongly dominated by forma <u>marginata.</u>

<u>Globobulimina pyrula</u> (D'Orbigny 1846) - Parker (1958): <u>G. affinis.</u>

<u>Uvigerina mediterranea</u> Hofker 1932 - Borsetti et al. (1986).

<u>Uvigerina peregrina</u> Cushman 1923 - Borsetti et al. (1986).

<u>Trifarina angulosa</u> (Williamson 1858) - Parker (1958): <u>Angulogerina angulosa.</u>

<u>Epistominella rugosa</u> (Phleger and Parker 1951) - Our forms are similar to <u>E. rugosa convexa</u> of Parker (1958).

<u>Hyalinea balthica</u> (Schröter 1783) - Loeblich and Tappan (1964).

<u>Cibicides lobatulus</u> (Walker and Jacob 1798) - Von Daniels (1970).

<u>Cibicides pachydermus</u> (Rzehak 1886) - D'Onofrio (1959). Biconvex (Parker, 1958: <u>C</u>. aff. <u>C. floridanus</u>) as well as planoconvex morphotypes (Parker, 1958: <u>C. kullenbergi</u>) have been included here.

<u>Cibicides wuellerstorfi</u> (Schwager 1866) - Parker (1958).

<u>Cassidulina crassa</u> D'Orbigny 1839 - Parker (1958).

<u>Cassidulina laevigata</u> D'Orbigny 1826 - Loeblich and Tappan (1964).

<u>Cassidulina subglobosa</u> Brady 1881 - Brady (1884).

<u>Nonion barleeanum</u> (Williamson 1858) - D'Onofrio (1959): <u>N. padanum. Nonionina formosa</u> Seguenza 1880 and <u>Nonion padanum</u> Perconig 1952 are included in this species.

<u>Chilostomella czizeki</u> Reuss 1850 - Parker (1958): <u>C. mediterranensis.</u>

<u>Gyroidina altiformis</u> R.E. and K.C. Stewart 1930 - Parker (1958).

<u>Gyroidina orbicularis</u> D'Orbigny 1826 - Brady (1884): <u>Rotalia orbicularis.</u>

<u>Hoeglundina elegans</u> (D'Orbigny 1826) - D'Onofrio (1959).

Core	Water depth	Latitude	Longitude	Length	P	B
IN 68-23 (381)	64 m	42 11'1	14 55'5	411 cm		+
IN 68-22 (384)	129 m	42 23'0	15 00'0	544 cm		+
IN 68-16 (388)	194 m	42 36'9	15 01'3	466 cm		+
IN 68-21 (394)	252 m	42 53'2	14 47'5	719 cm	+	+
IN 68-28 (400)	396 m	41 59'5	16 55'3	396 cm	+	
IN 68-29 (401)	797 m	42 00'0	17 08'5	554 cm	+	+
IN 68-9 (362)	1234 m	41 47'5	17 54'5	609 cm	+	+
IN 68-5 (372)	1030 m	41 14'0	18 32'0	643 cm	+	+
IN 68-7 (365)	1225 m	41 56'0	18 14'1	410 cm	+	+
IN 68-38 (404)	716 m	41 07'6	17 34'8	643 cm	+	
IN 68-3 (369)	868 m	40 42'8	18 45'3	539 cm	+	+
CS 73-34	680 m	35 57'4	13 25'8	713 cm	+	+
BS 78-12	626 m	42 40'1	9 49'0	585 cm	+	+

Table I; core localities; the numbers between brackets refer to the core identification numbers used by Van Straaten (1966, 1967, 1972, 1985). Lithological data can be found in these papers and in Colantoni and Galignani (1977) and UU.OO. Gruppo Bacini Sedimentari (1979). The right-hand columns indicate whether planktonic foraminifera (P), benthic foraminifera (B), or both have been studied.

Sample number	Laboratory Code	Depth in core	Material	Zone	Age (in years YBP)		

Central Adriatic Sea:

Core IN 68-23:

381-1	UTC-505	0- 2 cm	bf		400	+/-	90
381-1	UTC-536	0- 2 cm	pm		Recent		
381-3	UTC-677	41- 46 cm	bf		1030	+/-	70
381-6	UTC-678	116-121 cm	bf		2180	+/-	70
381-10	UTC-506	216-221 cm	bf		2670	+/-	150
381-17	UTC-507	376-381 cm	bf		4590	+/-	100

Core IN 68-22:

384-1	UTC-850	0- 1 cm	br		1140	+/-	90
384-4	UTC-851	58- 59 cm	mo		4360	+/-	100
384-9	UTC-852	197-198 cm	bf		6000	+/-	140
384-14	UTC-853	321-322 cm	bf		8450	+/-	130
384-24	UTC-895	542-543 cm	br/mo	II	9700	+/-	160

Core IN 68-16:

388-17	UTC-508	255-256 cm	bf	III	15100	+/-	500
388-28	UTC-509	461-462 cm	bf/mo	III	19900	+/-	400

Core IN 68-21:

394-1	UTC-510	0- 2 cm	bf		830	+/-	100
394-10	UTC-511	163.5-165.5 cm	mo/bf		7160	+/-	140
394-14	UTC-512	244-247 cm	mo		9510	+/-	130
394-19	UTC-513	439.5-442.5 cm	bf	II/III	13300	+/-	400
394-Sc	UTC-896	700-725 cm	bf	III	15800	+/-	500

Southern Adriatic Basin

Core IN 68-29:

401-14	UTC-897	390-397 cm	bf	III?	27100	+/-	600
401-19	UTC-898	542-555 cm	bf	III?	23600	+/-	500

Core IN 68-9:

362-2	UTC-500	11- 12 cm	bf		3160	+/-	120
362-18	UTC-501	155.5-157.5 cm	bf	I/II	9280	+/-	180
362-25	UTC-502	241-242 cm	pf	top III	13100	+/-	200
362-30	UTC-503	322-323 cm	pf	III	14200	+/-	300
362-44	UTC-504	510-511 cm	pf/pt	III	17200	+/-	300

Core IN 68-7:

365-1	UTC-854	0- 5 cm	pf		1290	+/-	120
365-10	UTC-855	180-185 cm	pf	III	15400	+/-	200
365-12A	UTC-856	248-253 cm	pt	III?	23200	+/-	600
365-16	UTC-857	335-340 cm	pt	IV?	18500	+/-	300
365-19	UTC-858	401-406 cm	pf	IV?	>42000		

Core IN 68-5:

372-1/1A	UTC-899	10- 20 cm	bf		5800	+/-	100
372-5A/3	UTC-900	190-200 cm	pt	I/II	9870	+/-	170
372-9	UTC-901	330-340 cm	bf	II	11900	+/-	300
372-12A	UTC-902	460-470 cm	bf	II/III	13700	+/-	300
372-16A	UTC-903	617-626 cm	bf	III	14700	+/-	300

Core IN 68-3:

369-13	UTC-904	221.5-224 cm	mo	II/III	13060	+/-	190
369-18	UTC-905	338-340.5 cm	mo	III	13400	+/-	200

```
369-30   UTC-906   524.5-527 cm   bf    III    16300    +/- 200
```

<center>Sicily channel</center>

Core CS 73-34:

```
CS-5B    UTC-910   29.5- 31 cm    bf    I/II    10780    +/- 160
CS-5P    UTC-893   29.5- 31 cm    pt    I/II    10340    +/- 150
CS-8B    UTC-911   74.5- 76 cm    bf    II/III  15070    +/- 190
CS-8P    UTC-894   74.5- 76 cm    pt    II/III  15400    +/- 300
CS-17    UTC-912   274-275.5 cm   pt    III     21800    +/- 400
CS-28    UTC-913   487-488.5 cm   bf    III/IV? 34200    +1600/-1300
CS-38    UTC-914   696-697.5 cm   bf    IV?     26000    +6000/-4000
```

<center>Tyrrhenian Sea</center>

Core BS 78-12:

```
BS-9B    UTC-907   146.5-148 cm   bf    I/II    10600    +/- 200
BS-9P    UTC-892   146.5-148 cm   pt    I/II    10050    +/- 140
BS-16    UTC-908   282-283.5 cm   bf    II/III  13820    +/- 190
BS-29    UTC-909   550.5-552 cm   bf    III     21100    +/- 400
```

Table II: ^{14}C-results. bf = benthic foraminifera, pm = plant material
mo = molluscs, pt = pteropods, pf = planktonic foraminifera.

Locality	Core	Depth	Extrap. Age
Central Adriatic	IN 68-22	429.25 cm	9060 YBP
" "	IN 68-21	275.75 cm	10100 YBP
Southern Adriatic	IN 68-9	163.5 cm	9620 YBP
" "	IN 68-5	215 cm	10180 YBP
Sicily channel	CS 73-34	22.5 cm	9780 YBP
Tyrrhenian Sea	BS 78-12	157.25 cm	10330 YBP

Table III: Interpolated ages of the I/II-boundary.

```
Locality                Core    Depth   Extrap. Age

Central Adriatic    IN 68-21  431.25 cm  13110 YBP
Southern Adriatic   IN 68-9   233 cm     12680 YBP
    "      "        IN 68-5   455 cm     13590 YBP
    "      ", sill  IN 68-3   212.5 cm   12870 YBP
Sicily channel      CS 73-34  75.25 cm   13610 YBP
Tyrrhenian Sea      BS 78-12  272 cm     13630 YBP
```

Table IV: Interpolated ages of the II/III-boundary.

2nd frequency increase Neogloboquadrina spp. and

   G. inflata in top S_1:   5800 YBP

1st frequency increase Neogloboquadrina spp. and

   G. inflata in top S_1:   6800 YBP

Frequency increase SPRUDTS-group: 7600 YBP

G. glutinata acme at basis S_1:   8500 YBP

G. inflata acme in basal part zone I: 9300 YBP

Zone I/II-boundary: 9600 YBP

Frequency increase G. inflata in

   basal part zone II: 11700 YBP

change in coiling direction (dextral --> sinistral)

   G. truncatulinoides: 11700 YBP

Zone II/III-boundary: 12700 YBP

exit G. scitula):   12700 YBP

Re-entry G. inflata in top zone III: 13700 YBP

Table V: Interpolated ages (in core IN 68-9) of main events in the planktonic foraminiferal record. No corrections have been made for the reservoir age.

entry Cassidulina subglobosa: topmost sample

exit Bolivina spathulata: 6100 YBP

exit Siphotextularia affinis   8500 YBP

exit Bolivina albatrossi   8500 YBP

exit Cibicides wuellerstorfi   9300 YBP

exit Trifarina angulosa (I/II-boundary)   9600 YBP

acme Cibicides pachydermus   11000-10000 YBP

exit Karreriella bradyi (II/III-boundary):   12700 YBP

exit Sigmoilina sellii (II/III-boundary):   12700 YBP

entry Sigmoilina sellii   15300 YBP

Table VI. Interpolated ages (in core In 68-9) of main events in the benthic foraminiferal record. No corrections have been made for the reservoir age.

131

FIGURE CAPTIONS

Fig. 1. Map showing core localities (1a,b) and bathymetry (1b).

Fig. 2. Relative frequencies of planktonic foraminifera plotted against core depth.

Fig. 3. Relative frequencies of planktonic foraminifera plotted against core depth.

Fig. 4. Outline of the biozonation and ^{14}C-dates of the studied cores.

Fig. 5. Review of interpolated ages of a number of lithological horizons in cores IN 68-9 and IN 68-5, used by Van Straaten (1967, 1985) for intercore correlations. Note the apparently structural age differences between the two cores.

Fig. 6. Control points used for interpolations and accumulation rates for the thirteen cores studied. Fig. 13a: central Adriatic Sea; 13b: southern Adriatic Sea; 13c: Sicily Channel and Tyrrhenian Sea.

Fig. 7. Relative frequencies of planktonic foraminifera plotted against apparent ^{14}C-ages based on a calibration with core IN 68-9. For the hatched part of the curve the time control is uncertain. The position of sapropel S_1 is indicated with the age constraints determined in standard core IN 68-9.

Fig. 8. Relative frequencies of planktonic foraminifera plotted against apparent ^{14}C-ages based on a calibration with core IN 68-9. For the hatched part of the curve the time control is uncertain. The position of sapropel S_1 is indicated with the age constraints determined in standard core IN 68-9.

Fig. 9. Relative frequencies of benthic foraminifera plotted against apparent ^{14}C-ages based on a calibration with core IN 68-9. For the hatched part of the curve the time control is uncertain. The position of sapropel S_1 is indicated with the age constraints determined in standard core IN 68-9.

Fig. 10. Relative frequencies of benthic foraminifera plotted against apparent ^{14}C-ages based on a calibration with core IN 68-9. For the hatched part of the curve the time control is uncertain. The position of sapropel S_1 is indicated with the age constraints determined in standard core IN 68-9.

Fig. 11. Relative frequencies of benthic foraminifera plotted against apparent ^{14}C-ages based on a calibration with core IN 68-9. For the hatched part of the curve the time control is uncertain. The position of sapropel S_1 is indicated with the age constraints determined in standard core IN 68-9.

Fig. 12. Relative frequencies of benthic foraminifera plotted against apparent ^{14}C-ages based on a calibration with core IN 68-9. For the hatched part of the curve the time control is uncertain. The position of sapropel S_1 is indicated with the age constraints determined in standard core IN 68-9.

Fig. 13. Stable isotope records from four central mediterranean piston-cores; figs. 12a,b and d are (re-)calibrated according to our biochronology; for fig. 12c the calibration of Fontugne et al. (1989) is followed, but in this case the correction made for the apparent age of marine carbonate (reservoir age, 400 years) has been omitted.
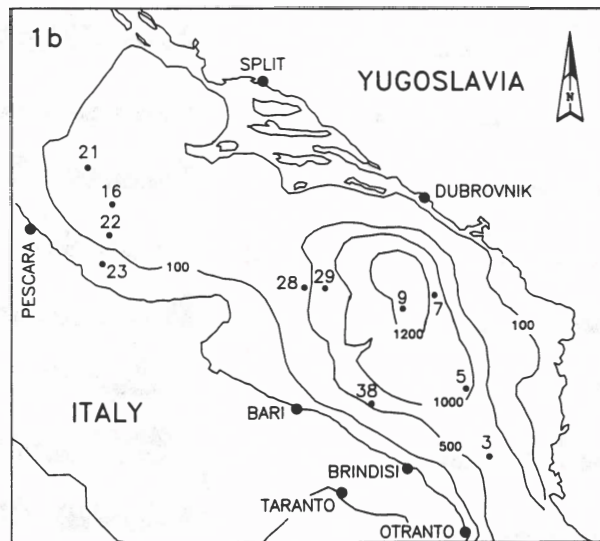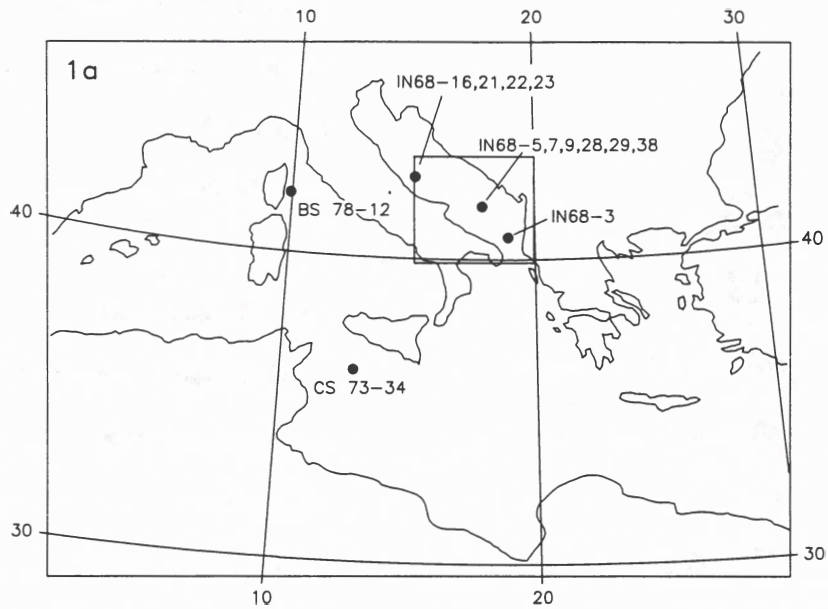
Figure 1
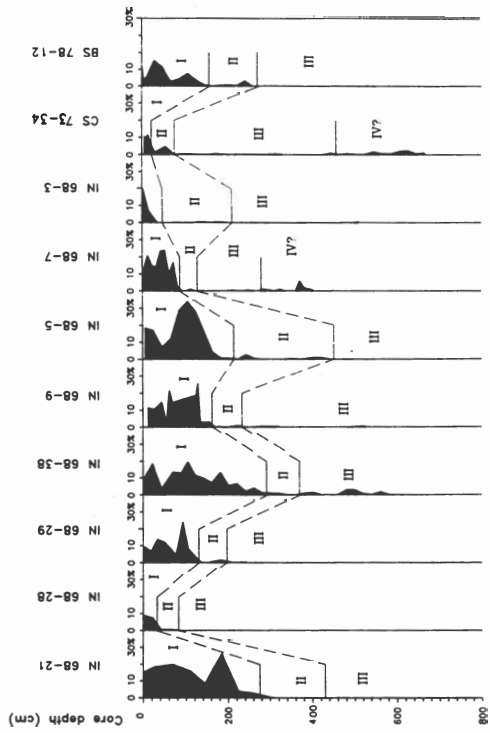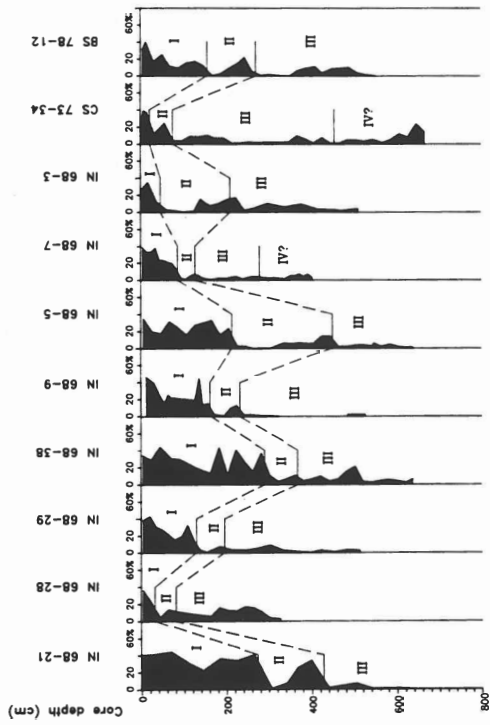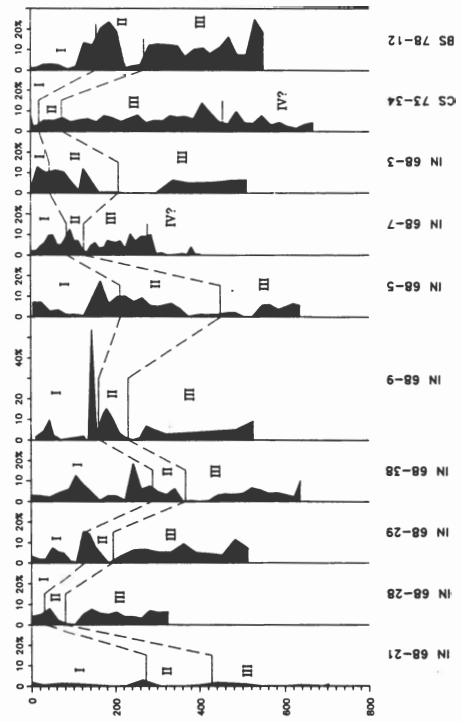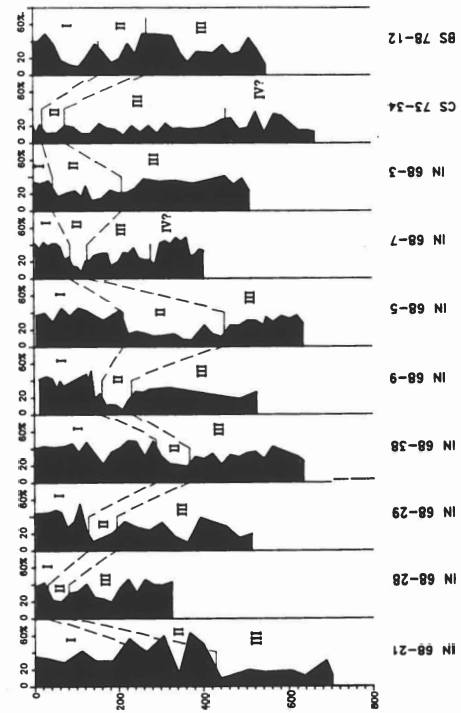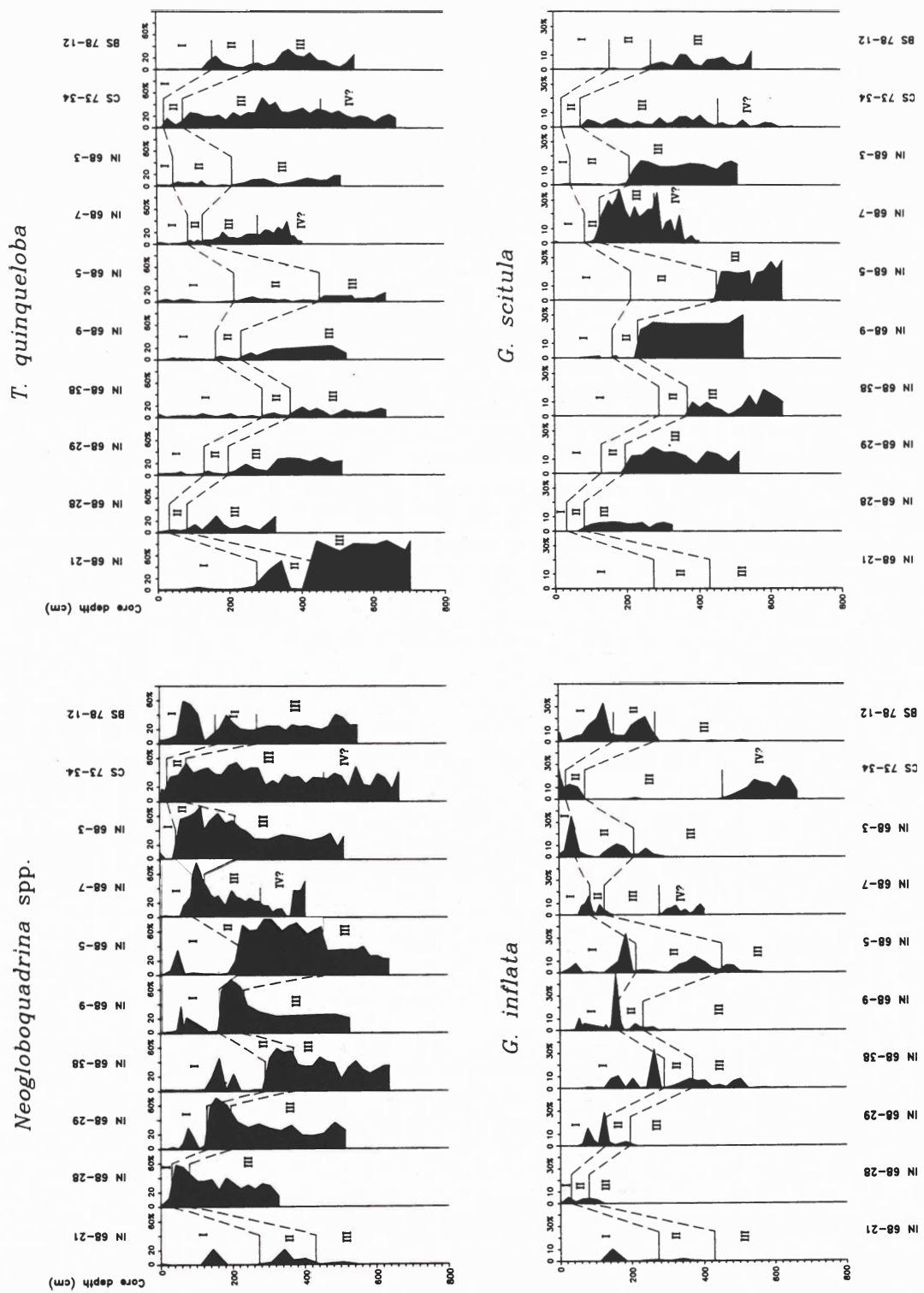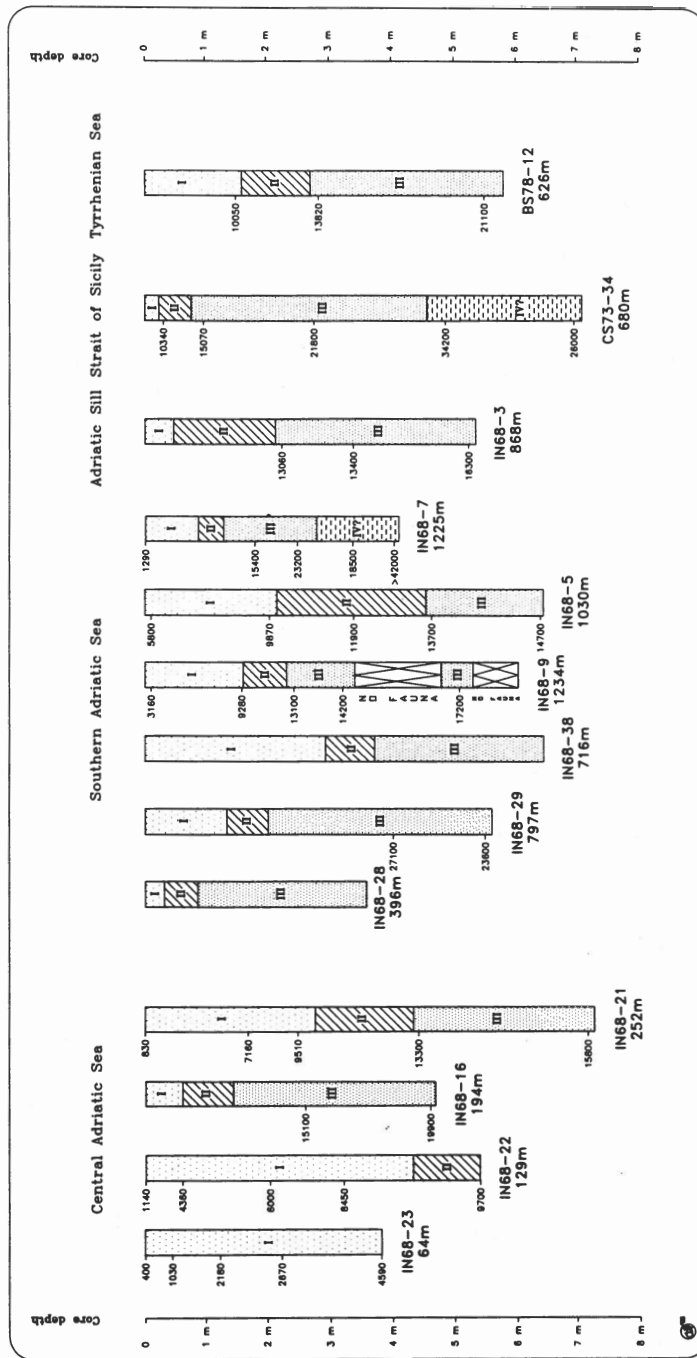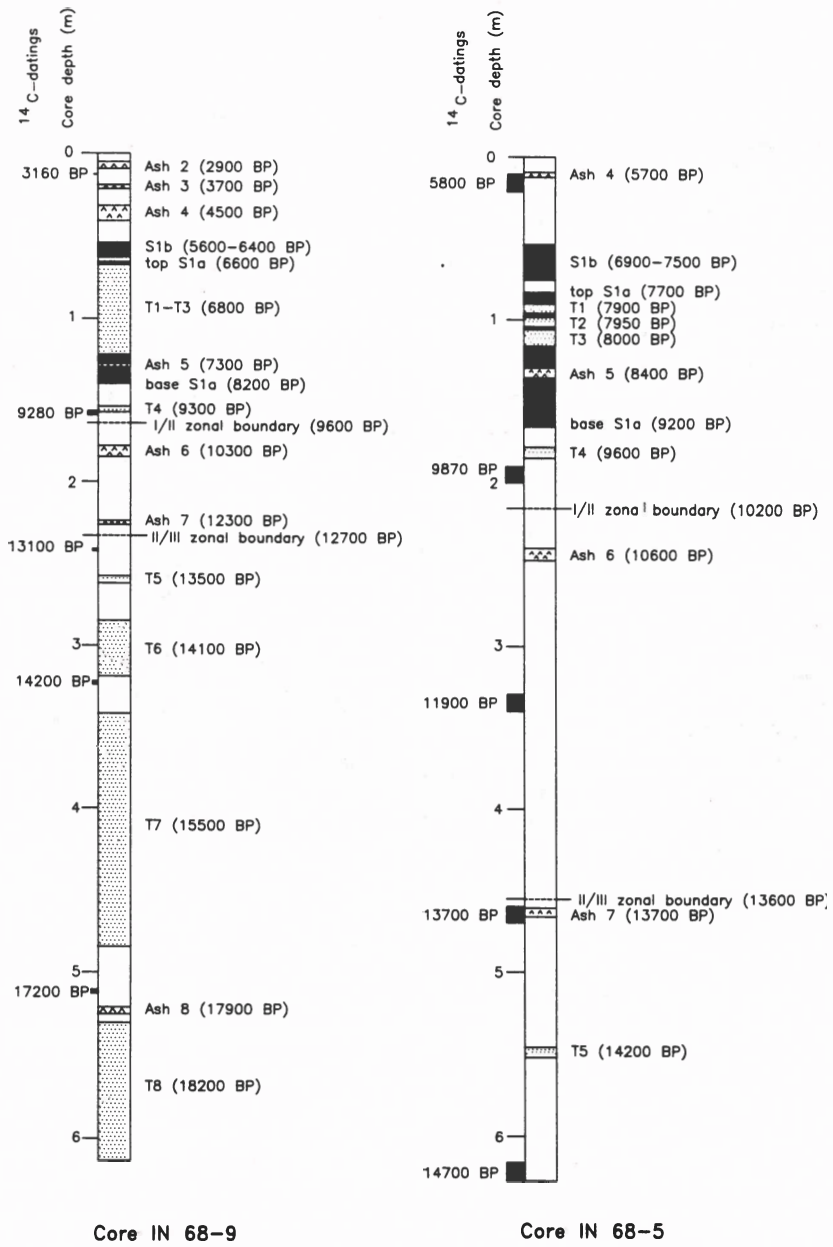
1a

1b

Figure 1

133

Figure 2

134

Figure 3

135

Figure 4

136

Core IN 68-9

Core IN 68-5

Figure 5

137

Figure 6

138

Figure 7

139

Figure 8

140

Bolivina albatrossi   *Bolivina spathulata*

Bulimina costata   *Bulimina marginata*
forma *marginata* + forma *denudata*

Cassidulina crassa   *Cassidulina laevigata*

Figure 9

141

Cassidulina subglobosa

Cibicides pachydermus

Cibicides wuellerstorfi

Epistominella rugosa

Globobulimina pyrula +
Chilostomella czizeki
Cassidulinoides bradyi

Gyroidina altiformis

Figure 10

142

Figure 11

143

Figure 12

144

Figure 13

145
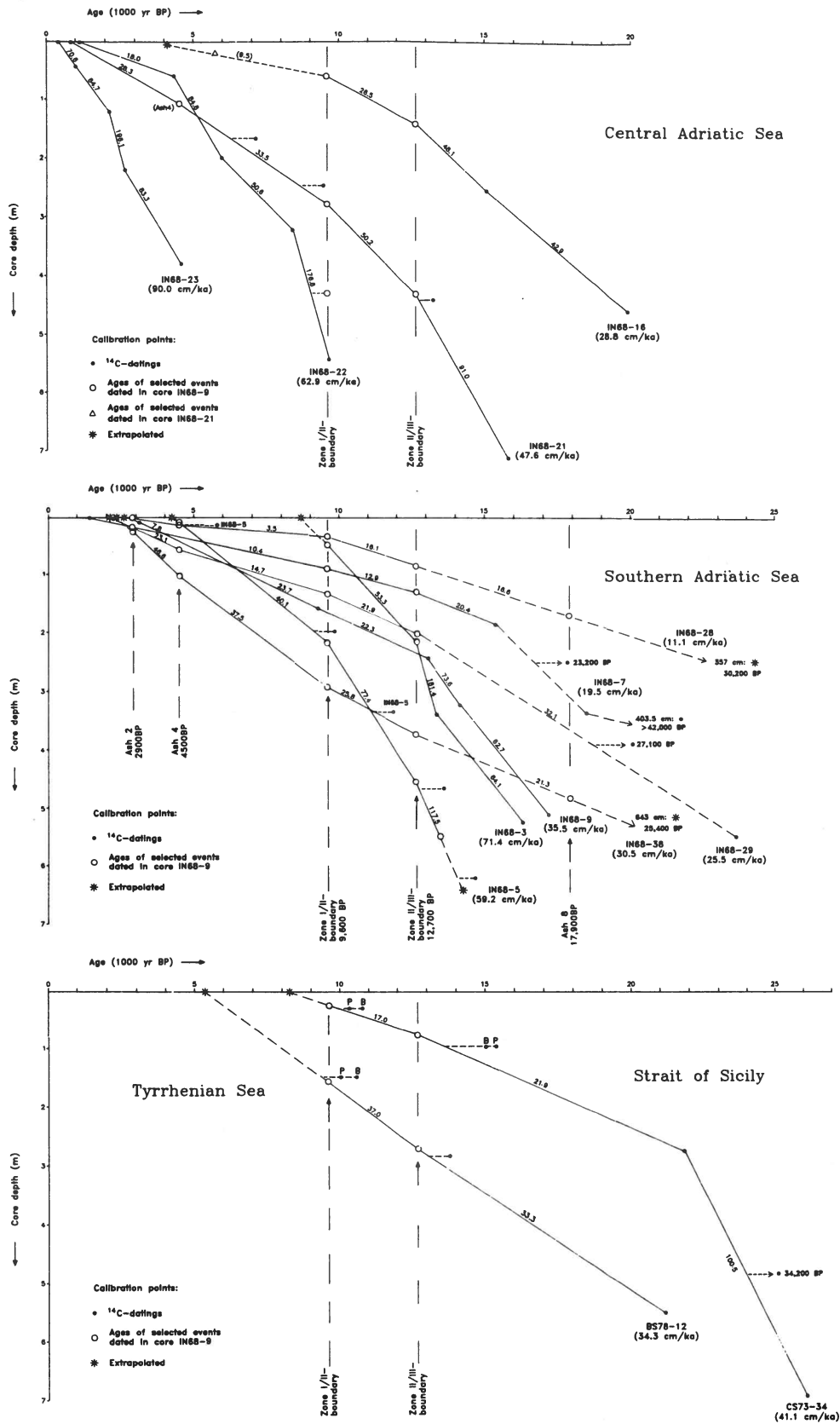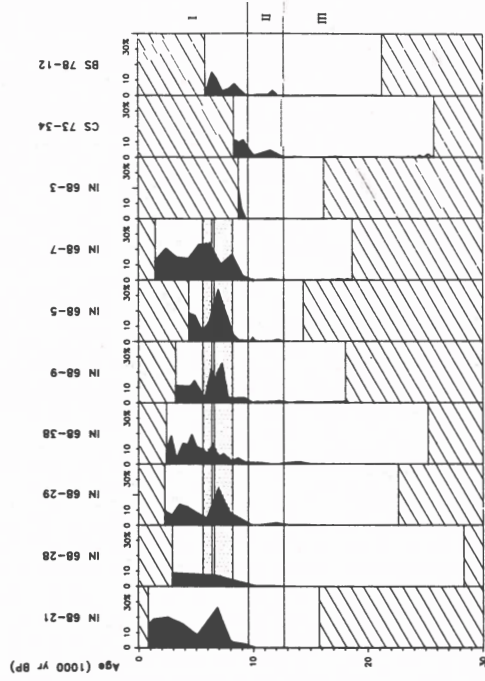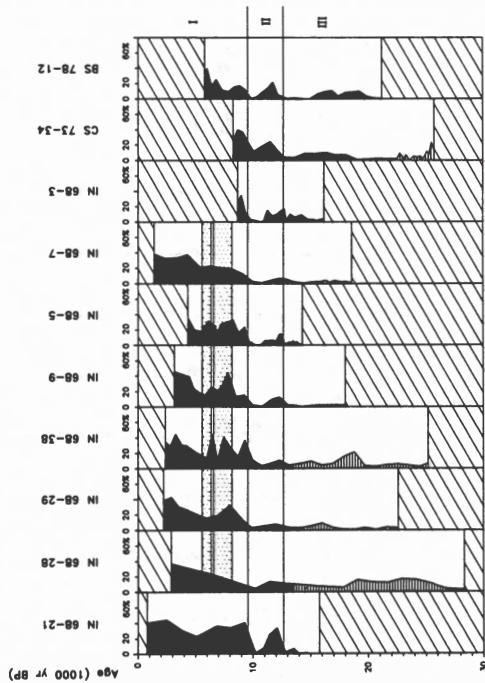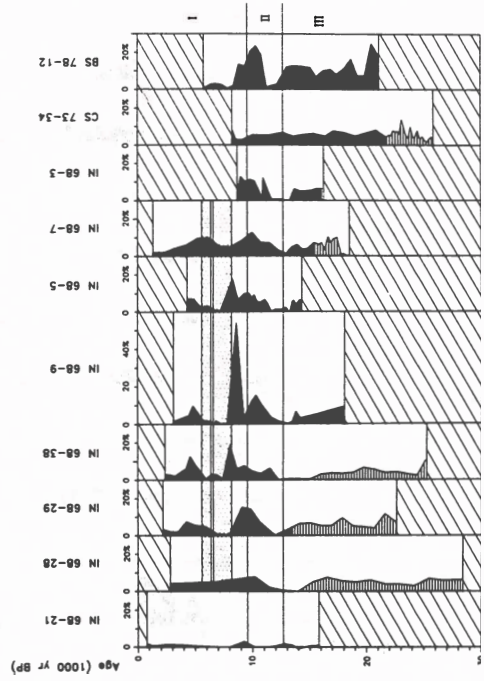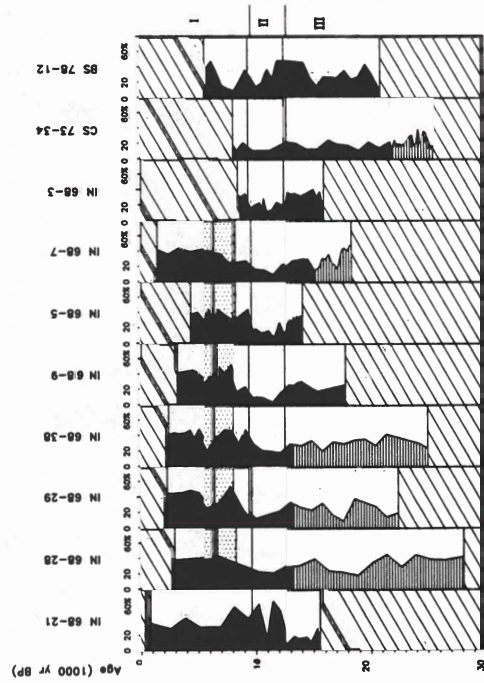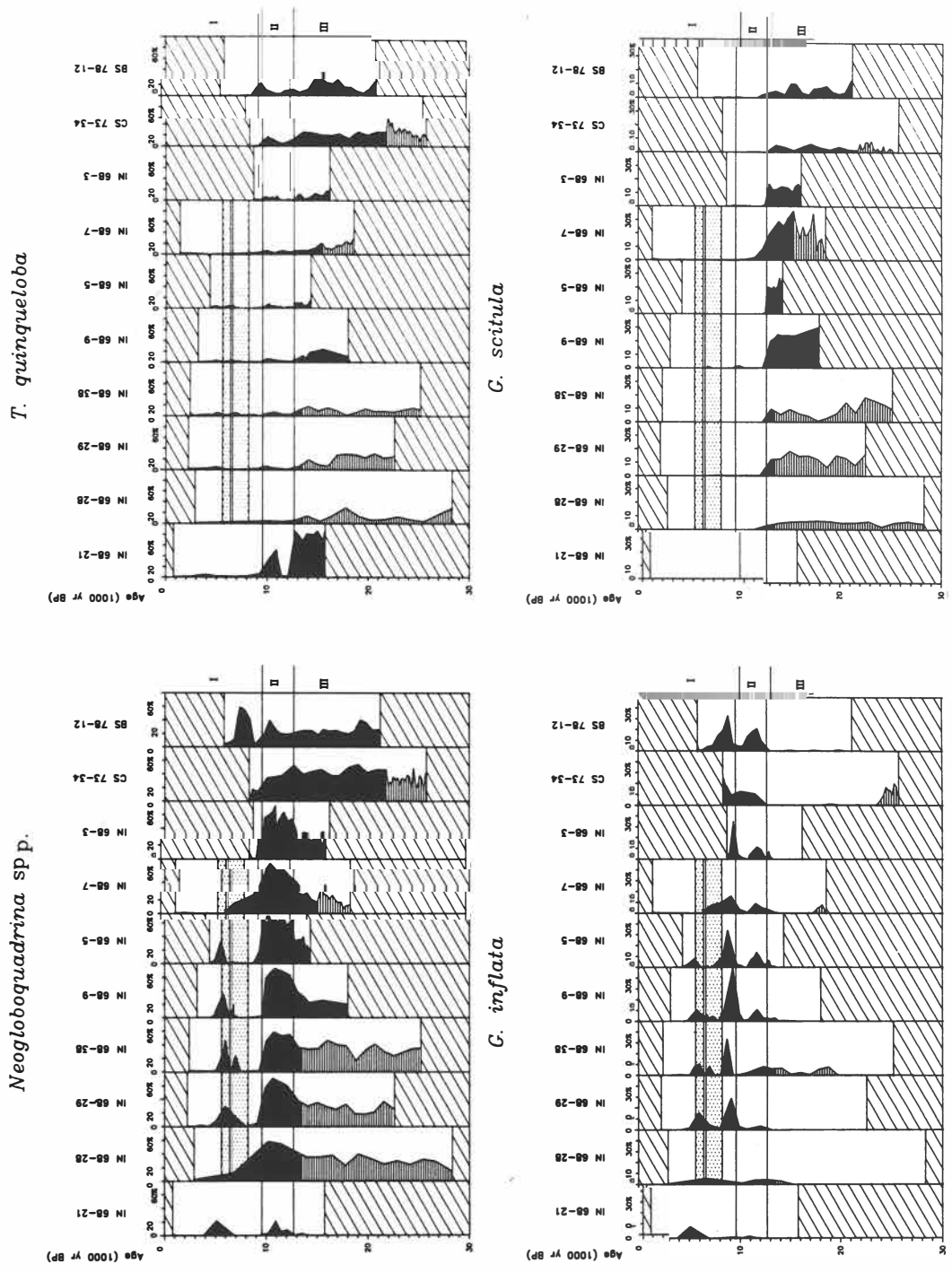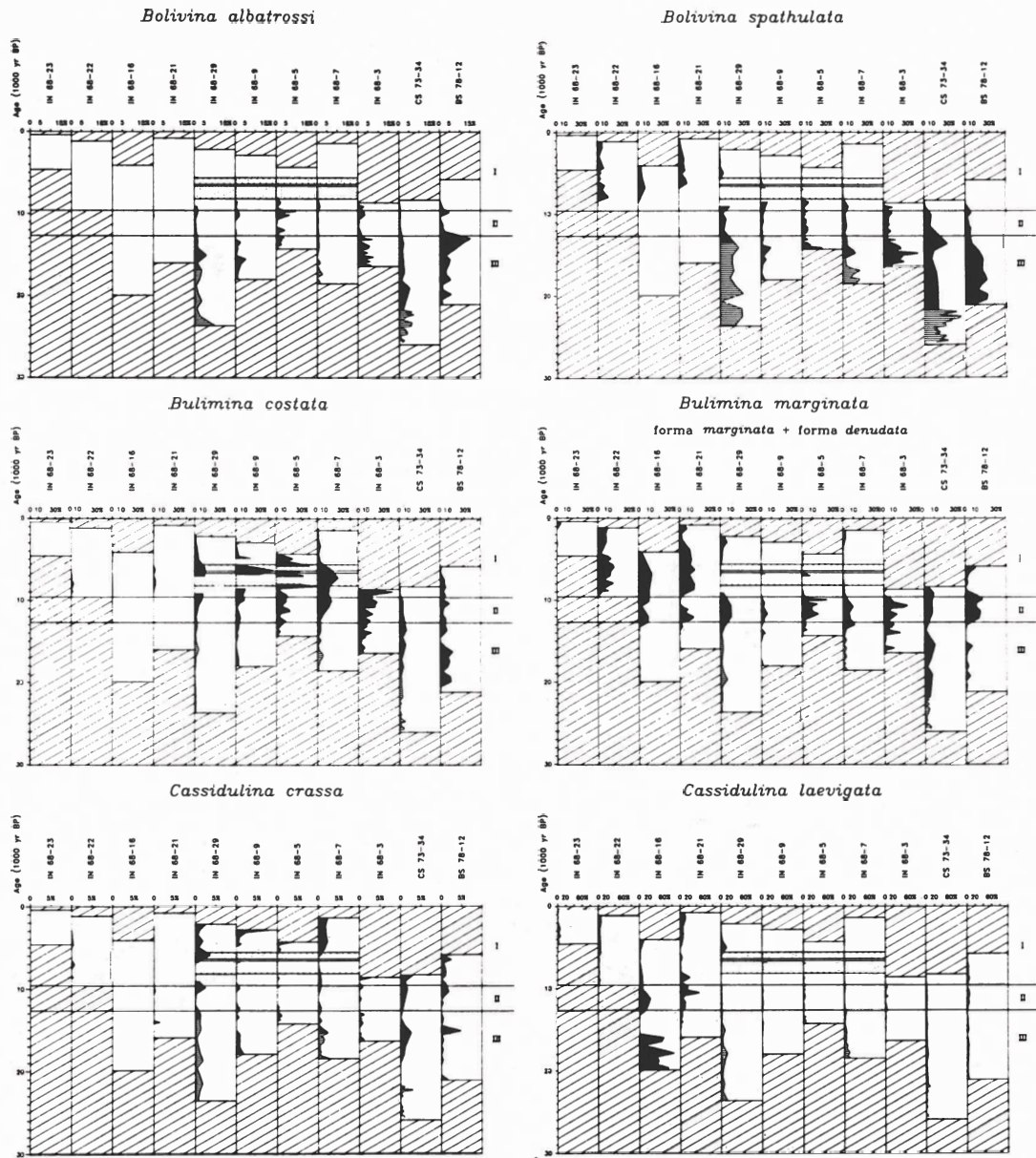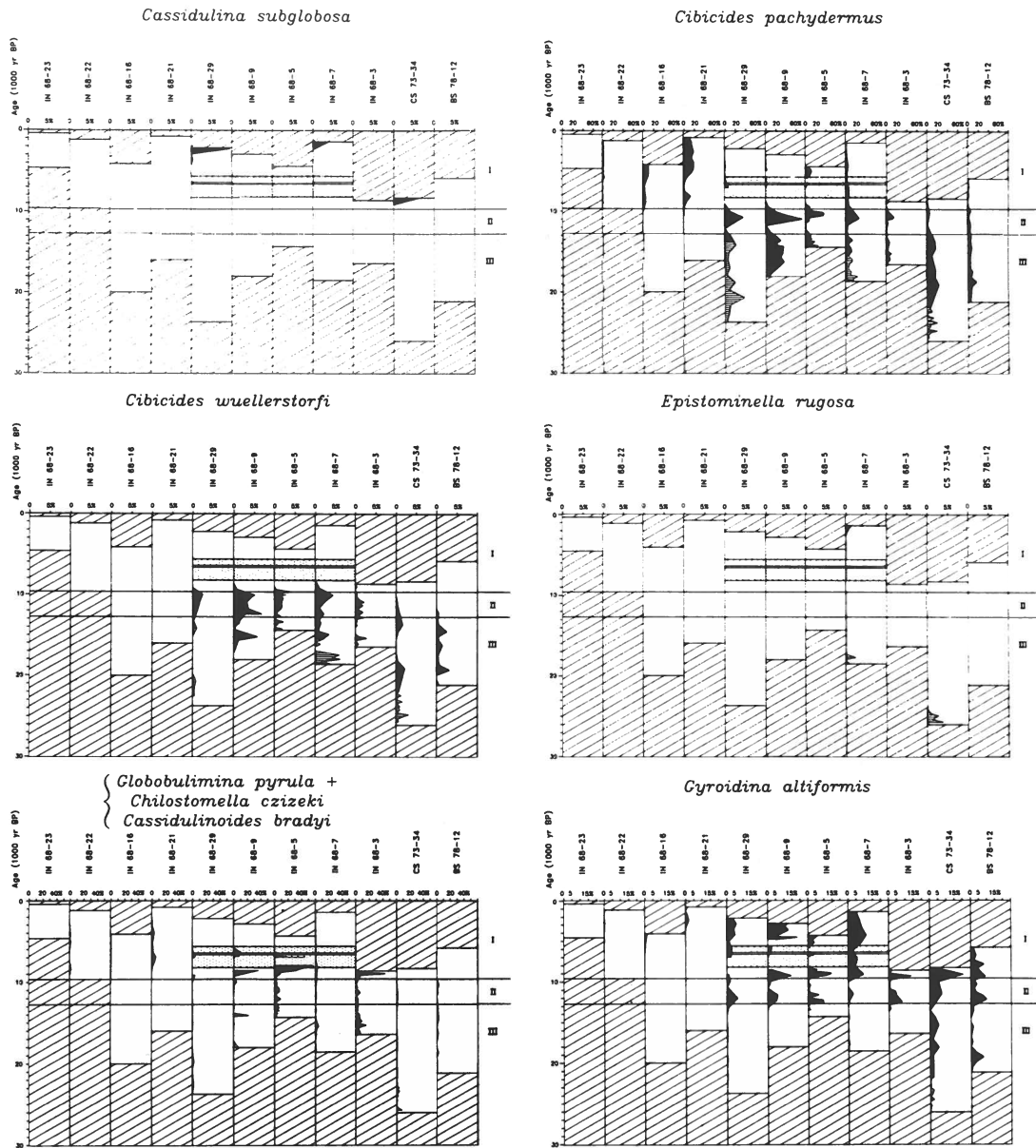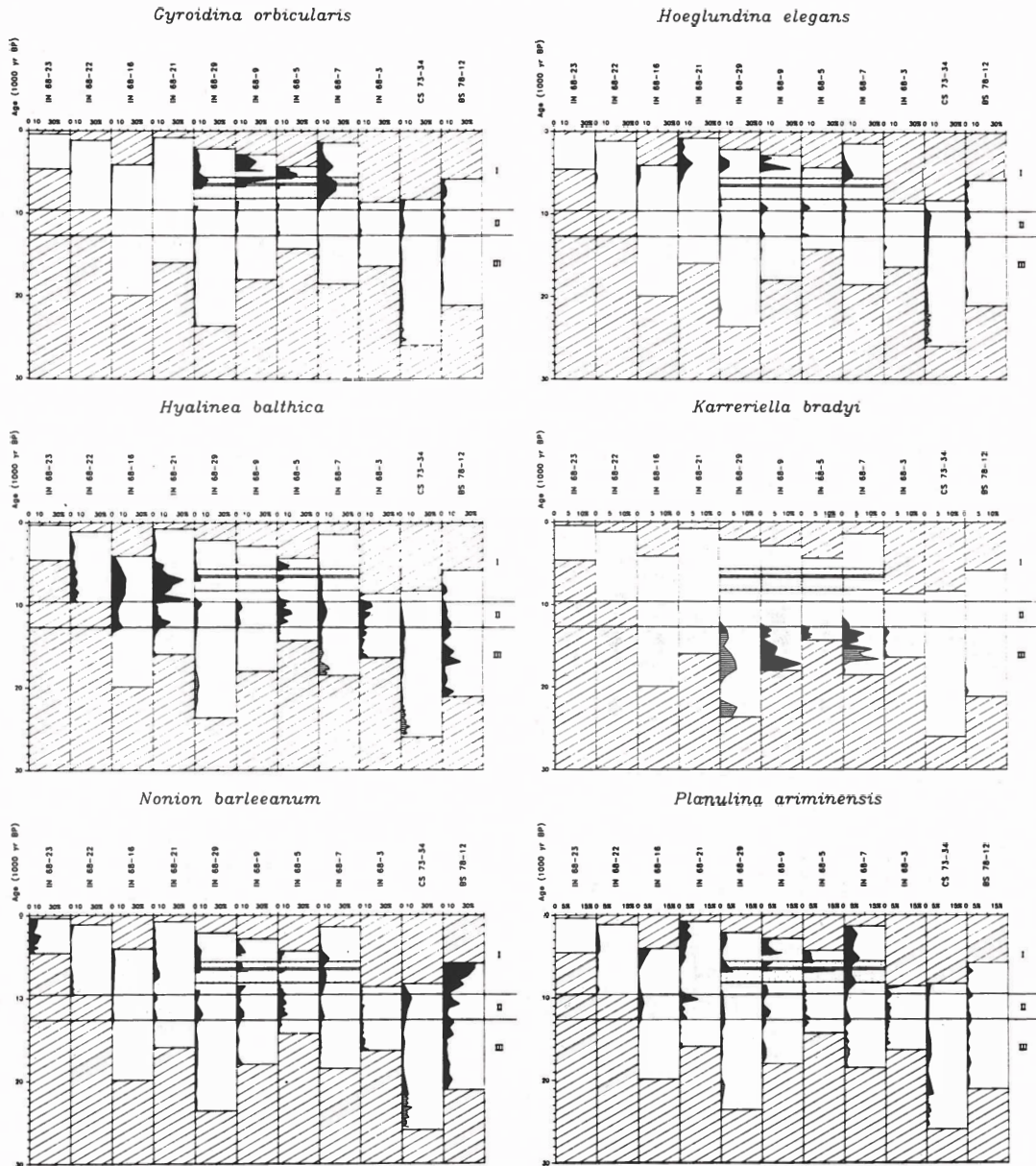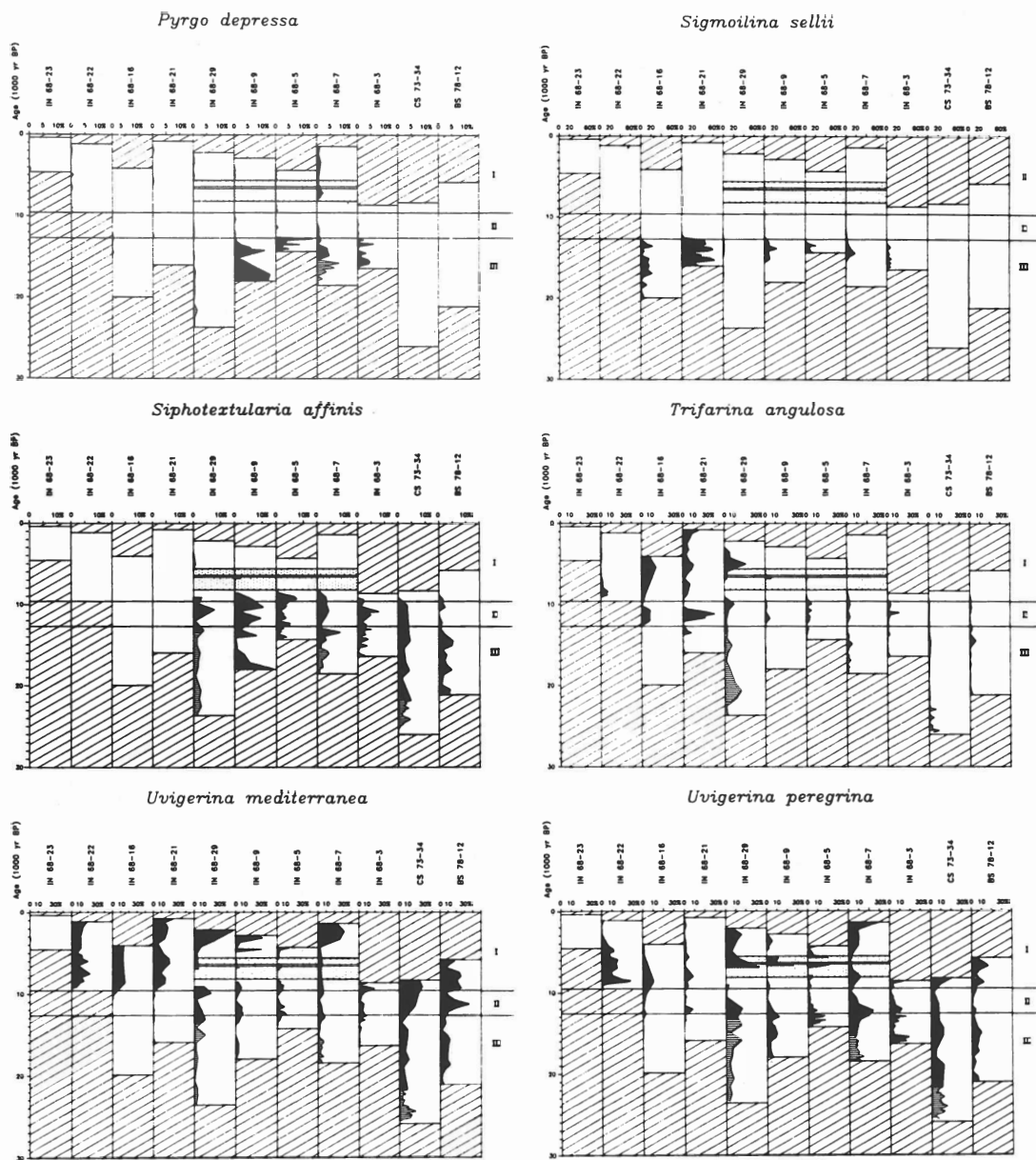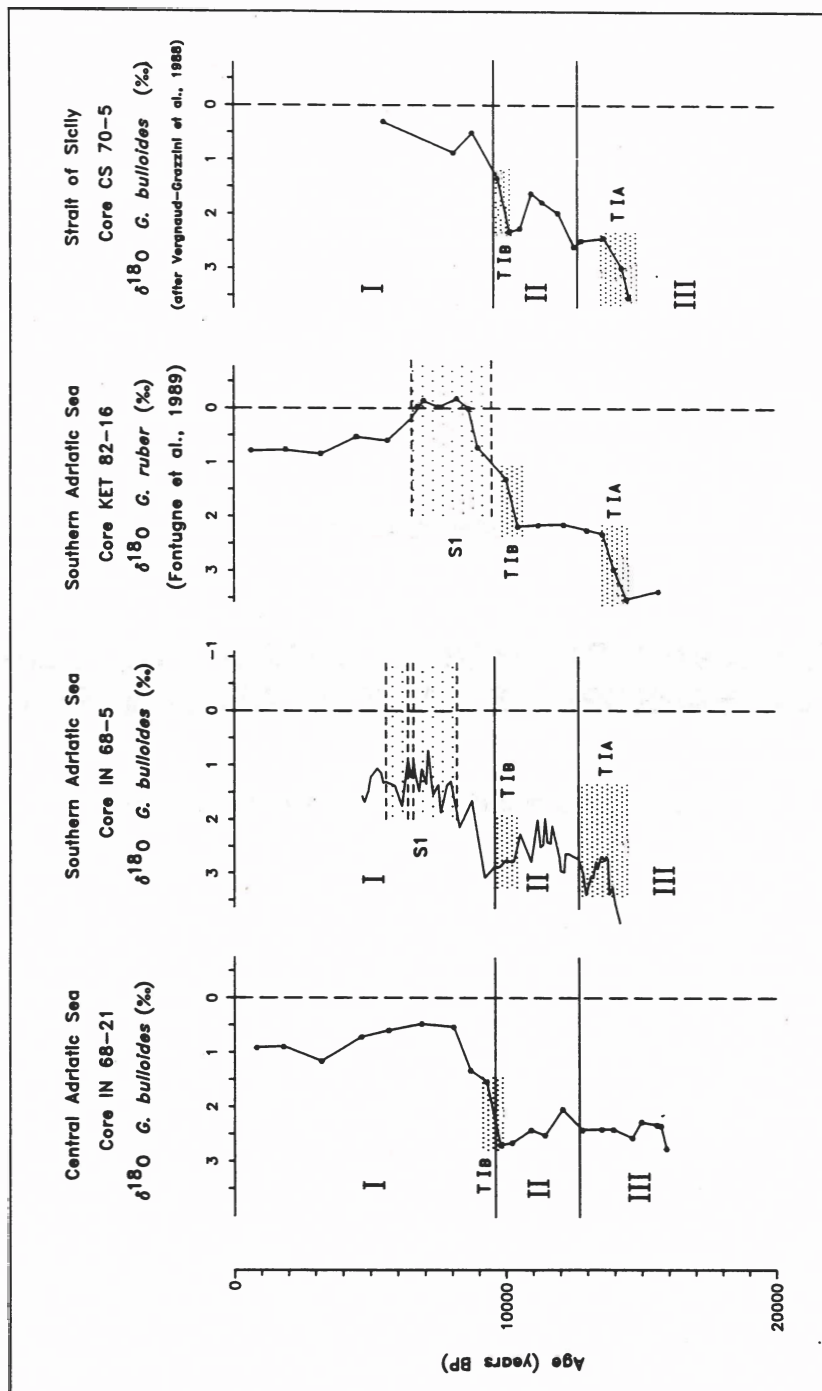
appendix 3

INCREASED RIVER DISCHARGE DURING THE DEPOSITION OF SAPROPEL S$_1$ IN THE AEGEAN SEA

INCREASED RIVER DISCHARGE DURING THE DEPOSITION OF SAPROPEL S₁ IN THE AEGEAN SEA

W.J. Zachariasse[1], F.J. Jorissen[1], C. Perissoratis[2], E.J. Rohling[1], V. Tsapralis[2]

1. Department of Stratigraphy and Micropaleontology, Institute of Earth Sciences, University of Utrecht, P.O.Box 80021, 3508 TA, Utrecht, The Netherlands.

2. Institute of Geology and Mineral Exploration, 70 Messoghion str., Athens 11527, Greece.

ABSTRACT

Three major changes in the planktonic foraminiferal record of core SK1 (Sporades Basin; western Aegean Sea) are correlated with similar, well-dated, changes in IN68-9 (Adriatic Sea). Thus, we could place core SK1 in a well-constrained time-stratigraphic framework. The interval between 300 and 520 cm in core SK1 is time-equivalent to sapropel S₁ in core IN68-9, and contains a large number of turbidites and high abundances of the planktonic foraminifer G. bulloides. This suggests a marked increase of the discharge of sediments and nutrients by Greek rivers at times of the formation of S₁. Slope instability seems to lag surface water eutrophication by approximately 1 000 years. This may be attributed to the fact that increased slope instability requires a period of enhanced sediment-loading, which started at the same time as the river induced surface water eutrophication (9 600 yrs BP).

INTRODUCTION

During the 1982 cruise of the British RV Discovery, piston core SK1 was recovered from the deepest part of the Sporades Basin. This basin is a ca. 1 000 m deep circular depression in the western Aegean Sea, south of Skopelos Island (figure 1). A foraminiferal study of this core has been carried out to determine the timing of climatic and hydrographic changes in the area. Therefore, the faunal succession was correlated to the recently designed late Quaternary biochronology for the Adriatic Sea (Appendix 2), which is based on a large number of AMS ^{14}C datings.

MATERIAL AND METHODS

Piston core SK1 measures 820 cm, and consists mainly of olive-brown coloured hemipelagic mud and silty to sandy intervals representing the coarse-grained parts of turbidites. These turbidites are especially frequent between 300 and 510 cm (figure 2). Planktonic foraminiferal counts were made on the 150 to 595 micron fraction of 55 samples. An Otto microsplitter was used to reduce residues into suitable aliquots of about 300 specimens. Benthic foraminifera were collected from the same aliquots, but their small numbers allow only some general remarks.

CHRONOLOGY OF CORE SK1

Abundances of planktonic foraminiferal species in core SK1 (figure 3a) show three levels of major faunal change, which can be correlated to similar changes in the well-dated core IN68-9 from the Adriatic Sea (figure 3b). The latter core serves as a chronologic standard for late Quaternary sequences in the Adriatic Sea (Appendix 2).

(1) The level at 283 cm is characterized by a peak abundance of neogloboquadrinids (figure 3a). A similar peak occurs in IN68-9, with an interpolated age of 5 800 yrs BP (figure

3b). The 283 cm level is the only horizon in core SK1 where *Globorotalia inflata* attains substantial numbers.

(2) The level at about 570 cm is characterized by a distinct upward decrease in the abundance of neogloboquadrinids, whereas those of *Globigerina bulloides* show an inverse change (figure 3a). The changes at 570 cm in SK1 are similar to those defining the Zone I/II boundary in IN68-9 (figure 3b). The I/II zonal boundary marks the base of the Holocene and was dated at 9 600 yrs BP.

(3) High numbers of *Globorotalia scitula* and *Turborotalita quinqueloba* below ca. 680 cm in SK1, are succeeded by low numbers above this level (figure 3a). This change is similar to that defining the Zone II/III boundary in IN68-9. The II/III zonal boundary marks the end of the pleniglacial and was dated at 12 700 yrs BP (Appendix 2).

EARLY HOLOCENE ENVIRONMENTAL CONDITIONS

The interval between 300 and 520 cm in SK1 contains high percentages of the benthic foraminiferal genera *Chilostomella* and *Globobulimina*. High percentages of these genera are indicative of low bottom water oxygen concentrations (Mullineaux and Lohmann, 1981). The organic carbon concentrations are distinctly raised within this interval, relative to the values below and above (table I). This may be the result of better preservation of organic carbon due to low bottom water oxygen concentrations during the deposition of the interval between 300 and 520 cm. The interpolated age-range of 6 000 to 8 700 yrs BP for this interval indicates that the section from 300 to 520 cm is time-equivalent to sapropel S_1 in core IN68-9. A distinct dark coloring, so characteristic of sapropel S_1 in pelagic settings, has not been observed in core SK1, but turbidites are markedly frequent (figure 2).

These turbidites are essentially planktonic foraminiferal grainstones, and possibly resulted from overloading of the slopes with fine-grained sediments. Levels devoid of foraminifera (samples 26, 27, 32 and 34) and levels showing high abundances of the small-sized *Turborotalita quinqueloba* (samples 22, 25, 29 and 33) are explained by sorting. The levels devoid of foraminifera larger than 150 micron proba-

SAMPLE	$C_{org.}$
10	0.37
13	0.37
16	0.41
19	0.31
21	0.44
24	0.86
27	1.37
29	0.86
31	0.89
33	0.88
34	0.67
36	0.35
38	0.31
40	0.35
43	0.33
45	0.30

Table I. Organic carbon concentrations (weight percentages) in several samples of core SK1. Sample positions are indicated in figure 2.

bly represent the fine-grained tails of turbidites. Since the average test size of *Turborotalita quinqueloba* in the present-day Mediterranean is only slightly larger than 150 micron (Kroon et al., 1989), sorting of particles in this size-range will enrich this species in the studied residues.

Although probably all foraminifera in the interval between 300 and 520 cm have been transported by turbidity currents, sorting certainly does not explain the high abundances of *Globigerina bulloides*, since this species has an extremely large size-range. *Globigerina bulloides* is a eutrophic species thriving in (coastal) upwelling areas (Thiede, 1983; Zhang, 1985; Hemleben et al., 1989) and in high-fertility areas off river mouths (Barmawidjaja et al., 1989; Van Leeuwen, 1989). High abundances of this species between 570 and 300 cm indicate that the surface waters in the Sporades Basin were eutrophicated from 9 600 to about 6 000 yrs BP.

EVIDENCE FOR INCREASED RIVER DISCHARGE AT EARLY HOLOCENE TIME

We reasoned that the low-oxygen conditions in the deep Sporades Basin between 8 700 and 6 000 yrs BP were coeval with similar conditions throughout the rest of the eastern Mediterranean. This widespread dysoxic to anoxic event resulted in the formation of the early Holocene sapropel S_1. Increased input rates of freshwater are generally invoked to explain these widespread low-oxygen conditions in the deep eastern Mediterranean. Amongst the freshwater sources most commonly referred to are the Black Sea and the Nile river (for overview, see chapter 1), but evidence is growing that also Turkish and Greek rivers were important (Shaw and Evans, 1984; Cramp et al., 1988). Eutrophication of surface water and higher rates of redeposition in the Sporades Basin at early Holocene time suggest an increased supply of river-borne nutrients and sediments.

One possibe source for these river-borne nutrients and sediments is the nearby Sperchios river (figure 1), which presently discharges 81 m^3 s^{-1} into the nearby Maliakos Gulf (Therianos, 1974). This efflux mixes with seawater, while transported into the western Aegean through the 50 km long and minimally 43 m deep Oreon Strait. Similar conditions prevailed back to about 10 000 yrs BP, when sea-level stood ca. 45 m below the present-day level (Cramp et al., 1988; Barmawidjaja et al., 1989; Fairbanks, 1989).

More plausible sources for the increased flux of nutrients and sediments into the Sporades Basin are the much larger rivers which presently discharge into the northern Aegean Sea (figure 1). Increased fluxes from these rivers may have generated large plumes of suspended matter, transported southward along the east coast of Greece by the generally cyclonic surface water circulation in the Aegean Sea (Ovchinnikov, 1966; Theocharis et al., 1988).

Surprisingly, the record of *Globigerina bulloides* marks the onset of enhanced nutrient fluxes into the Sporades Basin already at 570 cm in core SK1 (ca. 9 600 yrs BP), whereas enhanced sediment loading resulted in increased turbiditic activity some 50 cm further upcore; i.e. some 1 000 years later. At that time, bottom water oxygen concentrations throughout the eastern Mediterranean had dropped sufficiently to initiate the widespread S_1 formation.

CONCLUSIONS

The similarity between late Quaternary faunistic changes in the Adriatic and Aegean Sea shows that the recently designed late Quaternary biochronology for the Adriatic Sea provides a useful standard for calibrating undated late Quaternary sequences in the eastern Mediterranean.

Dysoxic conditions prevailed in the deep Sporades Basin between ca. 8 700 and 6 000 yrs BP. At that time, similar conditions prevailed throughout the eastern Mediterranean, which resulted in the widespread formation of sapropel S_1. In pelagic settings, sapropel S_1 is usually characterized by a distinctly dark colour. In the Sporades Basin, there is no distinct colour change across this interval. Enhanced turbiditic activity and surface water eutrophication, however, suggest that the discharge of Greek rivers had increased substantially at times of the S_1 formation.

A time-lag of roughly 1 000 years between surface water eutrophication and increased turbiditic activity in the Sporades Basin is suggested. This may be attributed to the fact that increased slope instability requires a period of enhanced sediment-loading, which started at the same time as the river induced surface water eutrophication at 9 600 yrs BP.

ACKNOWLEDGEMENTS

REFERENCES

Barmawidjaja, D.M., Van der Borg, K., De Jong, A.F.M., Van der Kaars, W.A. and Zachariasse, W.J., 1989. Kau Basin, Halmahera, a late Quaternary paleoenvironmental record in a poorly ventilated basin. *Proc. Sellius II Symp. Jakarta, Neth. J. Sea Research, 24*: 591-605.

Cramp, A., Collins, M. and West, R., 1988. Late Pleistocene-Holocene sedimentation in the NW Aegean Sea: a palaeoclimatic palaeoceanographic reconstruction. *Palaeogeogr. Palaeoclimatol. Palaeoecol., 68*: 61-77.

Fairbanks, R.G., 1989. A 17,000-year glacio-eustatic sea level record: influence of glacial melting rates on the Younger Dryas event and deep-ocean circulation. *Nature, 342*: 637-642.

Hemleben, Ch., Spindler, M. and Anderson, O.R., 1989. *Modern planktonic foraminifera.* Springer-Verlag New York, 363 pp.

Jorissen, F.J., 1987. The distribution of benthic foraminifera in the Adriatic Sea. *Mar. Micropaleontol., 12*: 21-48.

Jorissen, F.J., 1988. Benthic foraminifera from the Adriatic Sea; principles of phenotypic variation. *Utrecht Micropaleontol. Bull., 37*: 174 pp.

Kroon, D., Wouters, P., Moodley, L., Ganssen, G., and Troelstra, S.R., 1988. Phenotypic variation of *Turborotalita quinqueloba* (Natland) tests in living populations and in the Pleistocene of an eastern Mediterranean piston core. In: Brummer, G.J.A. and Kroon, D. *Planktonic foraminifers as tracers of ocean-climate history.* Free University press, Amsterdam, pp. 131-147.

Mullineaux, L.S. and Lohmann, G.P., 1981. Late Quaternary stagnations and recirculation of the Eastern Mediterranean: changes in the deep water recorded by fossil benthic foraminifera. *J. Foraminiferal Res., 11*: 20-39.

Ovchinnikov, I.M., 1966. Circulation in the surface and intermediate layers of the Mediterranean Sea. *Oceanologica, 6*: 48-59.

Shaw, H.F. and Evans, G., 1984. The nature, distribution and origin of a sapropelic layer in sediments of the Cilicia Basin, northeastern Mediterranean. *Mar. Geol., 61*: 1-12.

Theocharis, A., Georgopoulos, D., Krestenitis, Y., and Koutitas, C., 1988. Observations and modeling of upwellings in the Aegean Sea. *Rapp. Comm. Int. Mer. Medit., 31*: 212.

Therianos, A.D., 1974. The geographical distribution of river water supply in Greece. *Bull. Geol. Soc. Greece, 11*: 25-28.

Thiede, J., 1983. Skeletal plankton and nekton in upwelling water masses off northwestern South America and northwest Africa. In: E. Suess and J. Thiede (Editors), *Coastal Upwelling, pt. A*, Plenum Publishing Corp., pp. 183-207.

Van Leeuwen, R.J.W., 1989. Sea-floor distribution and late Quaternary faunal patterns of planktonic and benthic foraminifers in the Angola Basin. *Utrecht Micropaleontol. Bull. 38*: 288 pp.

Zhang, J., 1985. Living planktonic foraminifera from the Eastern Arabian Sea. *Deep Sea Res., 32*: 789-798.
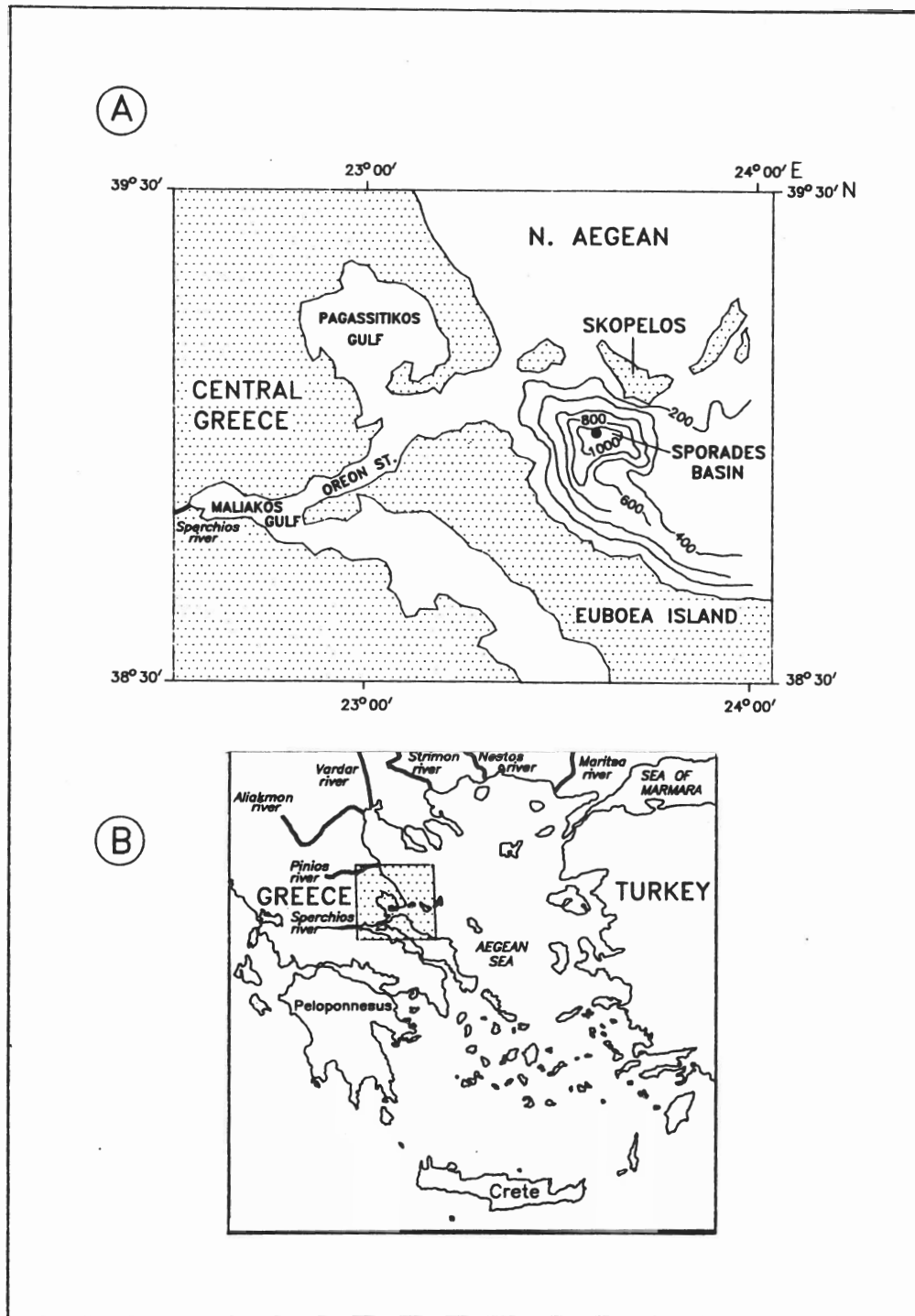
Figure 1.   A. The location of core SK1.
B. The regional setting.
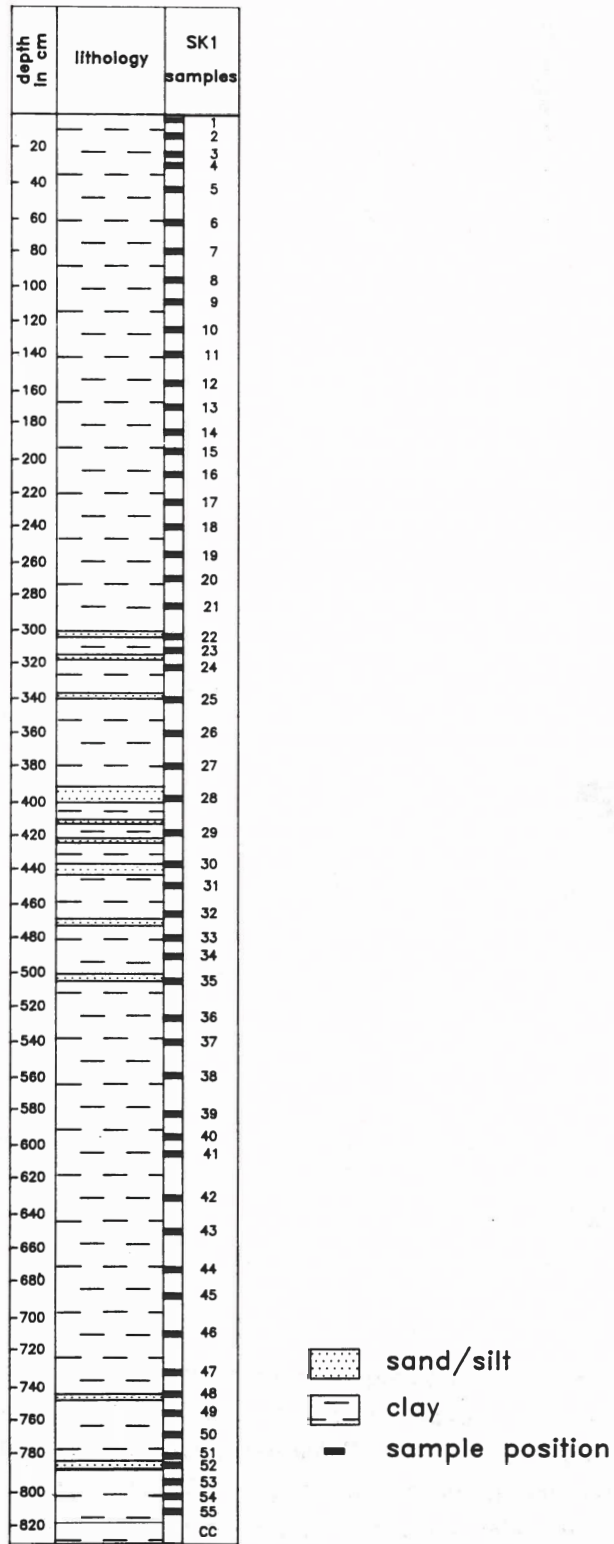
Figure 2. Lithology core SK1 and sample positions.

153
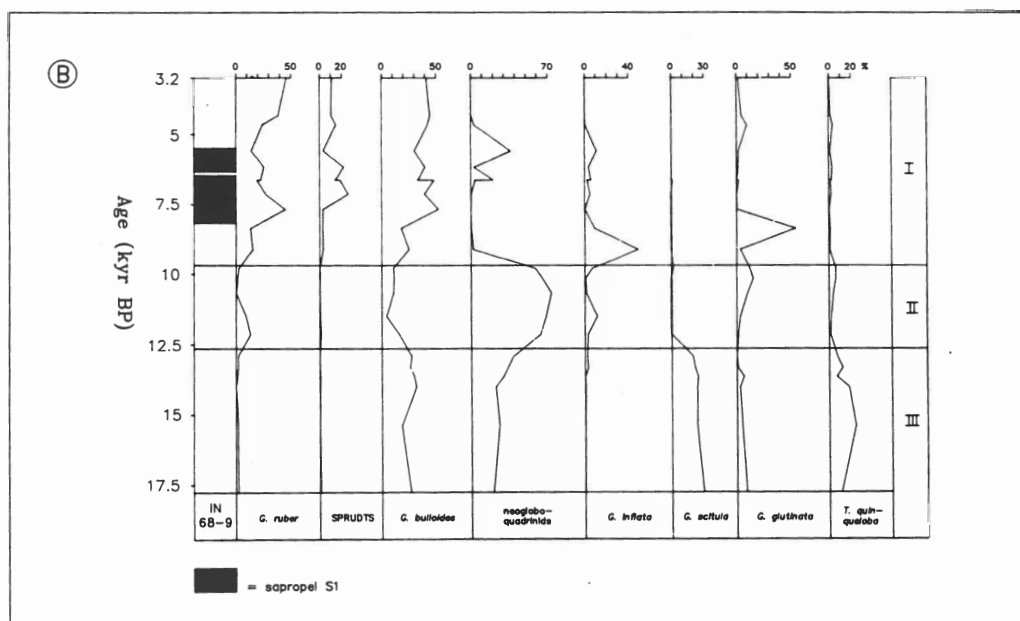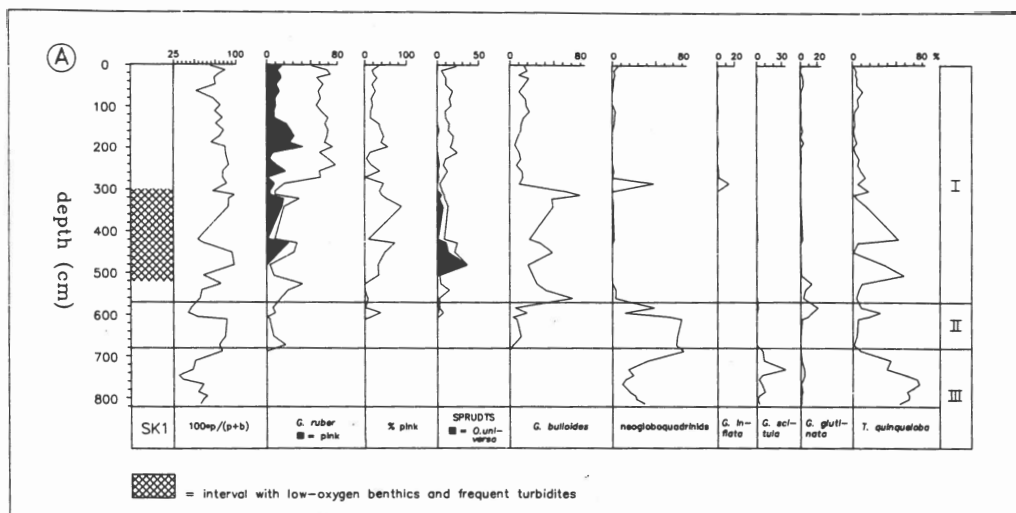
Figure 3 **A.** Downcore faunal frequency distribution in core SK1. The SPRUDTS-group consists of *Globogerinoides sacculifer*, *Hastigerina pelagica*, *Globoturborotalita rubescens*, *Orbulina universa*, *Globigerina digitata*, *Globoturborotalita tenella* and *Globigerinella siphonifera*. Percentage pink denotes the percentage of pink *Globigerinoides ruber* with respect to total *G. ruber*. Roman numerals refer to the biozonation of Jorissen et al. (Appendix 2).

       B. Faunal frequency distribution in core IN68-9, from the Adriatic Sea, plotted versus time. Samples were calibrated to ^{14}C ages on the basis of AMS ^{14}C datings and linear interpolation and extrapolation, in which turbidites were assumed to contain very little time (Appendix 2). The Zone I/II boundary was dated in this core at 9 600 yrs BP, and the Zone II/III boundary at 12 700 yrs BP.

ACKNOWLEDGEMENTS

CURRICULUM VITAE

Eelco Johan Rohling was born in Heiloo, The Netherlands, on the 19th of September 1963. After attending secondary school from 1975 to 1981, he studied Earth Sciences at the University of Leiden for 1 year, and completed this study at the University of Utrecht. He obtained the Masters ('doctoraal') degree in stratigraphy and micropaleontology, with physical oceanography/climatology and sedimentology as subsidiary subjects, on the 31st of August 1987. On the 1st of september 1987 he became employed by the University of Utrecht as a Ph.D.-candidate. The dissertation was completed in May 1991.